Identification and Characterisation of a Lithium Mimetic: Enzymatic, Cellular and Animal Investigations

Nisha Singh

St. Peter's College



Thesis submitted for the degree of

DPhil in Pharmacology

Hilary term 2012

Abstract

It has been six decades since the discovery of lithium for the treatment of bipolar disorder. There is, as yet, no conclusive evidence as to how lithium produces this therapeutic effect, since it is known to interact with multiple cellular targets. One of the most credible targets is the enzyme, inositol monophosphatase (IMPase), which plays a crucial role in cell signalling. My aim was to find a novel IMPase inhibitor and evaluate it as a possible lithium-like mood stabiliser by using enzyme, cell and whole animal experiments.

To achieve this, I created recombinant human and mouse IMPase enzymes and then used these for screening and crystallisation. I used two different approaches for the small-molecule screening: substrate-based virtual screening and drug repositioning using a library of compounds with clinically proven safety. I identified ebselen as a novel IMPase inhibitor suitable for drug repositioning.

I determined that ebselen inhibited IMPase noncompetitively, likely through a covalent modification on a cysteine. In cell cultures, ebselen was found to inhibit not just IMPase but other steps that resulted in accumulation of higher inositol phosphates. When injected intraperitoneally into mice, ebselen crossed the blood-brain barrier and exhibited inhibition of IMPase *ex vivo*. Moreover, in mice, ebselen simulates some, but not all, of the behavioural effects of lithium.

I have determined that ebselen inhibits IMPase and acts as a partial lithium mimetic. Given that ebselen is safe in man, it warrants clinical testing for the treatment of bipolar disorder.

Table of Contents

Abstract

Table of contents…….…….....…..i

Acknowledgments……...…..viii

Abbreviations……..…….x

Chapter 1 Introduction

1.1 The history of bipolar disorder..... 1

1.1.1 Pre- 19th century 1

1.1.2 19th century and beyond.....2

1.2 Symptoms of bipolar disorder 3

1.2.1 Cycling 3

1.2.2 Classification and Diagnosis.....5

1.2.3 Aetiology.....5

1.3 Treatment of bipolar disorder 6

1.3.1 The discovery of lithium.....7

1.3.2 Early clinical trials with lithium 8

1.3.3 Lithiums effects on mice models of bipolar disorder 9

1.3.4 Shortcomings of lithium therapy 14

1.4 Mechanisms of lithium's actions 15

1.4.1 Lithium's effects on sodium channels.....15

1.4.2 Lithium's effects on neurotransmitters 17

1.4.3 Lithium's effects on second messengers *25*

1.5 Inositol depletion hypothesis **33**

1.5.1 Evidence for the inositol depletion hypothesis *35*

1.5.2 Evidence against the inositol depletion hypothesis *36*

1.6 Selection of IMPase as a target **37**

1.7 IMPase **38**

1.7.1 Structure of function of IMPase *38*

1.7.2 IMPase as the target of lithium inhibition *40*

1.8 Drug development **42**

1.8.1 Developing small molecules for target validation *43*

1.9 Aims **46**

Chapter 2 Inositol monophosphatase: Cloning, Expression, Purification and Crystallography

2.1 Introduction **46**

2.1.1 Crystal structure of IMPase *46*

2.1.2 Mechanism of substrate hydrolysis *47*

2.1.3 Lithium and IMPase *50*

2.1.4 Aims *52*

2.2 Materials and Methods **53**

2.2.1 Chemicals and reagents: *53*

2.2.2 Bioinformatics *54*

2.2.3 Protein expression and analysis *54*

2.2.4 Chromatography *59*

2.2.5 IMPase activity and concentration analysis *62*

2.2.6 Protein characterisation *66*

2.2.7 Mass spectrometry *67*

2.2.8 Crystallography *68*

2.3 Results **71**

2.3.1 Cloning *71*

2.3.2 Protein expression *74*

2.3.3 Protein purification *77*

2.3.4 Protein characterisation *84*

2.3.5 Crystallography *90*

2.4 Discussion **97**

2.4.1 Specific activity *97*

2.4.2 The 'interfering' band *97*

2.4.3 Crystallography *98*

2.4.4 Comparison of human and mouse IMPase 1 ..... *98*

Chapter 3 Screening for an IMPase inhibitor

3.1 Introduction **104**

3.1.1 Ligand-based drug design *104*

3.1.2 Drug repositioning *109*

3.1.3 Aims *109*

3.2 Materials and methods 111

3.2.1 Virtual screening protocol 111

3.2.2 Drug repositioning 112

3.2.3 Biological assay 113

3.3 Results 117

3.3.1 Lithium and L-690330: Dose–response and enzyme kinetics 117

3.3.2 Biological testing of virtual screening hits 119

3.3.3 IMPase activity in presence of NIS-15 125

3.3.4 In silico docking of NIS-15 into the active site of IMPase 126

3.3.5 Biological testing of compounds in the NIH clinical collection 127

3.3.6 Possible non-specific effects of ebselen on IMPase 130

3.3.7 Ebselen's effect on the kinetics of IMPase 133

3.3.8 Reversibility of ebselen inhibition 135

3.3.9 Ebselen inhibition: Covalent or non-covalent? 137

3.3.10 Interaction with cysteine in glutathione 140

3.3.11 Interaction with GSK-3β 141

3.4 Discussion 143

3.4.1 Virtual screening 143

3.4.2 NIH compounds screen 144

3.4.3 Ebselen inhibition of IMPase 145

3.4.4 Other applications of Ebselen 149

Chapter 4 Evaluation of ebselen in cells and tissues

4.1 Introduction 150

4.1.1 Effects of lithium on inositol phosphates 150

4.1.2 Aims 151

4.2 Materials and Methods 153

4.2.1 Materials 153

4.2.2 IP_1 ELISA 154

4.2.3 Michaelis–Menten kinetics with reduced ebselen 157

4.2.4 Calcium release assay 157

4.2.5 Inositol phosphate profiling and separation 159

4.2.6 Mouse brain homogenate IMPase kinetics 161

4.3 Results 163

4.3.1 Effect of ebselen on Ins1P levels in cells 163

4.3.2 Effects of reduced ebselen on IMPase activity 166

4.3.3 Calcium release experiments 167

4.3.4 Inositol phosphate profile 174

4.3.5 Ex vivo IMPase inhibtion 177

4.4 Discussion 184

4.4.1 Effect of ebselen on PI-linked signalling pathway in cells 184

4.4.2 Effect of ebselen on PI-linked signalling pathway in cells 190

Chapter 5 Ebselen and behaviour

5.1 Introduction 192

5.1.1 Exploratory activity using the open-field test 192

5.1.2 Amphetamine-induced hyperactivity test....193

5.1.3 Behavioural despair test (Forced swim test)....195

5.1.4 Pilocarpine seizure test....195

5.1.5 Aims....197

5.2 Materials and Methods....198

5.2.1 Legal compliance....198

5.2.2 Experimental animals....198

5.2.3 Drugs....199

5.2.4 Activity monitor setup....199

5.2.5 Open field test....201

5.2.6 Amphetamine-induced hyperactivity....202

5.2.7 Forced swim test....203

5.2.8 Pilocarpine seizures....203

5.2.9 In situ hybridisation....205

5.3 Results....209

5.3.1 Open field test....209

5.3.2 Amphetamine-induced hyperactivity....213

5.3.3 Forced swim test....222

5.3.4 Pilocarpine seizure test....227

5.3.5 Tremor analysis....232

5.3.6 In situ hybridisation....234

5.4 Discussion....241

5.4.1 Ebselen's effect on exploratory activity 241

5.4.2 Ebselen's effect on amphetamine-induced hyperactivity 242

5.4.3 Ebselen's effect in the forced swim test 243

5.4.4 Effect of ebselen in the pilocarpine seizure test 245

Chapter 6 Final discussion 248

Bibliography 254

Acknowledgments

Firstly, I would like to thank my parents. You are my faith and my inspiration. Everything I have achieved today is because of your unwavering support and conviction in me. I would also like to thank my sister, who is, and will always be my best friend.

The Churchill lab, Grant, Parv, Sri, Alex, Duncan, and Amy, you are the best lab ever. You have made working in the lab, even on the most mundane days, something I always looked forward to. Grant, you are the best teacher and supervisor I have ever known. You inspire me to be better, and you challenge me to think differently. Parv, thank you for being my 'mother-hen', my colleague and my friend, all in one. Sri and Alex, anytime I have asked for any help, scientific, technical or otherwise, you have unhesitatingly volunteered. Duncan and Amy, thank you for your exceptional company for all your advice and patience with me. I am grateful to all of you for putting up with me!

A very big thank you to Michael Field, without whom, this thesis would be incomplete. I am indebted for how much you have done for me. Also, a big thanks to Clive Garnham, who is always there with a helping hand, with or without a tool! Michael and Clive, your enthusiasm is infectious.

Thank you to Dr. Trevor Sharp, Dr. Florence Serres, Mr. Dave Smith, Dr. Nathan Lack, Dr. Robert Sim, Dr. Ali Ryan, Dr. Ed Lowe, Dr. Esther Woon for all your scientific input. Dr. Justyn Thomas, Olga Kuznetsova, Matthew Knight and Simon Hackett; thank you for being involved with the project. Your ideas and contributions have been much appreciated.

I am indebted to the Department of Pharmacology, University of Oxford for providing my funding, without which none of this work would have been possible.

Thank you to Dr. Edith Sim, my college advisor, and to St. Peter's College. Thank you also to the Dr. Antony Galione and the Galione lab.

Parv, Sri, Aarti, thank you for being my surrogate family, and being my support system, in times when I have needed it the most.

I would like to conclude by a very apt Chinese proverb that my supervisor, Grant, showed me:

"Were I to await perfection, my book would never be finished."

Abbreviations

5-HT	5-hydroxytryptamine or serotonin
ADME	Absorption, distribution, metabolism and excretion
AIH	Amphetamine-induced hyperactivity
APS	Ammonium persulphate
ATP	Adenosine triphosphate
BCA	Bicinchoninic acid
BSA	Bovine serum albumin
CHO	Chinese hamster ovary
CMP-PA	Cytidine monophosphate- phosphatidic acid
CNS	Central nervous system
DOI	2,5-dimethoxy-4-iodoamphetamine
DTNB	5,5'-dithiobis-(2-nitrobenzoic acid)
DTT	Dithiothreitol
EDTA	Ethylenediaminetetraacetic acid
EGTA	Ethyleneglycoltetraacetic acid
ELISA	Enzyme linked immunosorbent assay
ER	Endoplasmic reticulum
ESI-MS	Electrospray ionisation -mass spectroscopy
FBPase	Fructose 1,6-bisphosphatase
FR counts	Front to rear counts
FST	Forced swim test
GABA	γ-amino butyric acid
GPCR	G-protein coupled receptor
GRK-3	G-protein receptor kinase 3
GSH	Glutathione (reduced)
HBSS	Hanks balanced salt solution
HPLC	High performance liquid chromatography
HRP	Horse radish peroxidase
Hs	*Homo sapiens*
i.p.	Intraperitoneal
IBPase	Inositol-1,4-bisphosphatase

IMPase	Inositol monophosphatase
IP-5Pase	Inositol polyphosphate 5-phosphatase
IP_1	Inositol monophosphate
IP_2	Inositol bisphosphate
IP_3	Inositol trisphosphate
IP_3-3inase	Inositol trisphosphate 3-kinase
IP_4	Inositol tetrakisphosphate
IP_5	Inositol pentakisphosphate
IP_6	Inositol hexakisphosphate
IPPase	Inositol polyphosphate 1-phosphatase
mAb	Monoclonal antibody
MALDI	Matrix-assisted laser desorption ionisation
MIPS	1-D-*myo*-inositol-3-phosphate synthase
Mm	*Mus musculus*
PAPase	3′- phosphoadenosine-5′-phosphatase
PI	Phosphatidyl inositol
PIP	Phosphatidyl inositol 4-phosphate
PIP_2	Phosphatidyl inositol 4, 5-bisphosphate
PK/PD	Pharmacokinetic/Pharmacodynamic
PKC	Protein kinase C
PLC	Phospholipase C
R.T.	Room temperature
s.c.	Subcutaneous
SSRI	Selective serotonin reuptake inhibitor
TEMED	Tetramethylethylenediamine

CHAPTER 1

INTRODUCTION

1 Introduction

1.1 The history of bipolar disorder

1.1.1 Pre- 19th century

Mental diseases have been identified and documented from the 5th and 4th centuries BC (Jackson, 1986; Roccatagliata, 1986). According to Hippocrates' treatise *On the Nature of Man*, the conditions of 'melancholia' and 'mania' were thought to be due to imbalances in black bile and yellow bile, respectively. Hippocratic followers did not support the then prevalent idea that illnesses were due to supernatural forces, but went as far as to say that melancholy was a "*psychological manifestation of an underlying biological disturbance, specifically, a perturbation in brain function*" (Goodwin *et al.*, 2007). At the time, however, the lines between the different states of mental illnesses were blurred. There was no distinction between what we now know as 'depression' (melancholy), 'mania' and 'schizophrenia'. Most writers and physicians kept meticulous records of the manifestations of melancholy and mania, and attributed these two states to one underlying disease. For example, Aretaeus, a clinician in the second century AD, described what we now know as bipolar disorder. He said, "*Some patients after being melancholic have fits of mania…so that mania is like a variety of being melancholy*." (Goodwin *et al.*, 2007).

This notion persisted, as illustrated by Thomas Willis, an English physician (incidentally, M.A. Oxford) in 1672 when he said, "*manics and melancholics are so much akin, that these Distempers often change, and pass from one into the other; for the Melancholick disposition growing worse, brings on Fury; and Fury or Madness growing less hot, oftentimes ends in a Melancholick disposition. These two, like*

smoke and flame, mutually receive and give place to one another" (Goodwin *et al.*, 2007).

In 1851, a French psychiatrist, Jean-Pierre Falret, published a seminal paper *'De la folie circulaire ou forme de maladie mentale caracterisée par alternative régulière de la manie et de la melancholie,'* ('Of insanity or circular form of mental illness characterized by regular alternation of mania and melancholy'). He described an illness that he called *'la folie circulaire'* ('circular insanity') in which a patient swings between mania and depression. This is the first documented diagnosis of what we now know as 'bipolar disorder' or 'manic depression' (Pichot, 2004). Even then, differing patterns in the different types of mental illness had been observed, but no clear distinctions were made for a further 50 years.

1.1.2 19th century and beyond

Emil Kraeplin was a German psychiatrist who modernised the practise of psychiatry and psychopharmacology. He carried out a detailed analysis of the symptoms presented by a variety of mentally ill patients. He defined and classified 'dementia praecox' and distinguished it from 'manic-depressive' illness. We now know dementia praecox as 'schizophrenia' and manic-depressive illness as 'bipolar disorder'. In his book titled 'Manic Depressive Insanity and Paranoia' he writes,

"*We include here certain slight and slightest colourings of mood, some of them periodic, some of them continuously morbid, which on the one hand are to be regarded as the rudiment of more severe disorders; on the other hand, pass without sharp boundary in to the domain of personal predisposition. In the course of the years I have become more and more convinced that all the above mentioned states only*

represent manifestations of a single morbid process." (Kraepelin and Robertson, 1921)

In his meticulous descriptions of the different mental illnesses, he observed that it was unlikely that melancholy and manic-depression were the same illness, but he was reluctant to state this definitively (Goodwin *et al.*, 2007). In 1957, Leonhard, another German psychiatrist, observed that some patients had histories of both mania and depression as a recurrent theme and that there was also a strong familial trend, whereas in other patients only depression was seen. He segregated these two types of mental illnesses and coined the terms 'bipolar depression' for the former and 'monopolar depression' for the latter.

1.2 Symptoms of bipolar disorder

Bipolar disorder is a type of mental illness that is classified under a broader spectrum of mental illnesses called 'affective disorders'.

1.2.1 Cycling

Bipolar disorder is characterised by extreme fluctuations in mood, varying from an elevated high-energy, high-mood manic phase to an unusually low-energy, low-mood depressed state, interspersed with a symptom-free period. The manic phase is characterised by exaggeration, grandiosity, pleasure-seeking behaviour, substance abuse, high sexual energy and decreased need for sleep. The depressed state is characterised by low energy levels, anhedonia, lack of interest or motivation — similar to unipolar depression.

Cycling between the two polar states usually occurs a minimum of four times a year, with a recovery phase that is symptom-free. When the patient cycles between

these states more frequently it may be termed 'rapid cycling' (Figure 1.2.1) In extreme cases suffers can progress to ultradian cycles: *"There've been times where I've been cycling so rapidly I was laughing and crying at the same time…one minute way up, the next minute in the total pit of despair, literally mere seconds between the two extremes…"* (Mackinnon and Pies, 2006)

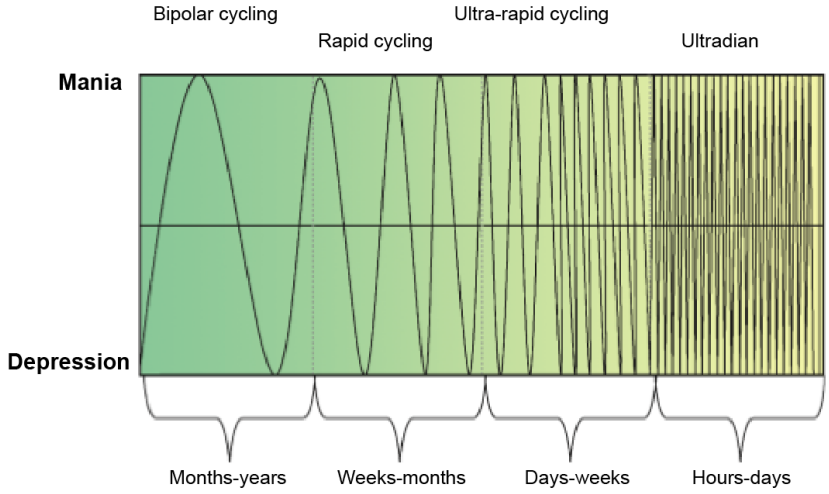


Figure 1.2.1. Cycling in bipolar depression. Schematic representation of cycling between the states of mania and depression in patients with bipolar disorder. The classification of patients is dependent on the frequency, not the quality, of episodes (Mackinnon and Pies, 2006).

However, the cycling between the two polar states is not usually as prescribed as that. There are ambiguous states in which symptoms of the manic phase may present concomitantly with symptoms of the depression phase. These are called 'mixed states'. Traditionally, when mood, energy and intellect are all high and synchronous, this is a classic manic state, and when they are all low and still synchronised, this is a classic depressed state. When there is a phase shift in mood, energy and intellect (Figure 1.2.2), such that they become unsynchronised, this is called a mixed episode. For example, a bipolar patient is most likely to commit suicide when the energy levels are high, but mood is low. This is also called the state of 'agitated depression'.

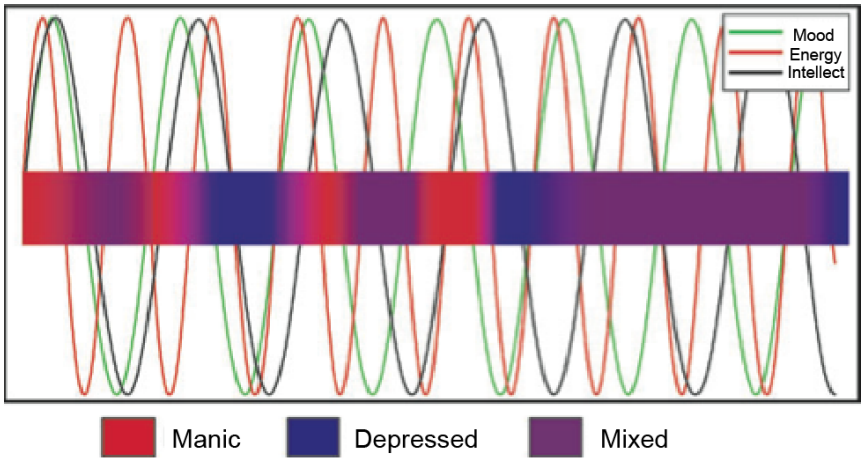


Figure 1.2.2. Mixed cycling in bipolar disorder. Mixed episodes are characterised by asynchronous shifts in mood, energy and intellect. The red portions of the bar across the graph show the states of pure mania, the blue shows pure depression and the purple signifies the mixed states (Mackinnon and Pies, 2006).

1.2.2 Classification and Diagnosis

Bipolar disorder can be classified as 'bipolar disorder I' and 'bipolar disorder II', depending on the presentation of the illness (American Psychiatric Association, 2000). The lifetime prevalence of bipolar disorder I and II is 3.9% of the population, and the median age of onset is 25 years (Kessler *et al.*, 2005). The difference between bipolar I and bipolar II is that the latter is characterised by transitions between 'hypomania' (rather than mania) and depression. Hypomania is a less severe form of mania, where the elevation in mood does not impair the functioning of the patient or require hospitalisation. Hence, bipolar disorder II is sometimes confused with unipolar depression and, if treated with antidepressants, may precipitate mania (Bunney, 1978; Peet, 1994).

1.2.3 Aetiology

The cause of bipolar disorder is still unknown. What is certain, however, is that there is a strong genetic component. Studies involving families of a bipolar

patient, denoted in studies as the 'proband', have shown that first-degree relatives have a higher risk of developing bipolar disorder or an alternative affective disorder such as schizophrenia, substance abuse disorder and/or schizoaffective disorder. According to studies, the lifetime risk of a first-degree relative developing bipolar disorder I is 4.1% higher in families with a bipolar proband, with a 16.9% increase in developing affective disorders, which include (Gershon, 1982; Gershon *et al.*, 1989). The heritability of bipolar disorder I and bipolar disorder II is 0.77 and 0.68, respectively (where 1.0 indicates complete heritability) (Bertelsen *et al.*, 1977). However, since the heritability is not 1.0, this indicates that there is likely to be an environmental or an epigenetic involvement in bipolar disorder.

Despite a strong genetic component, it is an environmental trigger, such as stress or substance abuse, which will usually precipitate the first episode of illness. After onset, bipolar disorder remains a lifetime illness and episodes do not need environmental triggers. The disease starts with bipolar cycling (Figure 1.2.1) but as it progresses, the cycles become more rapid, and mixed, if left untreated.

1.3 Treatment of bipolar disorder

Before the advent of effective drugs, lobotomy was widely practised as the treatment for mental illness. In the early 20th century, electroconvulsive therapy was introduced as an alternative. Perhaps surprisingly, it is only in the last 60 years that a pharmacological approach was approved, and this came in the form of lithium.

Lithium has become the drug of choice for bipolar disorder. It is the only true mood-stabiliser; because it has the ability to buffer the polarities of mania and depression, although it is better know for its anti-manic properties. Alternative drugs include anticonvulsants, antidepressants, atypical antipsychotics and benzodiazepines

(Goodwin *et al.*, 2003; Hayes *et al.*, 2011; Sachs *et al.*, 2000). However, the latter are only used to sedate manic patients and are usually only used acutely. Other than lithium, anticonvulsants have been the most widely prescribed drugs for the treatment and prophylaxis of bipolar disorder. Some antidepressants have been found to be useful when given in combination with lithium and/or anticonvulsants. However, antidepressant therapy in bipolar disorder carries the risk of precipitation of mania. This has particularly been seen in patients treated with tricyclic antidepressants such as imipramine (Peet, 1994). Atypical antipsychotics, such as quetiapine, have also found to be beneficial when given in combination with lithium and/or anticonvulsants (Porcelli *et al.*, 2011; Young *et al.*, 2010a; Young *et al.*, 2010b). Still, lithium remains the gold standard in the treatment of bipolar disorder (Cipriani *et al.*, 2005; Goodwin *et al.*, 2003) and is the only known drug with anti-suicidal properties.

1.3.1 The discovery of lithium

Lithium water had been used as the treatment for gout, and lithium bromide for epilepsy, for almost a century before its anti-manic properties were described (Shorter, 2009). In the late 19th century a Danish psychiatrist, Frederik Lange, had used lithium for treating 'melancholic depression' with positive outcome. However, most of this Danish literature passed unnoticed, and lithium treatment remained obscure until 1949, when it was rediscovered by John Cade.

John Cade hypothesised that bipolar disorder was a dysfunctional metabolic condition, and in an attempt to isolate this metabolic compound he injected guinea pigs with urine extracts taken from schizophrenic patients (Cade, 1949).

It was widely established that uric acid was psychoactive, so Cade needed soluble urate for a control. He used lithium urate and observed that guinea pigs

became less responsive and lethargic, despite being fully conscious. He repeated his finding with lithium carbonate and found the same to be true, so attributed this effect to lithium.

1.3.2 Early clinical trials with lithium

John Cade was a psychiatrist and realised that this calming effect of lithium might be useful in the treatment of bipolar disorder and trialled lithium citrate in 10 patients. All but one (who was probably schizophrenic) seemed to benefit from therapy, and withdrawal of lithium caused relapse into mania (Cade, 1949). Cade also tried lithium in a handful of schizophrenic and chronically depressed patients. In the former, he found that although lithium seemed to attenuate agitation it did not have any fundamental benefit. In the chronically depressed patients, he observed no change in symptoms (Cade, 1949).

At the time, Cade's research went largely unnoticed, as the Australian journal in which he had published was unknown. A clinical trial in Melbourne in 1951 had shown that lithium was beneficial and that the risk/benefit ratio was favourable (Noack and Trautner, 1951). But all of this was confined to the shores of Australia until 1952, when Mogens Schou began conducting randomised lithium trials in bipolar patients in Aarhus, Denmark. He found that lithium was incredibly useful in mania and could be used to replace electroconvulsive therapy (Schou *et al.*, 1954). His findings sparked off many more lithium-associated trials in Europe throughout the 1950s and 1960s, for both the treatment and prophylaxis of bipolar disorder. Lithium was also found to decrease suicides (Cipriani *et al.*, 2005; Coppen *et al.*, 1991). America, however, was slow to respond. Lithium had a maligned history due to cardiac-related problems. Lithium chloride was, chemically, a simple salt, like sodium chloride, and not many were convinced that such a simple salt could produce such a

dramatic effect in bipolar patients. The publisher Robert Giroux records the words of Robert Lowell, a poet who suffered from manic depression,

"*Of all our conversations, I remember most vividly Robert Lowell's words about the new drug, lithium carbonate, which had such good results and gave him reason to believe he was cured*": "*It's terrible Bob, to think that all I've suffered, and all the suffering I've caused, might have arisen from the lack of a little salt in my brain.*" (Goodwin *et al.*, 2007).

The FDA finally approved lithium for the treatment of bipolar disorder in 1970 — after two decades and a lot of pressure — and for prophylaxis of bipolar disorder in 1975 (Shorter, 2009).

Remarkably, although lithium is the mainstay of bipolar therapy, it has not been found to be of much use in schizophrenia and unipolar depression. It is intriguing that something as simple and universal as lithium can have such a significant effect on one type of mental illness but not others.

Lithium has been routine therapy for six decades, and yet we still do not know how it works, neither do we know much about the pathophysiology of bipolar disorder itself. Lithium has the ability to permeate extensively in the body. Because of this, it has many different targets, and it remains unclear as to which are central to the therapeutic action of bipolar disorder and which are non-specific side effects, even though probably no other drug has been studied on so many different systems.

1.3.3 Lithiums effects on mice models of bipolar disorder

Rodent models of psychiatric disorders are still as challenging as they were a few decades ago. We are limited by our understanding of the neurobiology of most psychiatric disorders. Genetic technology has ensured a wide assortment of mutant mice, but their phenotyping, and relation to disease pathology leaves much to be

desired (Wotjak, 2004). Animal models are usually judged based on 3 criterions (Kato *et al.*, 2007);

1. Face validity- the association between human symptoms of disease and features of the model.
2. Construct validity- the association between mechanism of model and the disease pathology.
3. Predictive validity- the efficacy of drugs used therapeutically in the model.

Lithium has been widely studied in a variety of different animal models and some of its effects are discussed below.

1.3.3.1 Exophenotypic models of bipolar disorder

Exophenotypic models are generally used to mimic symptomatic aspects of a disease. In bipolar disorder, these models aim to replicate one aspect of the disease trait, for example, either mania or depression. These models usually have high face validity and, in case of bipolar disorder, high predictive validity. They do not usually have construct validity since they are not suggestive of mechanism, only of output.

Exploratory behaviour:

These tests generally measure activity in a novel environment. Rodents are, by nature, inquisitive animals and will explore a new environment. Lithium in a variety of studies alters this behaviour. Exploratory activity is assessed by tests such as the open field test, in which ambulation and rearing, among other parameters, can be measured. The hole-poking test is also widely used in which the number of times the animal pokes its head through a hole created in a surface is measured. Other variations of the test include the activity wheel, head dips and Y-maze, all of which employ different methods to measure exploration. Lithium decreases exploratory

activity in almost all cases after taking strain differences into account (O'Donnell and Gould, 2007). This effect is reproducible and consistent and hence this model offers good predictive validity.

Although this test had previously not been directly translated to symptoms of bipolar patients, recently, it has been shown that there was increased ambulation and exploration of novel objects in bipolar patients compared to normal volunteers (Perry *et al.*, 2009). Hence, this suggests that exploratory behaviour may have face validity as predictive validity.

Stimulant induced hyperactivity

These experiments are used to model the mania phase of bipolar disorder. The most common stimulant used is d-amphetamine, although combinations of d-amphetamine and chlordiazepoxide, apomorphine, phencyclidine have also been used (O'Donnell and Gould, 2007; Van Kammen and Murphy, 1975). The experiment involves inducing hyperactivity and then measuring the attenuation of this by drugs. Lithium consistently attenuates amphetamine-induced hyperactivity in rodents, although different strains have differential responses to d-amphetamine and lithium. This test does have clinical translatability because the therapeutic effects of lithium on mania are proven. Anti-psychotics also reduce psychostimulant-induced hyperactivity (Arnt, 1995) and may be used for the treatment of manic episodes in bipolar disorder. These tests have good face and predictive validity, and some amount of construct validity.

Depression-like behaviour

Although no model yet exists that can show the cyclical nature of bipolar disorder, mania and depression can be separately modelled and many models of depression do exist (Cryan *et al.*, 2002). The forced swim test (FST) is a behavioural despair model and one of the most commonly for depression. In this test, the rodent is placed in a cylinder containing water without being able to touch the bottom of the cylinder for a few minutes. There is an initial rush of activity followed by a period of test, which measures whether the animals swims or makes just enough movement to keep its head above the water. The more it swims, the lower the immobility time. The tail suspension test is similar to the FST. Here, the rodent is suspended by its tail, and its immobility is measured. Antidepressants have a robust effect on reducing immobility time compared to control animals. Lithium also reduces immobility time, although not as much as some of the antidepressants.

In the clinic, lithium does have an antidepressant effect, although it is used only in adjunct with other classes of antidepressants such as selective serotonin reuptake inhibitors (SSRIs) for the treatment of refractory depression (Bauer and Dopfmer, 1999). Antidepressants have been used less commonly in the treatment of bipolar disorder since studies show that they may precipitate a manic episode (Peet, 1994). This test therefore has good face validity and some amount of construct and predictive validity.

Table 1.3.1 outlines some of the most commonly used rodent behavioural models used to mimic bipolar disorder and how lithium affects them.

Table 1.3.1. Summary of rodent bipolar disorder behavioural tests and the effect of lithium.

Test	Effect	No. of studies	Consistency of effect	Effect of other mood-stabilisers, antidepressants and antipsychotics
Exploratory behaviour	↓	**	**	*
Rearing	↓	***	***	*
Amphetamine-induced hyperactivity	↓	***	***	**
Ouabain-induced changes	↓	*	*	*
Aggression	↓	**	***	*
Learned helplessness	↔	*	*	***
Learning and memory	↓	**	*	*
Forced swim test immobility	↓	**	***	***
Tail suspension test immobility	↓	*	*	***
Circadian Rhythm length	↑	**	***	*
Pilocarpine seizures	↑	***	***	*

The relative number and consistency of reports for each behavior is denoted with * for relatively low, ** intermediate, and *** relatively high consistency/number. For each model, we also indicate the consistency of the effect of other drugs used to treat both the depressive and the manic phases of bipolar disorder, namely antidepressants, mood stabilizers, and antipsychotics. We illustrate the most consistent action of lithium as attenuating (↓), potentiating (↑), or not affecting (↔) the particular behavior. Table adapted from (O'Donnell and Gould, 2007).

1.3.3.2 Endophenotypic models

The term 'endophenotype' was described as an internal, intermediate phenotype (i.e., not obvious to the naked eye) that fills the gap in the causal chain between genes and distal diseases (Gottesman and Gould, 2003; Gottesman and Shields, 1973). Put simply, it means models incorporating both a genetic and a behavioural component. 'Endophenotypes' are different from 'exophenotypes' because the former may or may not have any face validity but has a definite genetic

factor (O'Donnell and Gould, 2007) and is measurable in patients and rodent models (Cryan and Slattery, 2007). This is a more biomarker–related approach which aims to use one characteristic component of the disease or marker of the disease and model that, instead if the whole syndrome. Endophenotyes need to meet certain criteria: it must be associated with an illness, must be heritable, may be state independent (present even if illness is dormant), (Hasler *et al.*, 2006). These are newer models and further work is needed to establish the consistency of lithium's effects in these models (Lenox *et al.*, 2002).

1.3.4 Shortcomings of lithium therapy

There are two main weaknesses to lithium therapy: it can be very toxic on chronic use, and not all bipolar patients respond to therapy.

Lithium, despite being indispensable in the treatment of bipolar disorder, is a 'dirty drug' since it exhibits polypharmacology. The pathophysiology of BD and how lithium acts are still not fully understood. Since no single lithium target has been conclusively identified, the development of newer, more effective drugs is yet more challenging. Additionally, lithium has a number of toxic side effects that reduce compliance. Chronic lithium therapy can cause renal failure, hypothyroidism, polydipsia, diabetes insipidus and is teratogenic. Lithium also has a very narrow therapeutic index (the difference between therapeutic and toxic dose). Finally, small differences in physiology can cause relatively large changes in lithium plasma concentration, thereby precipitating toxicity. Thus, there is a need for a new mood-stabiliser that can duplicate the therapeutic actions of lithium but without its toxic side effects.

1.4 Mechanisms of lithium's actions

Genetic and imaging studies have, so far, not yielded any crucial insights into the pathology, disease progression or treatment of bipolar disorder. Most of what is known has come from lithium-related studies. Although these are useful, it is often challenging to elucidate the details of the mechanisms of action. It means that we have a lot of information, but no clear leads. Imagine trying to unravel an entangled ball of wool. You can see the threads, but you cannot find the starting point, the succession or the end point.

Lithium, a small cation, is the most non-specific drug available. It interacts with a number of channels, transporters, signalling cascades and neurotransmitters. It is thus very difficult to distinguish which interaction is responsible for its therapeutic effects and which are associated with side effects. Additionally, it is not ethical to withhold drug treatment from patients. As soon as patients are diagnosed, they must be treated pharmacologically, with consent. This means that it is very difficult to obtain extensive pre-treatment data and compare these with what happens during treatment. However, continued interest in lithium has inspired a tremendous amount of research, and has generated a number of hypotheses to explain lithium's mode of action.

1.4.1 Lithium's effects on sodium channels

Lithium, by virtue of its chemical and physical properties, is very similar to sodium (Table 1.4.1). Lithium permeability in the body is similar to that of sodium, and hence lithium affects a number of sodium exchangers and transporters. It is also known that lithium is transported actively into cells (Zerahn, 1955) and has the ability

to accumulate in cells since its entry into cells is easier than its removal. Plasma and red blood cells have traditionally been used to determine and calculate various parameters. For example, the ratio of red blood cell lithium to plasma lithium shows a wide degree of variability in patients treated with lithium, and may be useful to predict responsiveness to lithium therapy (Goodwin *et al.*, 2007). In spite of lithium's demonstrated effects on transporters, an association between this and its therapeutic action in bipolar disorder remains to be proven.

Table 1.4.1. Comparison of lithium and sodium

	Sodium	Lithium
Electrons in outer shell	1	1
Oxidation state	Strongly basic	Strongly basic
Electronegativity (Pauline scale)	0.93	0.98
Atomic radius	186	152
Van der Waal's radius (picometres)	227	182

Studies have shown that bipolar patients treated with lithium seemed to have higher Na^+/K^+ ATPase activity, and plasma lithium concentrations correlate positively with this (Naylor *et al.*, 1974). However, studies with bipolar disorder patients have shown mixed results in relation to Na^+/K^+ ATPase activity. Studies have shown decreased (Naylor *et al.*, 1973), increased (Sengupta *et al.*, 1980) and no difference (Hesketh *et al.*, 1977) in activity between controls and bipolar disorder patients. More recently, mania-like effects were seen in mice expressing a dysfunctional neuronal Na^+/K^+-ATPase pump (Kirshenbaum *et al.*, 2011), adding some support to the theory that lithium produces its therapeutic effects by correcting sodium imbalances in bipolar patients.

After lithium, anticonvulsants are the most commonly used drugs in the treatment of bipolar disorder. Although the primary site of action of valproate (the most commonly used drug after lithium) is an increase in GABA neurotransmission

by inhibiting GABA transaminase, valproate also inhibits voltage-gated sodium channels. Carbamazepine, another anticonvulsant, stabilises the inactive state of sodium channels making them more refractory. Lamotrigine and phenytoin, both sodium channel blockers, have been found to be useful in the prophylactic treatment of bipolar disorder (Calabrese *et al.*, 2003; Coxhead *et al.*, 1992; Kusumakar and Yatham, 1997; Mishory *et al.*, 2000).

Lithium's effects on these sodium channels may or may not contribute to its therapeutic effects, but its side effects show a distinct resemblance to interference with sodium exchange, although other mechanisms may be additionally involved. Lithium's narrow therapeutic index may possibly be due to the body's inability to distinguish between sodium and lithium and thus maintain membrane cationic gradients. As it interferes with the regulation of sodium and hence water levels in the body, lithium can cause dehydration, which can further elevate lithium concentrations. Lithium interferes with excretory pumps and transporters, which are regulated by sodium, and chronic lithium leads to kidney failure. It also causes hypothyroidism by interfering with the formation of sodium iodide, which is taken up by the thyroid gland to form thyroid hormones (Livingstone and Rampes, 2006).

1.4.2 Lithium's effects on neurotransmitters

Almost all drugs that are used to treat mental disorders seem to target, directly or indirectly, a neurotransmitter system(s). In Alzheimer's disease, the cholinergic system is primarily targeted (Babic, 1999), although more recently, memantine, a glutamatergic-NMDA antagonist, has also been used (Reisberg *et al.*, 2003). In Parkinson's disease and schizophrenia, it is the dopaminergic system that is modulated by drugs (Seeman and Van Tol, 1994). Antidepressants target the

serotonergic system (effects on the dopaminergic system are also seen) (Willner, 1985), and β-adrenergic blockers are used for their anti-anxiety effects (Hayes and Schulz, 1987). Lithium has the ability to modulate all of these systems, but, again, the target of its therapeutic effects in bipolar disorder remains unknown.

Neurotransmitters can be divided into four primary categories: acetylcholine, monoamine transmitters, amino acid transmitters and neuropeptide transmitters.

1.4.2.1 Acetylcholine (ACh)

Muscarinic involvement in bipolar disorder has been proposed since chronic lithium treatment seems to increase ACh synthesis, choline transport and ACh release in the brain (Jope, 1979; Simon and Kuhar, 1976). Studies of muscarinic receptor binding and receptor-coupled phosphatidyl inositol (PI) hydrolysis in rat hippocampus showed that atropine caused up-regulation of the muscarinic receptors (M1, M3 and M5) and increased the sensitivity of PI hydrolysis in response to agonists (Ellis and Lenox, 1990). In the presence of lithium, there was no change in the receptor up-regulation, although there was a decrease in the super-sensitivity of PI-hydrolysis. This suggests that lithium was influencing the muscarinic pathway downstream of the receptor level.

Therapeutically, cholinesterase inhibitors, such as physostigmine, produce depression in euthymic bipolar patients on lithium (Oppenheim *et al.*, 1979) and in normal volunteers (Janowsky and Risch, 1984; Risch *et al.*, 1981). RS-86 is a cholinergic agonist that has anti-manic and sleep-inducing properties (Riemann *et al.*, 1994). Muscarinic agonists likes xanomeline, which are been used in Alzheimer's patients, seem to reduce mood swings and psychotic symptoms in these patients (Bodick *et al.*, 1997).

1.4.2.2 Monoamine neurotransmitters

Monogenic amine (or monoamine) transmitters, such as those for noradrenaline, serotonin and dopamine, can be excitatory or inhibitory depending on the post-synaptic receptors they act on. They are believed to play roles in the limbic system, in the prefrontal cortex and in the striatum, and they affect behaviour, mood, emotionality and decision-making, amongst other things. These neurotransmitters are synthesised in the nerve termini and are either recycled or broken down.

1.4.2.2.1 Noradrenaline

In the 1960s and 70s, a number of theories about noradrenaline's role in bipolar disorder were formulated (Bunney and Davis, 1965; Janowsky *et al.*, 1972; Schildkraut, 1965). This led to multiple studies measuring the amount of noradrenaline and its metabolites in the plasma, urine and cerebrospinal fluid (CSF) of untreated and lithium-treated bipolar patients; most of these provided conflicting evidence. Lithium seems to influence aspects of noradrenaline signalling, such as turnover, but not overall amounts of noradrenaline itself. Schildkraut *et al.*, showed an increase in rat brain noradrenaline turnover after chronic and acute lithium treatment (Schildkraut *et al.*, 1969; Schildkraut *et al.*, 1966) although others have not found any significant differences (Ahluwalia and Singhal, 1980; Ho *et al.*, 1970). Lithium treatment both increased and decreased levels of the noradrenaline metabolite, 3-methoxy-4-hydroxy phenylglycol (MHPG) in CSF, plasma and urine of bipolar patients — depending on whether they were in bipolar mania or depression (Bond, 1972; Greenspan *et al.*, 1970; Maas *et al.*, 1968; Schanberg *et al.*, 1968a; Schanberg *et al.*, 1968b; Schildkraut *et al.*, 1965). Another study (Young *et al.*, 1994) showed, post-mortem, that in cortical brain regions of bipolar patients, the total noradrenaline turnover was higher than in control brains. Interestingly, lithium has the consistent

ability to increase the expression of activator protein-1 (AP-1) pathway *in vitro* (Yuan *et al.*, 1998).

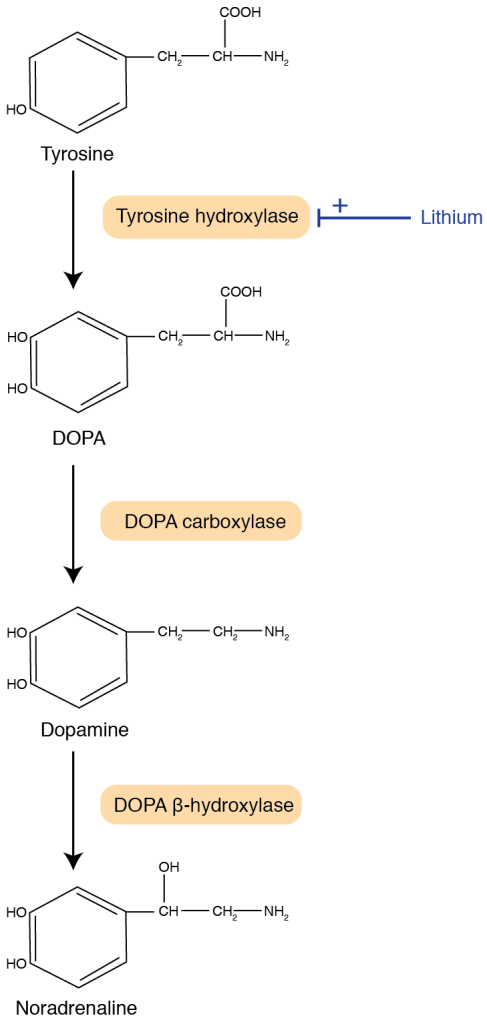


Figure 1.4.1. Noradrenaline and dopamine synthesis. Tyrosine is the precursor of dopamine and noradrenaline. Tyrosine hydroxylase is the enzyme that converts tyrosine into DOPA and is the rate-limiting step in the synthesis. Lithium enhances the activity of tyrosine hydroxylase indirectly (through altered gene expression).

This increase in expression, in turn increases the expression of genes included in the AP-1 complex. One of the proteins of this complex is tyrosine hydroxylase, which is an enzyme involved in the synthesis pathway of noradrenaline and dopamine (Figure 1.4.1). This suggests of an increase in brain noradrenaline turnover in the presence of lithium, i.e., increased synthesis and metabolism.

Additionally, Grossman and co-workers measured the levels of noradrenaline and it metabolites in the urine of drug-free bipolar depressed patients, and showed that the total turnover was decreased (Grossman and Potter, 1999). This suggested decreased tyrosine hydroxylase activity in these patients. Lithium has the ability to

reverse this by increasing tyrosine hydroxylase activity; lithium has been shown to increase tyrosine hydroxylase levels, both *in vitro* and *in vivo*, in rat brain and in neuroblastoma SH-SY$_5$Y cells (Chen *et al.*, 2000; Chen *et al.*, 1998).

No change in noradrenaline receptor binding in rat brain was observed (Schultz *et al.*, 1981). However, lithium attenuates α_2-mediated behavioural effects (Goodwin *et al.*, 1986; Smith, 1988).

The results from investigations in bipolar mania and bipolar depression states have proved slightly more consistent than those from preclinical lithium studies on the noradrenergic system, although these studies do not seem to show any delineation between bipolar depression and unipolar depression states (Potter and Linnoila, 1989). In bipolar mania, elevated levels of MHPG were found in the CSF and plasma (Ballenger and Post, 1984), whilst lower levels were found in the plasma during bipolar depression (Goodwin *et al.*, 1970; Siever, 1987).

Studies on bipolar depressed patients have shown elevated noradrenaline responses to stress, when compared to unipolar depressed patients (Potter and Manji, 1994; Roy *et al.*, 1985; Rubin *et al.*, 1985; Rudorfer *et al.*, 1985).

Further confirmation of the involvement of the noradrenergic system in bipolar disorder comes from drugs that target it with more specificity than lithium. Idaxozan, an α_2 antagonist, has been shown to have efficacy in small-scale trials for bipolar depression; this possibly arises because of increased synaptic noradrenalin levels due to inhibition of the α_2-autoreceptors (Grossman *et al.*, 1999). Clonidine, an α_2 agonist, also seemed to be beneficial in mania in small scale clinical trials (Bakchine *et al.*, 1989; Diacicov and Tudorache, 1990; Tudorache and Diacicov, 1991)

In 1972, Janowsky proposed the hypothesis that it was the balance of cholinergic to noradrenergic transmission that was disrupted in bipolar patients. Elevated cholinergic system activity has an overall effect resulting in depression and that for the noradrenergic system resulted in mania. He hypothesised that an increase in cholinergic transmission relative to noradrenergic transmission results in depression, whereas the reverse occurs in mania (Janowsky *et al.*, 1972). But with mounting conflicting evidence, this hypothesis has not received attention recently.

1.4.2.2.2 Dopamine

Lithium dose-dependently decreases dopamine levels in the brain (Poitou and Bohuon, 1975; Segal *et al.*, 1975) and also changes dopamine-linked behavioural effects (Bunney and Garland-Bunney, 1987). Additionally, overall dopamine turnover was found to be reduced in patients treated with lithium (Linnoila *et al.*, 1983). Dopamine binding studies using lithium have not shown the presence of any lithium bound to the receptors, and it is believed that lithium decreases dopamine transmission by influencing a post-receptor target, for example, by effecting receptor–effector coupling.

Most of the evidence for involvement of dopamine in bipolar disorder is indirect, coming from pharmacological studies. However, the argument that the dopaminergic system is involved is sound, since dopamine plays a role in a number of features that are characteristic of mania. For example, dopamine has been associated with impulsiveness and substance abuse, both of which are traits found in bipolar patients. L-dopa and amphetamine, both of which increase dopamine in the synaptic cleft, have the ability to elicit mania in bipolar patients (Goodwin *et al.*, 1970; Murphy *et al.*, 1971; van Praag and Korf, 1975). Joyce presented cases of episodic Parkinsonism before the onset of bipolar depression, which was reversed during

bipolar mania (Joyce *et al.*, 1995). Dopamine agonists, bromocriptine and piribedil, appear to have antidepressant activity in bipolar depression, although they can induce mania in these patients on prolonged use (Gerner *et al.*, 1976; Silverstone, 1984).

1.4.2.2.3 Serotonin (5-HT)

Lithium, rather than increasing or decreasing the levels 5-HT, seems to have an overall effect of stabilisation of 5-HT function(Knapp and Mandell, 1973; Linnoila *et al.*, 1984). It affects multiple aspects of the neurotransmitter synthesis, storage and release, and therefore modulates the serotonergic system (Bunney and Garland-Bunney, 1987; Price *et al.*, 1990). It seems that any effect that lithium has on the serotonergic system requires chronic treatment since a transient reduction in serotonergic function does not seem to affect bipolar patients on lithium (Price *et al.*, 1990).

Serotonin has not been as well characterised in bipolar disorder as it has in unipolar depression. Some studies have shown that 5-HIAA (a metabolite of 5-HT) levels are low in both bipolar depression and in mania, which led to the 'permissive' hypothesis of van Praag: that there is a general deficit in 5-HT in the CNS of bipolar patients. This leads to changes in other neurotransmitter systems, which, in turn, causes the two states of abnormal polarity that characterise bipolar disorder (van Praag and Korf, 1975). The synthesis of serotonin involves the enzyme tryptophan hydroxylase. Bellivier *et al*., 1998, found a polymorphism in the gene that codes for tryptophan hydroxylase that correlated positively with bipolar patients (Bellivier *et al.*, 1998).

Tryptophan depletion, however, did not cause relapse in lithium-treated bipolar patients (Hughes *et al.*, 2000). Sobczak *et al.*, conducted a study in which first-degree relatives of bipolar disorder I patients were given tryptophan-free diets

acutely, and their cognitive functions were tested. The results showed that in these relatives, information processing in a planning task was impaired. This has provided a possible endophenotype for bipolar depression (Sobczak *et al.*, 2002).

Additional support for the argument that serotonin may play a role in bipolar disorder comes from the fact that both atypical antipsychotics and antidepressants have found roles in the treatment of bipolar disorder, although none are as effective as lithium and they cannot be used as monotherapy. Indeed, some antidepressants when used in bipolar depression can precipitate mania or hypomania in bipolar patients making serotonin less than an ideal target.

1.4.2.3 Other neurotransmitters and neuropeptides

GABA and glutamate have also, more recently, been implicated in the pathophysiology and therapeutic actions of lithium; the involvement of GABA is illustrated by the successful use of GABAergic anticonvulsants in bipolar disorder. Evidence of glutamatergic involvement comes from studies that show that chronic lithium has also been shown to protect against glutamate-mediated excitotoxicity (Nonaka *et al.*, 1998). However, most of the evidence relating to the involvement of glutamate is still relatively indirect, and more studies are needed to establish consistency of effect.

It is known that the onset of the first episode in predisposed individuals is triggered by stress; both glucocorticoids and corticotrophin releasing hormone play crucial roles in physiological stress responses and in sleep patterns. There is some evidence for the involvement of the glucocorticoid receptor in bipolar disorder. Firstly, chronic lithium reduces glucocorticoid-receptor-mediated activity by attenuating the translocation of the receptor from the cytosol to nucleus (Zhou *et al.*, 2005).

1.4.3 Lithium's effects on second messengers

It has been established that lithium affects almost all the neurotransmitter systems in the brain, either directly or indirectly. It has also been established that none of these effects are elicited through direct receptor interaction, except possibly in case of the 5-HT_1 and 5-HT_2 receptors, where there may be some lithium-related binding (Plenge and Mellerup, 1982; Treiser *et al.*, 1981), but are more likely to be through an interference with the receptor–effector coupling mechanism. It is likely that lithium influences all of these neurotransmitters through an effect it has downstream of the receptor. It is likely that lithium imposes its therapeutic benefit by modulating the second messenger system. This would explain why it has the ability to increase both excitatory and inhibitory transmission and has the ability to modulate multiple pathways.

To date, no drug has been as beneficial as lithium in the treatment of bipolar disorder (Goodwin and Geddes, 2003). This might be because the drugs used target one transmitter system, (maybe two) and that this does not result in complete efficacy. It is quite possible that lithium acts by manipulation of one or more second messenger system that are common to a multiple receptors.

Lithium has effects on many different second messenger systems (Mork *et al.*, 1992). This is not surprising, since all these systems form an inter-connected network. A change in one signalling cascade will almost certainly influence another. The two most prominent second messenger targets of lithium are the phosphoinositide (PI)-linked signalling cascade (Berridge *et al.*, 1989) and the glycogen synthase kinase-3 (GSK-3) systems (Klein and Melton, 1996). Both are located at the strategically influential junction between the activator and effector systems of cell major cellular signalling cascades and both are inhibited by therapeutic concentrations of lithium.

1.4.3.1 Inositol monophosphatase (IMPase)

Lithium has been shown to reduce the accumulation of inositol in the lens of the eye (Varma *et al.*, 1970) and in the kidney (Hauser, 1969). The first studies showing that inositol levels were decreased in the rat brain came from Allison and Stewart (Allison and Stewart, 1971) who postulated that this reduction might to due to lithium interfering with active transport, synthesis or incorporation into phosphoinositides. A later study showed that although there was a decrease in myo-inositol levels in the cerebral cortex of rats treated with lithium, there was an increase in the levels of Ins1P (Allison *et al.*, 1976). They suggested that one of the ways that this might occur is inhibition of the enzyme that converts Ins1P into inositol.

Lithium at therapeutic concentrations inhibits inositol monophosphatase (IMPase). IMPase is involved in the phosphatidylinositol (PI) signalling pathway and catalyses the conversion of inositol monophosphate to inositol (Figure 1.4.2).

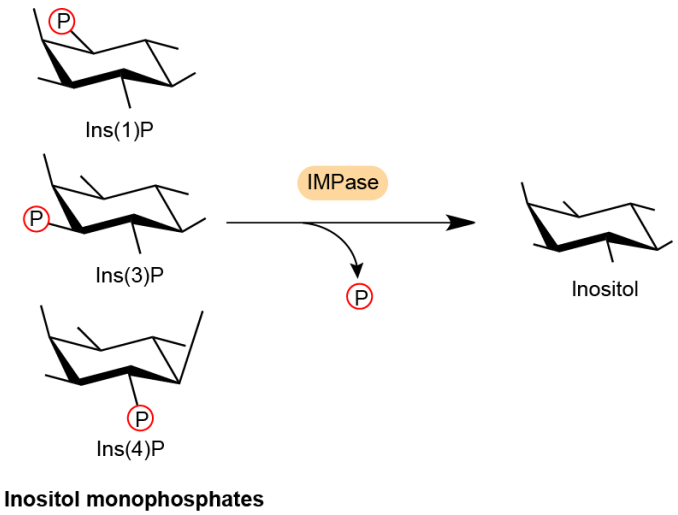


Figure 1.4.2. IMPase function. IMPase catalyses the conversion of inositol monosphosphates to inositol. Inositol monophosphates are named according to the position of the phosphate group.

Lithium inhibits IMPase uncompetitively with an IC_{50} of about 0.8 mM (Hallcher and Sherman, 1980). It was hypothesised that lithium's therapeutic actions result from inhibition of IMPase and consequently cause depletion of inositol and its precursor, phosphatidylinositol 4,5-bisphosphate (PIP_2). Inhibition of IMPase by lithium forms the basis of the inositol depletion hypothesis (Section 1.5).

1.4.3.2 Lithum's effects on phosphoinositides and inositol phosphates

Lithium plays a significant role in modulating the PI-linked cell-signalling cascade (Drummond *et al.*, 1987) and has been shown to increase Ins1P levels and decrease inositol trisphosphate (IP_3) and inositol tetrakisphosphate (IP_4) levels in a number of studies (Atack *et al.*, 1992; Atack *et al.*, 1994; Jenkinson *et al.*, 1994). It achieves this by inhibition of two enzymes directly involved in the PI-signalling pathway, IMPase and inositol polyphosphate 1-phosphatase (IPPase), and a number of other indirectly related enzymes.

IPPase hydrolyses inositol 1,3,4-trisphosphate and inositol 1,4-bisphosphate to inositol 3,4-bisphosphate and inositol 4-phosphate, respectively (Inhorn and Majerus, 1987), whereas IMPase converts Ins1P to free inositol which is then combined with PI to form the IP_3 precursor, PIP_2. In theory, lithium inhibition of IPPase and IMPase would reduce the availability of free inositol and therefore decreases IP_3 and subsequently PIP_2, thus having an overall effect of slowing down the PI pathway.

In cells and cerebral cortex slices pre-treated with lithium, stimulation of the G_q-coupled receptors (e.g. with pilocarpine) or the M_1 receptor (carbachol), or the 5-HT_{2A} and 5-HT_{2C} receptors (serotonin), produced distinct increases in the level of Ins1P (Batty and Nahorski, 1985; Brown *et al.*, 1984; Jenkinson *et al.*, 1994).

Besides increasing Ins1P levels (which does not have a recognised physiological consequence), lithium also decreased IP_3 and IP_4 levels *in vitro* (Atack

et al., 1993b), unrelated to receptor desensitisation. Decreased levels of membrane phospholipids like PIP and PIP_2 have also been observed, which can be rescued by the addition of myo-inositol (Jenkinson *et al.*, 1994). Although the levels of PIP_2 is extensively present in cells and would be difficult to deplete, it is postulated that only a small pool, 10–20%, is available for PI-signalling and hence is sensitive to seemingly small changes in level (Fain and Berridge, 1979; Monaco and Woods, 1983).

1.4.3.3 Glycogen synthase kinase-3

Glycogen synthase kinase 3 (GSK-3) is a serine/threonine protein kinase that modulates substrates by phosphorylation. It has two isoforms GSK-3α and β which have essentially the same function. GSK-3 phosphorylation of glycogen synthase renders it inactive.

Lithium was shown to inhibit GSK-3 uncompetitively at therapeutic concentrations with an IC_{50} of about 2 mM (Klein and Melton, 1996). This suggests that there is partial inhibition of GSK-3 *in vivo* (therapeutic concentration ~0.8 mM). However some evidence indicates that lithium also inhibits the phosphatase that activates GSK-3, thereby reinforcing the inhibition of GSK-3 activity (Zhang *et al.*, 2003) (Figure 1.4.3).

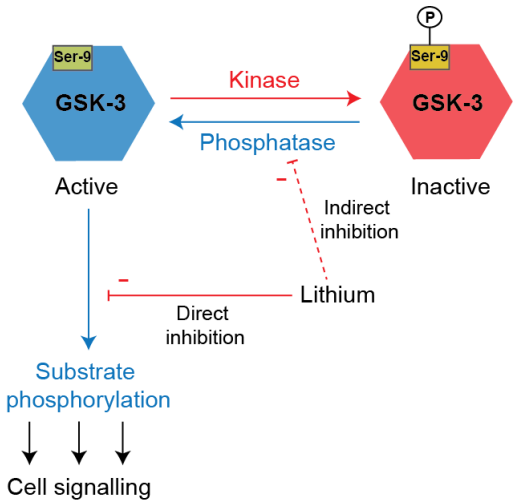


Figure 1.4.3. GSK-3 inhibition by lithium. GSK-3 is phosphorylated on the serine-9 residue by the action of kinases; this renders it inactive. The action of a phosphatase hydrolyses the phosphate on the serine-9 residue and thus re-activates GSK-3. Activated GSK-3 is involved in a number of substrate phosphorylation reactions. Lithium inhibits GSK-3 directly (inhibiting the activated protein) and indirectly (inhibiting the phosphatase which activates it).

GSK-3 has a role in neuroplasticity and cellular resilience and it is believed that lithium's neuroprotective effects may be partially mediated by GSK-3 inhibition, since neuronal loss and atrophy play a role in bipolar disorder. Inhibition of GSK-3 has an anti-apoptotic effect (Gould and Manji, 2005).

Circadian rhythm disruptions are seen in bipolar patients, and lithium has the ability to correct this. GSK-3 plays a crucial role in circadian regulation and it is believed that lithium might effect its ability to correct circadian rhythm patterns through GSK-3 inhibition (Gould and Manji, 2002; Gould *et al.*, 2004b). Moreover GSK-3 is at the crucial juncture of neurotransmitters, like noradrenaline, dopamine and 5-HT, and gene transcription. GSK-3 inhibition may be involved in the teratogenic effects seen with lithium treatment (Klein and Melton, 1996).

The most convincing evidence comes from the use of GSK-3 inhibitors in mouse models of preclinical mania and depression and from GSK-3 heterozygous knockout mice. The GSK-3 inhibitor AR-A014418 caused a decrease in immobility

time, and decreased amphetamine-induced hyperactivity. The GSK-3 knockout mouse showed reduced exploratory activity and increased immobility time in one study (O'Brien *et al.*, 2004) but not in another (Agam *et al.*, 2009).

Overall, GSK-3 has only recently been considered as a target for lithium, and hence requires further investigation to understanding lithium's therapeutic effects. In particular, given that it is known that lithium must be dosed chronically to be effective, more studies are needed to understand chronic GSK-3 inhibition.

1.4.3.4 Protein kinase C

Protein kinase C (PKC) is a serine/threonine kinase that phosphorylates substrates in order to activate or inactivate them and thus modulates cell-signalling pathways. PKC, itself, is activated by diacylglycerol (DAG) and Ca^{2+} (Figure 1.4.4). Chronic lithium treatment decreases the activity of certain isoforms of PKC, such as PKCα (Bitran *et al.*, 1995; Chen *et al.*, 2000). PKC, like the other second messengers discussed above, has the ability to modulate noradrenaline, dopamine and 5-HT pathways in the CNS (Apparsundaram *et al.*, 1998; Blakely *et al.*, 1998; Zhang *et al.*, 1998).

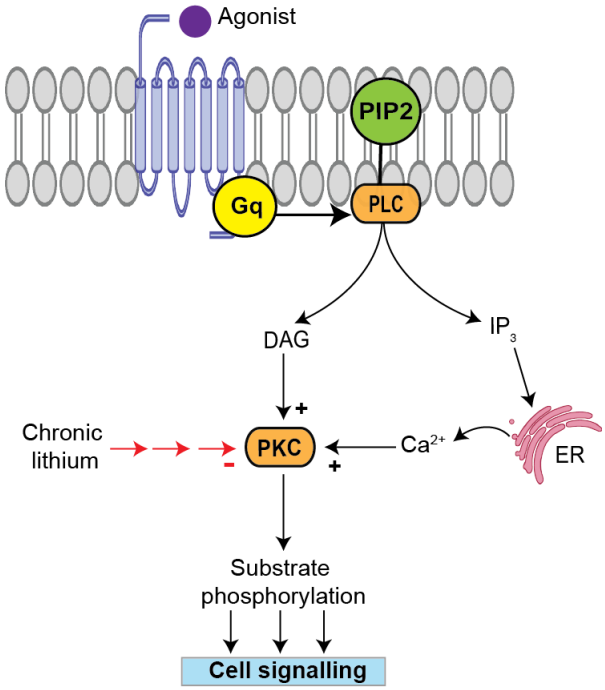


Figure 1.4.4. PKC is inhibited by chronic lithium. Stimulation of a G_q-coupled receptor by an agonist causes activation of phospholipase C (PLC) which catalyses the breakdown of PIP_2 to IP_3 and DAG. IP_3 causes calcium release from the endoplasmic reticulum (ER). DAG and calcium cause activation of PKC that in turn phosphorylates various substrates and thus modulates cell signalling. Chronic lithium inhibits activity of PKC and therefore affects cell signalling.

The antimanic effects of tamoxifen have further highlighted a possible role for PKC in bipolar disorder. Tamoxifen is an antiestrogenic drug, which also inhibits PKC at higher concentrations. Small-scale clinical trials of tamoxifen, showed that it has some efficacy in bipolar mania (Bebchuk *et al.*, 2000).

Although IMPase, PKC and GSK-3 have been treated as separate targets in the literature, this is not necessary the case. Signalling cascades are almost always interdependent. For example, IP_3 causes calcium release, which activates PKC, and PKC in turn inactivates GSK-3. Upon lithium treatment, IP_3 levels decrease, and chronic lithium treatment also decreases PKC activity. This in turn will increase GSK-3 activity because of the decreased PKC-dependent inhibition. However, lithium itself inhibits GSK-3 (Figure 1.4.5).

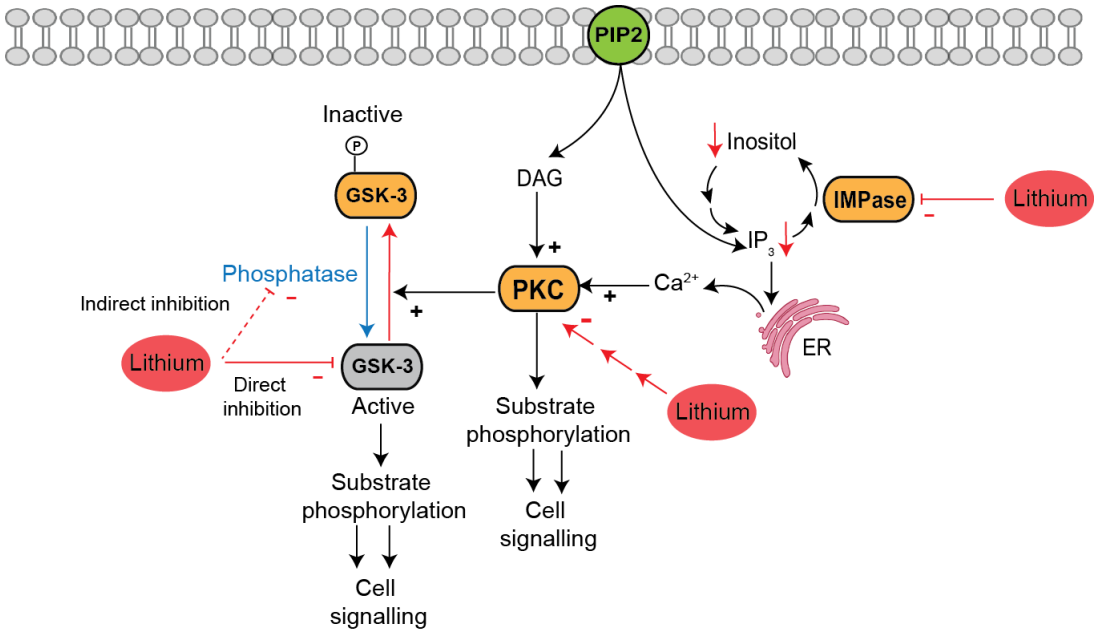


Figure 1.4.5. Interactions between lithium's second messenger targets. Lithium inhibits GSK-3, PKC and IMPase, directly or indirectly. All three are interconnected through different signalling pathways. Therefore an effect on any one of these will affect another.

Thus, the significance of lithium treatment lies not simply with whichever second messenger(s) it inhibits, but also with how this inhibition modulates downstream cell signalling. This is not be an all-or none action, it is a careful tweaking of various signals from a variety of pathways. Hence, it is quite likely that not just one but all affected second messengers are involved in the therapeutic effects of lithium,.

However, based on the evidence so far, IMPase as the target of lithium in bipolar disorder has gained considerable approval. This led to the formulation of the inositol depletion hypothesis.

1.5 Inositol depletion hypothesis

The inositol depletion hypothesis was formulated by Sir Michael Berridge (Berridge *et al.*, 1982, 1989) and suggests that in bipolar patients, the PI signalling pathway is hyperactive (Figure 1.5.1). Lithium, by inhibiting IMPase, impedes this pathway by depleting the cell of inositol, which is required for the regeneration of active signalling molecules such as IP_3. It also leads to an increase in inositol monophosphates and in cytidine monophosphate-phosphatidic acid (CMP-PA) and a decrease in IP_3 and IP_4. IMPase is also a member of another inositol recycling pathway. Glucose 6-phosphate is converted by 1-D-*myo*-inositol-3-phosphate synthase (MIPS) into Ins1P (Majumder *et al.*, 1997), which is then converted to inositol by IMPase (Figure 1.5.1). Therefore, inhibition of IMPase ensures that both pathways (inositol recycling and synthesis) in the brain are inhibited.

Lithium does not significantly alter PI signalling in the periphery, relative to the extent in the CNS, because inositol depletion does not occur here. This is because the brain is reliant mostly on recycled inositol and is sensitive to small variations in inositol metabolism. Most of the brain's inositol is recycled within the cell; only about 2% of the inositol in the CSF in rat was via uptake from peripheral plasma (Barkai, 1981).

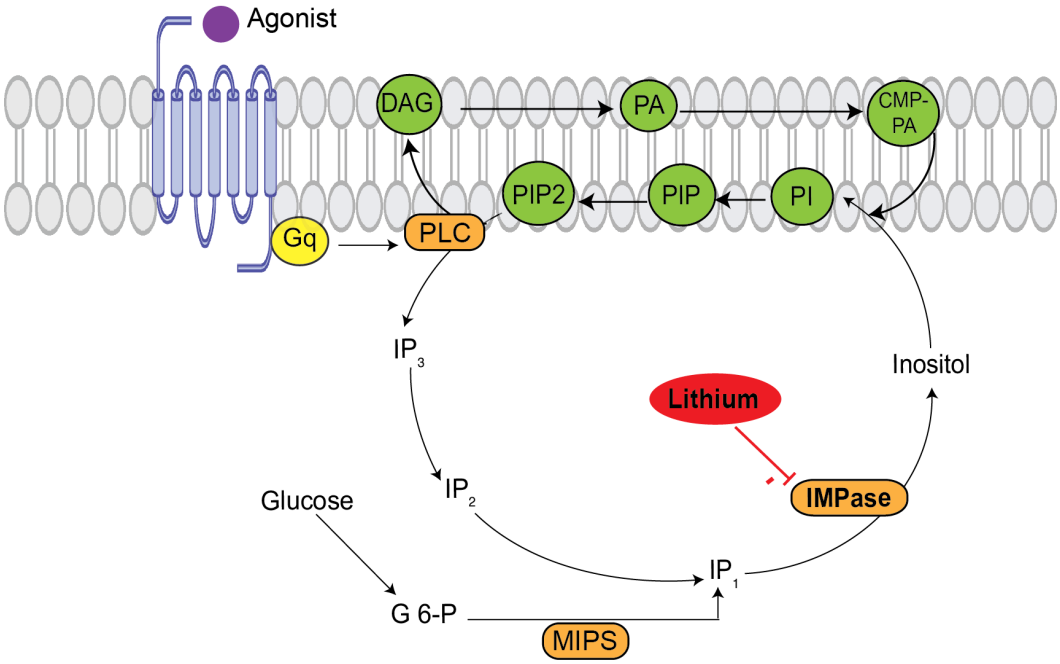


Figure 1.5.1. Lithium's effects on the PI signalling pathway. In a simplified representation of the PI-linked signalling pathway, agonist stimulation of the G_q-coupled receptor leads to the activation of phospholipase C (PLC) that hydrolyses PIP_2 in the plasma membrane to DAG and IP_3, both of which are second messengers. IP_3 is hydrolysed to inositol bisphosphate (IP_2), and then Ins1P and finally inositol. DAG is converted to phosphatidic acid (PA) and then to CMP-PA. CMP-PA combines with inositol to form PI which is then phosphorylated to PIP and finally to PIP_2. *De novo* inositol synthesis occurs from glucose, which is converted to G 6-P and then to Ins1P by MIPS. Lithium inhibits IMPase and causes an increase in Ins1P and a decrease in inositol. This gave rise to the inositol depletion hypothesis.

Thus, the brain is sensitive to inositol depletion whereas in the periphery inositol is easily replenished from the diet. Moreover, lithium inhibits the enzyme uncompetitively (Hallcher and Sherman, 1980), which means that lithium inhibits either the enzyme–substrate or enzyme–product intermediate. The level of inhibition increased with increasing substrate concentration (Nahorski *et al.*, 1991). Since lithium inhibits the enzyme uncompetitively, it is more effective on pathways that are hyper-functional, and not as much on those pathways that are effective at basal levels. An analogy of this would be antibiotics or anticancer drugs that target bacterial or cancer cells, respectively, better than normal cells since the former replicate much faster.

1.5.1 Evidence for the inositol depletion hypothesis

The strongest evidence for the inositol depletion hypothesis comes from lithium's inhibition of IMPase at therapeutic concentrations. This inhibition causes a decrease in inositol and PIP_2, which can be measured. Shimon *et al*., 1997, showed decreased levels of inositol in the prefrontal cortex in post-mortem brains of bipolar patients using gas chromatographic techniques (Shimon *et al.*, 1997). Magnetic resonance spectroscopy has also been extensively used (Silverstone *et al.*, 2005) and has shown that decreased levels of *myo*-inositol were present in the frontal lobe of bipolar patients treated acutely and chronically with lithium compared to controls (Moore *et al.*, 1999). Additionally, increased levels of phosphomonoesters (including Ins1P) have been shown to be increased in the frontal lobe of both bipolar manic and bipolar depressed patients treated with lithium (Kato *et al.*, 1992). According to the inositol depletion theory, a decrease in inositol leads to a reduction in the phosphoinositides, such as PIP_2, a precursor for IP_3. This was demonstrated by showing that reduced PIP_2 levels were found in platelets from bipolar I patients treated with lithium, compared to control volunteers (Soares *et al.*, 2000a; Soares *et al.*, 2000b).

Further evidence for the inositol depletion hypothesis came from the pharmacology of the drugs used to treat bipolar disorder. Lithium inhibits IMPase and causes a reduction in inositol levels. Valproate and carbamazepine, the two alternative drugs for the treatment of bipolar disorder, also reduce inositol levels via the MIPS pathway (Harwood, 2005; Williams *et al.*, 2002).

Some evidence also comes from genetic linkage studies that suggest that a susceptibility locus for bipolar disorder exists on chromosome 18p11. One of the genes that codes for IMPase is at this locus (Shamir *et al.*, 2001; Sjoholt *et al.*, 2004).

In a genome-wide association study, the strong link between bipolar disorder and DAG kinase was seen (Baum *et al.*, 2008). As previously mentioned, DAG is a second messenger in the PI-signalling cascade and is involved in the activation of PKC. Another possible genetic component is polymorphisms in the gene that codes for G- protein receptor kinase-3 (GRK-3) in bipolar patients (Barrett *et al.*, 2003). GRK-3 phosphorylates G-protein coupled receptors (GPCR) upon excessive stimulation and causes desensitisation. The mutant enzyme is not able to cause receptor desensitisation, and hence there is receptor overstimulation and increased neuronal activity and stress. This is consistent with the suggestion of 'hyper-active' PI-signalling that has been postulated in the inositol depletion hypothesis, which is targeted by lithium.

1.5.2 Evidence against the inositol depletion hypothesis

The inositol depletion hypothesis does have weaknesses, the most important being that the decrease in inositol is rapid, but the therapeutic effect of lithium in bipolar patients is only seen weeks after the treatment.

Another weakness is that lithium plasma concentration of about 0.8 mEq/L corresponded to a concentration of about 0.22 mEq/L in CSF and a significantly lower IMPase inhibition (Atack, 1996). Assuming that the brain and CSF lithium levels correspond, this means much lower inhibition in the brain (about 9% compared to 78% in the erythrocytes (Atack, 1996). This might suggest that although brain inositol is being depleted at a very slow rate and is incomplete. In another study it was shown that, PIP_2 and PIP have decreased levels in stimulated cells in presence of lithium, but that there was also a significantly reduced stimulation in the absence of lithium (Jenkinson *et al.*, 1994). Two IMPase genes are encoded in mammalian

genomes. Genetic studies have also linked the isoform of the gene that codes for IMPase that is less predominant in the brain, rather than the more predominant IMPase isoform, to bipolar patients.

1.6 Selection of IMPase as a target

There were three primary reasons for choosing IMPase over other targets of lithium as the focus of screening for inhibitors.

The first was the compelling evidence supporting the inositol depletion hypothesis. It is uncertain whether inhibition of IMPase and depletion of inositol are responsible for the beneficial effects in patients on lithium, or whether inhibition of IMPase leads has some alternative beneficial consequences. Either way it is clear that IMPase is involved in some, if not all, of lithium's therapeutic effects.

Secondly, there are well-established assays (enzymatic, cellular and behavioural) for assessing IMPase inhibition and its effects, as well as extensive literature describing the enzyme, and known inhibitors (lithium and L-690330/690488) provide convenient positive controls. IMPase knockout mice and inositol reversibility of certain lithium phenotypes have been extensively characterised, and testing in these models may be possible.

And finally, inhibitors for the other identified lithium target, GSK-3β, are widely available. No bioavailable IMPase inhibitors, other than lithium, exist.

Hence, IMPase was used as a starting point for screening to identify novel IMPase inhibitors.

1.7 IMPase

IMPase is a soluble, cytosolic enzyme that catalyses the conversion of inositol monophosphate to inositol. It is highly conserved and found in species as diverse as archaebacteria (Chen and Roberts, 1998), plants (Gillaspy *et al.*, 1995) and mammals (Gee *et al.*, 1988; Hallcher and Sherman, 1980; Takimoto *et al.*, 1985). The enzyme assembles as a homodimer and requires the presence of magnesium for catalytic activity, although it is inhibited by high concentrations of magnesium, as well as by calcium and — of therapeutic significance in bipolar disorder — lithium (Hallcher and Sherman, 1980).

Typically, mammalian genomes encode two isoforms of the protein, each 277 amino acids in length with a mass of 30 kDa, with the coding region of each gene distributed across eight exons.

1.7.1 Structure of function of IMPase

As detailed above, IMPase, by catalysing the conversion of Ins1P to inositol, is a pivotal enzyme for both inositol recycling in the PI signalling pathway (Figure 1.5.1), and the injection of new inositol derived from G 6-P via MIPS.

Mammalian IMPase has 2 isoforms, IMPase 1 and IMPase 2, coded by *impa*1 and *impa*2 genes, respectively. Compared to human and mouse IMPase 1 (*Hs*IMPase 1, *Mm*IMPase 1; 277 amino acids), *Hs*IMPase 2 has an additional 11 residues, and *Mm*IMPase an additional 13, at the N terminus. *Hs*IMPase 1 and 2 have highly similar 3D structures, and, excluding the N-terminal extension, the sequences are 54% identical (Arai *et al.*, 2007) (Figure 1.7.1).

A

```
  1 ----------MADPWQECMDYAVTLARQAGEVVCEAIKNEMNVMLKSSP     39
              .|.||:||...||.||.:||:::.:|:..|..|..|:|.
  1 MKPSGEDQAALAAGPWEECFQAAVQLALRAGQIIRKALTEEKRVSTKTSA     50

 40 VDLVTATDQKVEKMLISSIKEKYPSHSFIGEESVAAGEKSILTDNPTWII     89
    .||||.||..||.::||.::|::|||.||.||:.|:|.|.:||.:|||||
 51 ADLVTETDHLVEDLIISELRERFPSHRFIAEEAAASGAKCVLTHSPTWII    100

 90 DPIDGTTNFVHRFPFVAVSIGFAVNKKIEFGVVYSCVEGKMYTARKGKGA    139
    ||||||.|||||||.|||||||||.:::||||:|.|.|.::||.|:|:||
101 DPIDGTCNFVHRFPTVAVSIGFAVRQELEFGVIYHCTEERLYTGRRGRGA    150

140 FCNGQKLQVSQQEDITKSLLVTELGSSRTPETVRMVLSNMEKLFCIPVHG    189
    |||||:|:||.:.|::|:|::||:|..|.|.|:::.|||||:|.....||
151 FCNGQRLRVSGETDLSKALVLTEIGPKRDPATLKLFLSNMERLLHAKAHG    200

190 IRSVGTAAVNMCLVATGGADAYYEMGIHCWDVAGAGIIVTEAGGVLMDVT    239
    :|.:|::.:.:|.:|:|.|||||:.|:||||:|.|.:|:.||||:::|.:
201 VRVIGSSTLALCHLASGAADAYYQFGLHCWDLAAATVIIREAGGIVIDTS    250

240 GGPFDLMSRRVIAANNRILAERIAKEIQVIPLQRDDED    277
    |||.|||:.||:||:.|.:|..||:.:|.|...||||.
251 GGPLDLMACRVVAASTREMAMLIAQALQTINYGRDDEK    288
```

B

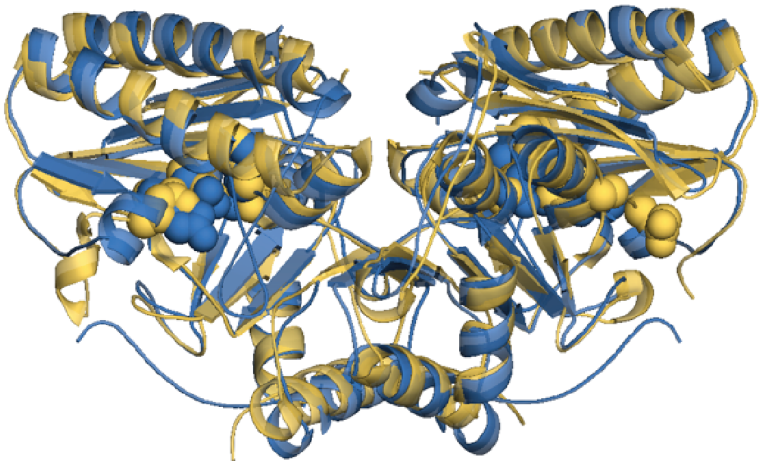


Figure 1.7.1. Comparison of *Hs*IMPase 1 and 2. A) Alignment of the amino acid sequences of *Hs*IMPase 1 and *Hs*IMPase 2. The sequences are 51% identical and 72.6% similar with no gaps. One dot indicates corresponding residues (aligned) in the structure, and double dots identify residues within 5 angstroms in distance (aligned). The alignment was produced using Expasy software from PDBs 2HHM and 2CZK. **B) Overlay of *Hs*IMPase 1 and *Hs*IMPase 2.** *Hs*IMPase 1 (blue, PDB 2HHM) and *Hs*IMPase 2 (yellow, PDB 2CZK). The structures exhibit 73% similarity and are 54% identical (Arai *et al.*, 2007).

The absence of secondary structure interactions in the 13 residue N-terminal extension in *Hs*IMPase 2 and the fact that it is not proximal to the active site suggests that it is unlikely to be involved in any substrate interactions, and likely serves as a signal peptide element.

Compared with rat IMPase 1, the activity of rat IMPase 2 for Ins1P is significantly lower, and the enzyme is less sensitive to lithium (Ohnishi *et al.*, 2007a). High expression levels of IMPase 1 and *impa*1 mRNA were found in the rat brain. *impa*2 mRNA and IMPase 2 were also found in the brain, but their expression levels were much lower, except in the mid-hind brain and the visual cortex (Ohnishi *et al.*, 2007a). Cardiac tissue, the epithelium of the small intestine and the distal convoluted tubules of the kidneys in rats contained IMPase 2 almost exclusively (Ohnishi *et al.*, 2007a).

Although studies have shown that IMPase 1 is the predominant isoform in the brain, genetic studies have not revealed any associations between IMPase 1 and bipolar disorder. IMPase 2, however, has been linked to the disease. The *impa*2 gene is found on the 18p11.2 chromosome, which is considered to be a susceptibility region for bipolar disorder, schizophrenia and febrile seizures. (Esterling *et al.*, 1997; Sjoholt *et al.*, 1997; Yoshikawa *et al.*, 1997). Furthermore, in Japanese and Palestinian Arab bipolar patients, there is evidence of an association with a single nucleotide polymorphism (SNP) in *impa*2 (Ohnishi *et al.*, 2007b).

1.7.2 IMPase as the target of lithium inhibition

Much has been published to suggest that IMPase is the therapeutic target of lithium in the treatment of bipolar disorder, based on the inositol depletion hypothesis. However, the target has not been conclusively validated. Knockout and knock-in mice have been generated in order to elucidate the pathophysiological role of IMPase.

1.7.2.1 IMPase transgenic mice

*impa*1 and *impa*2 knockout mice have been created, but these have not resolved the questions surrounding the interaction of lithium or provided significant insights into bipolar disorder. These knockout mice should correlate with lithium's phenotypic behavioural actions in mice. However, they only replicate some of the actions and are counterintuitive. For example, the *impa*1 homozygote knockout showed increased motor activity (Cryns *et al.*, 2008) whereas lithium treated mice, chronic and acute, show reduced activity (Johnson and Wormington, 1972; Smith and Smith, 1973). Moreover, *impa*1 knockout mice did show antidepressant-like activity and increased susceptibility to pilocarpine seizures (Cryns *et al.*, 2008). It is possible that these effects are due to the increased motor activity of the knockout mouse itself. Additionally, although pilocarpine seizure in the *impa*1 knockout mice could be reversed by inositol, it has no face validity in context of bipolar disorder. The IMPA *impa*2 knockout mice did not show any phenotypic effects of lithium treatment (Cryns *et al.*, 2007).

There was also some residual IMPase activity in the *impa*1 knockout mice that could not be accounted for by compensation by IMPase 2. This led to the suggestion that there may be a third IMPase isoform, although no evidence for it exists (Cryns *et al.*, 2008).

*impa*1 and *impa*2 knock-in transgenic mice, showed no behavioural phenotype of bipolar disorder. (Ohnishi *et al.*, 2010).

1.8 Drug development

Another approach to establishing IMPase as the target of lithium is to identify small molecule inhibitors that target the enzyme and comparing their effects with those of lithium. A major benefit of this approach is that these small molecule inhibitors can potentially be further developed as therapeutic drugs.

Drug development represents a formidable challenge. It requires intense resources, both financial and scientific, and the probability of success is low. There are essentially four stages in conventional drug development before a molecule can enter preclinical and clinical stages.

1. Target identification
2. Target validation
3. Lead identification
4. Lead optimization

The first stage involves identification of a protein or gene implicated in a particular disease. In the second stage, the putative target (protein or gene) is validated for the specified disease. For example, modifying the protein or knocking out the gene can be shown to have a pathophysiological impact. In the third stage, a 'lead', or an active small molecule, is identified by screening a library of compounds. In the final stage, the molecule is further optimised, to obtain enhanced potency and to ensure clinical safety.

Once optimised, the compound is then subjected to a battery of preclinical tests for efficacy, toxicity and ADME (absorption, distribution, metabolism and excretion) characteristics, before it can be approved for human use in clinical trials. If the drug exhibits better efficacy and safety than current commercial alternatives, it is likely to be approved for human treatment.

The process of drug development takes an average of 10–17 years and has a less than 10% probability of success (Ashburn and Thor, 2004). The cost of launching a new drug, from bench discovery into the market, is typically $1.7 billion (Gilbert *et al.*, 2003). Given the high-risk, high-investment model of the current pharmaceutical industry, a useful alternative strategy is to utilize existing drugs (thus, ones know to be safe) in novel applications.

1.8.1 Developing small molecules for target validation

Once a target has been identified, it can be validated using small molecules. To develop or discover new molecules, essentially three methods are employed: traditional medicinal chemistry, virtual screening and drug repositioning.

1.8.1.1 Traditional medicinal chemistry

Medicinal chemistry has been the traditional method for drug discovery. Typically, this involves identifying/synthesising a potential molecule (or adapting an existing compound) using organic chemical synthesis, then introducing modifications to chemical groups with the goal of yielding a compound that is either more potent or less toxic than the starting compound. Two design approaches are commonly employed: structure-based, where the three-dimensional structure of the target is used; or ligand-based, where the starting compound is a compound that is known to bind to the biomolecular target.

Merck, starting with the substrate, Ins1P, used medicinal chemistry to develop an inhibitor for IMPase. After a series of chemical derivatives of Ins1P (Figure 1.8.1), they arrived at a novel compound, L-690330, that inhibited IMPase competitively with an IC_{50} value of 0.33 μM *in vitro*.

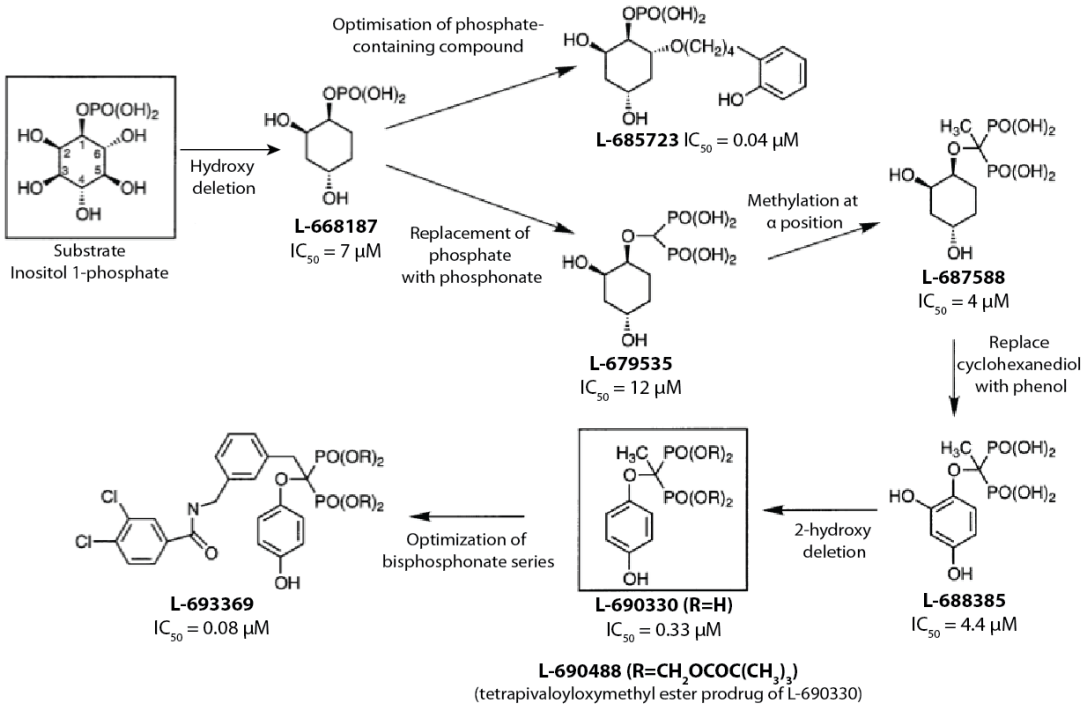


Figure 1.8.1. Development of L-690330 and L-690488 from Ins1P. Starting with the IMPase substrate Ins1P as the template, different functional groups were modified using medicinal chemistry, and a series of bisphosphonate inhibitors were developed. L-690330 and L-690488 were found to be the most promising, based on cell permeability and potency (Atack, 1997).

This compound, although potent, had a bisphosphonate group and was thus too highly charged to cross the cell membrane effectively. They compensated for the charge by esterification of the bisphosphonate, but the resulting compound (L-690488) was too hydrophobic and accumulated at the site of the injection *in vivo*. Although these compounds are not suitable for use in animal models of mania and depression, they do provide valuable insight into the effects of IMPase inhibition *in vitro* or in cells.

1.8.1.2 Virtual screening

Virtual screening is a more recent approach to identify inhibitors. This involves using computers and sophisticated software can predict the strength of interactions between a small molecule and a target macromolecule, such as a protein.

A library of compounds is screened, and candidates are ranked to identify the best 'lead' (or 'hit'). A hit is a compound that has the required functional groups and permissible spatial orientation to bind to the protein (Wilson *et al.*, 2004). Virtual libraries can contain millions of compounds; they can be general, focussed or targeted (Walters *et al.*, 1998).

Virtual screening is both cost- and time-effective. Rather than directly synthesising a large series of compounds, it is much more efficient to first screen a vast library *in silico*, identify compounds with best probability of a hit, and then synthesise and screen these for biological activity. A major advantage of virtual screening is that it enables the discovery of molecules (or scaffolds) that might otherwise have been overlooked.

Virtual screening can also be performed by one of two methods: ligand-based and structure-based screening. Ligand-based drug design starts with a known ligand of the protein and then virtually screens libraries to identify compounds that have similar physical and chemical properties. Structure-based drug design uses a model of the target protein, simulates docking of molecules at specific sites on the protein and determines those with the best fit. Usually, the active site is used.

1.8.1.3 Drug repositioning

More recently, there has been growing recognition of the fact that a drug usually has more than just one target. This has lead to testing of drugs approved for one indication to be clinically tested in another. This technique is termed 'drug repositioning' (Figure 1.8.2). For example, duloxetine, which was developed for depression, is now also indicated for stress urinary incontinence (Ashburn and Thor, 2004).

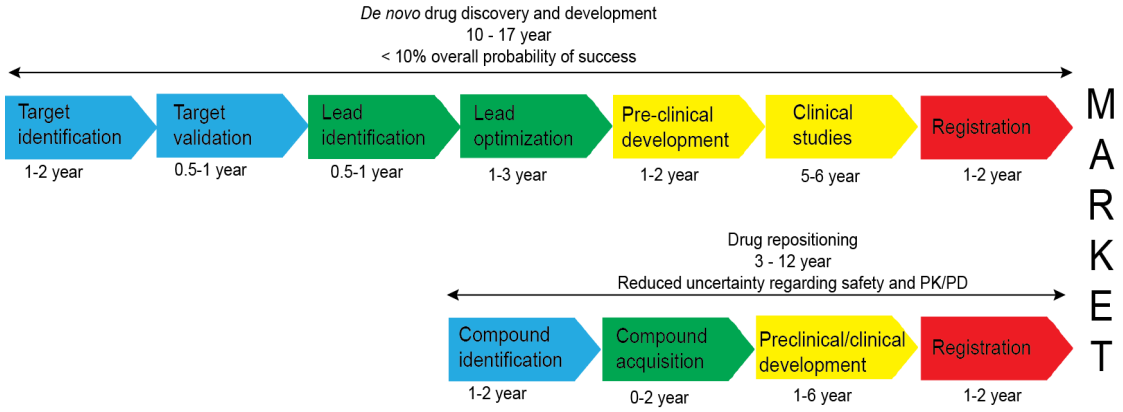


Figure 1.8.2. Comparison of *de novo* drug development and drug repositioning. *De novo* drug development takes 10-17 years on average and has a less than 10% probability of success. Drug repositioning takes an average of 3-12 years and has decreased risk due to the known safety and ADME profile (adapted from (Ashburn and Thor, 2004).

Drug repositioning has several advantages over traditional drug discovery, the most significant of which is that the safety and the ADME profile of the drug are known. Most drugs fail in clinical trials for two principal reasons: lack of efficacy and lack of safety. With drug repositioning, one major hurdle in safety is taken care of. Additionally, the time to reposition a drug is 3–10 years (Ashburn and Thor, 2004), considerably shorter than that for *de novo* drug discovery (Figure 1.8.2).

1.9 Aims

The aim of this project was to develop or identify a novel IMPase inhibitor and evaluate it for lithium-mimetic activity using enzymatic, cellular and whole animal systems.

These were addressed by four lines of investigation as described in each of the following chapters:

Chapter 2: Enzymatic studies. To express recombinant human and mouse IMPase, for use in screening and to perform enzymatic studies in order to characterise

the mechanism of inhibition of inhibitor(s) found in the screening process. Additionally, to crystallise and obtain X-ray structures of the resulting proteins ideally in complex with any inhibitors found to show the site of binding.

Chapter 3: Screening. To find novel IMPase inhibitors using two approaches. The first was to use virtual screening to develop a novel selective IMPase inhibitor *de novo*, with the ultimate aim of proving the inositol depletion hypothesis. The second was to reposition orphan drugs for IMPase inhibition, with the ultimate aim of developing a new drug for the treatment of bipolar disorder.

Chapter 4: Cellular and tissue evaluation. To test the novel IMPase inhibitor(s) in cells for the effects on inositol phosphate metabolism, and to obtain evidence of inositol depletion in cells. These data are compared to those obtained with lithium. Additionally, to test the inhibitor(s) for *ex vivo* IMPase inhibitory activity in mouse brain homogenate.

Chapter 5: Behavioural evaluation. To assess the inhibitor(s) in behavioural tests using mouse models of bipolar disorder that show reproducible results with lithium (open-field test, amphetamine-induced hyperactivity test, forced swim test and the pilocarpine seizure test).

CHAPTER 2

INOSITOL MONOPHOSPHATASE: CLONING, EXPRESSION, PURIFICATION AND CRYSTALLOGRAPHY

2 Inositol monophosphatase: Cloning, Expression, Purification and Crystallography

2.1 Introduction

2.1.1 Crystal structure of IMPase

Bovine and human recombinant IMPases have been crystallised and shown to be 79% identical (McAllister *et al.*, 1992). The human protein has been crystallised to a resolution of 2.1 Å (Bone *et al.*, 1992) and the bovine protein to a resolution of 1.4 Å (Gill *et al.*, 2005). Each subunit of the homodimer is composed of 3 α-helices and 2 β-sheets arranged as αβαβα (Bone *et al.*, 1992). The subunits are essentially hydrophilic, except for the dimerisation surface, which is more hydrophobic (Bone *et al.*, 1992; Gill *et al.*, 2005). The active site is a large hydrophilic cavity, much larger than required for IP_1 (Bone *et al.*, 1992). This is possibly why IMPase has the ability to hydrolyse substrates larger than IP_1, for example, 2′-adenosine monophosphate (Gee *et al.*, 1988). From crystallographic and modelling analysis of human and bovine IMPase 1, the key amino acid residues involved in substrate binding and catalysis have been identified as Glu70, Asp90, Ile92, Asp93, Thr95, Glu213 and Asp220 (Bone *et al.*, 1992; Gill *et al.*, 2005; Leech *et al.*, 1993; Pollack *et al.*, 1994; Pollack *et al.*, 1993).

This αβαβα structure is also found in other phosphatases, such as fructose 1,6-bisphosphatase (FBPase), inositol polyphosphate 1-phosphatase (IPPase), 3′-phosphoadenosine-5′-phosphatase (PAPase), inositol-1,4-bisphosphatase (IBPase) (Gill *et al.*, 2005), all of which are Mg^{2+}-dependent and inhibited by lithium. Based on the structural similarity that IMPase shares with these phosphatases, a catalytic model that involved two metal-binding sites (‘2-metal catalysis’) for IMPase Ins1P

hydrolysis was proposed by Pollack *et al.* (Pollack *et al.*, 1994). More recently, the crystal structure of bovine IMPase has been resolved to 1.4 Å and this showed three Mg^{2+} ions coordinated by active-site residues; this led to the proposal of the '3-metal catalysis' model for Ins1P hydrolysis (Gill *et al.*, 2005).

2.1.2 Mechanism of substrate hydrolysis

IMPase has an absolute requirement for magnesium for catalytic activity. Concentrations from 0.05 – 5 mM are activating *in vitro*, but concentrations above 5 mM become inhibitory (Hallcher and Sherman, 1980). The presence of the 6-OH functional group on the substrate is also necessary for activity, as substrates without this group show decreased catalytic rates (Gill *et al.*, 2005; Pollack *et al.*, 1994). IMPase does not have the same mechanism of hydrolysis as that of other phosphatase enzymes such as acid and alkaline phosphatases (Leech *et al.*, 1993), but its mechanism is similar to that of fructose 1,6-bisphosphatase (Pollack *et al.*, 1994). Initial studies suggested that IMPase uses a 2-metal catalysis mechanism (Pollack *et al.*, 1994) but later studies have proposed a 3-metal catalysis mechanism (Gill *et al.*, 2005).

2-site metal binding:

The 2-site metal catalysis model (Figure 2.1.1) postulates that at least two metal ions are required to stabilise the protein at the time of catalysis. *Hs*IMPase crystallographic studies showed the presence of one gadolinium cation and a sulphate anion coordinated at the active site of IMPase (Bone *et al.*, 1992).

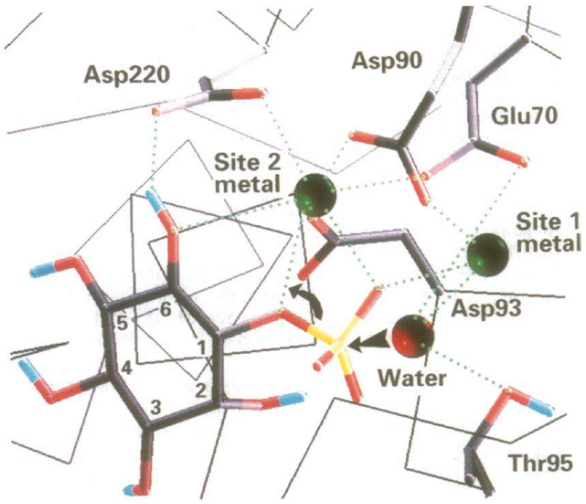


Figure 2.1.1. 2-site metal catalysis model. The figure shows the proposed two metal-binding sites at the active residues of *Hs*IMPase. Residues involved in catalysis are numbered. The aspartate (Asp) residues and the glutamate (Glu) residue are shown coordinating two metal ions (green spheres). The water molecule (red sphere), coordinated partly by the threonine (Thr95), is shown attacking the phosphate arm of inositol 1-phosphate (Pollack *et al.*, 1994).

However, the crystallisation conditions included high lithium concentrations. Lithium is a small cation and does not diffract X-rays; hence some detail regarding the substrate-binding site may have evaded detection. The crystallisation was repeated using manganese (Mn^{2+}, (Pollack *et al.*, 1994). These studies revealed that 3 Mn^{2+} ions coordinated to the active site residues: two high affinity sites and one low affinity site (Pollack *et al.*, 1994). The metal in the low affinity site could be displaced easily, and this model supported the 2-site catalytic mechanism. In this model, substituting manganese with magnesium (an endogenous ion), the first metal binding site coordinates a Mg^{2+} ion, probably at Glu70 and Thr95, then activates a water molecule for nucleophilic attack. This Mg^{2+} ion remains bound throughout the catalytic process. The other Mg^{2+} (at the second metal binding site) is coordinated by three aspartate residues (Asp90, Asp93 and Asp220) and stabilises the leaving inositol oxyanion by acting as a Lewis acid (Pollack *et al.*, 1994). This second Mg^{2+} dissociates during catalysis to allow the phosphate to leave; it becomes inhibitory if it remains bound

(Pollack *et al.*, 1994). Modelling data suggested that there was no requirement for a third metal binding site, so the presence of the third Mn^{2+} might have been an artefact. (Bone *et al.*, 1994).

3-site metal binding:

By contrast, the 3-metal catalysis model postulates that all three coordinating Mg^{2+} ions are required for IMPase catalytic activity (Figure 2.1.2). Gill *et al.* used the bovine IMPase crystal structure at a resolution of 1.4 Å with Mg^{2+}, an endogenous cofactor, in the crystallisation conditions (Gill *et al.*, 2005). Their structure showed the presence of three metal binding sites, with the third Mg^{2+} possibly being occupied only at high Mg^{2+} concentrations.

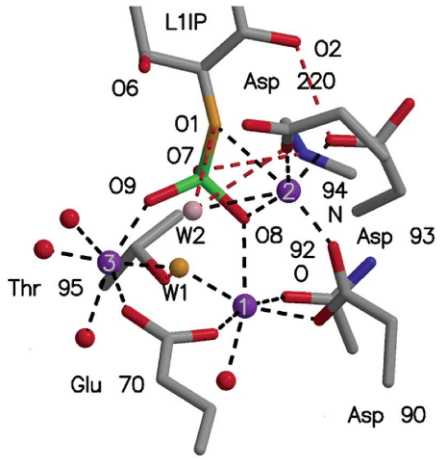


Figure 2.1.2. 3-site metal catalysis model. The figure shows the proposed three metal-binding sites at the active site of *Hs*IMPase 1. The aspartate (Asp) residues, glutamate (Glu) and threonine (Thr) residue coordinate three metal ions (numbered purple spheres). There are two water molecules (brown spheres); one (W1) is shown coordinating two of the metals, and the other (W2) is shown attacking the phosphate arm of inositol 1-phosphate (L1IP). Oxygen atoms (O) are numbered (Gill *et al.*, 2005).

The nucleophile is generated by protonation of Thr95 by a water molecule (W1) coordinated by a Mg^{2+} ion at site 1 (Mg^{2+}-1) and a second Mg^{2+} at site 3 (Mg^{2+}-3). The activated water then attacks the phosphoester bond thereby forming a low-energy, negatively charged trigonal bipyramidal transition state. The Mg^{2+} ion at site

2 (Mg^{2+}-2) and the hydrogen binding to the 6-hydroxyl (6-OH) group stabilises this negatively charged transition state before the transfer of a proton from a second water molecule (W2) to the leaving oxygen group, thereby resulting in phosphate hydrolysis and collapse of the trigonal bipyramidal intermediate structure. The sequence of product release from IMPase is likely to be: Mg^{2+}-3, followed by the inositolate ion, then Mg^{2+}-2 and finally Mg^{2+}-1. The dissociation of Mg^{2+}-2 is hindered at high magnesium concentrations, as this causes the inorganic phosphate to be trapped in the enzyme–product transition complex, and thereby inhibiting the enzyme from reverting to its original state (Gill *et al.*, 2005).

Both postulated mechanisms have their strengths and weaknesses. The 2-site model explains the process of phosphate hydrolysis satisfactorily and is in agreement with kinetic data obtained for the enzyme (Strasser *et al.*, 1995). However, this model ignores the presence of the third Mg^{2+} and does not provide a significant role for the 6-OH group, which has been shown to be necessary for catalytic activity. The 3-site metal explains the role of the 6-OH group and also of the third Mg^{2+} seen in the crystallographic structure. It is also in agreement with some other studies using archael IMPase and FBPase (Stieglitz *et al.*, 2002). However, in the presence of phosphate, only two metal binding sites were occupied. Phosphates are competitive inhibitors of IMPase. Also, high concentrations of Mg^{2+} inhibit IMPase, so if Mg^{2+} has a low affinity for this third binding site and is easily displaced, the physiological relevance of this model remains questionable.

2.1.3 Lithium and IMPase

For all IMPases examined to date, lithium has been shown to inhibit both *in vitro* and *in vivo*, with an IC_{50} value of about 0.8 mM (Berridge *et al.*, 1982; Hallcher

and Sherman, 1980). Initial kinetic experiments revealed that lithium inhibits IMPase uncompetitively, as does Mg^{2+} at high concentrations (Hallcher and Sherman, 1980). Further experiments showed that lithium acts as an uncompetitive inhibitor at concentration up to 4 mM, after which it becomes a non-competitive inhibitor of IMPase (Leech *et al.*, 1993). Lithium, by virtue of being an uncompetitive inhibitor, has been postulated to bind either to the enzyme–substrate or to the enzyme–product complex. Leech *et al*. also showed that lithium binding caused a burst of inositol release followed by inhibition, and concluded that lithium causes inhibition by binding to the enzyme–product complex. Inorganic phosphate competitively inhibits both lithium and magnesium binding. Also, magnesium is uncompetitive and inhibitory at high concentrations, and both lithium and magnesium bind in a mutually exclusive manner, suggesting that they bind to the same site. Hence it was concluded that lithium binds to the second metal binding site after magnesium (Mg^{2+}-2) has left, to form an inhibited enzyme–Mg^{2+}-1–phosphate–lithium complex (Leech *et al.*, 1993). Although there was much kinetic evidence for lithium binding IMPase, since lithium does not diffract X-rays sufficiently to be detected on a diffraction map, it is hard to show conclusively where lithium binds. The first study to directly show lithium binding to IMPase employed nuclear magnetic resonance (NMR; (Saudek *et al.*, 1996). This study confirmed previous findings that lithium binds to the enzyme–phosphate complex, but it could not distinguish between the different metal binding sites to identify the exact binding location. The NMR studies also showed that that lithium had an affinity for the enzyme even in the absence of substrate, and that there was a single binding-site for lithium (Saudek *et al.*, 1996).

2.1.4 Aims

To date, bovine, human and rat IMPases have been purified. However, despite many mouse IMPase-related studies, a murine isoform has not been purified nor has a crystal structure been obtained. The enzyme is highly conserved; however, given the significant benefits of mouse models in the development of therapeutic agents, any significant differences between mouse and human IMPase might compromise the validity of mouse IMPase as a model in inhibition assays. *In vitro* data on mouse IMPase activity might help to gain an understanding of the kinetics and mechanism of inhibition *in vivo*. More importantly, a mouse model will provide insights into the mechanism and behavioural phenotypes, as *impa* knockout or knock-in mice could be used to test novel inhibitors in mutant mice.

For these reasons, I decided to clone and express the recombinant mouse protein. I decided to use *Mm*IMPase 1 rather than *Mm*IMPase 2, despite the established genetic association between BD and IMPase 2, for a number of reasons:

1. Although IMPase 1 has not been directly linked with BD, it is the predominant isoform in human and mouse brains.
2. Lithium inhibits IMPase 2, but only at concentrations higher than therapeutic levels *in vivo* (Ohnishi *et al.*, 2007a).
3. IMPase 2 knockout mice exhibited no distinct lithium-like behavioural phenotype (Cryns *et al.*, 2007), unlike IMPase 1 (Cryns *et al.*, 2008).

To identify a novel lithium mimetic, it is essential to characterise the mimetic's effects in tissues and in behavioural models of BD, and to compare it with lithium at therapeutic concentrations. For these reasons, *Mm*IMPase 1 was selected for the screening of compounds.

2.2 Materials and Methods

2.2.1 Chemicals and reagents:

All chemicals were purchased from Sigma–Aldrich, UK unless otherwise stated.

Bovine IMPase (Sigma) was bought as a lyophilized powder and reconstituted in Tris buffer at 0.5 mg/mL. It was aliquoted (100 μL) and stored at −80°C until required. It was used at a final concentration of 5 μg /well. QIAprep Spin Miniprep (#27104) and QIAquick Gel Extraction (#28704) kits were purchased from Qiagen (Crawley, UK). Phusion Hot Start DNA polymerase (# F-540S, 100U), dNTPs, and restriction endonucleases (*NdeI* and *PstI*), were obtained from New England Biolabs (NEB, Hitchin, UK). Necessary buffers were provided in the kits.

IMAGE cDNA clones *Hs*3682657 and *Mm*6413389 were purchased from Source Biosciences (Cambridge, UK). Oligonucleotide primers were synthesised by Sigma Genosys. The protein ladder was bought from Fermentas.

2.2.1.1 Buffers

The following buffers were used for protein purification.

Buffer A: 20 mM Tris.HCl, 1 mM EDTA, pH 7.8

Buffer B: 20 mM Tris.HCl, 1 mM EDTA, 1 M NaCl, pH 7.8

Tris buffer: (50 mM Tris-HCl, 1 mM EGTA, 3 mM $MgCl_2$, 150 mM KCl, 0.5 mg/mL BSA and 0.01% *w/v* Triton-X),

2.2.2 Bioinformatics

Sequences for the IMAGE cDNA clones of *Hs*IMPase 1 and *Mm*IMPase 1 and genomic data were retrieved from http://www.ncbi.nlm.nih.gov/. The nucleotide sequences were aligned using ClustalW2 (http://www.ebi.ac.uk/Tools/msa/clustalw2/) and the alignments were visualised with ESPript 2.2 (http://espript.ibcp.fr/ESPript).

Expasy (http://expasy.org/) was used for obtaining predicted mass spectrometry fragmentation patterns. NEB cutter (http://tools.neb.com/NEBcutter2/) was used to determine restriction sites within the genes. Protein sequences alignment was done using EMBOSS software (Rice, 2000); http://www.ebi.ac.uk/Tools/psa/emboss_needle/).

2.2.3 Protein expression and analysis

2.2.3.1 Plasmid, cDNA and primers

The pRSET5a vector was a gift from Dr. Ralf Schoepfer (UCL London)(Schoepfer, 1993). This is a 2831 bp expression plasmid that had been previously used for expression of human and rat recombinant IMPase (McAllister *et al.*, 1992). The vector has a T7 promoter, which is transcribed following the addition of isopropyl β-D-thiogalactopyranoside (IPTG) when hosted in a BL21(DE3) *Escherichia coli* . The vector has multiple restriction sites and confers ampicillin resistance (Schoepfer, 1993).

2.2.3.2 Bacterial strains

E. coli bacterial strains were used throughout. DH5α (a gift from Prof. Sim, Dept. of Pharmacology, University of Oxford) and JM109 competent cells (Promega) were used for the cloning of DNA; BL21(DE3) pLysS (a gift from Dr. Parrington,

Dept. of Pharmacology, University of Oxford) was used for gene expression and production of recombinant protein. Cells (both stock and transformed) were mixed (1:1) with 50% sterile glycerol in cryovials and stored at −80°C.

2.2.3.3 Media and antibiotics

Lysogeny broth (LB), agar, sorbitol, betaine, chloramphenicol and ampicillin were bought from Melford, UK. All media were prepared and sterilised by autoclaving at 121°C, 15 psi pressure for 30 min. Betaine and ampicillin were sterilised by passing through a 0.2 μm filter. Chloramphenicol was made up in ethanol and hence there was no need to sterilise. All procedures were carried out under aseptic conditions using aseptic technique. Details of the media concentrations and the antibiotics used are given in Table 2.2.1.

Table 2.2.1. Media and antibiotics

Media / Antibiotic	Composition
Lysogeny broth (LB)	10 g/L Bacto-Tryptone, 5g/L Bacto-yeast extract, 10g/L NaCl
LB Agar	15 g/L Bacto-agar in LB medium
LB-Sorbitol media	660 mM sorbitol, 2.5 mM betaine in LB medium
Ampicillin sodium	50 μg/mL (Stock solution: 50 mg/mL)
Chloramphenicol	34 μg/mL (Stock solution: 34 mg/mL)

2.2.3.4 Transformation and extraction of DNA

The heat shock method was used for bacterial cell transformation throughout. DH5α cells (66 μL) or competent JM109 cells (50 μL) were incubated with plasmid (2 μL, 200 μg) on ice for 10 minutes. Transformation was carried out by placing in a water bath at 42°C for 45 s, followed by immediately placing on ice for 2 min. Then, 3 mL of LB was added, and samples were placed in an incubator (180 rpm, 37°C, 1.5

h). The culture was then centrifuged (3000×g, 10 min, R.T.) and the supernatant was discarded. The pellet was resuspended in a minimal quantity of LB and streaked onto antibiotic-containing LB–agar plates. These were incubated at 37°C overnight. Transformed single clones from the sample plate were selected and grown overnight (180 rpm, 37°C) in LB medium containing ampicillin.

The following morning, plasmid DNA was extracted using the Qiaprep Spin Miniprep kit according to the manufacturer's instruction.

2.2.3.5 Polymerase chain reaction (PCR)

PCR was performed in a final volume of 50 μL containing 100 μM sense and antisense primers, 0.5 μL of template DNA, 5 μL of 10× Phusion HF buffer (provided with the polymerase), and 200 μM dNTPs. Phusion Hot Start DNA polymerase (1 μL, 2 U/μL) was added immediately prior to the reaction. Following an initial phase (98°C, 30 sec) to denature the template, the amplification was carried out for 30 cycles (Figure 2.2.1) in a thermal cycler (MK Research PTC-0200 Peltier, GMI Inc., Ramsey, USA).

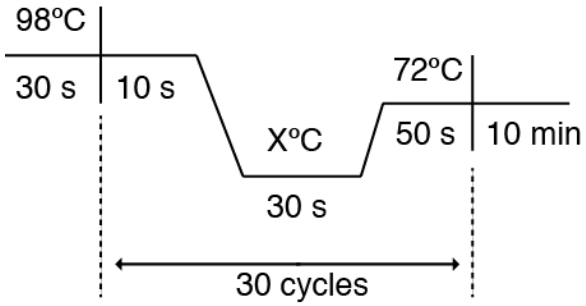


Figure 2.2.1. Protocol for PCR reaction. For annealing temperature (X°C) as required.

2.2.3.6 Agarose gel electrophoresis

A 1% *w/v* agarose gel was prepared in 1× TAE buffer (running buffer: 40 mM Tris, 20 mM acetic acid, 1 mM EDTA, pH 8) containing 0.5 μg/mL ethidium bromide. The DNA samples were prepared by mixing (DNA/loading buffer, 1:5) with 20% *v/v* gel loading buffer (30% *v/v* glycerol, 0.25% *w/v* bromophenol blue and 0.25% *v/v* xylene cyanol FF and loaded onto the gel. A 1kb DNA ladder (O'Gene Ruler 1kb Plus, Fermentas, UK) was run simultaneously to determine the size of the DNA samples. The gel was run at 100 volts for 20 min. The gels were visualised using a Gel Doc 2000 UV/visible illuminator (BioRad, Hemel Hempstead, UK).

2.2.3.7 DNA purification and determination of concentration

DNA was extracted from agarose gel by careful excision of the required band with a scalpel and the purification carried out using a QIAquick Gel extraction kit (Qiagen, Crawley, UK). The yield of DNA was determined spectrophotometrically at 260 nm (A_{260}) using a BioPhotometer (Eppendorf, Cambridge, UK). (A_{260} = 1 corresponds to approximately 50 μg/mL of double stranded DNA; (Sambrook *et al.*, 1989).

2.2.3.8 Restriction endonuclease digestion

PCR products and vector pRSET5a (1 μg) were digested by incubating with NdeI and PstI (10 U; NEB, Hitchin, UK) at 37°C for 1 h in 1× NEB buffer C. The digestion volume was 20 μL.

2.2.3.9 Ligation

The ligation mixture was prepared by mixing 1 µL of 10× T4 DNA ligase buffer, 1 µL of T4 DNA ligase (# M0202T, NEB), 2 µL of ddH_2O and 6 µL of DNA (1:1 molar ratio of plasmid to DNA insert) in a reaction volume of 10 µL, following the ligation protocol provided by the manufacturer. The reaction was incubated overnight at 4°C.

2.2.3.10 Protein expression

Cultures were grown overnight at 37°C with constant shaking at 180 rpm, in 25 g/L sterilized LB broth containing 50 µg/mL ampicillin. 10 mL of this culture was then transferred to a flask containing 1 L of sterilized 25 g/L LB broth containing 660 mM sorbital and 2.5 mM betaine (Blackwell and Horgan, 1991) and grown to an OD_{600} of 0.9 at 37°C with constant shaking at 180 rpm. IPTG (final: 0.4 mM) was added to the culture to induce expression and the culture was incubated overnight (30°C, shaking at 180 rpm). The next morning the cultures were centrifuged (1360×g, 20 min, R.T.), the supernatant was discarded and the bacterial cell pellet was stored at -80°C.

2.2.3.11 Isolation of soluble protein from large-scale culture

A pellet from previously expressed bacterial culture was resuspended in Buffer A containing a protease inhibitor cocktail. The resuspension volume was one tenth that of the original culture volume. The suspension was sonicated on ice using a Soniprep ultrasonicator for 20 cycles of on and off periods at 10Å, then centrifuged at 30,000×g for 30 min at 4°C. The supernatant was collected, and heated at 68°C for 1 h before being centrifuged again (30,000×g for 30 min at 4°C) and used for activity and protein assays.

2.2.4 Chromatography

2.2.4.1 Anion exchange chromatography Stage 1: Q-sepharose

The separation of proteins based on their charge is called anion exchange chromatography. When a protein is negatively charged at pH 7, for example, IMPase has a net negative charge at pH 7 (IMPase 1 theoretical isoelectric point = 5.14), it can be purified using a column that has a positively charged resin on it. This is called anion exchange chromatography.

The samples were passed through a Q-sepharose column using a gradient of buffer A and buffer B. See Tables 2.2.2 and 2.2.3 and Figure 2.2.2.

Table 2.2.2. Stage 1 chromatography.

	Stage 1
Column	Q-Sepharose Hi-Load 16/10 FF
Loading volume	25 mL
Flow Rate	3 mL/min
Fraction volume	2 mL

Table 2.2.3. Q-sepharose elution gradient

Volume (mL)	Q-sepharose elution gradient
0 to 10	Wash with 2% Buffer B
10 to 35	Injection of 25 mL sample
35 to 75	Loading of sample
75 to 135	2 to 55% Buffer B
135 to 155	55 to 100% Buffer B
155 to 165	100% Buffer B
165 to 170	100% to 2% Buffer B
170 to 200	Wash with Buffer A

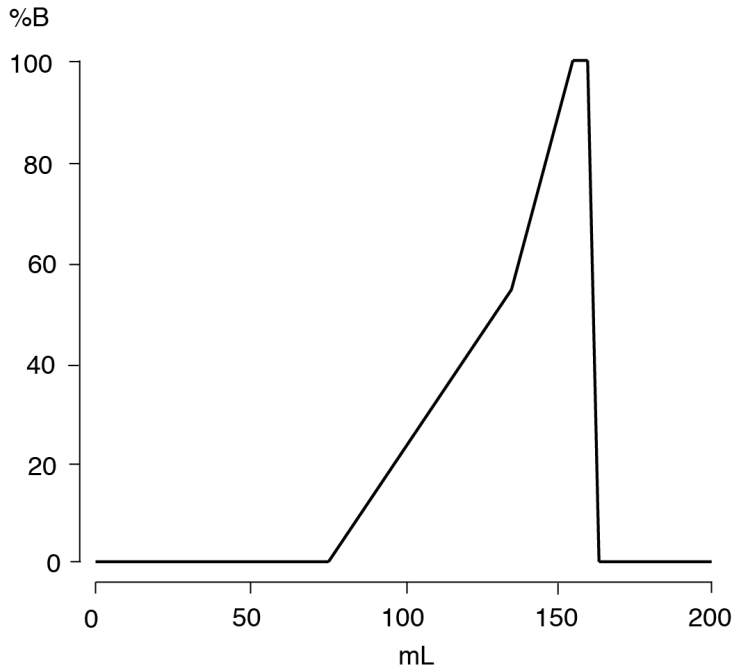


Figure 2.2.2. The elution gradient for Q-sepharose chromatography.

The selected fractions were placed in a 10 kDa dialysis tubing (Medicell, UK) and placed in 2 L of buffer A for 6 h with 1 buffer change. After dialysis 20 mM β-mercaptoethanol was added to prevent aggregate formation.

2.2.4.2 Anion exchange chromatography Stage 2: Mono-Q

Samples were passed through a Mono-Q column using a gradient of buffer A and buffer B. See Tables 2.2.4 and 2.2.5 and Figure 2.2.3.

Table 2.2.4. Stage 2 chromatography.

	Stage 2
Column	MonoQ 5/50 GL
Loading volume	5 mL
Flow Rate	1 mL/min
Fraction volume	0.5 mL

Table 2.2.5. Mono-Q elution gradient

Volume	Mono-Q elution gradient
0 to 2	Wash with Buffer A
2 to 10	Loading of sample (5 mL)
10 to 30	0% to 55% Buffer B
30 to 35	55% to 100% Buffer B
35 to 36	100% Buffer B
36 to 37	100% to 0% Buffer B
37 to 40	Wash with Buffer A

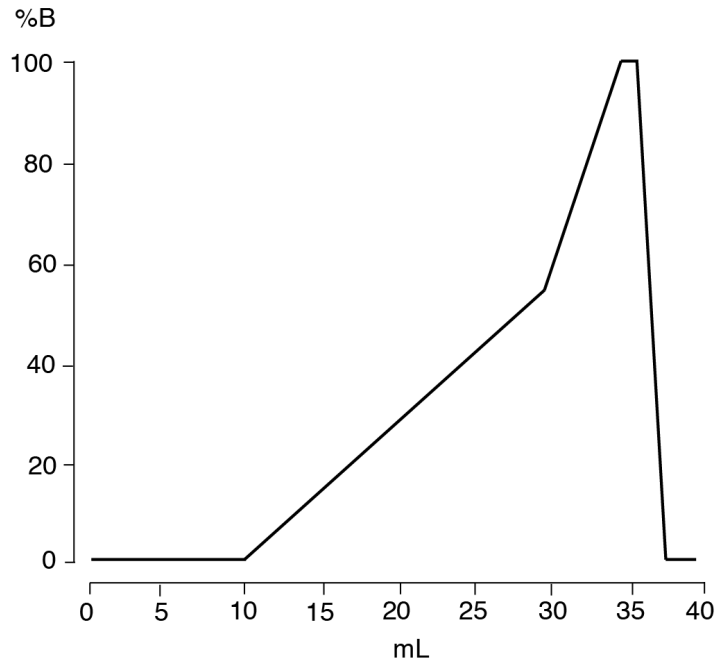


Figure 2.2.3. The elution gradient for Mono-Q chromatography.

The selected fractions were combined and concentrated to 1 mg/mL using Millipore spin columns with a cut-off of 10 kDa.

2.2.4.3 Size exclusion chromatography

The protein was passed through a GE Superdex-75 column at an isocratic gradient of 13% Buffer B (Table 2.2.6).

Table 2.2.6. Stage 3 chromatography

Superdex-75 parameters	
Column	Superdex 75 10/300 GC
Loading volume	1 mL
Flow Rate	0.5 mL/min
Fraction volume	0.5 mL
Gradient	Isocratic at 13% Buffer B

2.2.5 IMPase activity and concentration analysis

2.2.5.1 Malachite green phosphatase activity assay

IMPase catalyses the hydrolysis of the phosphate from Ins1P; the released phosphate reacts with Malachite Green (MG) reagent, in the presence of molybdate ions, to give a green colour complex (Figure 2.2.4). The assay (Itaya and Ui, 1966) was carried out in a 96 well plate. 2 µL of protein solution was added to a well containing 1 mM Ins1P, and the volume was made up to 20 µL with Tris buffer (50 mM Tris-HCl, 1 mM EGTA, 3 mM $MgCl_2$, 150 mM KCl, 0.5 mg/mL BSA and 0.01% *w/v* Triton-X), and the plate was incubated (1 h, 37°C). MG reagent was prepared 15 min before addition to the plate, by mixing 0.045% *w/v* MG solution with 4.2% *w/v* ammonium molybdate (3:1). 180 µL of the mixture was added to each well and the plate was incubated for 2 min for the colour to develop (to a green colour). The absorbance (595 nm) was read in a BMG Fluostar plate reader (BMG Labtech, UK).

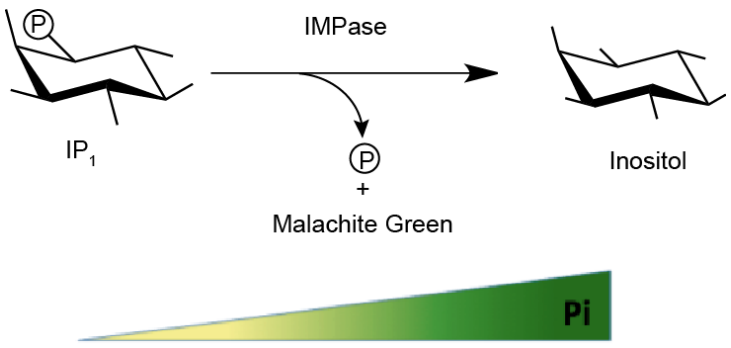


Figure 2.2.4. Malachite green assay. Reaction between IMPase and Ins1P releases phosphate, which then forms a complex with MG/molybdate that is green in colour. The absorbance at 595 nm is directly proportional to the phosphate concentration.

For quantification of specific activity of the IMPase enzyme, potassium dihydrogen orthophosphate (KH_2PO_4) standards (0 – 6 nmol) were prepared. 20 μL of these standards were added (in duplicate) to each plate, and MG reagent was added as for the samples. The (linear) standard curve derived from these (Figure 2.2.5) was used to quantify phosphate released by the IMPase sample catalysis.

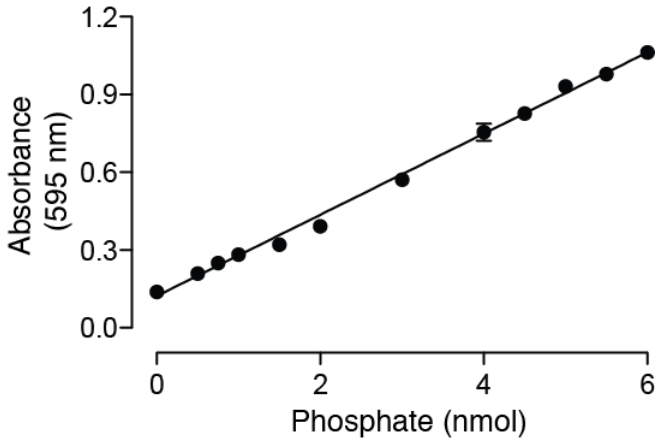


Figure 2.2.5. Typical Malachite Green standard linear plot using KH_2PO_4 A linear relationship between the phosphate present and the absorbance at 595 nm is observed.

2.2.5.2 Protein concentration assay

Protein concentration was estimated by the bicinchoninic acid (BCA) method (Smith *et al.*, 1985), in which peptide bonds reduce copper(II) to copper(I), the latter forming a complex with BCA that has a characteristic purple colour (Figure 2.2.6)

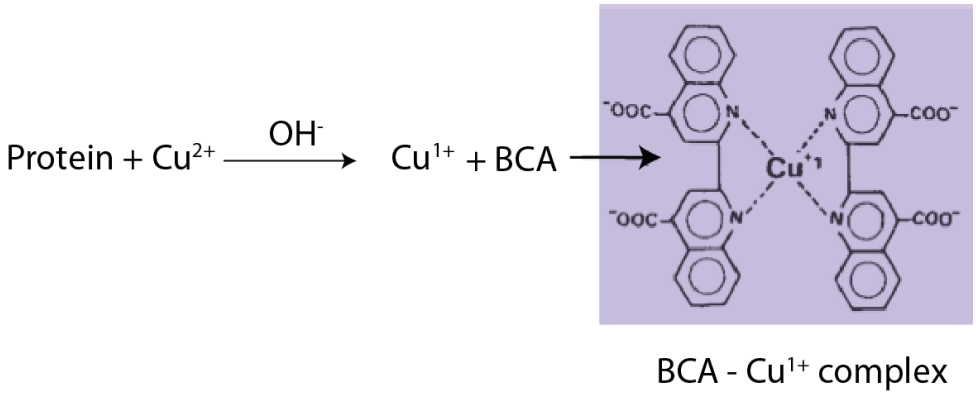


Figure 2.2.6. Bicinchoninic assay for determination of protein concentration. In the presence of protein in an alkaline environment (OH^-), cupric ions (Cu^{2+}) are reduced to cuprous ions (Cu^+) which then combine with bicinchoninic acid (BCA) to form a BCA–Cu^{1+} purple-coloured complex (peak absorbtion 560 nm). The absorbance is approximately proportional to the amount of protein.

Bovine serum albumin (BSA, 0 – 2 mg/mL in Buffer A was used as the standard. 200 µL of a solution of 50 parts bicinchoninic acid and 1 part 4% *w/v* copper sulphate was added to 25 µL protein sample or standards. In the presence of protein, the colour changes from bluish-green to purple (Figure 2.2.7). The plate was left at R.T. for 30 min for the colour to develop and then the absorbance was measured at 595 nm using a BMG Fluostar plate reader.

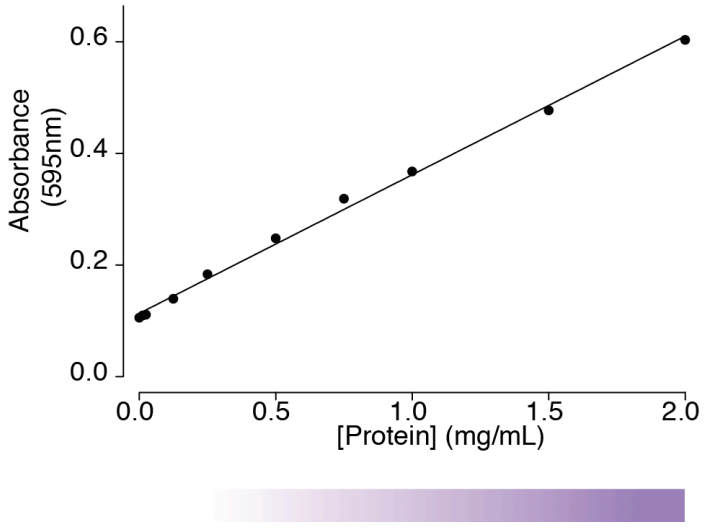


Figure 2.2.7. Example BSA protein standard linear plot A linear relationship between the protein concentration (mg/mL) and the absorbance at 595 nm is observed.

2.2.5.3 SDS-Page

Sodium dodecyl-sulphate polyacrylamide gel electrophoresis (SDS-PAGE) was performed using the Mini-PROTEAN vertical electrophoresis system (Bio-Rad). 10% Resolving gels (8.6×7.3×0.1 cm) were prepared by diluting 30% *v/v* acrylamide/bis-acrylamide (37.5:1; National Diagnostics) in 375 mM Tris-HCl pH 8.8, 0.1% *w/v* SDS, 0.1% *w/v* ammonium persulphate (APS) and 0.1% *v/v* tetramethylethylenediamine (TEMED). Resolving gels were covered with butanol and allowed to polymerise for at least 25 minutes. The butanol layer was then removed by washing twice with ddH_2O before adding the stacking gel layer. The stacking gel comprised 4% *v/v* acrylamide, 125 mM Tris-HCl pH 6.8, 0.1% *w/v* SDS, 0.1% *w/v* APS and 0.1% v/v TEMED, into which a comb (1 mm thick) was placed to create the wells; this was left to polymerise for ~20 minutes. Protein standards were loaded in one of the wells (PAGE Ruler Plus, Fermentas). In some experiments precast 10% acrylamide gels were used (Precise, Pierce). These required a running buffer of 100 mM Tris, 100 mM HEPES, 3 mM SDS, pH 8.

Protein samples (20 μL) were prepared by mixing with 5μL of 5× Laemmli buffer (# 39000; Pierce, UK) containing a pink tracking dye. The mixture was heated for 10 min at 95°C, and then loaded into the wells. Electrophoresis was performed at 100 V in running buffer (25 mM Tris-base, 192 mM glycine and 0.1% w/v SDS, pH 8) at R.T.

After electrophoresis, the gel was removed from the casing, and washed twice with ddH_2O for 10 min. The gel was then placed in solution that contained coomassie brilliant blue R-250 (Imperial Blue, Pierce) and left to incubate (1 hour, R.T., with agitation). The gel was then washed repeatedly with ddH_2O and left overnight for the bands to emerge.

2.2.6 Protein characterisation

2.2.6.1 Time course of activity

Time-course analyses of enzymatic reactions were performed, based on the MG assay (Section 2.2.5.1). Wells of a 96-well plate were filled with 2 μL of 10 mM Ins1P (final concentration: 1 mM) and Tris buffer to a final volume of 20 μL. 2 μL of each IMPase sample was added to each well along, or phosphate standards (in duplicate), and the plate was incubated at 37°C. The reactions were examined at successive time points (typically every ten minues) by the MG assay, and the phosphate produced was recorded against time.

2.2.6.2 Magnesium dependency assay

$MgCl_2$ concentrations (0 – 300 mM in Tris buffer) were used to assess magnesium dependence in IMPase enzymatic activity assays. The added concentration of magnesium was assumed to be the free concentration in solution. In 96-well plates, each well contained 2μL of IMPase and 16 μL of $MgCl_2$, and was incubated at R.T. for 5 min. Following subsequent addition of 1 mM Ins1P (final volume, 20 μL), the plate was left in a incubator (37°C, 60 min) and tested for activity by addition of 180 μL of MG reagent.

2.2.6.3 Effect of calcium

To determine the effect of calcium on the kinetics of the enzyme, a calcium clamping experiment was employed. As calcium is buffered by EGTA, free calcium in a solution containing EGTA can be calculated by using the program MaxChelator (version 5; C. Patton, University of Stanford, USA). $CaCl_2$ (1 μM – 10 mM) was dissolved in Tris buffer. 2μL of IMPase was incubated (5 min, R.T.) with 16 μL of the $CaCl_2$ containing buffer, followed by addition of Ins1P (final concentration, 1

mM) in the total volume of 20 μL in a 96-well plate. The plate was incubated for one hour, and then the inorganic phosphate was assessed using the MG assay.

2.2.6.4 Michaelis–Menten kinetics

2 μL of IMPase (in 16 μL of buffer) was added to each well of a 96-well plate followed by the addition of 2 μL of varying concentrations of Ins1P. The phosphate standards were added to the plate in duplicate and the plate was incubated at 37°C for 1 h. MG solution was then added and the absorbance was measured at 595 nm. The phosphate produced was evaluated by using the standard curve, and was plotted against substrate concentration.

In drug screening experiments, 2 μL of drug per vehicle was added to the enzyme in buffer, and the plate was incubated for 10 min at R.T., after which 2 μL of substrate was added to make the volume up to 20 μL. The V_{max} and K_m values were obtained from the graphs.

2.2.7 Mass spectrometry

IMPase (100 μM) was desalted using a Bio-Spin 6 Column (Bio-Rad, Hemel Hempstead, UK) in 15 mM ammonium acetate (pH 7.5). A stock solution (100 mM $MgCl_2$ in 20 mM HCl) was diluted to 500 μM $MgCl_2$ in ddH_2O. The protein was mixed with the $MgCl_2$ solution to give a solution with a final concentration of 10 μM protein, and 50 μM $MgCl_2$. This was incubated on ice for 15 min at 37 °C prior to non-denaturing electrospray ionisation mass spectrometry (ESI-MS) analysis. Data was acquired on a Q-TOF mass spectrometer (Q-TOF micro, Micromass, Altrincham, UK) connected to a Nanomate (Advion Biosciences, Ithaca, NY, USA) with a chip voltage of 1.70 kV and a delivery pressure 0.25 psi. The sample cone voltage was

typically 80 V- 100 V with a source temperature of 40 °C and acquisition/scan time of 10 s/1 s. Calibration and sample acquisition were performed in the positive ion mode (500–5,000 *m*/*z*). The pressure at the interface between the atmospheric source and the high vacuum region was fixed at 6.60 mbar. Data was processed with MASSLYNX 4.0 (Waters)[1].

The purified recombinant human IMPase protein was also subjected to matrix-assisted laser desorption/ionization analysis (MALDI) MS before and after tryptic digest, to confirm purity.[2] The molecular weights of the trypsin-digested peptides were measured and analysed with the program MASCOT (www.matrixscience.com). The purified protein was confirmed as IMPase by comparison with the fragmentation pattern predicted by the Expasy MS fragmentation software.

2.2.8 Crystallography

Crystals were grown using the sitting drop method (Figure 2.2.8). Both human and mouse recombinant IMPase proteins were crystallised using this method. Crystal screening was carried out using a Tecan Genesis Pro Team 150 Robot (Tecan, Theale, UK) and a Mosquito crystallisation robot (TTP Labtech, Melbourn, UK) in 96-well plates.

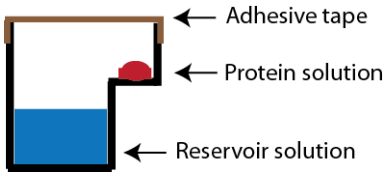


Figure 2.2.8. Sitting drop method for crystal formation. Each well contains a reservoir below a flat surface where the protein drop is placed.

[1] Performed by Dr. Esther Woon in Prof.. Schofield's laboratory, Dept. of Chemistry, University of Oxford.

[2] Performed by Dr Benjamin Thomas, Central Proteomics Facility, Sir William Dunn Pathology School, Oxford University.

2.2.8.1 Crystallisation of *Hs*IMPase 1

Commercial screens JCSG (Molecular Dimensions Limited, MDL), Wizard (Emerald Biosystems), Molecular Dimensions (MDL) I and II and Index (Hampton Research) containing various combinations of protein precipitating reagents were used. SwissSci 96-well 3 lens plates (# 3W96T-UVP) were used 100 nL of 10 mg/mL protein solution was placed in each well, and was mixed with the reagent at a ratio of 2:1, 1:1 or 1:2. The reservoir well contained 40 μL of reagent.

Apo-crystals were then soaked with a cryo-protectant, 50% *w/v* glycerol. Crystals were flash-cooled, collected at 100 K and stored in liquid nitrogen.

Data were collected at the European Synchrotron Radiation Facility (ESRF), Grenoble, France to 1.7 Å resolution at 100 K, using crystals of 150 μm. A Q315r ADSC detector was used(wavelength, 0.97625 Å). The data were processed with MOSFLM (Battye *et al.*, 2011) and SCALA (Evans, 2006), subjected to multiple repeated rounds of model building (COOT) (Emsley *et al.*, 2010) and refinement using (REFMAC5) (Murshudov *et al.*, 2011). Molecular replacement was carried out with PHASER (McCoy *et al.*, 2007) using a 2.1 Å resolution published structure (PDB 2HHM, (Bone *et al.*, 1992) to determine initial phases.

2.2.8.2 Crystallisation of recombinant *Mm*IMPase 1

The crystallisation of the recombinant *Mm*IMPase was carried out in SwissSci 96-well 2 lens plate (# MRC96T-UVP) using 100 nL of protein (7.5 mg/mL) in a 1:1 ratio with reagent. 50 μL of reagent was placed in the reservoir.

Crystals were soaked with a cryo-protectant, 33% *w/v* ethylene glycol, flash-cooled, collected at 100 K and stored in liquid nitrogen.

Data were collected at the Diamond Light Source, Didcot, UK to 2.2 Å resolution at 100 K, using crystals of 150 µm (beam wavelength 0.980 Å, size 120 µm x 80 µm). The detector type was ADSX Q315 CCD. The data were processed as above using molecular replacement.

2.3 Results

2.3.1 Cloning

IMAGE clones containing human and mouse *impa*1 cDNA were obtained as plasmids (Table 2.3.1). These were transformed into DH5α cells, cultured in the presence of the indicated antibiotic and stored for later use. The pRSET5a expression vector was similarly transformed into DH5α and stored.

Table 2.3.1. IMAGE clones

	IMAGE	Accession	Antibiotic
Human inositol (*myo*)-1(or4)-monophosphatase 1 (IMPA1)	3682657	BC009565	Chloramphenicol 34 μg/mL
Mouse inositol (*myo*)-1(or 4)-monophosphatase 1 (IMPA1)	6413389	BC055722	Ampicillin 50 μg/mL

To express the two proteins (*Hs*IMPase I and *Mm*IMPase I), the genes were first amplified from the IMAGE plasmids, ligated into pRSET5a and transformed into BL21(DE3) cells, as detailed in the following sections.

2.3.1.1 PCR amplification of *impa* cDNA

Sequence data for the two cDNAs (BC009565, BC055722) were obtained from GenBank, and compared by BLAST search against the genomic reference database (NCBI) to confirm that the reported IMAGE sequences were 100% accurate. The sequences were then submitted to NEB Cutter to identify restriction sites of the pRSET multiple cloning site (MCS) that were absent from the cDNA sequences. Both *NdeI* and *PstI* were thus identified (for both genes), and primers were designed

accordingly so that these sites would be appended 5′ and 3′ of the PCR-amplified genes, respectively. Primers were designed manually (Table 2.3.2).

Table 2.3.2 Primers for PCR amplification of human and mouse *impa*1 cDNA. Restriction sites (fwd: *NdeI*, rev: *PstI*) are underlined.

cDNA	Name	Orientation	Sequence (5′ - 3′)
Human ***Hs*555086**	Hs_F	Forward	AATATTTTCAGCATATGGCTGATCCTTG
	Hs_R	Reverse	ATGACTATGAGCTGCAGTAATTAATCTTC
Mouse ***Mm*183042**	Mm_F	Forward	AGGCATATGGCAGACCCTTGGCA
	Mm_R	Reverse	AGGCTGCAGTAATCAGTCTAAATCAGTGAC

Using the IMAGE clones as templates with the above primers, the genes were amplified by PCR at three different annealing temperatures: 50°C, 55°C and 65°C and the products examined on agarose gel (Figure 2.3.1).

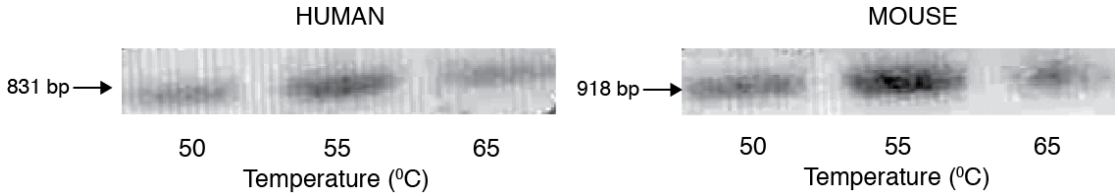


Figure 2.3.1. PCR amplification of impa1 genes at three annealing temperatures.

Products were obtained at the expected sizes (831 bp and 918 bp) as determined from the locations of the primers relative to their respective cDNA sequences. The optimum temperature for amplification was found to be 55°C, so this was used in a subsequent PCR amplification.

DNA from the second PCR amplification was extracted from the gel and purified.

In separate reactions, the two PCR products and the pRSET5a vector were co-digested with restriction enzymes *NdeI* and *PstI* in NEB buffer C. The three digested products were then electrophoresed on agarose gel to isolate the digested DNA and purified, as above.

The concentrations of the digested products were determined spectrophotometrically, and ligation reactions were performed to obtain expression vectors pRSET-*Hs*Impa1 and pRSET-*Mm*Impa1. The ligation products were then transformed into competent JM109 cells and cultured overnight in the presence of ampicillin (pRSET5a resistance).

Plasmids were extracted from the cultured cells. A small sample was taken from each (2 μL), digested with *NdeI* and *PstI*, and examined on a gel to confirm that the plasmids contained inserts of the expected sizes (Figure 2.3.2).

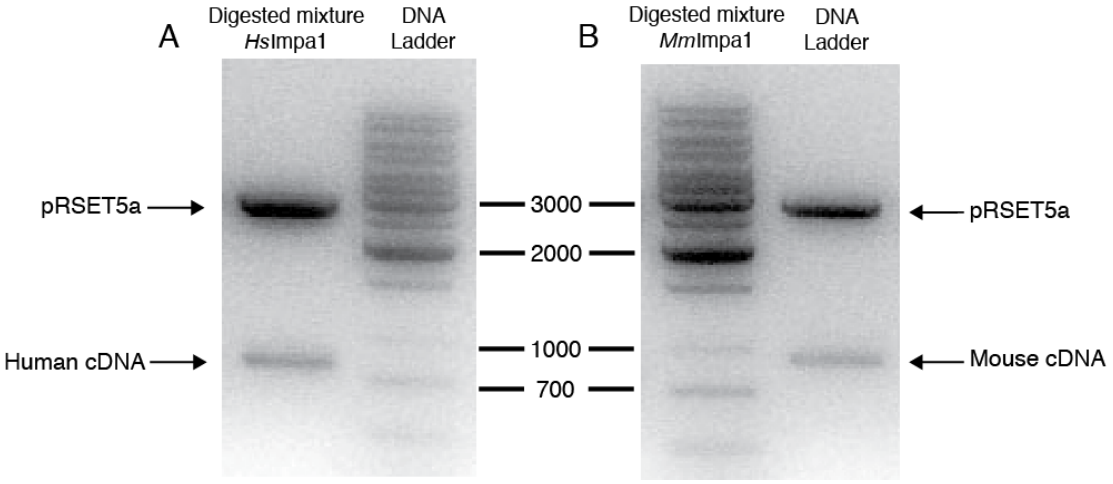


Figure 2.3.2 Analysis of *impa*1 genes cloned into pRSET5a. A) Human and B) mouse *impa*1 vectors were digested with NdeI and PstI and electrophoresed on agarose gel. The top band is linear pRSET5a vector (~2800 bp) and the lower band is the *impa*1 insert (~850 bp).

A further 2 μL of each was used to transform the plasmids into the BL21(DE3) pLysS expression cells. The remainder was dissolved (10 ng/μL) in 10

mM Tris-HCl (pH 8.5) and submitted for sequencing (Geneservice, Oxford, UK). This confirmed that no errors had been introduced into the gene sequences.

2.3.2 Protein expression

The combination of pRSET5a vector and BL21(DE3) host cells has previously been used successfully to express IMPase protein (Diehl *et al.*, 1990; McAllister *et al.*, 1992). In this system, addition of IPTG induces expression of a chromosomally encoded T7 bacteriophage polymerase under control of a modified *lac* promoter. The gene of interest is located immediately downstream of a T7 promoter on pRSET5a, so is transcribed/translated by the expressed T7 polymerase.

First, the BL21(DE3) cells harbouring the pRSET clones containing human and mouse *impa1* genes were cultured to confirm satisfactory exponential growth. From overnight cultures, 1 mL was placed in 100 mL LB containing 50 μg/mL ampicillin and incubated (37°C, 180 rpm). Samples were taken every 30 min and assessed for cell density by measuring optical density (OD, absorbance at 600 nm), until OD_{600} reached 0.9 (Figure 2.3.3).

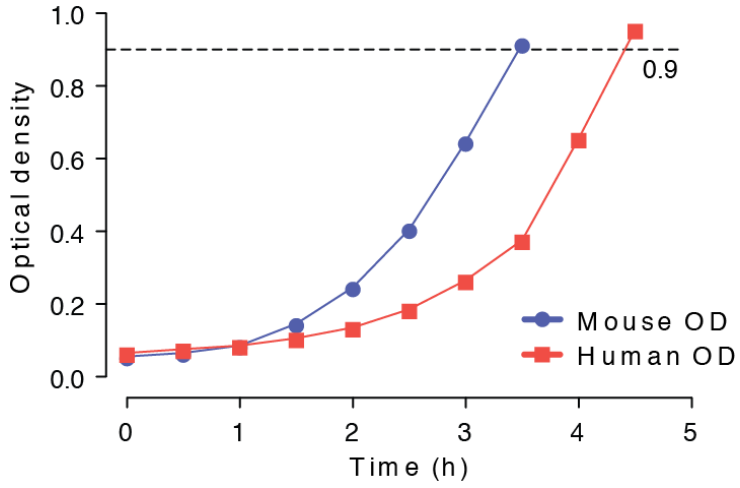


Figure 2.3.3 Time course of growth of BL21(DE3) pLysS containing human or mouse *impa1*. Protein expression is induced by IPTG when the cell density reaches $OD_{600} = 0.9$.

To optimise the yield of functional protein, various expression conditions were tested, including medium composition, duration of expression and temperature (Table 2.3.3). In all cases the base medium was 25 g/L LB. The final expression conditions used were those for Batch G.

Table 2.3.3 Optimisation of expression conditions. Different expression conditions (Batches A–H) for human and mouse IMPase were used to achieve optimal protein expression.

Name	Media additives	Time (h)	Temperature (°C)	Shaking (rpm)
Batch A	-	16 h	37°C	180
Batch B	-	5 h	37°C	180
Batch C	-	24 h	37°C	180
Batch D	50 μg/mL ampicillin	5 h	37°C	180
Batch E	50 μg/mL ampicillin	24 h	37°C	180
Batch F	-	16 h	30°C	180
Batch G	660 mM sorbitol, 2.5 mM betaine	16 h	30°C	180
Batch H	660 mM sorbitol, 2.5 mM betaine	5 h	37°C	200

Following induction, soluble protein was isolated, the protein concentration was measured and the specific activity was determined to discover which Batch condition would yield the optimum performance (Figure 2.3.4).

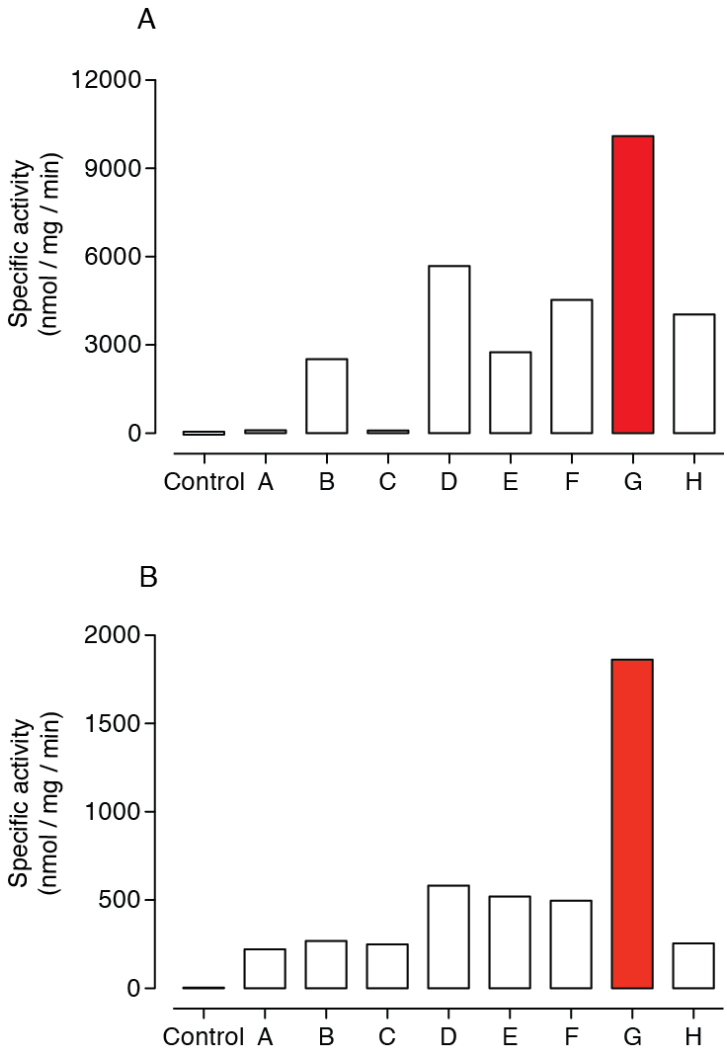


Figure 2.3.4. Specific activity under the tested expression conditions. A) Recombinant *Hs*IMPase activity, and **B)** recombinant *Mm*IMPase activity. In both cases, batch G was found to have the highest specific activity. Control: BL21(DE3) transformed with pRSET5a containing no insert (n=1).

The conditions for Batch G (660 mM sorbitol, 2.5 mM betaine, 16 h overnight growth at 30°C) proved optimal. The protein concentration in the case of the *Hs*IMPase 1 and *Mm*IMPase 1 was ~5 mg/mL. The 'Batch G' parameters were used in all further experiments.

Next, *Hs*IMPase 1 and *Mm*IMPase 1 were expressed in 1 L cultures (as above), sonicated, and centrifuged to separate soluble and insoluble (membrane)

protein fractions. The latter was resuspended in Buffer A. The fractions were analysed for protein distribution by denaturing SDS-PAGE (Figure 2.3.5).

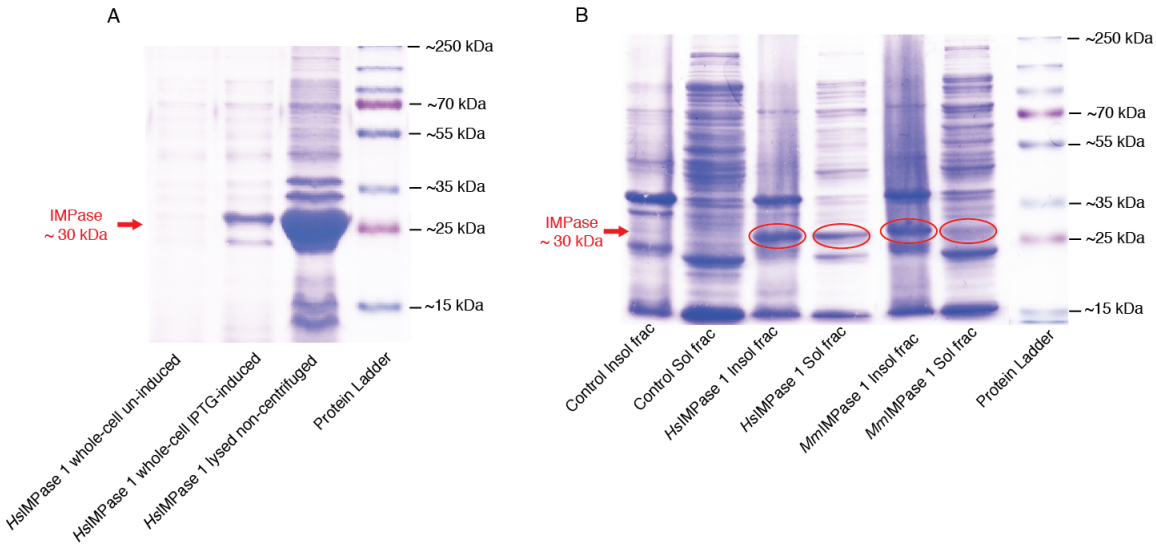


Figure 2.3.5. SDS-PAGE showing protein content in the different fractions during protein purification. A) The three fractions shown are the whole cell fraction (non-induced), whole cell fraction (IPTG-induced) and the induced and lysed cell fraction, containing both the soluble and insoluble *Hs*IMPase 1 protein. **B)** The fractions here show the soluble and insoluble fractions (resuspended in Buffer A) for the control, *Hs*IMPase 1 and *Mm*IMpase 1. The control was BL21(DE3) transformed with pRSET5a containing no insert..

This confirmed that both human and mouse IMPase was being expressed at about 28 kDa. Since IMPase is a homodimer of 60 kDa, after denaturing the expected band for IMPase would be around 30 kDa. It also revealed the presence of interfering bands (i.e. protein of similar mass to IMPase) at around 25kDa that would be of particular concern in subsequent purification. It was also evident that there was an IMPase band in the insoluble fractions.

2.3.3 Protein purification

In light of the presence of the 25 kDa 'interfering band', it was decided that, instead of single-stage anion exchange with Mono-Q (as used previously for

*Hs*IMPase; (McAllister *et al.*, 1992), a two-step anion exchange protocol would be employed: Q-sepharose followed by Mono-Q.

Prior to chromatography, the soluble cell lysate fraction was heated at 68°C for 1 h, as per McAllister *et al.*, 1992, and centrifuged at 30,000×g for 30 min at 4°C.

The traces are representative of both the human and mouse IMPase 1 proteins.

2.3.3.1 Anion exchange chromatography

The heated soluble fraction was passed through a Q-sepharose column for anion exchange chromatography. This was performed in an attempt to separate the interfering band and also to reduce the protein load before passing through the Mono-Q column (the next stage of purification). The fractions collected were all tested for IMPase phosphatase activity and the active fractions were then separated on SDS-PAGE reducing gel.

The active fractions were found to be 11 to 37, with the highest activity in fractions 18–25 (Figure 2.3.6). It was only possible to separate the interfering band slightly (it overlaps quite considerably with the active fractions. It seemed that in trying to purge the interfering band, a lot of the IMPase protein would also be lost. The SDS-PAGE gel showed that most of the interfering band at ~ 25 kDa seemed to be in the latter half of the active fractions and was inactive in the MG assay. Hence, the fractions 16 – 25 were combined and dialysed, while the rest were discarded.

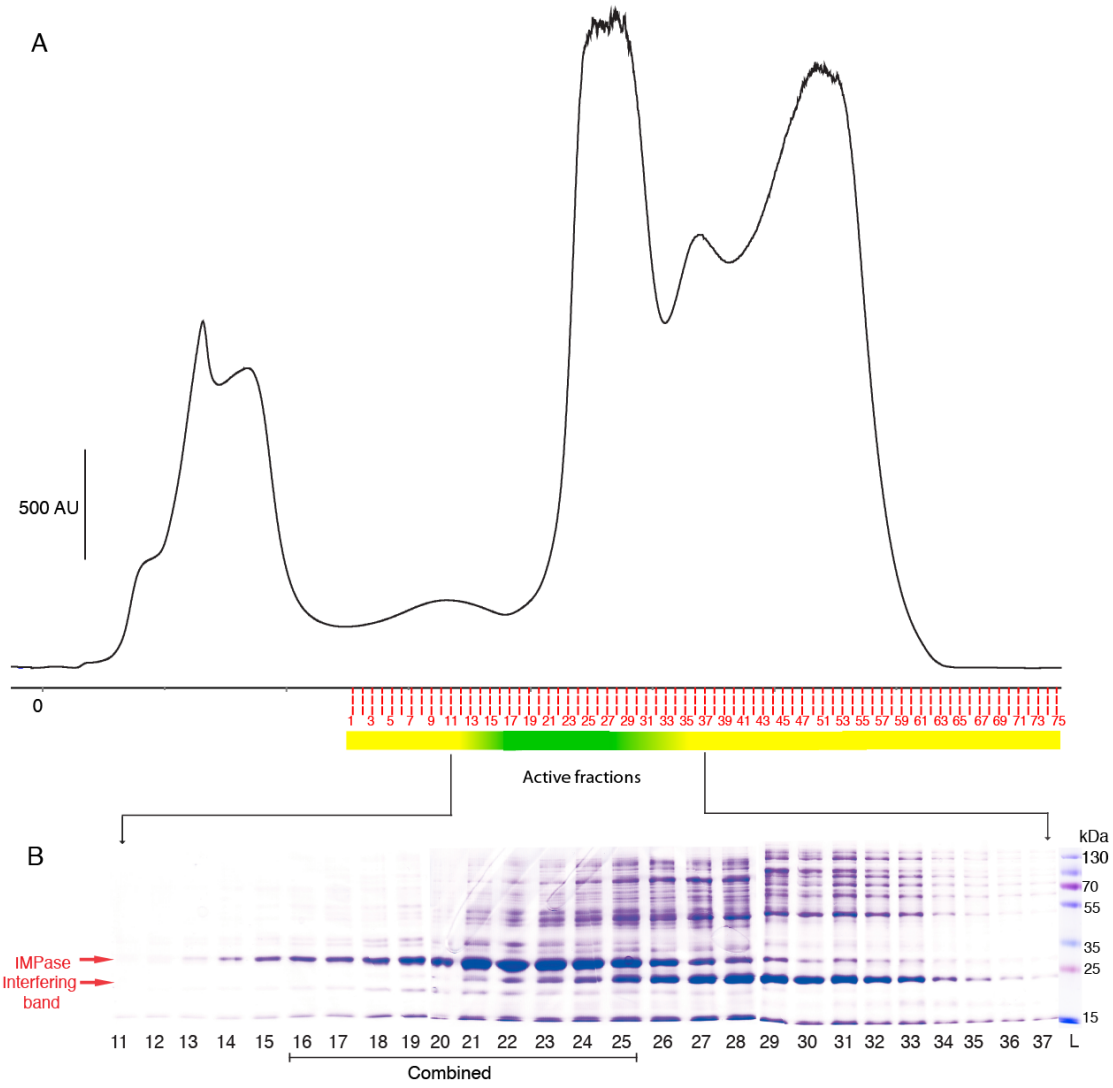


Figure 2.3.6. Example Q-sepharose anion exchange chromatogram showing the purification of *Hs*IMPase 1 and *Mm*IMPase 1. Recombinant IMPase expressed in BL21(DE3)pLysS was run on a Q-Sepharose Hi-Load 16/10 FF column. **A)** Black line shows UV absorption at 280 nm. Collected fractions are labelled in red. Beneath: active (green) and inactive fractions (yellow) as determined by an MG assay. **B)** SDS-PAGE of active fractions (fraction 11–37). The IMPase band and the 'interfering band' are identified (red arrows). 'L' denotes the protein ladder.

After dialysis and concentration, it was found to be necessary to add a reducing agent before proceeding with the next stage of chromatography (Mono-Q anion exchange). The protein was initially purified without the addition of a reducing agent, and this caused it to aggregate. It precipitated and not did separate into its individual components, but as a single high molecular weight aggregate which eluted in the void volume in the final stage of size exclusion chromatography. It was

hypothesized that the free cysteine groups present in the protein were causing it to aggregate and hence, a reducing agent would be required. Addition of 20 mM β-mercaptoethanol resolved the aggregation problem.

Following Mono-Q chromatography (Figure 2.3.7), a gel was prepared using the fractions that had exhibited IMPase activity (MG phosphatase assay; fractions 7–24), When these fractions were run on the gel they were found to have the desired IMPase band at around 28 kDa. Most of the fractions did not show the interfering band, except for fractions 22 and 23, where it was very faint. Fractions 10 – 23 were combined before concentrating and further purification by size exclusion chromatography. It was important to ensure, as far as possible, elimination of the interfering band as size exclusion chromatography is not capable of separating IMPase (~28 kDa) from a protein at 25 kDa.

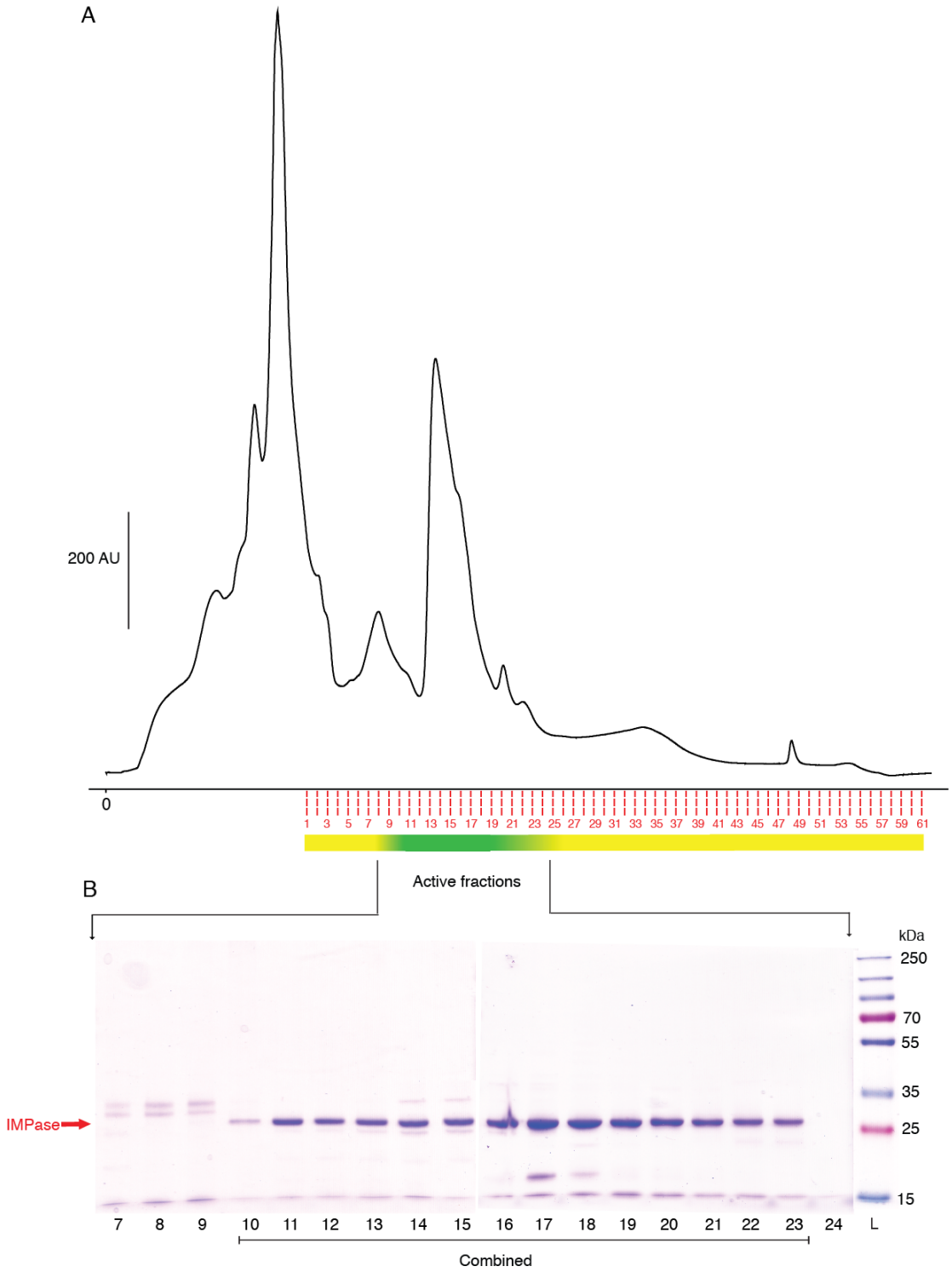


Figure 2.3.7. Example Mono-Q anion exchange chromatogram showing the purification of *Hs*IMPase 1 and *Mm*IMPase 1. The combined active fractions from Q-sepharose (16–25) were dialysed and run on a Mono-Q GL 5/50 column. **A)** Black line shows UV absorption at 280 nm. Collected fractions are labelled in red. Beneath: active (green) and inactive fractions (yellow) as determined by an MG assay. **B)** SDS-PAGE of active fractions (fraction 71–24). The IMPase band is identified (red arrow). 'L' denotes the protein ladder.

2.3.3.2 Size exclusion chromatography

The final stage of chromatographic purification was size exclusion with a GE Superdex-75 column (Figure 2.3.8) using the active fractions from the previous step.

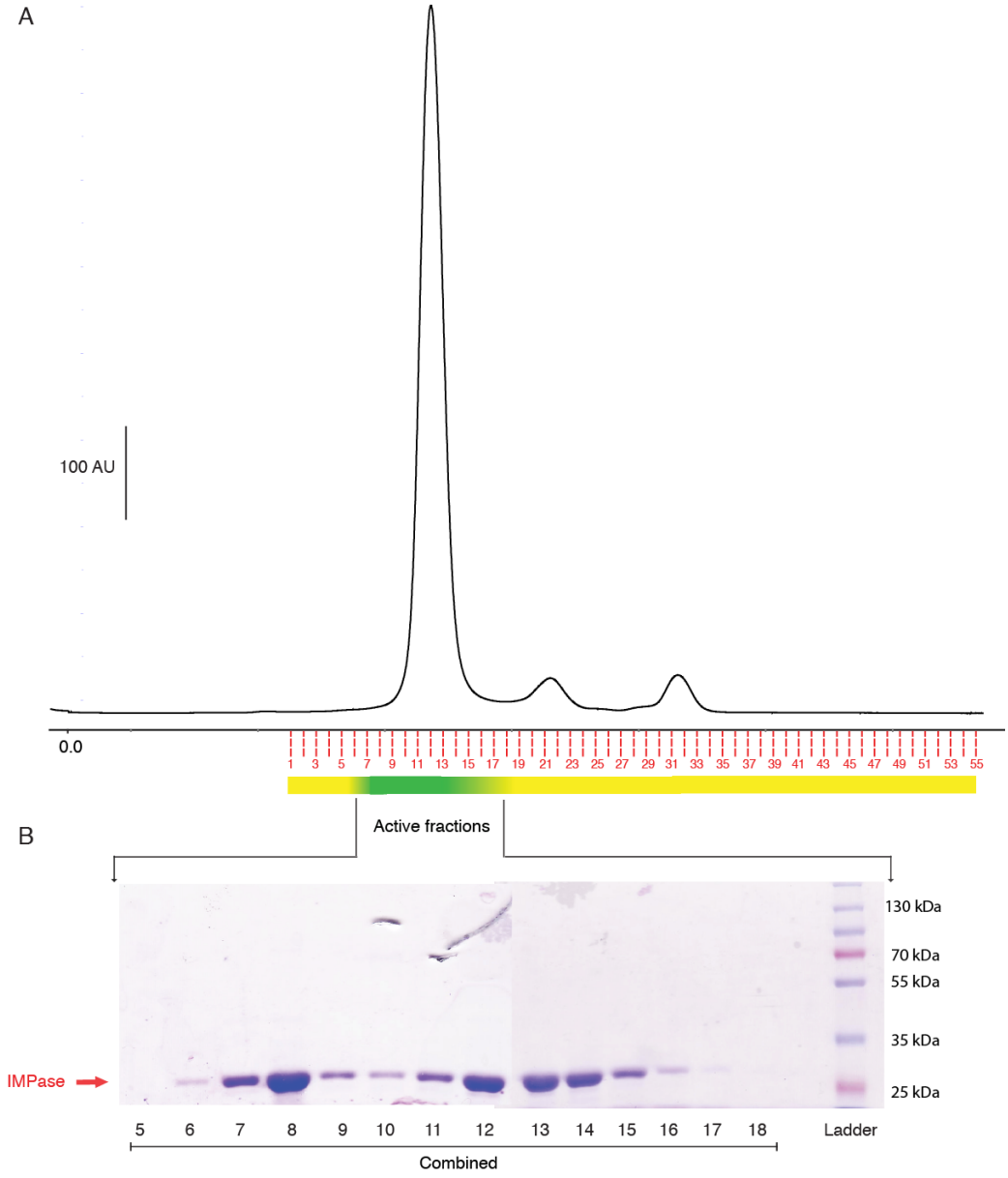


Figure 2.3.8. Example Superdex-75 size exclusion chromatogram showing the purification of *Hs*IMPase 1 and *Mm*IMPase 1. Enzymatically active fractions from Mono-Q exchange were combined and concentrated before being passed through the Superdex-75 10/300 GC column. **A)** Black line shows UV absorption at 280 nm. Collected fractions are labelled in red. Below: active (green) and inactive fractions (yellow) were identified by using the MG phosphatase assay. **B)** SDS-PAGE of fractions that were found to have IMPase activity (fraction 5–18).

In figure 2.3.8, it looks as though there were two IMPase peaks present. This was not the case, and unfortunately, there was improper gel loading which is why it looks that way. The active fractions after gel filtration were found to be 5–18. These were combined and concentrated to ~10 mg/mL for crystallography. Figure 2.3.9 shows an SDS-PAGE gel of denatured protein size composition following the purification steps.

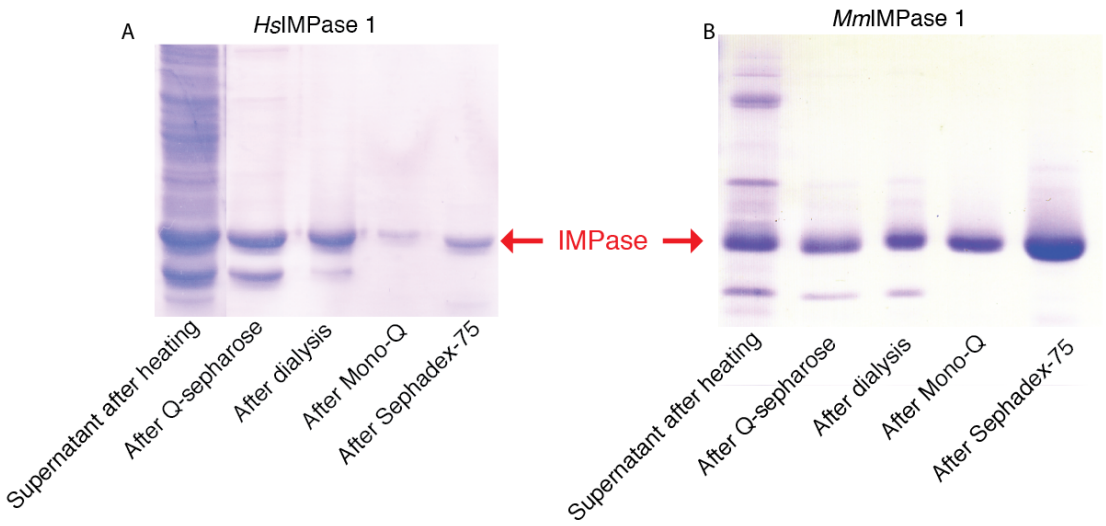


Figure 2.3.9. Protein content at different stages of purification. A) *Hs*IMPase **B)** *Mm*IMPase. Left to right: soluble protein fraction after heating for 1 h at 68°C; combined fractions after Q-sepharose; after diaslysis; combined eluate after Mono-Q; gel filtration through Superdex-75.

The gel images suggest that the mouse protein content was higher than that of the human. However, both had approximately the same amounts of protein: this anomaly probably arose since the gels were not normalised for protein content. One happened to be more concentrated than the other.

Following the purification steps, total IMPase yield was estimated at ~20% of the initial protein.

2.3.4 Protein characterisation

The enzymatic action of IMPase allows a simple assay for activity detection, as utilized in the purification (above). It also has characteristic properties that distinguish different isoforms, such as inhibition by lithium, calcium, manganese, high concentrations of magnesium (> 5 mM) (Hallcher and Sherman, 1980) and beryllium (Faraci *et al.*, 1993). This section reports characterisation of the purified enzymes.

Finally, mass spectroscopy was performed to further confirm correct identification of the enzyme, and ensure sufficient purity for crystallography. It was also necessary to check that the purified protein was sufficiently stable for further mass spectroscopy involving bound molecules.

2.3.4.1 Time-course assays

Using the recombinant human and mouse IMPase I, together with commercially available bovine IMPase, time-course studies of the phosphatase activity were performed to determine the linear region of the activity under particular conditions, From the results of these tests (Figure 2.3.10) it was determined that, for these samples, a 60 min time point was chosen as the limit for all further assays.

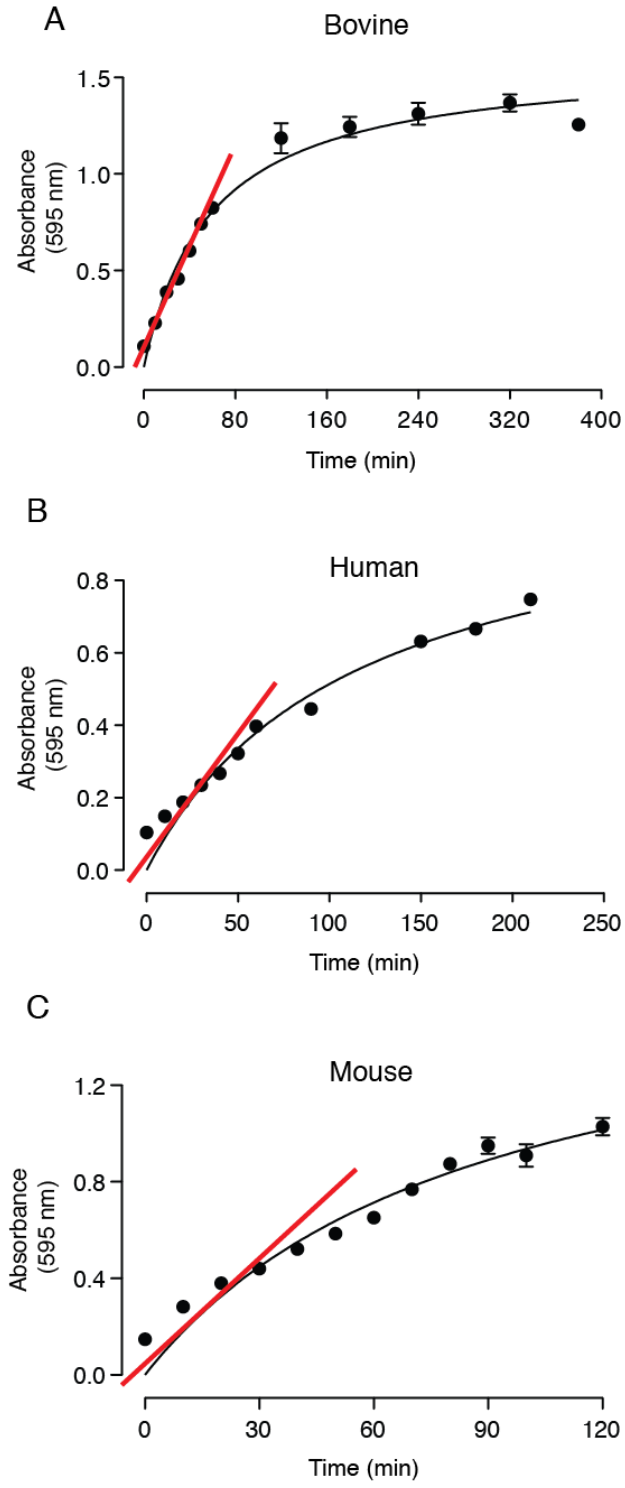


Figure 2.3.10. Time-course of IMPase activity. A) bovine, B) human and C) mouse IMPase activity was recorded at different time points with 1 mM Ins1P by measuring absorbance at 595 nm in an MG assay. The red line shows the linearity phase of IMPase activity. Since samples of all the three isoforms were linear within 1 h, this was chosen for all further IMPase assays, unless otherwise required.

2.3.4.2 Magnesium dependence

It is known that IMPase has a requirement for magnesium, but that activity is inhibited by high concentrations. Assays were performed with the human, mouse and bovine enzymes to assess the dependency on magnesium concentrations using the conditions for the time-course assay (above) and allowing a 60 min reaction time (Figure 2.3.11).

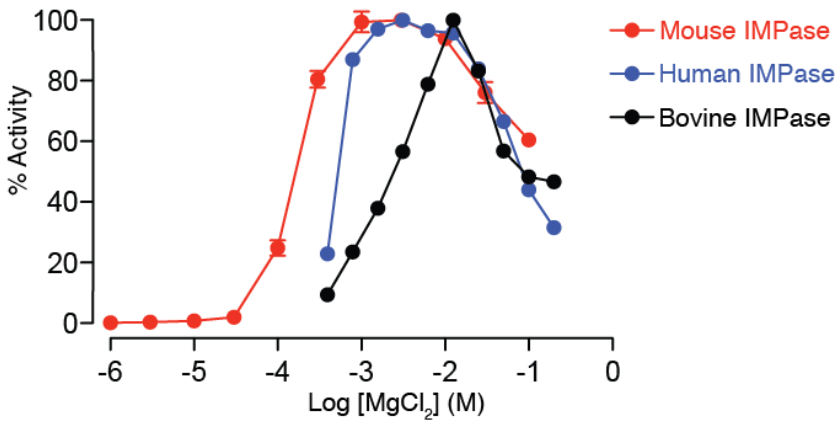


Figure 2.3.11. Effect of magnesium concentration on IMPase activity. The results showed the expected peak in activity, with declining activity as Mg^{2+} concentrations were reduced or increased. All three isoforms of IMPase, bovine, human and mouse, show this trend.

The enzyme shows characteristic magnesium dependence curve. The human enzyme appears more sensitive to magnesium concentration, consistent with the findings of McAllister (McAllister *et al.*, 1992). It is maximally activated at a lower concentration than the bovine enzyme. The latter exhibits a sharp peak at optimum activity, whereas the human enzyme shows a broader peak. Activity is progressively inhibited above ~10 mM of magnesium. The optimum magnesium concentration for the human enzyme is about 3 mM, and 10 mM for bovine. The mouse IMPase shows a similar trend to the human. These values are consistent with the reported values (Gee *et al.*, 1988) and thus confirm that at concentrations above 10 mM, magnesium becomes inhibitory, in all three cases.

2.3.4.3 Effect of calcium

A similar assay was performed to examine the reported inhibitory effects of calcium (Figure 2.3.12).

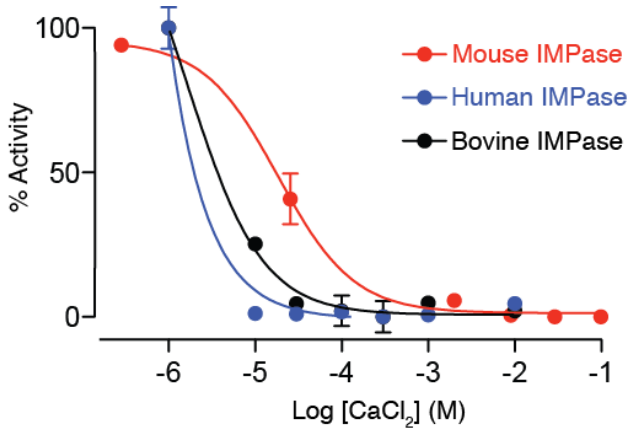


Figure 2.3.12. Effect of calcium on IMPase activity. Ca^{2+} becomes inhibitory above 1 µM (n = 2-3).

Bovine, human and mouse IMPase activity was found to be sensitive to the inhibitory effects of calcium (Figure 2.3.12). At 10 µM $CaCl_2$, the human IMPase was effectively completely inhibited (the bovine isoform was ~70% inhibited at this concentration) and the mouse IMPase was about 40% inhibited.

2.3.4.4 Enzyme kinetics

To establish enzyme kinetics parameters for the IMPase phosphatase reaction, assays were performed at different concentrations of substrate, Ins1P. Graphs were plotted to analyse the kinetics (Figure 2.3.13).

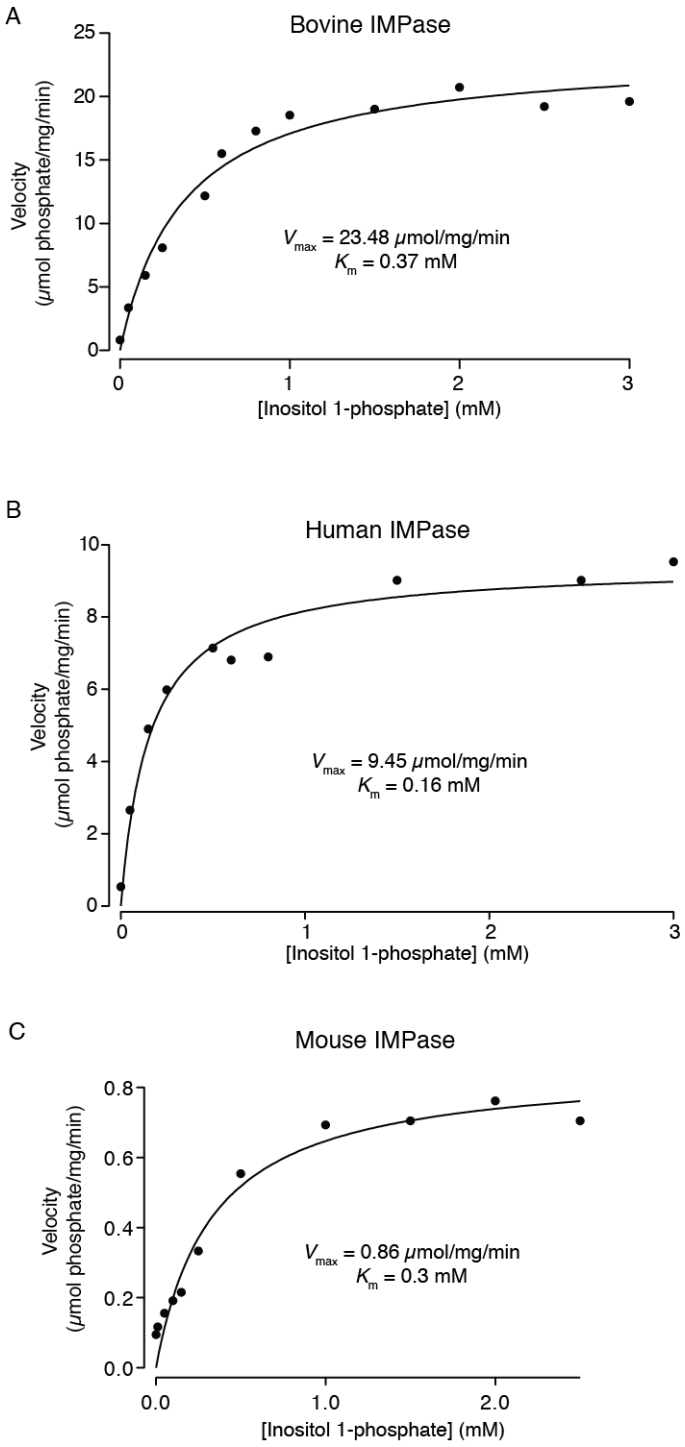


Figure 2.3.13. IMPase kinetics analysis. Michaelis–Menten kinetics curves for **A)** bovine **B)** human and **C)** mouse IMPase. Reactions were stopped after 60 min. (n=1) These are representative traces and the experiment has been repeated.

The graphs record velocity of the reactions against substrate concentration. From these, K_m and the V_{max} of the enzymatic reaction were calculated. K_m and V_{max}

for *Hs*IMPase 1 were found to be 0.16 ± 0.03 mM and 9.45 ± 0.39 μmol/mg/min, respectively. For *Mm*IMPase K_m was 0.3 ± 0.07 mM and V_{max} was 0.86 ± 0.06 μmol/mg/min. The human K_m value is comparable with previously reported values for bovine and human recombinant enzymes (Gee *et al.*, 1988; McAllister *et al.*, 1992). However, V_{max} value was about 5 times lower than previously reported (McAllister *et al.,* 1992), although it was comparable to that derived from the bovine brain. In case of the mouse IMPase, V_{max} was lower than that of the human isoform, while K_m was comparable. The bovine IMPase had a V_{max} value of 23.48 ± 1.06 μmol/mg/min, and K_m of 0.37 ± 0.06 mM.

2.3.4.5 Mass spectrometry

Mass spectroscopy of the trypsin digested IMPase and non-denatured protein was used to confirm the identity of the protein before crystallisation. The fragmentation pattern obtained from the trypsin-digested protein was similar to the pattern predicted by Expasy software (results not shown). The non-denaturing mass spectrum showed a single clean peak, which had a mass of about 60 kDa, which is the mass of the IMPase dimer (Figure 2.3.14). Mass spectrometry also confirmed that protein was of sufficient purity (> 95%) for crystallography.

The mouse IMPase 1 mass spectroscopy was not carried out.

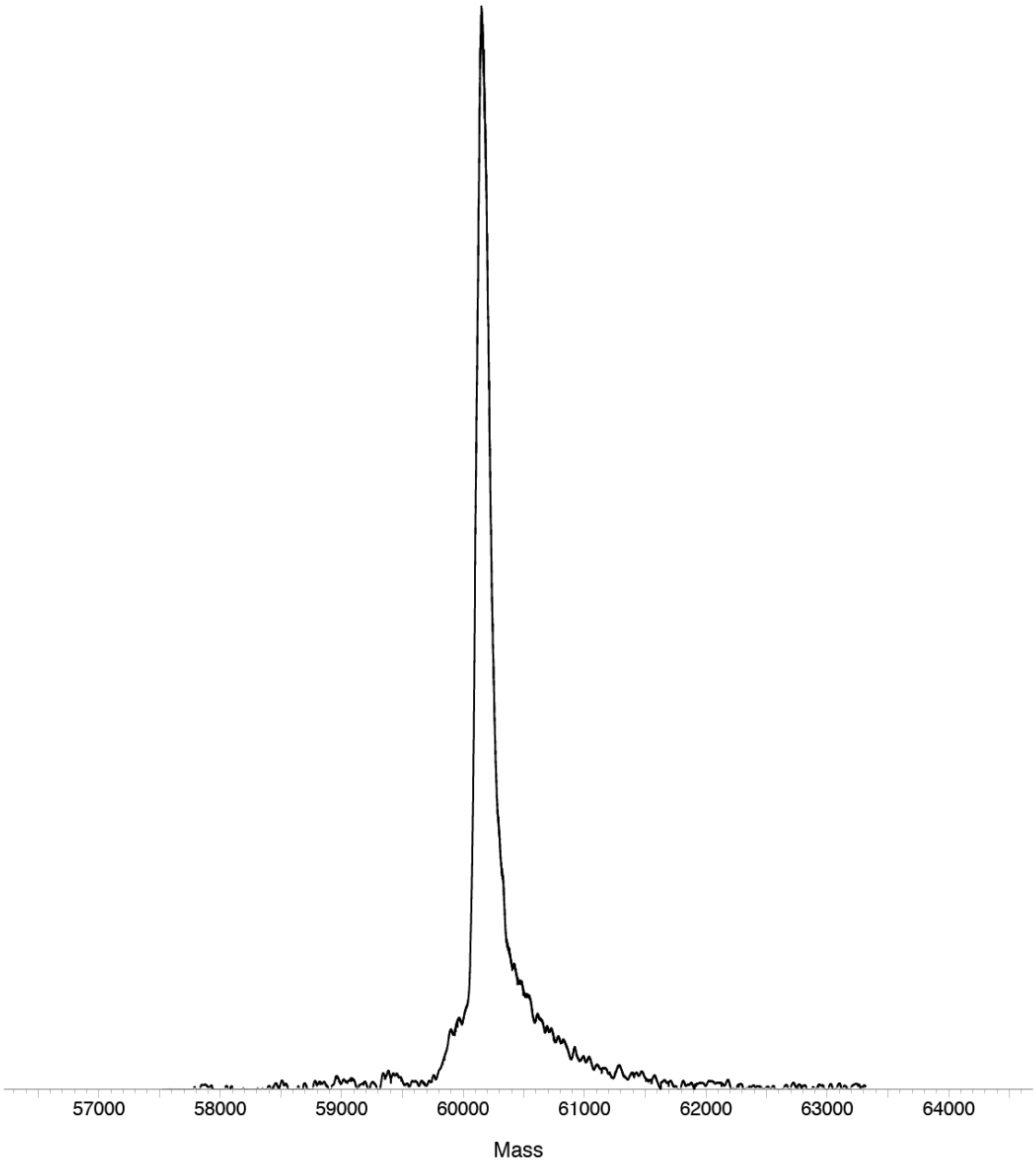


Figure 2.3.14. Non-denaturing mass spectrum of *Hs*IMPase 1. A single clean peak is observed with a mass of 60150.25 Da.

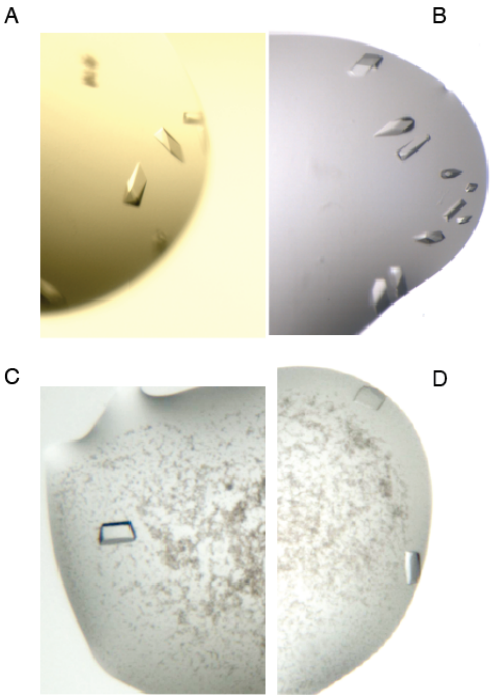
2.3.5 Crystallography

Using commercial kits, crystals were successfully grown for both human and mouse recombinant enzymes. Both proteins crystallised under conditions requiring high magnesium concentrations. The initial mouse screen for crystals was performed

without magnesium, but no crystals were observed. Magnesium was then added to the enzyme and then screened around different condition.

A number of different conditions produced crystals within a few days (Figure 2.3.15). The optimum conditions for human protein crystallisation were found with JCSG well A5. This contained 0.2 M magnesium formate and 20% w/v PEG 3,350. A 24-well crystal plate (Axygen Bioscience, Union City, USA) was then used for two-dimensional screening around the JCSG A5 conditions, (36 to 46% PEG and 0.1 to 0.25 M magnesium formate). The protein (10 mg/mL) and the precipitating reagent was added in a 1:1 ratio. This refined the optimum conditions to 40% PEG 3350 and 0.2 M magnesium formate. The optimum temperature was R.T.

The initial screen for *Mm*IMPase 1 was carried out both R.T. and 4°C, using commercial screens: JCSG, Morpheus, Proplex, PGA, PACT (all from MDL) and PEG-ION (Hamptons Research). None of these screens proved successful. The conditions were repeated using 7.5 mg/mL protein with 100 mM $MgCl_2$ or 20 mM β-mercaptoethanol, and the experiment was repeated at 4°C. Crystals were obtained under some conditions; the best were wells G3 and H3 of the PACT screen (G3: 0.2 M NaI, 20% *w/v* PEG 3350, 0.1 M Bis Tris propane, pH 7.5; H3: as G3 but pH 8.5) (Figure 2.3.15).



	A	B
	Human IMPase JCSG: Well A5, R.T. 0.2 M Magnesium formate, 20% w/v PEG 3350	Human IMPase INDEX: Well G12, R.T. 0.2 M Magnesium chloride hexahydrate, 0.1 M HEPES pH 7.5, 25% w/v PEG 3350
C	Mouse IMPase + 0.1 M magnesium chloride PACT: Well G3, 4ºC 0.2 M sodium iodide, 0.1 M Bis Tris propane pH 7.5, 20% w/v PEG 3350	Mouse IMPase + 0.1 M magnesium chloride PACT: Well H3, 4ºC 0.2 M sodium iodide, 0.1 M Bis Tris propane pH 8.5, 20% w/v PEG 3350
		D

Figure 2.3.15. IMPase crystals. **A)** and **B)** *Hs*IMPase crystals. **C)** and **D)** *Mm*IMPase crystals. The table on the right gives the crystallisation conditions.

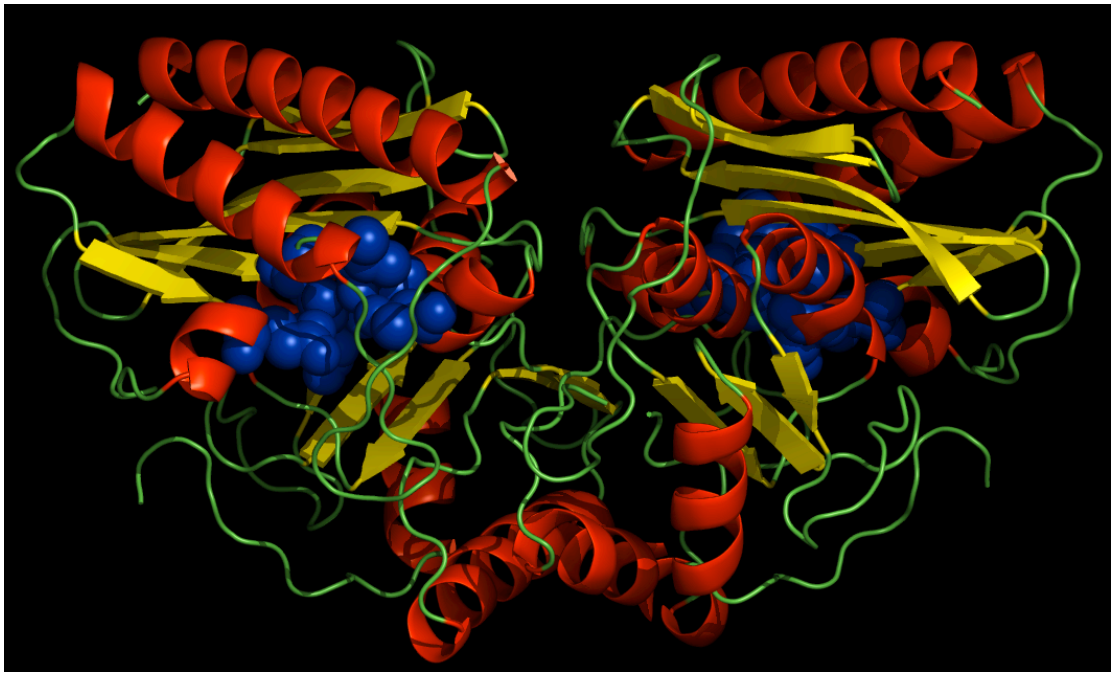


Figure 2.3.16. Crystal structure of human IMPase 1 at 1.7 Å. The individual monomers can be seen with the active site residues highlighted as blue spheres.

The crystal structure of human IMPase 1 (Figure 2.3.16) was obtained using molecular replacement of the structure present in the protein data bank (PDB 2HHM). The R and R_{free} values were 0.165 and 0.206, respectively. The completeness of the structure was 99.4% (Table 2.3.4).

Table 2.3.4. Refinement statistics for *Hs*IMPase 1. The table shows the refinement statistics for the crystal structure. The values in parentheses are for the highest resolution shell (1.7 Å).

Parameter	Value
Space group	$P2_12_12_1$
Unit-cell parameters (Å)	a = 60.68, b = 76.05, c = 118.09
Resolution (Å)	47.43 – 1.700 (1.79-1.7)
R merge %	0.047 (0.442)
I/σ(I)	15 (2.2)
Number of unique reflections	60344 (8763)
Average Multiplicity	4.7 (4.8)
Completeness (%)	99.3 (100.0)
R_{work}	0.154
R_{free}	0.186
Mean B value (Å^2)	33.14
Bond length (Å)	0.01
Bond angle (Å)	1.12

A similar structure was obtained for *Mm*IMPase (Figure 2.3.17). [3]

[3] Dr. Ed Lowe helped to carry out the crystallization experiments as well as with the refinement of the structures.

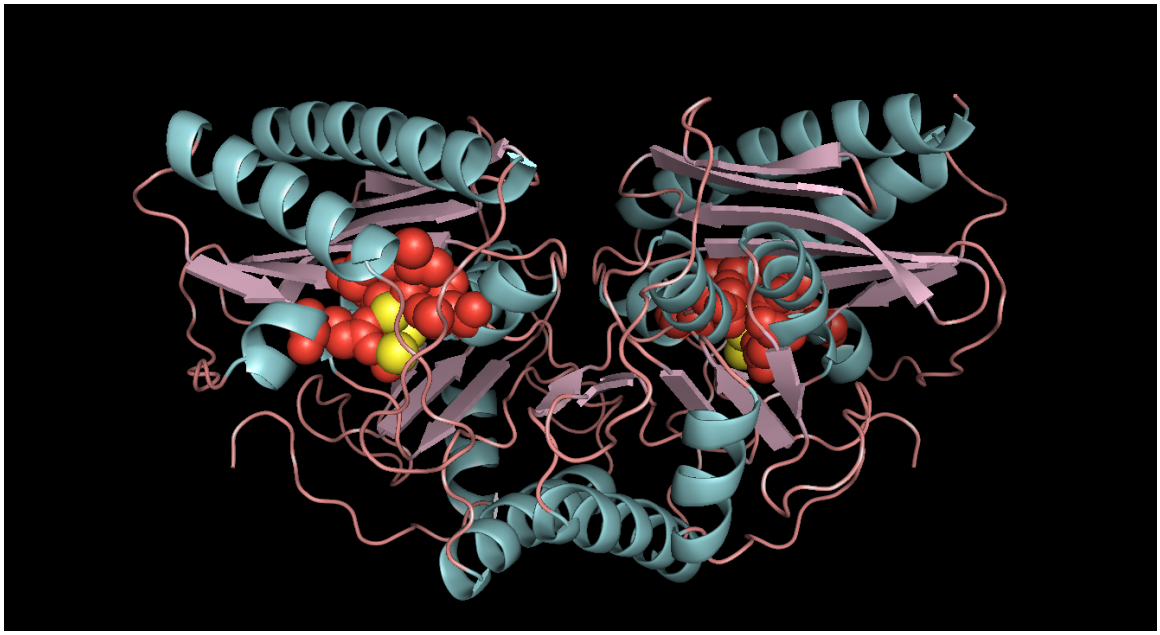


Figure 2.3.17. Crystal structure of *Mm*IMPase. The crystal structure of the mouse IMPase at a resolution of 2.2 Å. The red spheres represent active site residues and the yellow sphere represent the three magnesium cations coordinated in the active site. This coordination is shown in Figure 2.3.18.

The figure below, 2.3.18, shows the three magnesium ions being coordinated by the active site residues of the *Mm*IMPase 1. This is similar to that observed in previous studies using the bovine and human IMPase 1 (Gill *et al.*, 2005; Pollack *et al.*, 1993).

The mouse structure needs further refinement and hence the table of refinement statistics is not shown here.

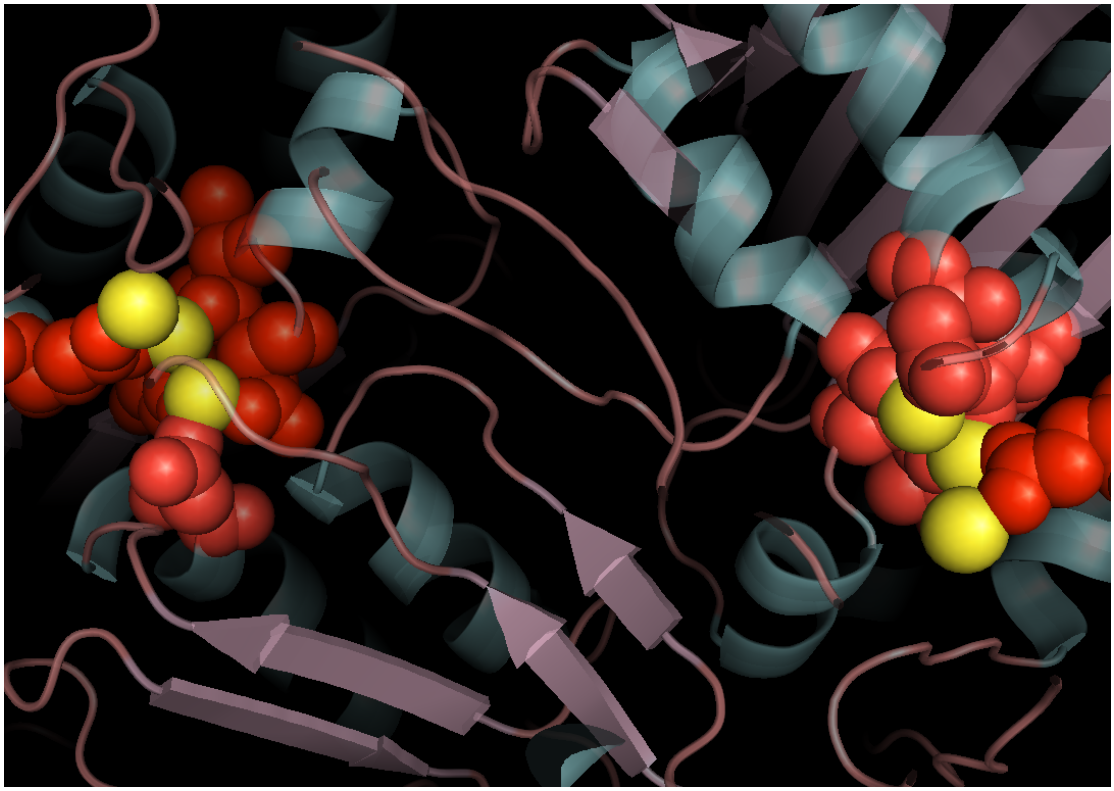


Figure 2.3.18. Coordination of the three magnesium ions. The yellow spheres present the magnesium ions. The red spheres represent the negatively charged residues, Glu-70, Asp-90, Ile-92, Asp-93 and Asp-220, are believed to be coordinating the three magnesium ions in the *Mm*IMPase 1.

When the *Hs*IMPase 1 and the *Mm*IMPase 1 are overlaid, there is no evident structural divergence between human and mouse IMPase 1 (Figures 2.3.19).

A

```
  1 MADPWQECMDYAVTLARQAGEVVCEAIKNEMNVMLKSSPVDLVTATDQKV   50
    |||||||||||||.|||||||::.||:||||:||:||||.||||.|||||
  1 MADPWQECMDYAVILARQAGEMIREALKNEMDVMIKSSPADLVTVTDQKV   50

 51 EKMLISSIKEKYPSHSFIGEESVAAGEKSILTDNPTWIIDPIDGTTNFVH  100
    ||||:||||||||.|||||||||||||::.|:.|||:||||||||||||
 51 EKMLMSSIKEKYPCHSFIGEESVAAGEKTVFTEQPTWVIDPIDGTTNFVH  100

101 RFPFVAVSIGFAVNKKIEFGVVYSCVEGKMYTARKGKGAFCNGQKLQVSQ  150
    ||||||||||||.|||::|||:||||||.||||.||||||||||||||||
101 RFPFVAVSIGFLVNKEMEFGIVYSCVEDKMYTGRKGKGAFCNGQKLQVSQ  150

151 QEDITKSLLVTELGSSRTPETVRMVLSNMEKLFCIPVHGIRSVGTAAVNM  200
    ||||||||||||||||||.|||:|:||||||||..||:||||||||||||
151 QEDITKSLLVTELGSSRKPETLRIVLSNMEKLCSIPIHGIRSVGTAAVNM  200

201 CLVATGGADAYYEMGIHCWDVAGAGIIVTEAGGVLMDVTGGPFDLMSRRV  250
    ||||||||||||||||||||:||||||||||||||||||||||||||||:
201 CLVATGGADAYYEMGIHCWDMAGAGIIVTEAGGVLMDVTGGPFDLMSRRI  250

251 IAANNRILAERIAKEIQVIPLQRDDE    276
    ||||:..||:||||||::||||||||
B 251 IAANSITLAKRIAKEIEIIPLQRDDE    276
```

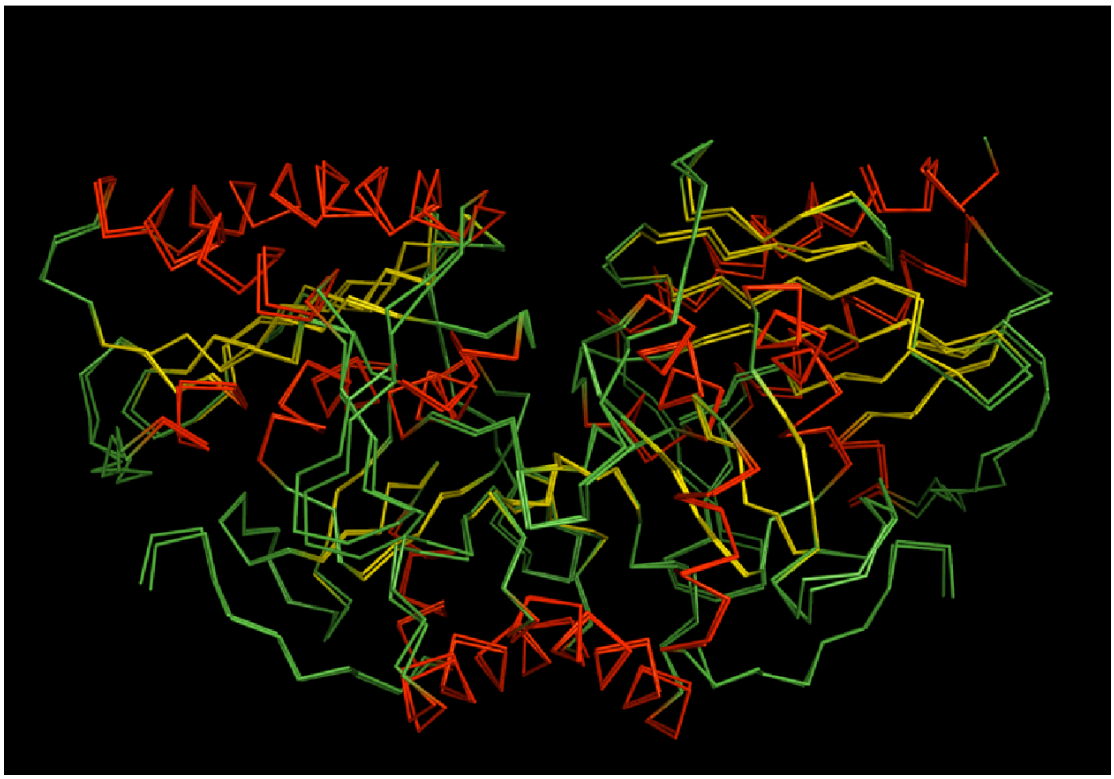


Figure 2.3.19. Comparison of *Hs*IMPase 1 and *Mm*IMPase 1. A) Alignment of the amino acid sequences of *Hs*IMPase 1 (above) and *Mm*IMPase 1 (below). The sequences are 86.6% identical and 96.4% similar with no gaps. One dot indicates corresponding residues (aligned) in the structure alignment, and double dots identify residues within 5Å that are aligned. The alignment was produced using Expasy software. **B)** Overlay of *Hs*IMPase 1 and *Mm*IMPase 1. Stick representation of backbone structures showing α-helices (red), β-strands (yellow) and the loops regions (green). There is a remarkably high degree of structural homology between the two proteins.

2.4 Discussion

The mouse and human recombinant protein was successfully cloned, expressed and crystallised. This is the first report of the crystal structure of mouse IMPase 1. Additionally, for the human IMPase 1, it is highest resolution structure available (1.7 Å compared to 2.1 Å (Bone *et al.*, 1992).

2.4.1 Specific activity

The human IMPase also exhibited lower specific activity than published values (McAllister *et al.*, 1992). The mouse IMPase was considerably lower. Whether this was due to the protein not folding correctly or just a characteristic of the protein is not known and needs further analysis.

In order to increase specific activity, it might be beneficial to assess more expression conditions, and to determine protein and activity by an alternative method. However, the purpose here was solely to obtain sufficient yield of active protein for crystallisation, and this was achieved. For the screening process (see following chapter), the partially purified proteins was used but verification with the pure bovine IMPase was done.

2.4.2 The 'interfering' band

As alluded to earlier, one of the other possible reasons for low specific activity could be due to an interfering protein band (evident in the SDS-PAGE gels). This migrated at about 20 kDa (IMPase at 26–28 kDa) and eluted with IMPase, but did not have activity with Ins1P. The identity of this interfering band could be determined

using protein sequencing analysis. Additionally, the band was also visible in the control BL21(DE3) bacteria (Figure 2.3.5). The control bacteria were transformed with the plasmid, not containing a cDNA insert. Hence, this interfering band may be related to the pRSET5a vector itself.

2.4.3 Crystallography

Both the human and the mouse IMPase proteins were crystallised successfully. On resolving the structure, both were found to contain 3 Mg^{2+} in the active site. This is consistent with previous studies that found 3 Mn^{2+} or Mg^{2+} at the active site (Bone *et al.*, 1994; Gill *et al.*, 2005). The sitting drop method was employed and the crystals were obtained within a week of screening, which is significantly quicker than for crystal conditions used for the human IMPase previously (Bone *et al.*, 1992). Initially, the human protein was resolved to 2.1 Å (data not reported). Another screen was tried with the Merck inhibitor, L-690330 (Atack *et al.*, 1993a). The human IMPase failed to co-crystallise with the inhibitor, but the best-resolved structure of *Hs*IMPase to date, was obtained, with the three Mg^{2+} ions at the active site. The final human IMPase structure was achieved at a resolution of 1.7 Å.

2.4.4 Comparison of human and mouse IMPase 1

This is the first time that the mouse protein has been crystallised. As expected, no significant differences were found between the two isoforms. A comparison of the sequences showed 86.6% identity (96.4% similarity) with no gaps. All the residues involved in metal binding in the active site were conserved.

As with the *Hs*IMPase 1, the *Mm*IMPase 1 crystallisation required inhibitory concentrations of magnesium. The crystal structure shows the three magnesium residues coordinated by the negatively charged residues, Glu-70, Asp-90, Ile-92, Asp-93 and Asp-220 (Figure 2.3.18, detail from Figure 2.3.17). More studies are required to determine whether this third magnesium is required for catalysis or is just an artefact of the high magnesium concentration of the crystallisation conditions, as suggested previously (Pollack *et al.*, 1994).

Although the human and mouse proteins proved highly homologous (both at the sequence and structural levels), surprisingly, their growth and expression patterns differed somewhat. The mouse clone consistently displayed a faster growth rate (Figure 2.3.3) prior to induction, and exhibited a higher total protein after 16 h induction. As expected, the specific activity of both mouse and human IMPases increased over the course of the purification; however, that of the mouse was lower. This may be because of the conditions used, or it may be because the mouse IMPase has lower specific activity compared to the bovine and human isoforms in general. Since the mouse IMPase 1 has not been crystallised previously, it is not possible to say with certainty that this was due to the expression conditions.

Also, much of the mouse protein was evident in the insoluble fraction (Figure 2.3.5). It is not uncommon for heterologously expressed eukaryotic protein to misfold in bacterial cells, and consequently aggregate and thus appear in insoluble fractions. It is also possible that the induction conditions (optimised for enzyme activity) caused a significant proportion of the protein to misfold. It has been suggested that IMPase protein may exist as both a cytosolic (soluble) as well as membrane-associated (Vadnal *et al.*, 1992). Thus, it is possible that the *Mm*IMPase 1 is predominantly present in the membrane fraction.

Although no obvious similarities are observed, there may be subtle differences contributing to differences in specific activity seen in comparison of the human and mouse IMPase. Additionally, Atack *et al.*, have previously observed that the specific IMPase inhibitor, L-690330, inhibits the IMPase present in the mouse brain homogenate less potently than it inhibits the recombinant human or bovine IMPase (Atack *et al.*, 1993a). Hence, there may be nuances in the two isoforms of IMPase that have not yet been characterised.

CHAPTER 3

SCREENING FOR AN IMPASE INHIBITOR

3 Screening for an IMPase inhibitor

3.1 Introduction

Enzymes are very attractive as drug targets; enzyme inhibitors currently represent 47% of all drugs in clinical use, followed by drugs acting at the G-protein coupled receptors (GPCRs) (Figure 3.1.1; (Hopkins and Groom, 2002). Typically, enzymes have large structures composed of a numerous amino acids, some of which are targeted by drugs to modify enzyme activity.

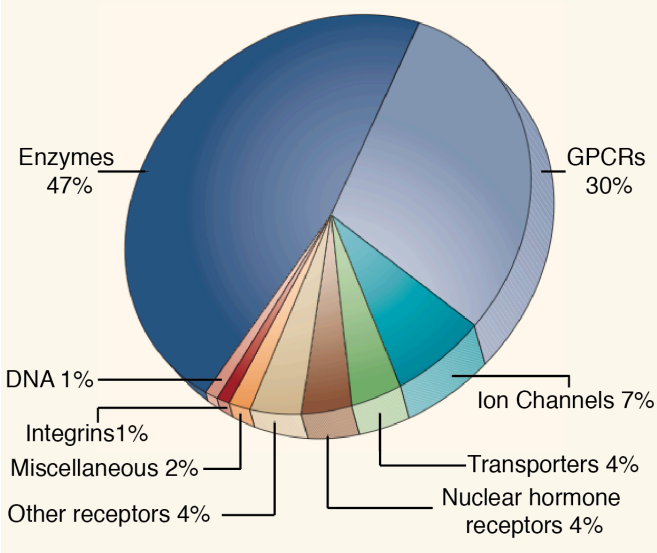


Figure 3.1.1. Targets of small-molecule drugs by chemical class. Drugs that modify enzymes represent the largest group of drug used clinically (Hopkins and Groom, 2002).

3.1.1 Ligand-based drug design

Before the advent of three-dimensional (3-D) screening, two-dimensional (2-D) or pharmacophore-based design was often used. A pharmacophore is a basic structure consisting of functional groups that are required for activity. 2-D screening is carried out by examining the chemical structure of this ligand, and then modifying different functional groups with the aim of obtaining an inhibitor of the enzyme. L-

690330 was developed in this way using from the IMPase substrate, Ins1P, as the starting molecule. Various groups were added and deleted, eventually resulting in L-690330, which is similar to the substrate in a two-dimensional representation (Figure 3.1.2).

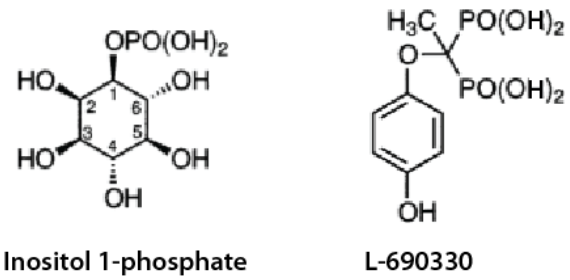


Figure 3.1.2. Two-dimensional similarity of Ins1P and L-690330. Ins1P contains a phosphate group, which is substituted by the bisphosphonate group in the IMPase inhibitor, L-690330. None of the hydroxyl groups, except the one in the *para* position to the phosphate head group, is necessary for inhibitory activity as shown by L-690330.

According to medicinal chemistry screening methodologies, the inclusion of a phosphate or phosphonate group was absolutely essential for IMPase inhibitory activity; however, the presence of this group resulted in problems of cell permeability. In the 3-D approach, molecules are screened as 3-D physical structures, because macromolecules such as proteins interact with small molecules dependent on their 3-D structures, not on their 2-D representational structures. Hence, in 3-D screening, the presence or absence of a particular functional group is not critical; rather, the overall shape of the molecule is important.

For example, the development of Ned-19, an inhibitor of calcium release by mimicking nicotinic acid adenine dinucleotide phosphate (NAADP), was achieved by 3-D screening. Although Ned-19 and NAADP are not very similar in their 2-D representations, their shapes and surface-charge areas are homologous (Figure 3.1.3) (Naylor *et al.*, 2009).

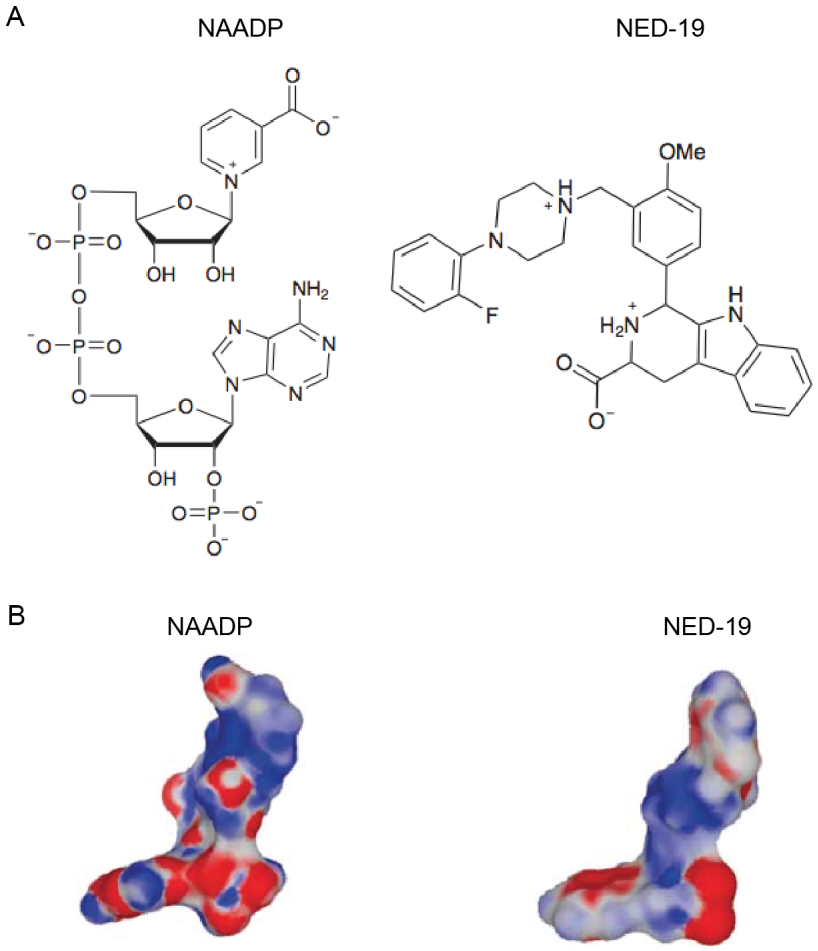


Figure 3.1.3. Comparison of the two and three-dimensional structures of Ned-19 and NAADP. **A)** The planar structures of NAADP and Ned-19 do not look similar. The phosphate groups in NAADP are absent in Ned-19, which contains a fluorine atom **B)** The shape of the inhibitor of NAADP-induced calcium release is similar to the endogenous NAADP. The electrostatic surfaces are represented in colour (red, negative; blue, positive) (Naylor *et al.*, 2009).

According to 2-D analysis, the presence of a phosphate group appeared essential, whereas in 3-D screening this was not found to be true: Ned-19 is similar in shape to NAADP but does not have a phosphate group, and is consequently cell permeable.

Hence, 3-D screening was selected as a suitable approach to find novel inhibitors of IMPase that did not contain a phosphate moiety (the moiety that rendered L-690330 cell-impermeant). To identify potential small-molecule inhibitors of

IMPase by 3-D virtual screening, a compound library and suitable software were required.

3.1.1.1 The ZINC Database

The ZINC (Zinc is Not Commercial) database is a collection of approximately 14 million commercially available compounds as 3-D models (Irwin and Shoichet, 2005). This database was used for the virtual screening for novel IMPase inhibitors since it was open access and fulfilled the criteria required for a 'clean' database (Irwin and Shoichet, 2005). According to Irwin, a 'clean' database should have compounds that are available for purchase; subsets of molecules with variable properties (functional groups, molecular weight, log P) should be easy to create and operate and the database should support varying isomers, stereochemistries, and 3D conformational sampling. In 2005, 68% of the compounds in the database were classified as 'drug-like', i.e. they followed Lipinski's Rule of Five[4]. Some of these compounds were 'lead-like' (molecular weight 150–350, LogP <4, hydrogen-bond donors ≤3, hydrogen-bond acceptors ≤6; (Teague *et al.*, 1999), and some were fragment-like (molecular weight <250, LogP −2 to −3, hydrogen-bond donors <3, hydrogen-bond acceptors <6, rotatable bonds <3; (Verdonk *et al.*, 2003). The 'drug-like' molecules (approximately 9.5 million compounds) were used for screening with IMPase.

3.1.1.2 Conformer generation: OMEGA

Omega software contains two main components, model building and torsion driving, each of which can function independently. This software builds initial models of structures by fragment assembly. Once a model structure is established, the

[4] Criteria for assessing potential drugs in terms of partition coefficient, number of atoms, molecular weight, surface charge and molar refractivity.

program then generates various conformations for the structure and ranks these according to the energy state. Molecules can exist in many different conformational states. Only a conformer that is recognised by the protein will bind to it; this is known as the 'bioactive' conformer.

OMEGA was used to generate up to 100 conformers of Ins1P and of the compounds in the ZINC database, which would all be virtually screened and compared for shape similarity.

3.1.1.3 Shape-based screening: ROCS

ROCS (Rapid Overlay of Chemical Structure) is a shape-based, ligand-centric superposition program. It computes the molecular shape of a subject ligand, and then compares this against a database for 3-D similarity and ranks the molecules in the database according to best match. The overlap analysis does not use 'hard-sphere' volumes, but rather a Gaussian-based comparison. Since proteins see structures in 3-D, this program successfully finds hits that would appear non-intuitive in 2-D analysis. ROCS is also capable of matching user-specified chemical alignment (referred to as 'colour matching') to refine shape-based matches; this allows ROCS to find hits that are both similar in shape and chemically matched.

ROCS assigns a rank (the 'Combo Tanimoto' score) to OMEGA-generated conformers of ZINC compounds, based on similarity of shape, and chemically alignment to the different OMEGA-generated conformers (e.g. of Ins1P). This virtual screening system allows user-defined setting of search parameters, such as 'flexible' or 'stringent'.

3.1.2 Drug repositioning

In order to screen compounds of known safety against IMPase, the 'NIH clinical collection' library was used. The NIH collection has 450 compounds, almost all of which have been in Phase I of clinical trials (Figure 3.1.4). They are known to be safe, at defined doses, in human, but have failed for their intended therapeutic indication. If they can be shown to have efficacy in preclinical animal models of an alternative condition (e.g. bipolar disorder), they may be taken into clinical trials much more swiftly and economically compared to *de novo* drugs. These drugs have major advantages over new molecules: known ADME and safety profile.

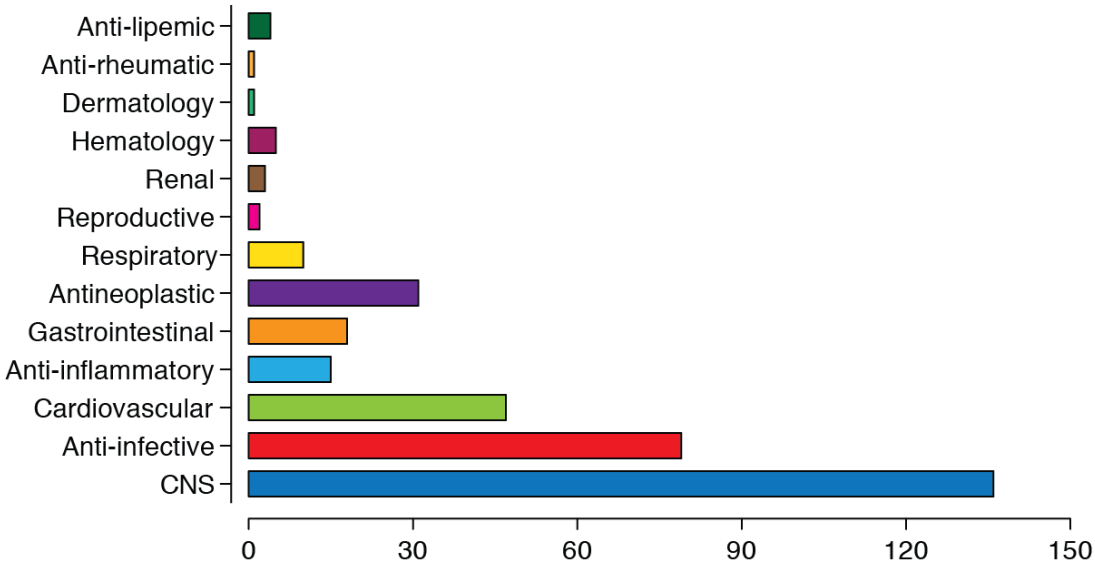


Figure 3.1.4. NIH Clinical Collection. Drug types are classified by therapeutic indication (www.NIHClinicalCollection.com).

3.3.3 Aims

The investigations described in this chapter had two principal goals:

1. **To identify a selective IMPase inhibitor by virtual screening.**

Although the inositol depletion hypothesis has been known for three decades, it has not been conclusively proven. The development of selective, small-molecule, cell-permeable IMPase inhibitors and their testing in animal models of BD, would yield significant evidence for/against the inositol depletion hypothesis. Also, validation of IMPase as the therapeutic target of lithium in bipolar disorder would enable further development of novel IMPase inhibitors for the treatment of this disease.

2. **To identify a novel IMPase inhibitor by drug repositioning.**

   This approach involves screening a library of compounds of known safety profiles, for subsequent IMPase inhibitory activity in biological assays. If any of these drugs show lithium-mimetic activity in an animal model of BD, they could, in theory, be directly used in bipolar patients in Phase II clinical trials to test for efficacy.

3.2 Materials and methods

All compounds and equipment were bought in the UK unless otherwise stated. All chemicals were purchased from Sigma–Aldrich, unless otherwise stated. Analysis was performed using GraphPad Prism (version 5; GraphPad Software, L Jolla, CA, USA).

Tris Buffer: 50 mM TRIS HCl, containing 3 mM $MgCl_2$, 1 mM EGTA, 150 mM KCl, 0.01% *v/v* Triton X, 0.5 mg/mL bovine serum albumin pH 7.4.

3.2.1 Virtual screening protocol

3.2.1.1 Computer

The computer had an Intel 3.2 GHz E7650 processor containing a 4Gb RAM with SUSE Linux version 10 operating system.

3.2.1.2 Database

The ZINC compound library (version 8) was available at http://zinc8.docking.org/ and contained approximately 9.5 million 'drug-like' compounds that were used for conformer generation. The database contains only one conformer per entry. Up to 100 conformations of the 'drug-like' compounds in the database were generated using OMEGA 1.8.1.

3.2.1.3 Ligand preparation

The D-myo-inositol 1-phosphate model was drawn using ChemDraw Ultra (CambridgeSoft, Cambridge, UK) and saved in .sdf format. 100 conformers were created using OMEGA 1.8.1 and used as inputs for shape-based and colour-based screening by ROCS.

3.2.1.4 Shape and colour screening using ROCS

The shape-based screen and colour-based refinement were performed using ROCS. The top 10,000 compounds were ranked according to the 'Combo Tanimoto' score; the highest-ranking conformer for each ligand was retained.

The highest ranked 18 commercially available compounds from the ROCS virtual screen were selected and purchased. Compound names were assigned based on their order of testing. Stock solutions (10 mM) were made in 100% DMSO. In general, compounds were tested at a final concentration of 1 mM, in duplicate. The control contained the same percentage of DMSO as the drug samples.

Mass spectroscopy was performed on all these compounds to confirm purity.

3.2.1.5 Docking of hits from the virtual screen

Docking studies on *Hs*IMPase 1 were performed using FRED 1.0 (OpenEye Scientific Software). The crystal structure was obtained from www.rspcb.org (PDB 2HHM). Hydrogen atoms were added to the structure using MolProbity (http://molprobity.biochem.duke.edu, (Lovell *et al.*, 2003). The resulting structure was saved in pdb format, then opened in FRED_receptor 2.2, where the active site of the protein was identified and the docking analysis was performed.

3.2.2 Drug repositioning

A total of 450 compounds were purchased from the NIH (Bethesda, USA) in 96-well plates (10 mM in DMSO). These compounds had been tested for purity prior to purchase. The compounds were all tested at a final concentration of 100 μM in duplicate. These compounds have all been used in clinical trials and were found to be safe in humans, at the concentrations tested.

3.2.3 Biological assay

The highest ranked 18 compounds from the virtual screen, along with 450 compounds from the NIH clinical collection, were tested for their ability to inhibit IMPase using a Malachite Green (MG) phosphatase assay, as described in the previous chapter. The buffer used for the assay was Tris buffer.

3.2.3.1 Biochemical reagents

Bovine IMPase 1 was used at 5 ng/well, unless otherwise specified. The enzyme was prepared and used according to the details outlined in the previous chapter (Section 2.2.1). *Hs*IMPase 1 was used at a concentration of 10 ng/well and *Mm*IMPase 1 at 33 ng/well. IMPase refers to IMPase 1 in all cases.

D-*myo*-Inositol 1-phosphate (Ins1P) was purchased from Enzo Life Sciences and was dissolved in Tris buffer to the indicated concentration.

3.2.3.2 Malachite Green Phosphatase Assay

IMPase activity was quantified as described in Section 2.2.5.1.

The standard curve was constructed using concentrations of KH_2PO_4 (0 – 6 nmol) in Tris buffer. 20 µL of each standard was pipetted out, in duplicate, into a 96-well plate. A 0.045% *w/v* solution of malachite green oxalate in ddH_2O was mixed, in a 3:1 ratio, with freshly made 4.2% *w/v* ammonium molybdate solution in 4M HCl. 180 µL of this MG-ammonium molybdate mixture was added to the standards in the 96-well plate. The plate was left aside for 2 min for the green colour to develop and then read at 595 nm, in a BMG FLUOstar Optima microplate reader. The absorbance was plotted against phosphate concentration (nmol), and the goodness of fit assessed. The standard curve is shown in the previous chapter (Section 2.2.5.1).

3.2.3.3 Enzyme kinetics

IMPase (2 μL) in Tris buffer was added to each well in a 96-well plate, along with 2 μL of varying concentrations of Ins1P to a final volume of 20 μL. The phosphate standards were added to wells of the plate in duplicate, and the plate was incubated at 37°C for 1 h. MG solution was added, the absorbance was measured at 595 nm, and activity was evaluated by reference to the phosphate standard curve.

In drug screening experiments, 2 μL of drug was added to the enzyme in Tris buffer, and the plate was incubated for 10 min at R.T. after which the substrate (2 μL) were added to make a final volume of 20 μL. V_{max} and K_m values were derived from Michaelis–Menten plots.

3.2.3.4 Concentration–response curves

Enzyme (2 μL) in buffer was incubated for 10 min at R.T. with 2 μL of varying concentrations of drug. Ins1P (1 mM) was then added to make a final volume of 20 μL. The reaction mixture was incubated at 37°C for 1 h, then, MG solution was added, and the phosphatase concentration was determined by the MG assay.

3.2.3.5 Testing for reversibility of drug inhibition

*Hs*IMPase (100×) was incubated with 20 μM drug (10 x IC_{50}) for different time periods and then diluted, to the appropriate IMPase concentration, into the assay buffer (Tris buffer) containing Ins1P. The reaction was allowed to proceed for 1 h as per the usual protocol of the MG assay.

3.2.3.6 Test for covalent versus non-covalent inhibition

Two methods were employed to test covalent binding.

Kinetics method

*Hs*IMPase 1 (20×) was incubated with test compound (2× IC_{50}) for 30 minutes. This was diluted to the appropriate enzyme concentration in Tris buffer containing the substrate and incubated for 1 h at 37°C. MG reagent was then added and absorbance was measured (595 nm).

Mass spectroscopy

Mass spectroscopy was used as described (Section 2.2.7) but with an additional mild denaturing step. The 100 μM *Hs*IMPase was incubated with 100 μM drug, and after 10 min, it was diluted to 10 μM enzyme with 15 mM ammonium acetate buffer pH 7.4/ 0.1% *v/v* formic acid, to denature the enzyme. This solution was then subject to mass spectroscopy using MS.

3.2.3.7 Cysteine residue binding study

In order to verify a covalent interaction of the drug with a cysteine residue, a glutathione (GSH) assay was used.

The thiol group in GSH reacts with Ellman's reagent (5,5'-dithiobis-(2-nitrobenzoic acid, DTNB) to form a yellow ionized compound, 2-nitro-5-thiobenzoate (NTB). This is quantified spectrophotometrically (450 nm) (Tietze, 1969). This reaction of thiol groups with DTNB is called Ellman's reaction and is shown in Figure 3.2.1.

The GSH standards and DTNB reagent were prepared in KPE buffer (16 mM KH_2PO_4, 83 mM $K_2HPO_4.3H_2O$, 11.2 mM EDTA).

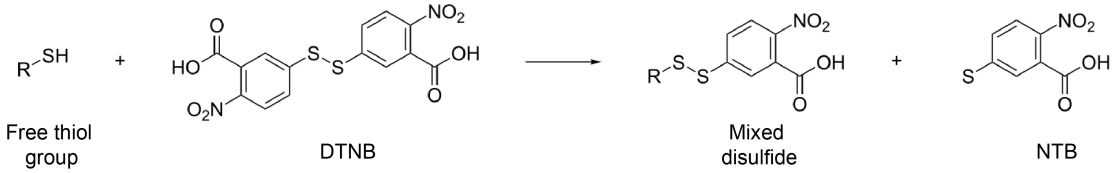


Figure 3.2.1. Ellman reaction. The reaction between a thiol-containing compound or protein (R-SH) and DTNB to form NTB^- (yellow).

100 μM of the ebselen was incubated with varying concentrations (0.02-0.2mM) of GSH, (final volume 50 μL) for 5 min in a 96-well plate before the addition of 1 mM DTNB (150 μL). The plate was then left at R.T. for 2 min. Absorbance at 450 nm was measured.

3.2.3.8 Glycogen synthase kinase 3β (GSK-3β) assay

Compounds were sent to the Millipore Kinase screening centre (Dundee, UK) for testing of GSK-3β inhibitory activity. The kinase, GSK-3β, was incubated with the substrate, test compound and ATP in presence of magnesium. The amount of phosphorylated substrate was measured to evaluate kinase activity.

3.3 Results

3.3.1 Lithium and L-690330: Concentration–response and enzyme kinetics

Lithium and L-690330 are known inhibitors of IMPase. In order to assess the inhibitory effects of screened compounds, and to verify the assay protocol, bovine IMPase 1 activity in the presence of varying concentrations of inhibitor was measured, and concentration–response curves were plotted for these know inhibitors (Figure 3.3.1).

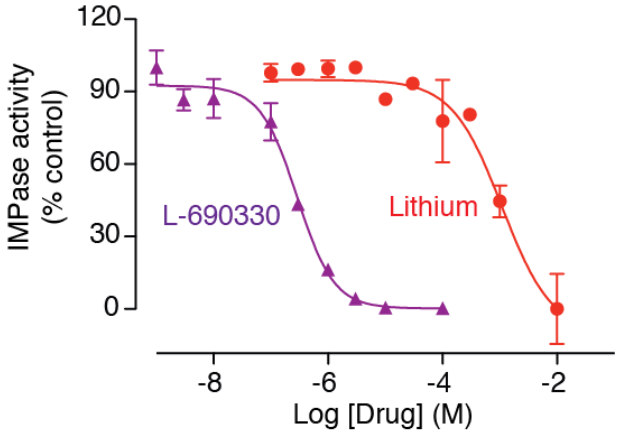


Figure 3.3.1. Concentration–response curves for lithium and L-690330. The concentration–response values were obtained using bovine IMPase 1 and Ins1P (IMPase substrate) at 1 mM. IC_{50} values were determined as 0.53 mM and 288 nM, respectively (n = 5), consistent with previous reported values.

IC_{50} values for lithium and L-690330 with bovine IMPase 1 were determined as 0.5 mM and 288 nM, respectively. These were comparable with previously reported values [0.8 mM for lithium (Hallcher and Sherman, 1980), 300 nM for L-690330 (Atack, 1997)].

Next, IMPase enzyme kinetics was characterised, both in the absence and presence of inhibitor (1 mM lithium or 300 nM L-690330). Phosphate release rates were measured, from which plots were made of release rate against enzyme

concentration (Figure 3.3.2). V_{max} and K_m values were deduced from the graphs and the mode of inhibition was assessed.

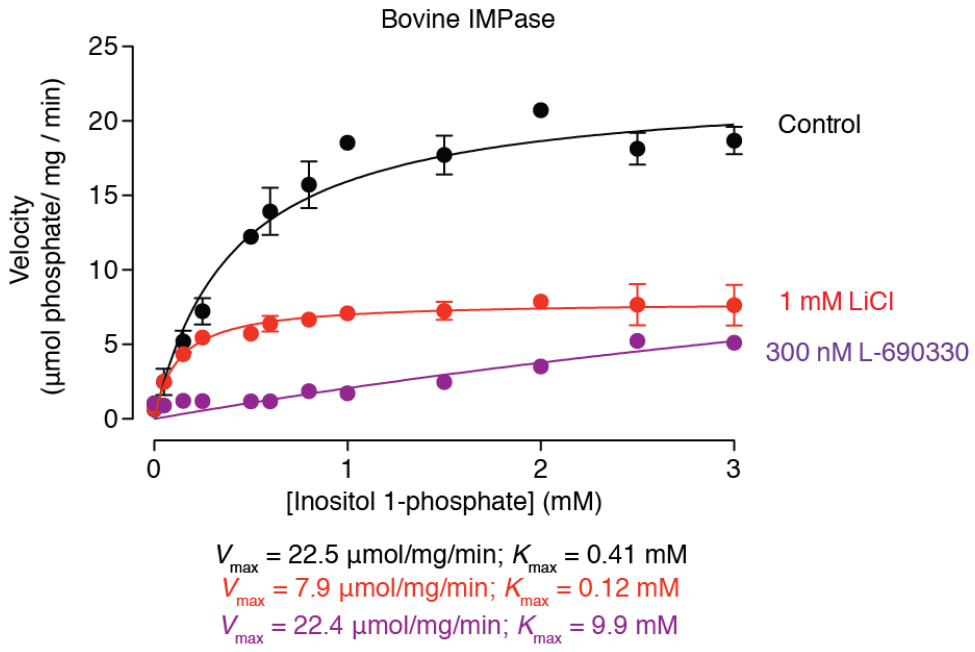


Figure 3.3.2. Kinetics of bovine IMPase in the presence and absence of inhibitors. The Michaelis–Menten graphs were plotted either in the absence (control) or presence of inhibitor at the indicated concentration (n = 3). Lithium is an uncompetitive inhibitor and L-690330 is a competitive inhibitor of IMPase.

In the absence of inhibitor, bovine IMPase 1 showed V_{max} and K_m values of 22.46 µmol phosphate/mg/min and 0.41 mM, respectively; in presence of inhibitor, these were 7.87 and 0.12 (1 mM lithium), or 22.40 and 9.87 (300 nM L-690330).

With lithium, both V_{max} and K_m values decreased significantly (unpaired t-test), which is indicative of un-competitive inhibition (Hallcher and Sherman, 1980). For L-690330, the K_m value increased while V_{max} did not change significantly (unpaired t-test). This indicates that L-690330 is a competitive inhibitor of IMPase. These results are consistent with previously published findings (Atack *et al.*, 1993a).

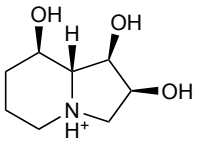
3.3.2 Biological testing of virtual screening hits

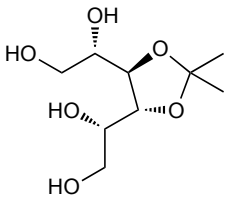
Starting with the 2-D structural model of Ins1P, 100 conformers were generated *in silico*. These were used to identify homologous molecules in the ZINC database according to ROCS algorithms. The 18 best ranking available compounds were selected (Table 3.3.1), purchased and subjected to biochemical testing for IMPase inhibitory activity. Structures are given in Table 3.3.2.

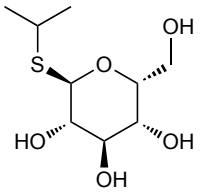
Table 3.3.1 Hits obtained from virtual screening. The table shows the molecular weight, ZINC ID and the Combo score of the top 18 purchasable compounds after virtual screening. The compounds were designated names from NIS-1 to NIS-18 dependent on the order of testing.

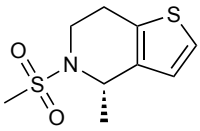
Compound	Molecular weight	Zinc ID	Tanimoto Combo score
NIS-1	173.2	391933	1.231
NIS-2	222.2	56733	1.192
NIS-3	238.3	391142	1.174
NIS-4	231.0	143635	1.279
NIS-5	424.3	1035046	1.178
NIS-6	240.2	18126067	1.148
NIS-7	211.2	16051380	1.320
NIS-8	239.5	39940	1.154
NIS-9	253.7	402889	1.140
NIS-10	340.4	5842537	1.159
NIS-11	223.3	1845986	1.353
NIS-12	365.1	980644	1.264
NIS-13	282.3	294576	1.278
NIS-14	210.1	518599	1.091
NIS-15	226.1	1871342	1.225
NIS-16	178.1	294739	1.307
NIS-17	198.2	402289	1.250
NIS-18	253.7	396677	1.279

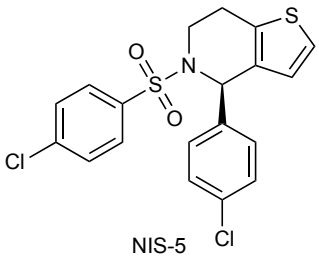
Table 3.3.2. Structures of NIS 1-18 compounds.

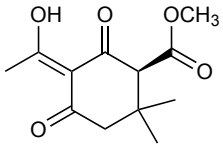

NIS-1

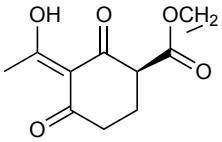

NIS-2

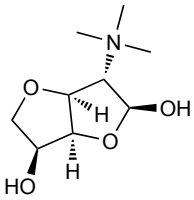

NIS-3

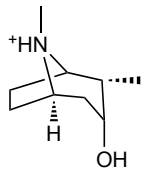

NIS-4

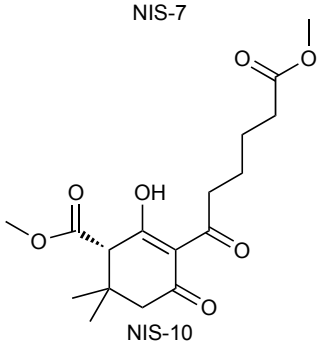

NIS-5

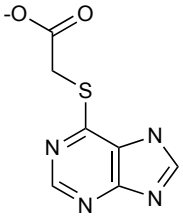

NIS-6

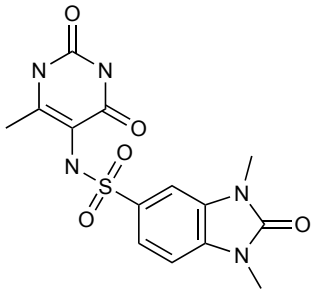

NIS-7

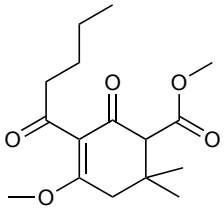

NIS-8

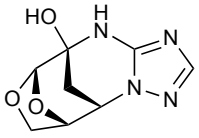

NIS-9

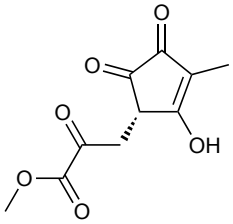

NIS-10

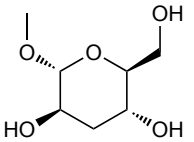

NIS-11

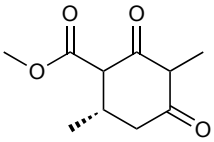

NIS-12

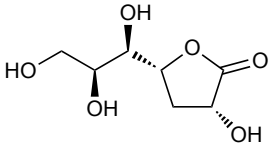

NIS-13


NIS-14


NIS-15


NIS-16


NIS-17


NIS-18

Compounds NIS 1–18 were tested at 1 mM enzyme kinetics assays (as above for lithium and L-690330), and their effects on V_{max} and K_m values were calculated and used to determine inhibition. Compounds that resulted in a decrease in V_{max} >50%, or increase in K_m of >50%, or both, were carried forward for further testing.

3.3.2.1 V_{max} and K_m of IMPase in presence of NIS 1–18

The 18 compounds were assessed based on changes in V_{max} and K_m. Relative changes in K_m and V_{max} can infer the mode of enzyme inhibition (Figure 3.3.3A). The fold decrease in V_{max} was calculated as the ratio of bovine IMPase V_{max} obtained in presence of the drug to the V_{max} in the absence of a drug. The fold increase in K_m was calculated as the ratio of the K_m of the enzyme in the absence of drug to K_m of the enzyme in the presence of drug. The distribution of the compounds according to the changes in both V_{max} and K_m is shown in figure 3.3.3B. Depending on the position of a drug on the graph, it is possible to predict its mode of inhibition.

The bovine IMPase was used, since the recombinant human and mouse protein was in the process of being produced and was not ready for assays at the time.

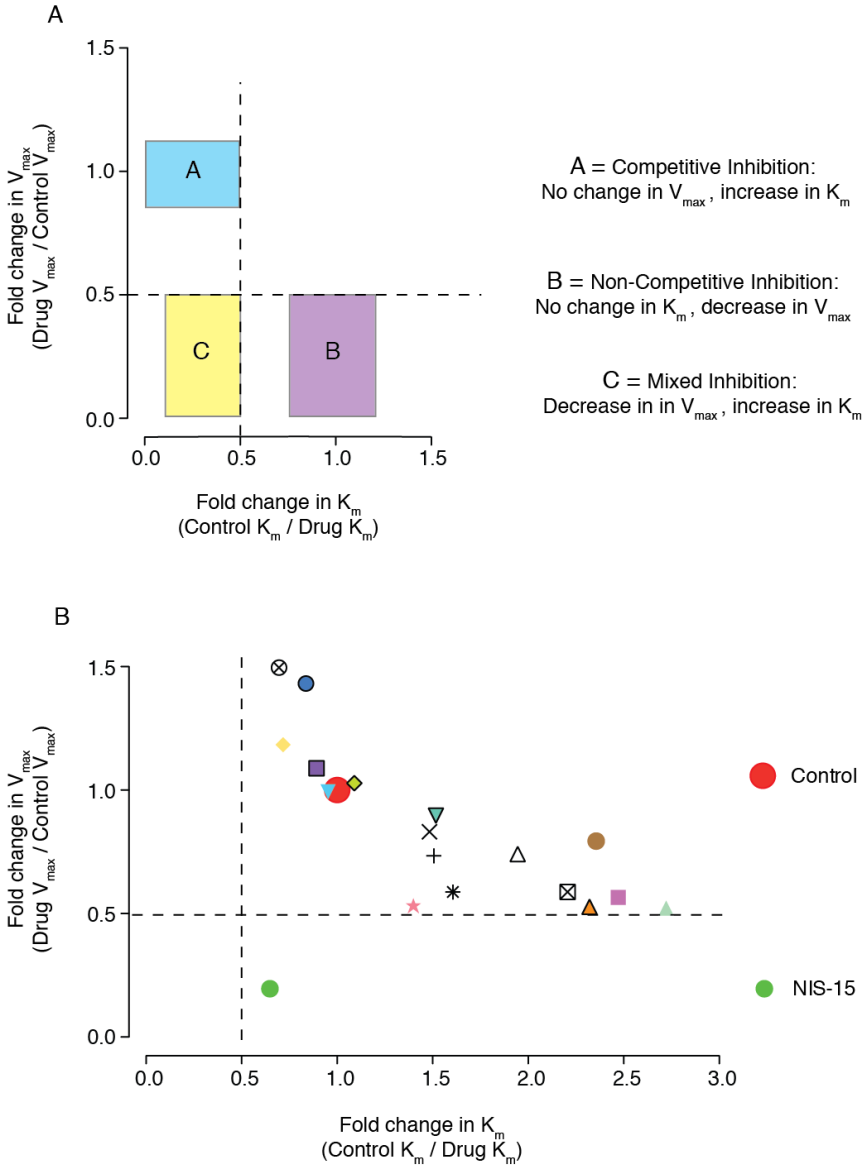


Figure 3.3.3. Analysis of V_{max} and K_m of bovine IMPase in presence of compounds NIS 1–18. A) Relationship between mode of inhibition and changes in V_{max} and K_m. Dashed lines (0.5 on both axes) represent 50% decrease in V_{max} and 50% increase in K_m. **B)** Plot of the compounds NIS 1–18 and vehicle (control). Only compounds in the lower right quadrant were classified as hits. NIS-15 and the control are specifically identified by circles, other symbols represent the other 17 compounds.

From Figure 3.3.3B, it is evident that only one compound, NIS-15, is classified as a hit, by these criteria. Additionally, its mode of inhibition was predicted to be either non-competitive or mixed. Independent comparisons of V_{max} and K_m are shown in Figure 3.3.4 and 3.3.5, respectively.

3.3.2.2 V_{max} analysis of IMPase in presence of NIS 1-18

The fold decrease in V_{max} was calculated as the ratio of the V_{max} obtained in presence of the drug to the V_{max} of the bovine IMPase in the absence of a drug as shown in Figure 3.3.4. Lithium and L-690330 were used as positive controls. Compounds that decreased the V_{max} by more than 50% were termed as 'hits'.

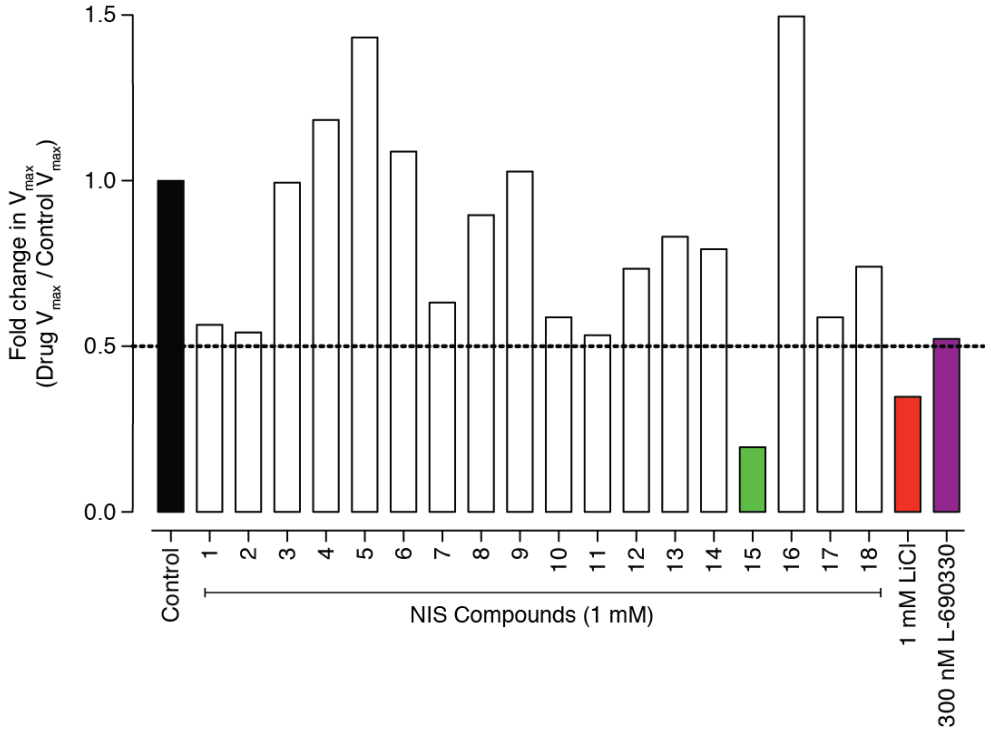


Figure 3.3.4. Fold decrease in bovine IMPase V_{max} for the NIS compounds. The bar graph represents the fold deacrease in V_{max} of IMPase in presence of NIS 1–18 Positive controls, lithium (red) and L-690330 (purple), were used at approximately their IC_{50} concentrations. The dashed line represents a 50% decrease in V_{max}. The hit (green) was selected based on its >50% decrease in V_{max}.

From the analysis of the V_{max} values, NIS-15 was deemed to be a hit since it decreased the V_{max} by 75%. The change in V_{max} also indicates that it is not a competitive inhibitor.

3.3.2.3 Analysis of IMPase K_m in the presence of NIS 1-18

Competitive inhibitors do not change V_{max} but cause an increase in K_m. Hence, to identify competitive inhibitors, the NIS compounds were also analysed for fold

increase in K_m (Figure 3.3.5). This was calculated as the ratio of the K_m of the enzyme without inhibitor to the K_m of the enzyme in the presence of the drug. Lithium and L-690330 were used as positive controls. Compounds that increased the K_m by more than 50% were deemed competitive.

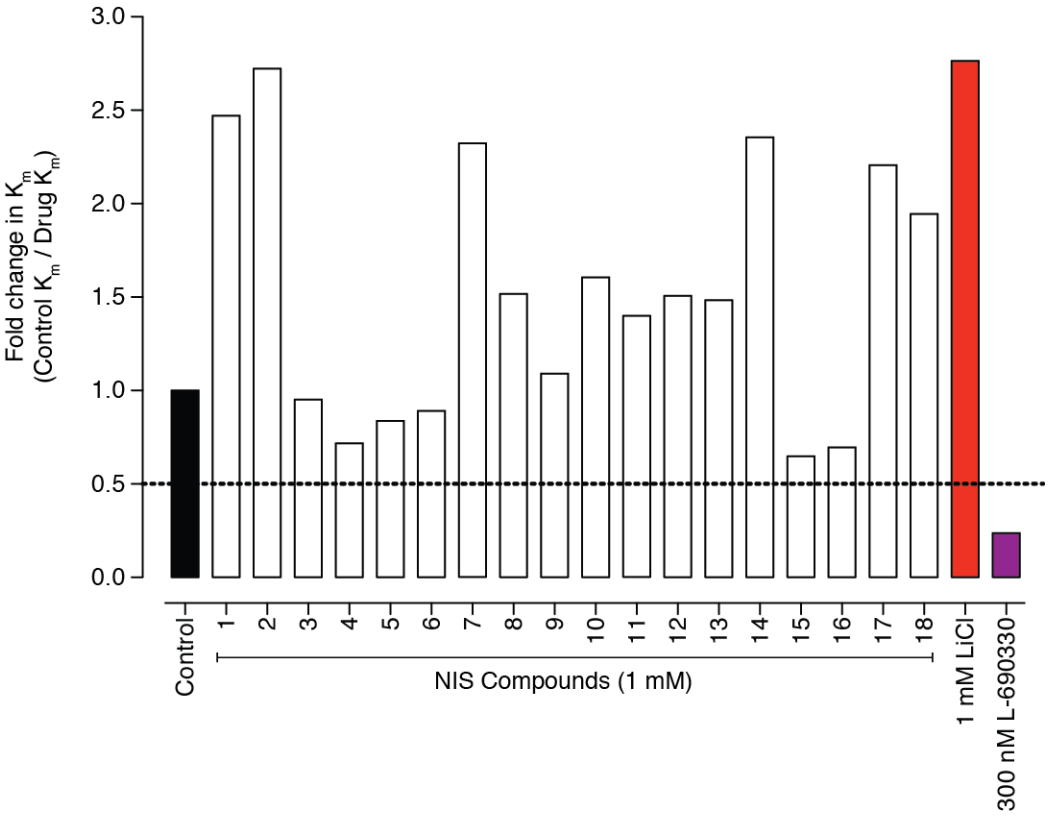


Figure 3.3.5. Fold increase in bovine IMPase K_m with NIS compounds 1–18. Positive controls: lithium (red) and L-690330 (purple) were used at approximately their IC_{50} concentrations. The dashed line shown at the 0.5 mark on the y-axis represents a >50% increase in K_m.

None of the NIS compounds caused an increase in K_m >50%; based on this, none was classified as 'hits' using the K_m as a measure.

NIS-15 caused a 35% decrease in K_m. This is likely to be within the error associated with the calculation of K_m.

Since NIS-15 caused a 75% decrease in V_{max} and produced an insignificant change in K_m it is likely that NIS-15 is a non-competitive inhibitor of IMPase.

3.3.3 IMPase activity in presence of NIS-15

Next, the effect of varying concentrations of NIS-15 on bovine IMPase activity was tested. A concentration–response curve was plotted (Figure 3.3.6) to analyse inhibition of IMPase activity with increasing concentration of NIS-15. The IC_{50} value of this inhibition was determined as a measure of potency.

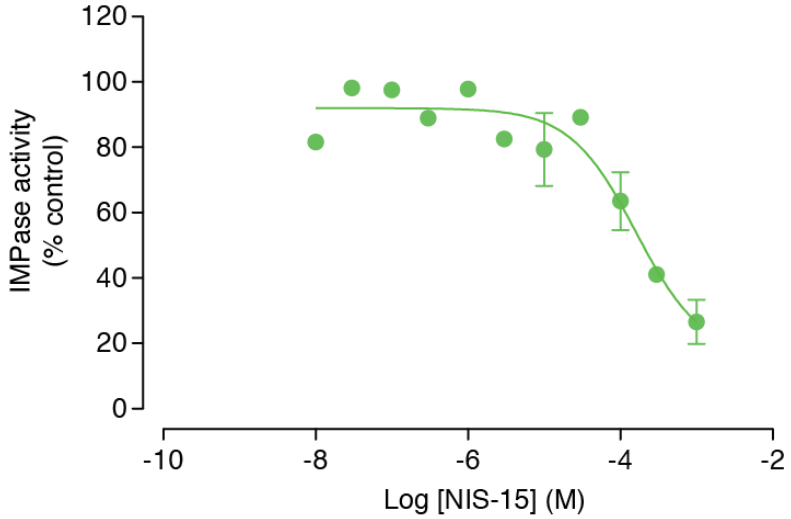


Figure 3.3.6. Concentration–response curve of NIS-15 on bovine IMPase activity. The concentration-dependent inhibition of NIS-15 on IMPase activity has an IC_{50} value of 160 μM.

NIS-15 showed concentration-dependent inhibition of IMPase activity. The IC_{50} was determined to be 160 μM, which is five times more potent than lithium, IC_{50} = 0.8 mM, (Hallcher and Sherman, 1980).

Enzyme kinetics experiments were carried out in the absence and presence of 1 mM NIS-15. A Michaelis–Menten graph was plotted to quantify the effect of NIS-15 on IMPase activity by comparing V_{max} and K_m values obtained with and without the drug (Figure 3.3.7).

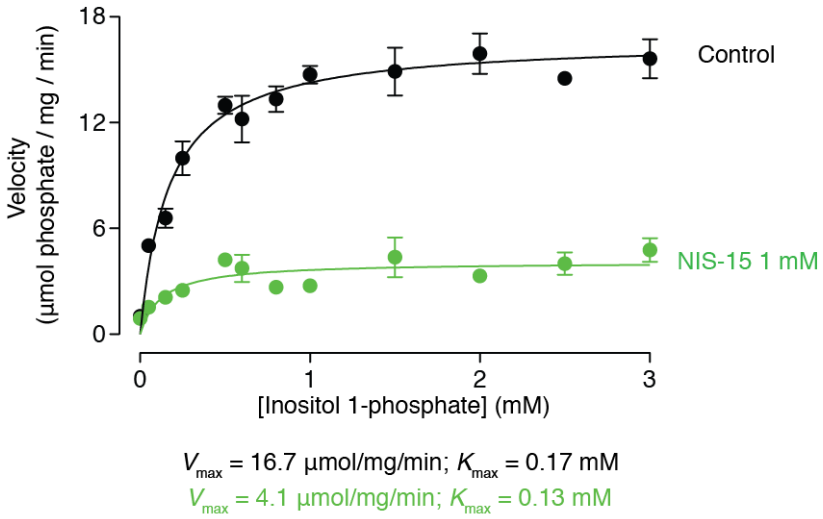


Figure 3.3.7. Change in bovine IMPase activity in presence of NIS-15. Michaelis–Menten plots of IMPase activity in the absence (black) and presence (green) of 1 mM NIS-15 clearly show that NIS-15 inhibits IMPase activity. V_{max} was significantly different, although the K_m was not, using the unpaired t-test.

The Michaelis–Menten graph shows that NIS-15 at 1 mM inhibits IMPase activity. The V_{max} values for the control (no drug) and NIS-15 were 16 ± 0.56 and 4 ± 0.34 µmol phosphate/mg/min, respectively. This shows a significant (75%) drop in V_{max} in presence of NIS-15. There was no significant change in K_m values (0.17 ± 0.03 and 0.13 ± 0.06 mM, respectively). The unpaired t-test was used to determine significance. This confirms that compound NIS-15 inhibited IMPase non-competitively.

3.3.4 *In silico* docking of NIS-15 into the active site of IMPase

NIS-15 was docked into the IMPase active site, *in silico*, in an attempt to gain insight into the binding of NIS-15 to IMPase (Figure 3.3.8).

NIS-15 is a lead-like compound: a log p of 0.98, 1 hydrogen bond donor, 6 hydrogen bond acceptors and a molecular weight of 226.184 Da.

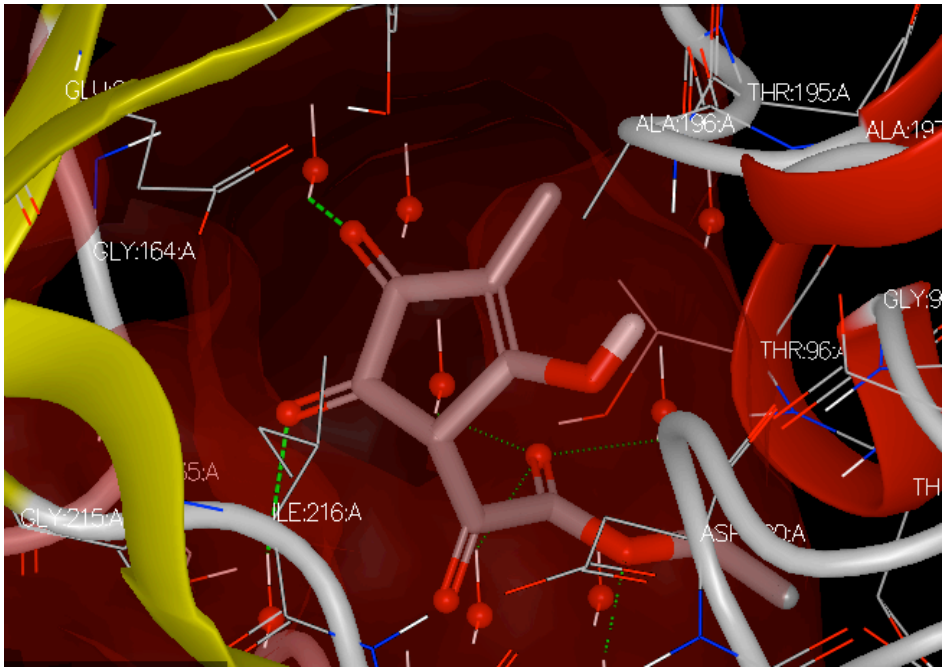


Figure 3.3.8. NIS-15 docked at the active site of *Hs*IMPase.

The simulation suggests that NIS-15 is sterically accommodated at the active site of IMPase but coordinated only with the water molecules and not with any amino acid residues. It also seems that the area of the active site cavity is much larger than that required by NIS-15.

3.3.5 Biological testing of the compounds in the NIH clinical collection

A total of 450 compounds in the NIH clinical collection were screened manually against recombinant *Hs*IMPase. The preliminary assay consisted of a 5-point kinetics curve for all the 450 compounds (data not shown). Of these, two, ebselen and dihidrexidine, were found to be inhibitors of IMPase activity and were tested further.

Concentration–response curves were plotted following incubation of bovine IMPase with varying concentrations of ebselen (Figure 3.3.9) or dihidrexidine (Figure

3.3.10) in presence of 1 mM Ins1P for 1 h. The phosphate released was measured to determine phosphatase inhibitory activity.

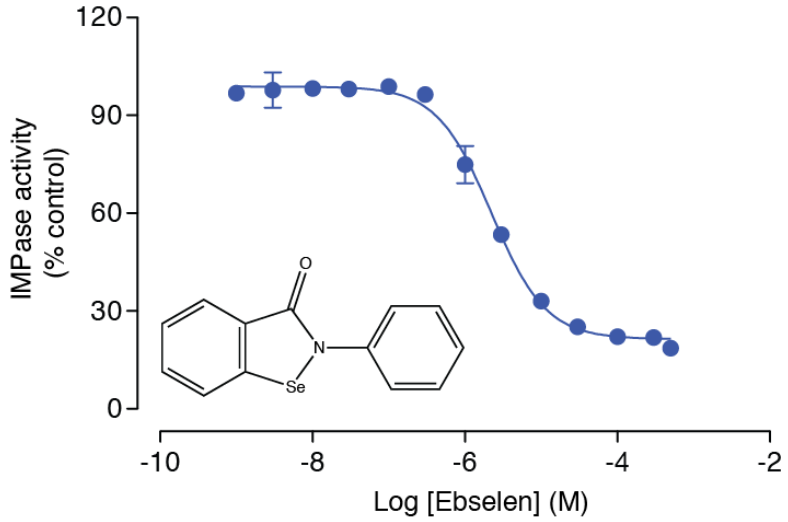


Figure 3.3.9. Concentration–response curve of ebselen. Ebselen inhibits *Hs*IMPase activity in a concentration-dependent manner (IC_{50} = 2.2 μM). The structure of ebselen is shown in the panel.

Ebselen inhibited IMPase activity in a concentration-dependent manner with an IC_{50} value of 2.2 μM. Since the IC_{50} value of lithium is about 0.8–1 mM, ebselen is about 500 times more potent than lithium. However, it was 10 times less potent than L-690330 with the bovine IMPase. This finding was reproduced in the bovine and mouse IMPase. as well.

Dihidrexidine, the other hit in the preliminary screen, was also tested by plotting a concentration–response curve (Figure 3.3.10).

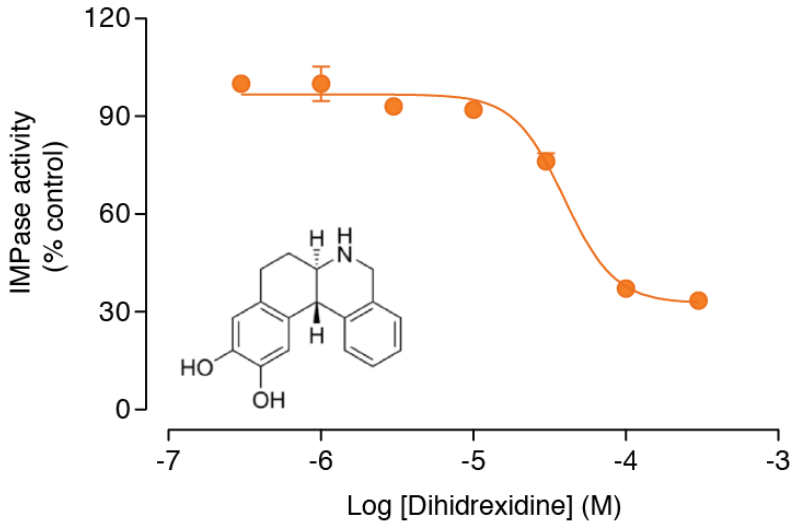


Figure 3.3.10. Concentration–response curve of dihidrexidine. Dihidrexidine inhibits *Hs*IMPase in a concentration-dependent manner (IC_{50} = 39.5 μM). The structure of dihidrexidine is shown.

Dihidrexidine concentration-dependently inhibited IMPase activity and was found to have an IC_{50} of 40 μM. This was about 25 times more potent than lithium and about 150 times less potent than L-690330. Ebselen was about 20 times more potent than dihidrexidine, so it was decided that it alone would be taken forward for further investigation.

IMPase kinetics experiments were carried out for *Hs*IMPase in the absence and presence of 300 μM ebselen (Figure 3.3.11). Michaelis–Menten graphs were plotted to investigate the mode of inhibition of ebselen on IMPase.

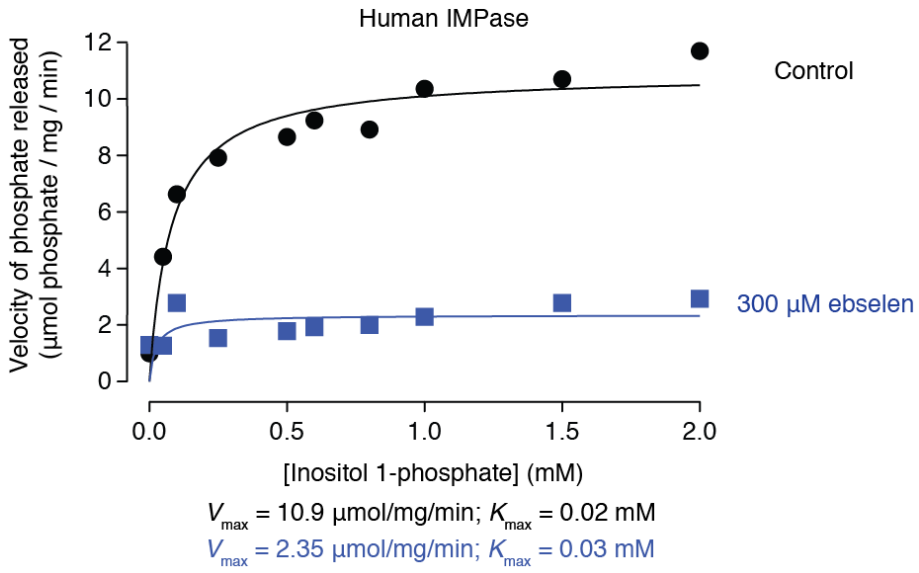


Figure 3.3.11. Effect of ebselen on *Hs*IMPase activity. Michaelis–Menten graphs were plotted from the enzyme kinetics experiments in the absence and presence of 300 µM ebselen. Ebselen inhibited the activity of *Hs*IMPase in a non-competitive manner (n=2).

Figure 3.3.11 shows that ebselen caused a significant change in V_{max} — from 11 (control) to 2.4 µmol phosphate/mg/min (~80% decrease) — but did not cause a significant change in K_m (unpaired t-test). This indicates that 300 µM ebselen inhibited IMPase non-competitively. Similar results were obtained for ebselen with bovine and mouse IMPase.

These results proved highly promising, so a more detailed study of ebselen's mechanism of IMPase inhibition was undertaken.

3.3.6 Possible non-specific effects of ebselen on IMPase

Ebselen inhibited *Hs*IMPase non-competitively (above). Similar results were obtained when the experiment was repeated with bovine and mouse IMPase 1 (data not shown).

Ebselen's distinctive structural feature, almost uniquely among drugs, is the presence of a selenium atom (Figure 3.3.9). Free selenium tends to be toxic and

reactive; however, in ebselen the selenium is not free, but bound within the molecule. Nonetheless, it was considered prudent to check that ebselen inhibition was not due to some non-specific effect resulting from the selenium in its structure.

3.3.6.1 Possible non-specific selenium effect

In order to eliminate a non-specific selenium effect, two compounds containing bound selenium were used to check for inhibitory effects on IMPase activity. The compounds were selenium dioxide and dibenzyl diselenide (Figure 3.3.12).

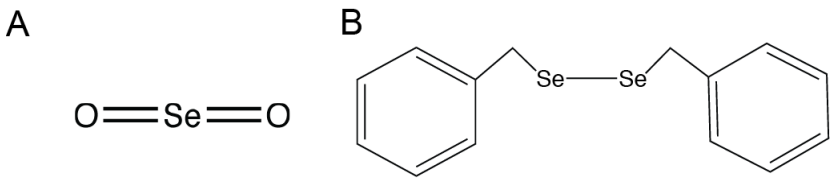


Figure 3.3.12. Structures of two selenium containing compounds. A) selenium dioxide, and **B)** dibenzyl diselenide.

These two selenium-containing compounds were tested at 1 mM for inhibitory effects on IMPase activity using kinetics experiments (Figure 3.3.13).

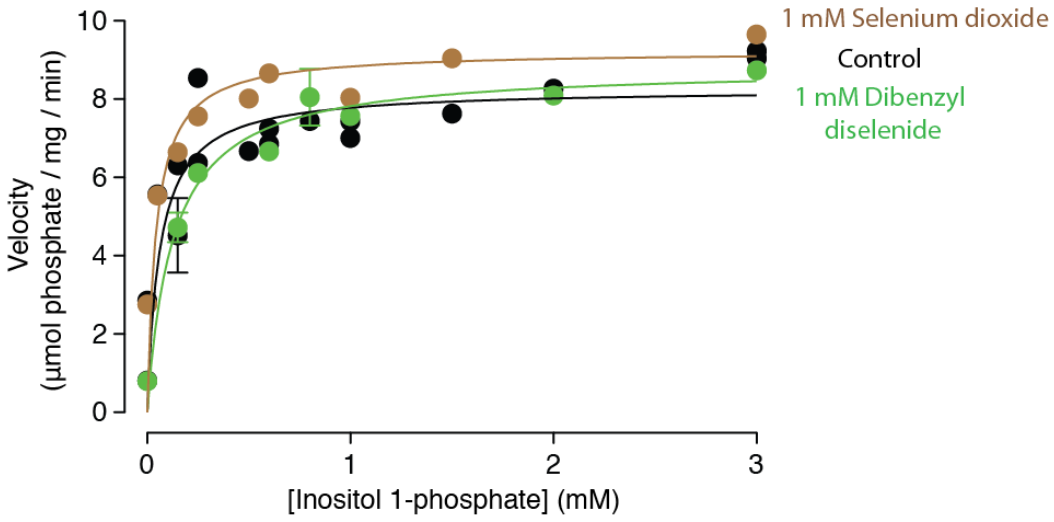


Figure 3.3.13. Effects of alternative selenium-containing molecules on *Hs*IMPase activity. The Michaelis–Menten graph of IMPase kinetics activity shows that neither dibenzyl diselenide (green) nor selenium dioxide (brown) had a significant effect. Control: IMPase without inhibitor (black).

Neither selenium dioxide not dibenzyl diselenide inhibited IMPase activity. There was no significant change in V_{max} or in K_m. It was therefore possible to conclude that IMPase inhibition in presence of ebselen was not due to a non-specific effect resulting from the presence of selenium in the compound.

3.3.6.2 Possible non-specific interference with malachite green

It was also possible that ebselen interfered with the Malachite Green reagent or the absorbance measurement (595 nm). To test this, potassium dihydrogen phosphate standards were incubated with and without ebselen; after the addition of Malachite Green reagent, absorbance was measured (Figure 3.3.14).

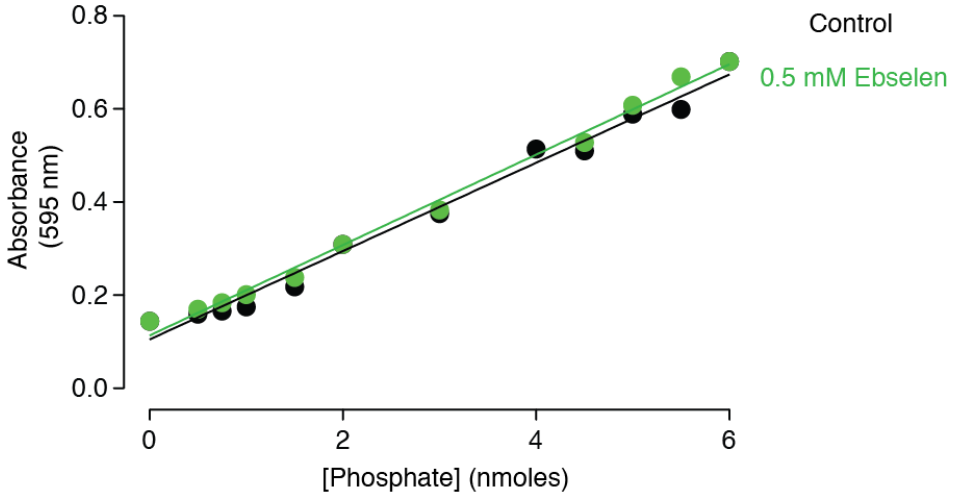


Figure 3.3.14. Absorbance of phosphate standards in presence of ebselen. The figure shows the absorbance (595 nm) of potassium dihydrogen phosphate in the absence and presence of 0.5 mM ebselen after addition of Malachite Green reagent.

There was no observable change in the absorbance at 595 nm. Hence, it was concluded that ebselen, at up to 0.5 mM, does not interfere with the Malachite Green assay.

3.3.7 Ebselen's effect on the kinetics of IMPase

Having established that ebselen's inhibitory effects on IMPase were highly unlikely to be non-specific, a study was made of IMPase enzyme kinetics in the presence of ebselen over a range of concentrations.

*Hs*IMPase was incubated with different concentrations of ebselen and substrate for 1 h before the addition of Malachite Green reagent. Absorbance at 595 nm was measured, and the velocities of the reactions were calculated (μmol phosphate/mg/min). A Michaelis–Menten graph was plotted for velocity against substrate concentration (Figure 3.3.15.A), and the mode of ebselen inhibition was determined using V_{max} and K_m analysis and a Lineweaver–Burk plot (Figure 3.3.15.B).

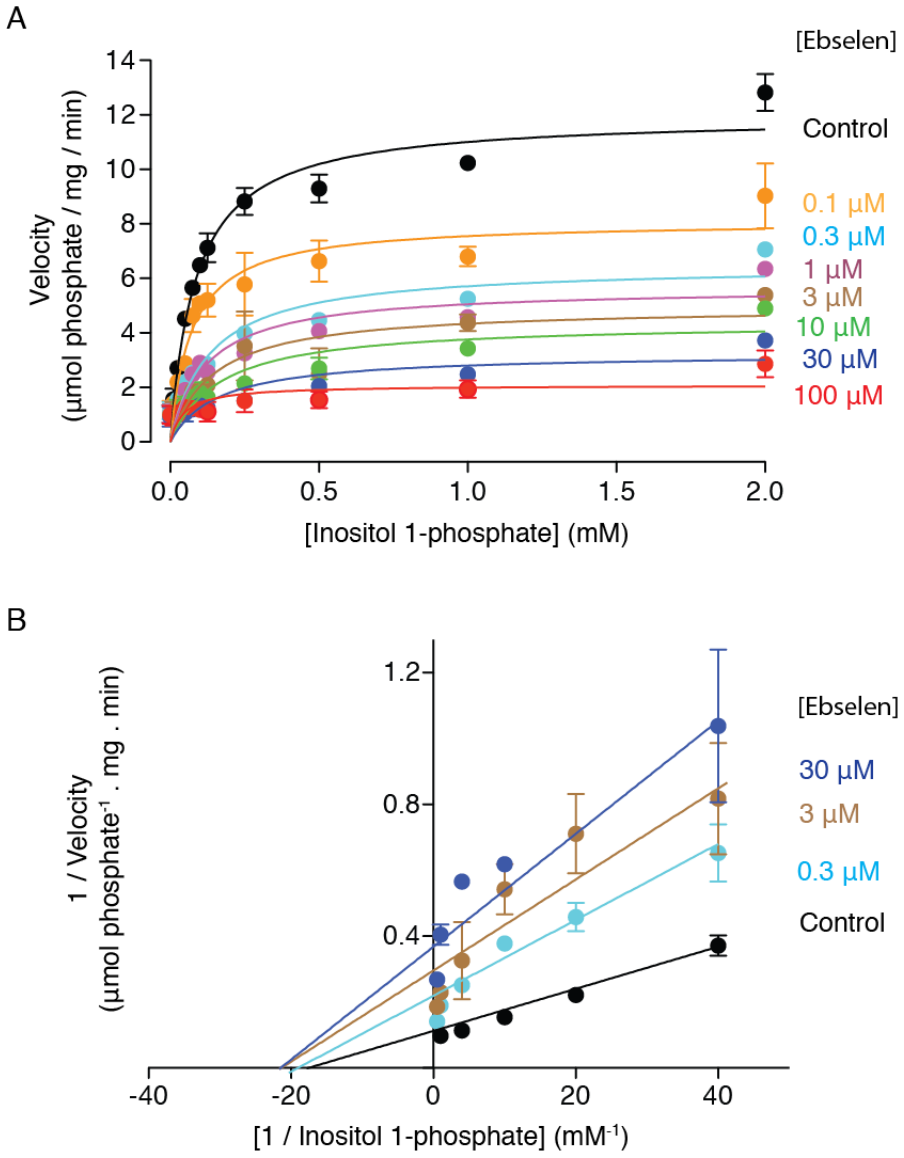


Figure 3.3.15. Ebselen concentration-dependent inhibitory effect on IMPase activity. Increasing concentrations of ebselen increased *Hs*IMPase inhibition. **A)** Michaelis–Menten plots of IMPase in presence of increasing ebselen concentrations (0–100 µM). **B)** Lineweaver–Burk plot of ebselen concentrations: 30, 3, 0.3 µM and control (black). The trend suggests convergence on the x-axis, with different y-axis intercepts.

Figure 3.3.15A shows the kinetics of IMPase inhibition in presence of increasing concentrations (0–100 µM) of ebselen. The trend of inhibition shows a decrease in V_{max}, thus suggesting that mechanism of inhibition is either non-competitive or un-competitive. The V_{max} and K_m values for the different concentrations were calculated (Table 3.3.3).

Table 3.3.3. Effect of ebselen (0–100 μM) on V_{max} and K_m values of *Hs*IMPase

[Ebselen] (μM)	0	0.1	0.3	1	3	10	30	100
V_{max} (μmole/mg/min)	11.96	8.09	6.47	5.66	4.96	4.38	3.25	2.08
K_m (mM)	0.09	0.07	0.13	0.12	0.14	0.17	0.16	0.05

Ebselen caused a significant and concentration-dependent decrease in V_{max}, without any significant change to K_m. This suggests that ebselen inhibits IMPase non-competitively. A Lineweaver–Burk plot, using some of the ebselen concentration data, confirmed non-competitive inhibition (Figure 3.3.15B).

3.3.8 Reversibility of ebselen inhibition

The foregoing analysis suggests that ebselen inhibits IMPase non-competitively. Ebselen's mode of binding was next investigated in detail.

First, using a dilution experiment similar to the method in Copeland's Evaluation of Enzyme Inhibition in Drug Discovery (Copeland, 2005), concentrated IMPase solution was incubated with 20 μM ebselen. This was then diluted 100 times to the required IMPase concentration at different time points (0 – 24 h), then Ins1P (substrate) was added, and after a further 1 h the activity was assayed.

If ebselen binds reversibly, it would become progressively dissociated from IMPase at different time points, and hence would be diluted out. Its inhibitory effect would be concomitantly diluted and the enzyme activity would tend to that of uninhibited enzyme. Conversely, if it bound irreversibly (or only very slowly reversible), it would remain bound to IMPase and not be diluted out and IMPase activity would remain more or less constant.

The results (Figures 3.3.16A and B) show that ebselen inhibition of IMPase activity is irreversible (or, at most, very slowly reversible). The V_{max} analysis shows that the extent of IMPase activity is very slightly higher in the 5 h and the 24 h sample compared to the 10 min sample, although still significantly lower than the control. At the 10 min time point, there was an 85% reduction in IMPase activity, and at 1 h it was about the same (90% decrease compared to control) and continued to be about the same till 5 h. At 24 h there still remained a 65% reduction in activity.

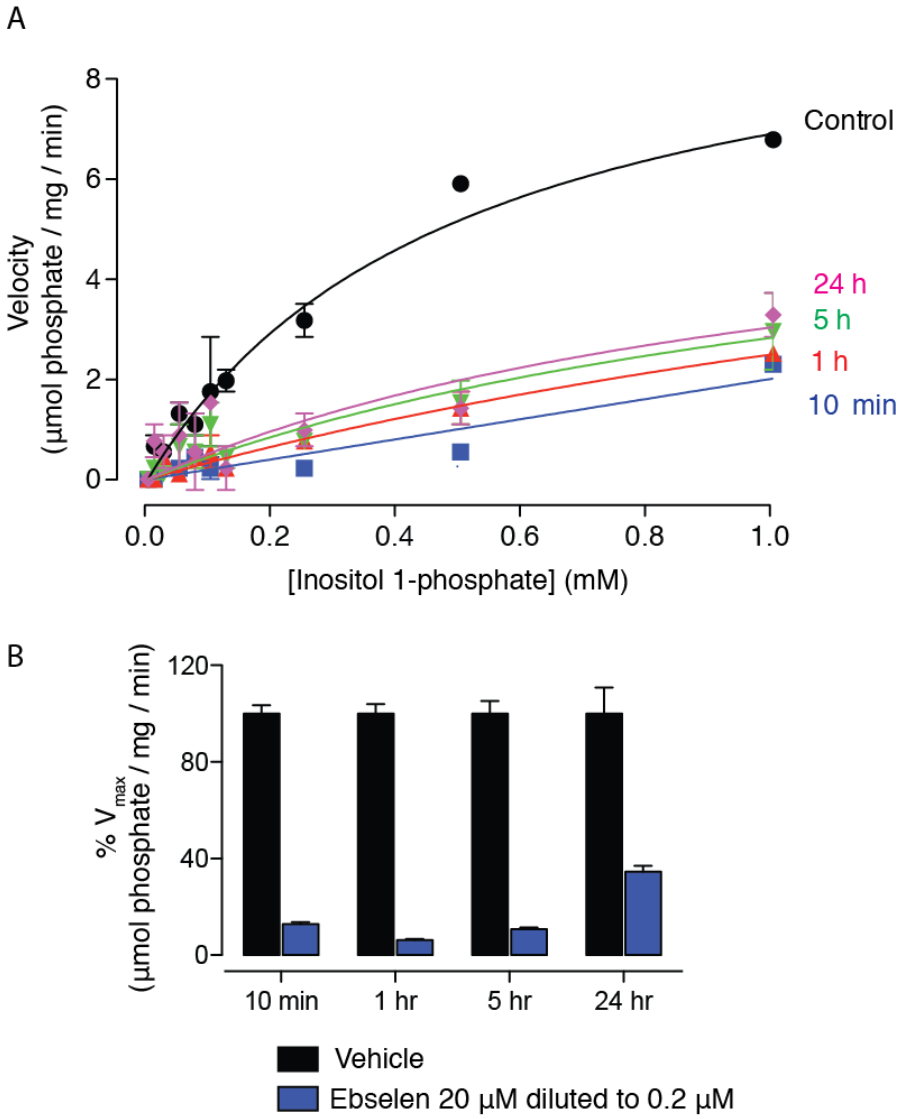


Figure 3.3.16. Test for reversibility of *Hs*IMPase inhibition by ebselen. A) Michaelis–Menten plots of IMPase activity following incubated with ebselen for indicated times and the control which was the vehicle incubated with *Hs*IMPase for the same length of time). **B)** V_{max} of the kinetics reactions.

Irreversible (or slowly reversible) reactions tend to involve covalent binding to the target. Hence, the following experiments were conducted to determine if ebselen did indeed bind covalently to IMPase.

3.3.9 Ebselen inhibition: Covalent or non-covalent?

3.3.9.1 *Hs*IMPase kinetics experiment to test for covalent binding

A concentrated solution *Hs*IMPase was incubated with 4 μM ebselen for 10 min before being diluted, to the appropriate enzyme concentration, into buffer containing the substrate. The phosphatase reaction was allowed to proceed for 1 h and then assessed by an MG assay. Simultaneously, the same concentration of ebselen (4 μM) was incubated with the appropriate concentration of *Hs*IMPase and the phosphatase reaction was allowed to proceed for 1 h (Figure 3.3.17).

If ebselen binds covalently, it would not be diluted out, and so the extent of inhibition in both (enzyme treated with 4 μM ebselen, and the concentrated enzyme treated with 4 μM ebselen which was diluted to a final concentration of 0.2 μM ebselen) would be the same. Conversely, if ebselen does not bind covalently, it will become diluted, and the IMPase specific activity in the 4 μM ebselen-treated enzyme will be lower than in the sample that was initially concentrated but then diluted (final ebselen concentration 0.2 μM).

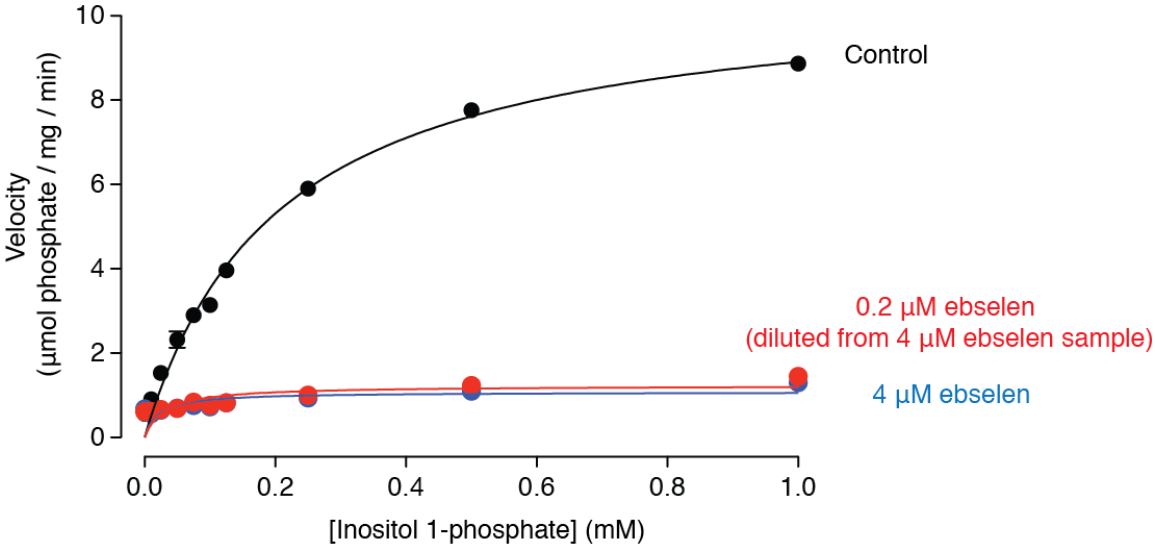


Figure 3.3.17. Test for covalent binding. Michaelis–Menten plot for *Hs*IMPase in the absence of drug and in presence of 4 µM ebselen and in presence of 0.2 µM ebselen that has been diluted from a concentrated enzyme–drug sample.

The 4 µM ebselen and the 0.2 µM ebselen (diluted from a concentrated enzyme–drug mixture), both inhibited the enzyme to the same extent (no significant difference V_{max} or K_m using the unpaired t-test) so it was concluded that ebselen binds covalently to the enzyme.

3.3.9.2 *Hs*IMPase mass spectroscopy to investigate covalent binding

Covalent binding of ebselen to *Hs*IMPase was further tested using mass spectroscopy. The enzyme was incubated with 10 µM ebselen, and then treated with 0.1% formic acid to mildly denature the enzyme. This solution was then subject to ESI-MS (Figure 3.3.18).

If ebselen bound non-covalently to the enzyme, the denaturation step would dissociate it from the enzyme so only a single peak (in the region of the molecular weight of IMPase) would be seen in the MS spectrum. However, if it bound covalently, mild denaturation would not break the bond, so there would be a shift in

the mass of the protein compared to the native protein (equal to, or a multiple of, the molecular weight of the drug).

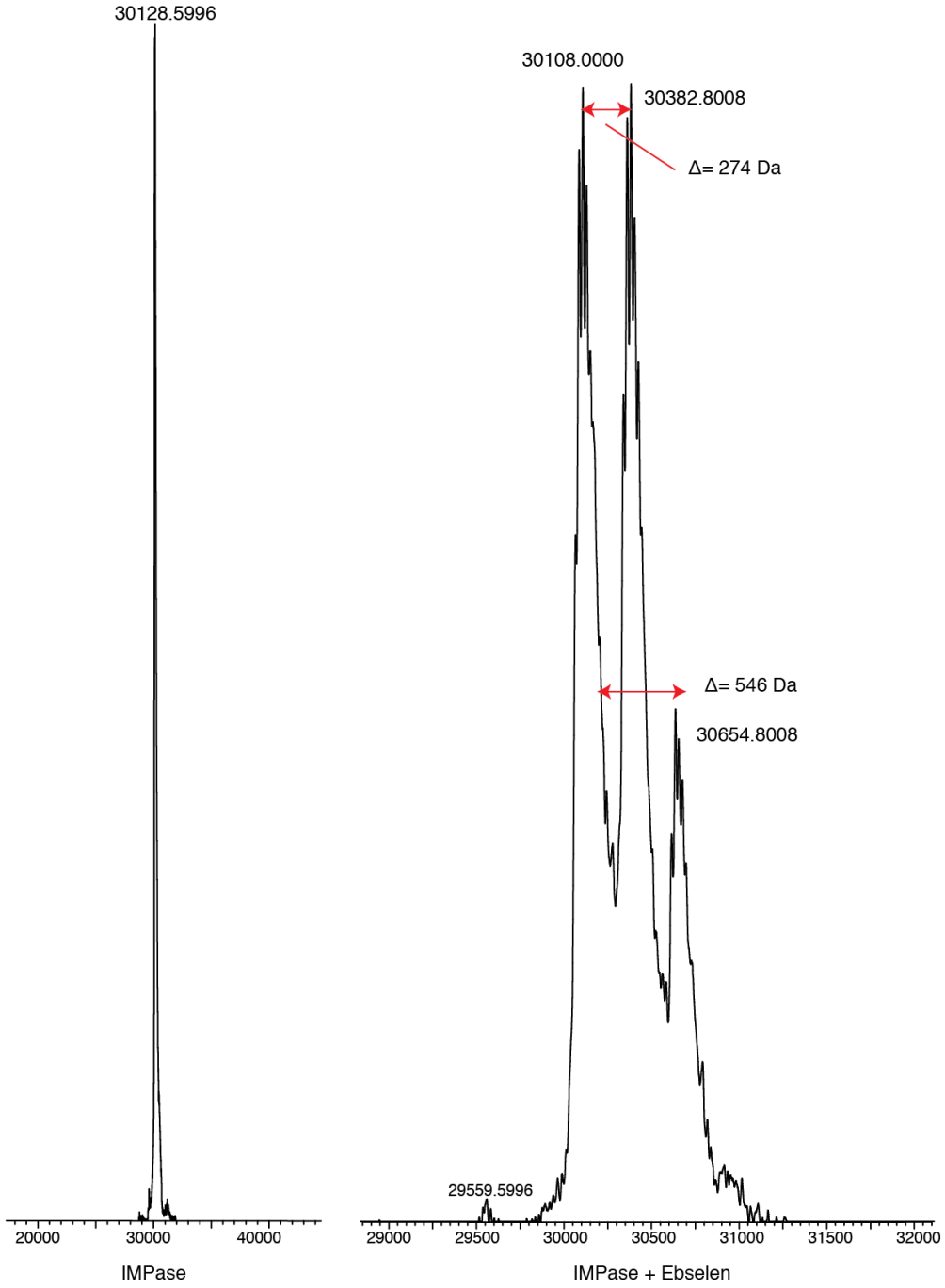


Figure 3.3.18. MS spectra of *Hs*IMPase with and without ebselen after mild denaturation. Left: IMPase alone, a single IMPase peak is observed. Right: IMPase treated with ebselen, three distinct peaks are observed. The peaks differ by a 274 Da (or a multiple thereof).

Mass spectroscopy was carried out following addition of ebselen. The presence of ebselen resulted two additional peaks with shifts corresponding to a molecular weight of about 274 Da (the molecular weight of ebselen). Since the denaturation step did not remove the bound ebselen, it was concluded that ebselen binds non-covalently to IMPase. Additionally, since three peaks were observed, it is possible to conclude that each IMPase monomer binds two molecules of ebselen.

3.3.10 Interaction with cysteine in glutathione

Mass spectroscopy results (above) suggest that two molecules of ebselen bind to each monomer of IMPase. According to some studies, although there are six cysteine residues in each monomer (bovine IMPase), only two are accessible and reactive (Greasley *et al.*, 1992; Knowles *et al.*, 1992). This raises the possibility that the selenium group in ebselen reacts with these free, accessible thiol groups. To check if ebselen can react with free thiol groups, reduced glutathione (GSH) was used.

GSH contains one free thiol group with which ebselen might react. The thiol group in GSH reacts with DTNB to form a yellow compound, NTB, which can be measured spectrophotometrically (450 nm). If ebselen binds covalently to the thiol of cysteine in glutathione, this reaction will not take place and the absorbance at 450 nm will be less than that in the control reaction (Figure 3.3.19).

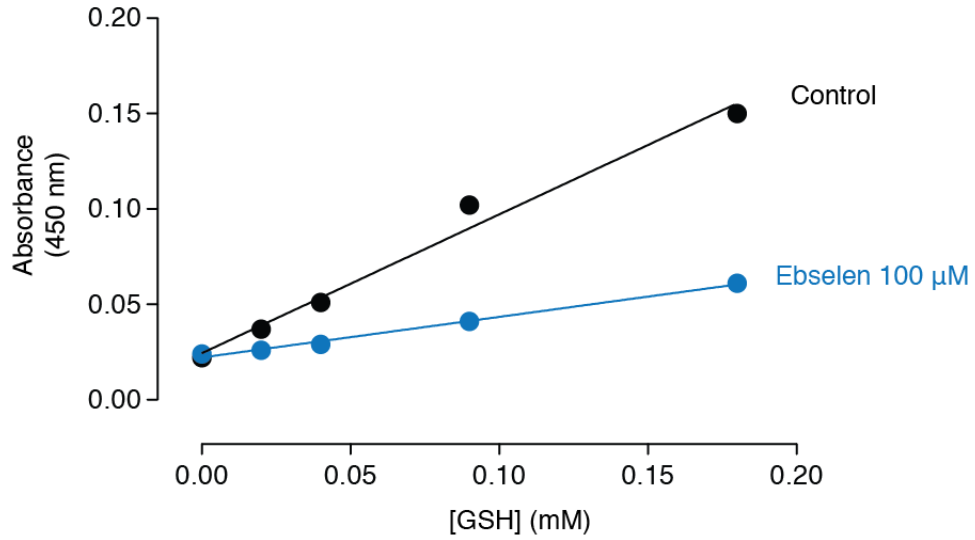


Figure 3.3.19. Ebselen reaction with cysteine residue in GSH. Ebselen (100 µM) decreased the absorbance at 450 nm (decrease in the production of NTB^-).

The data showed reduced NTB production in the presence of ebselen, thus demonstrating that ebselen binds to free thiols.

3.3.11 Interaction with GSK-3β

In the preceding evaluation of ebselen inhibition, IMPase was used as the target. However, it was important to check if ebselen had any effect on the activity of the other prominent target of lithium, GSK-3 (Klein and Melton, 1996).

This was tested at the Millipore Kinase Profiling facility, Dundee, UK. Varying concentrations of ebselen were incubated with GSK-3β, and the decrease in phosphorylation of substrate was measured as an indicator of inhibition (Figure 3.3.20).

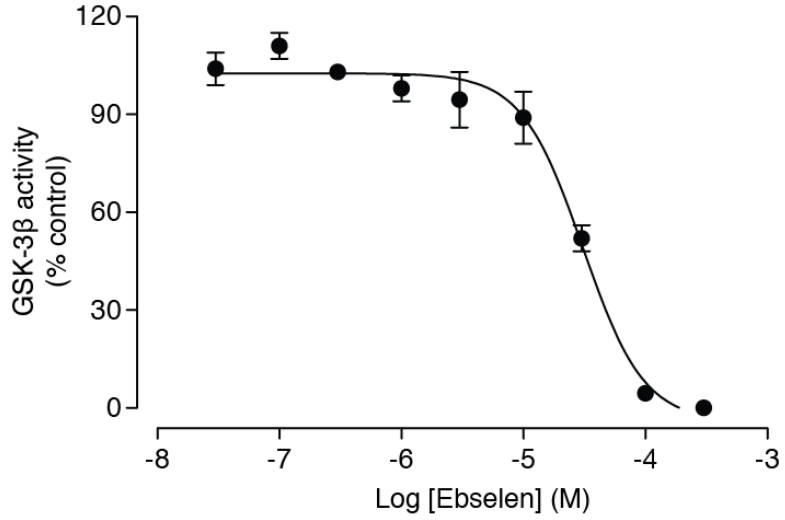


Figure 3.3.20. Ebselen inhibitory effect on GSK-3β. Ebselen inhibits GSK-3β in a concentration-dependent manner (IC_{50} = 30 μM).

Interestingly, ebselen inhibited GSK-3β activity concentration-dependently with an IC_{50} value of 30 μM. This is about ten-fold higher than ebselen inhibition of IMPase. By comparison, lithium inhibits GSK-3β with an IC_{50} of about 2 mM (Klein and Melton, 1996).

3.4 Discussion

3.4.1 Virtual screening

Using virtual screening, NIS-15 was found to inhibit IMPase non-competitively with an IC_{50} in the high micromolar range. As the NIS compounds were selected based on the 3-D shape of the IMPase substrate, Ins1P, it was expected that biochemically active compounds would exhibit competitive inhibition. Although, in general, competitive inhibitors bind to active sites, and non-competitive inhibitors bind elsewhere, this is not always necessary. However, it is difficult to explain why NIS-15 is non-competitive there is a precedent for virtual screening using the endogenous ligand resulting in such compounds as demonstrated by Ned-19 (Naylor *et al.*, 2009).

From the docking study, it was observed that NIS-15 did indeed fit into the active site, but did not form hydrogen bonds with any amino acid residues (only with a coordinated water molecule). The high IC_{50} value (160 μM) might reflect this inability to form tight bonds with the active site residues. Additionally, since the virtual screening was carried out using the Ins1P as the query molecule, it is possible that all the compounds that were output by the screening as 'hits' had similar IMPase binding affinity. Human and bovine IMPase have a K_m of approximately 100 μM for Ins1P, its substrate (Hallcher and Sherman, 1980; McAllister *et al.*, 1992). Hence, in retrospect, it is not surprising perhaps that NIS-15 had an IC_{50} of 160 μM. It would be interesting to use, L-690330 as the query molecule for virtual screening in order to obtain a more potent 'hit'. On a more positive note, NIS-15 is a small molecule (226 Da) with plenty of chemical space that can be manipulated making it a ideal lead compound for future medicinal chemistry

In conclusion, the virtual screening did lead to an inhibitor, albeit with a high IC_{50} value. It was decided that it would be unsuitable for pursuing at this stage.

3.4.2 NIH compounds screen

A total of 450 compounds were screened for IMPase inhibitory activity and two, ebselen and dihydrexidine, were identified as IMPase inhibitors. Ebselen has an IC_{50} of about 2 μM and dihydrexidine has an IC_{50} of about 30 μM. The latter compound was developed as a dopaminergic agonist (D_1 and D_5 receptor agonist more specifically) for use in Parkinson's disease (Lovenberg *et al.*, 1989). It was later withdrawn due to severe side effects such as hypotension (Blanchet *et al.*, 1998), but more recently has been revisited for potential therapy addressing cognitive deficits in schizophrenia (George *et al.*, 2007; Mu *et al.*, 2007).

Ebselen was developed as a glutathione peroxidase mimic (Schewe, 1995) and was used in Phase II clinical trials for its neuroprotective effects in stroke patients (Parnham and Sies, 2000; Yamaguchi *et al.*, 1998). It was determined to be a safe drug, i.e., patients on ebselen reported fewer incidences of adverse effects compared to patients on placebo (Kil *et al.*, 2007; Saito *et al.*, 1998). Ebselen was safe at a dose of 1,600 mg daily for one week in normal human volunteers (Lynch and Kil, 2009). Based on the information publicly available at this time there is no doubt that Ebselen is a "safer" drug than dihidrexidine. However, a more detailed report on the safety data has not been released, and more verification on safety is required. Nonetheless, it has successfully passed Phase II clinical trials, which suggests that there are no major safety issues.

Although ebselen contains selenium (potentially toxic), safety is not compromised as the selenium is not released as free selenium. ADME studies have

shown that ebselen is metabolised into 3 metabolites which can be detected in the plasma – 2-methyl selenobenzanilide, 2- glucuronyl selenobenzanilide, and N-(4-hydroxyphenyl)-2-methylselenobenzamide) (Lynch and Kil, 2009) an no free selenium was detected above the normal physiological levels.

In the present work, ebselen was selected for further investigation as a possible new drug for bipolar disorder, since it has high potency against IMPase, a better safety profile compared to dihydrexidine, and was commercially available. Another important reason for choosing ebselen over dihydrexidine was because it is known to be an antioxidant. Studies have suggested that bipolar disorder has a strong oxidative stress component (Benes *et al.*, 2006; Benes *et al.*, 2003), so the combination of antioxidant and IMPase inhibitory activity seemed promising for a possible new drug for bipolar disorder. Also, dihidrexidine is a dopamine agonist (elevated dopamine levels can precipitate mania), so it was deemed prudent not to develop dihidrexidine further as a drug for bipolar disorder.

Thus, ebselen was further evaluated for lithium-mimetic properties.

3.4.3 Ebselen inhibition of IMPase

Investigations into the kinetics of ebselen inhibition of IMPase suggested that it acted non-competitively. Although traditionally, competitive inhibitors have been preferred for therapeutic application, more interest is being focused on non-competitive inhibitors, because increasing concentrations of substrate do not reverse inhibition, as is the case with competitive inhibitors.

An analogue of ebselen, in which the selenium was substituted by sulphur (Figure 3.4.1), was also tested; inhibition of IMPase specific activity was also seen,

but not to the same extent. Further studies on the inhibitory effects of different analogues of ebselen may prove fruitful.

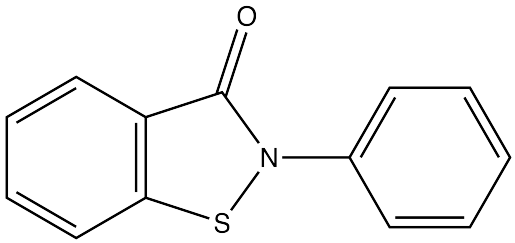


Figure 3.4.1. Analogue of ebselen. This analogue of ebselen contains a sulphur in place of the selenium in ebselen (ZINC ID 478097).

Ebselen was also shown to bind either irreversibly or with slow reversibility. This inhibition profile usually reflects covalently binding. Further investigation by kinetics and mass spectroscopy experiments, supported the conclusion that ebselen binds covalently to IMPase. Since the mass spectrum revealed that two ebselen molecules bind to each monomer, it was postulated that the selenium in ebselen was reacting covalently with cysteine residues in IMPase. The *Hs*IMPase 1 monomer contains seven free cysteine residues (Figure 3.4.2), and it is possible that ebselen reacts with two of these, which are in the accessible surface of the protein. These cysteine groups do not form disulphide bonds within the enzyme and are thus reduced (potentially reactive).

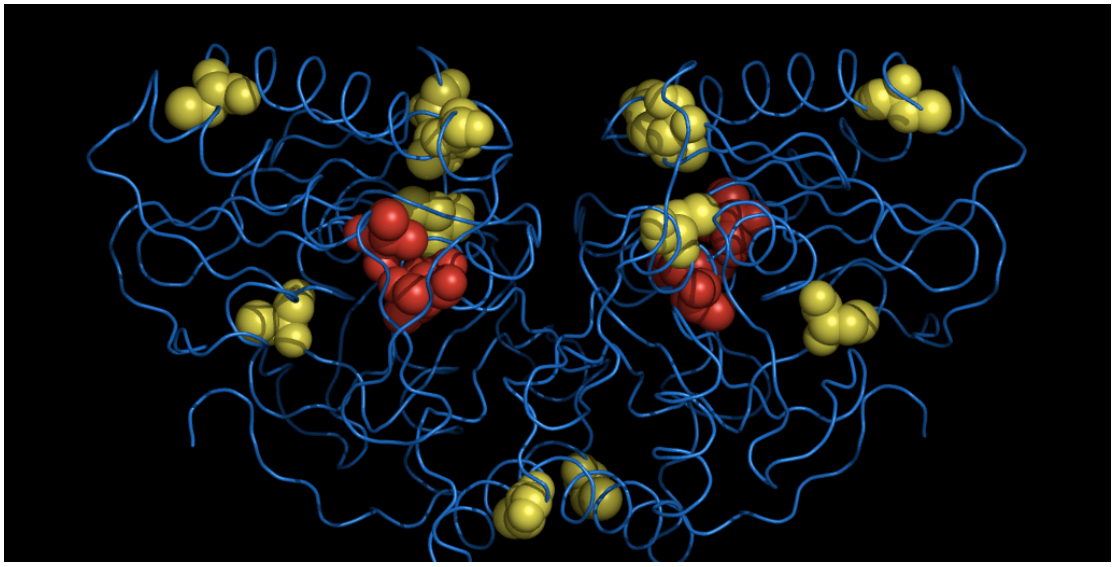


Figure 3.4.2. *Hs*IMPase 1 showing cysteine residues. Two monomers are shown; cysteine residues are displayed as yellow spheres; red spheres indicate the active site amino acid residues.

In bovine IMPase 1, only two cysteine residues are accessible despite the presence of a total of six cysteine residues in each monomer (Greasley *et al.*, 1992; Knowles *et al.*, 1992). The mass spectroscopy results in the present work indicated that two molecules of ebselen bound to each monomer of *Hs*IMPase 1. This finding is consistent with the idea that both the enzyme isoforms are comparable, such that even though there are seven cysteine residues present in human only two are accessible.

It was necessary to confirm that ebselen reacts covalently with free cysteines. For this, ebselen inhibition of the reaction of (cysteine-containing) GSH with DTNB was analysed. This showed that ebselen has the ability to bind covalently to free cysteine residues, and thus supports the postulation that ebselen binds to free cysteines in IMPase. However, it is unlikely that binding to cysteine residues distal to the active site would result in conformation changes that inhibit catalysis. Such binding is more likely to result in inhibition if it occurs at residues proximal to the active site thus impeding access by substrates.

Examination of the structure (Figure 3.4.2) confirms that one of the two accessible cysteine residues, Cys-218, is proximal to the active site residue Asp-220, which is important for the coordination of magnesium at the time of catalysis. The others are buried in the protein and are thus not accessible. Interestingly, when Cys-218 was mutated to alanine, IMPase activity was retained, and the mutant was not inhibited by high magnesium concentrations (Greasley *et al.*, 1992; Knowles *et al.*, 1992). It is likely that ebselen inhibits the enzyme by binding covalently to Cys-218. If this is true, ebselen would not inhibit the activity of this mutant, as the free cysteine is not present.

Further biochemical investigation with a C218A mutant and ebselen would test this hypothesis, but the definitive proof of the residues involved in ebselen inhibition is likely to come from X-ray crystallographic studies. Attempts at co-crystallization and soaking experiments with the protein and the inhibitor were unsuccessful. Further attempts to co-crystallize ebselen with IMPase might prove successful. Alternatively, mass spectroscopic experiments could be carried out to determine residue–ebselen bonds by using trypsin fragmentation and denaturing with Matric-assisted Laser Desorption/Ionisation - Time of Flight (MALDI-TOF).

Traditionally, covalent enzyme inhibition has been regarded as inappropriate in drug discovery although in recent times more covalent drugs have made it to the market (Singh *et al.*, 2011). For example, aspirin binds covalently to cyclooxygenase (Mizuno *et al.*, 1982); and proton pump inhibitors bind covalently by disulphide-bridge formation (Shin *et al.*, 2004). If the target enzyme has a rapid turnover, irreversible inhibition is of minimal concern (the Expasy site implies that IMPase has a half-life of about 30 h in mammalian erythrocytes). Most importantly, ebselen,

which is a compound in the NIH clinical collection, has already passed rigorous clinical testing to assess non-specific and toxic effects.

3.4.4 Other applications of Ebselen

Ebselen was also found to be a GSK-3β inhibitor and not a selective IMPase inhibitor. Hence, it will not be possible to attribute any effects of lithium that ebselen simulates to IMPase inhibition alone. However, it may still be possible to segregate IMPase and GSK-3 specific effects by using GSK-3 inhibitors that are bioavailable. Any lithium-like effects seen using ebselen could be further analysed using a GSK-3 inhibitor.

Still, since ebselen was found through drug repsoitioning, its aim is to be evaluated as a lithium mimetic that can be used clinically, rather than a selective IMPase inhibitor. This inhibitory effect that ebselen has on GSK-3 may, in fact, make it a better lithium mimetic than envisaged.

Chapter 4

Evaluation of Ebselen in Cells and Tissues

4 Evaluation of ebselen in cells and tissues

4.1 Introduction

4.1.1 Effects of lithium on inositol phosphates

There have been numerous studies on the effects of lithium; unfortunately, these have raised more questions than they have answered. Nevertheless, some characteristic markers have been identified for lithium treatment in cells and tissue. Some are markers of IMPase inhibition, and some reflect substantial physiological effects. However, which effects are mediated exclusively through IMPase inhibition and which are secondary effects (due to alterations in signalling molecules) is hard to determine, since most signalling cascades are intrinsically interconnected. The PI signalling pathway itself is extensive (some PI-modifying steps are shown in figure 4.1.1), with 63 mathematically possible inositol monophosphates alone (Irvine and Schell, 2001). Small changes in part of one cascade may profoundly affect seemingly distinct signalling pathways. This is analogous to the 'butterfly effect': the development of a hurricane formation may be influenced by changes produced in the atmosphere by the flapping of a butterfly's wings (Gleick, 1988).

At present, published studies have focused on changes in inositol phosphates during lithium treatment. Although these are good markers for lithium and provide an insight into the interactions of lithium, they do not elucidate the relevance of these interactions. Additionally, numerous studies have been carried out on Ins1P levels (and some on IP_3 and IP_4); however, none of the higher phosphorylated inositol phosphate expression profiles have been studied or characterised during lithium treatment.

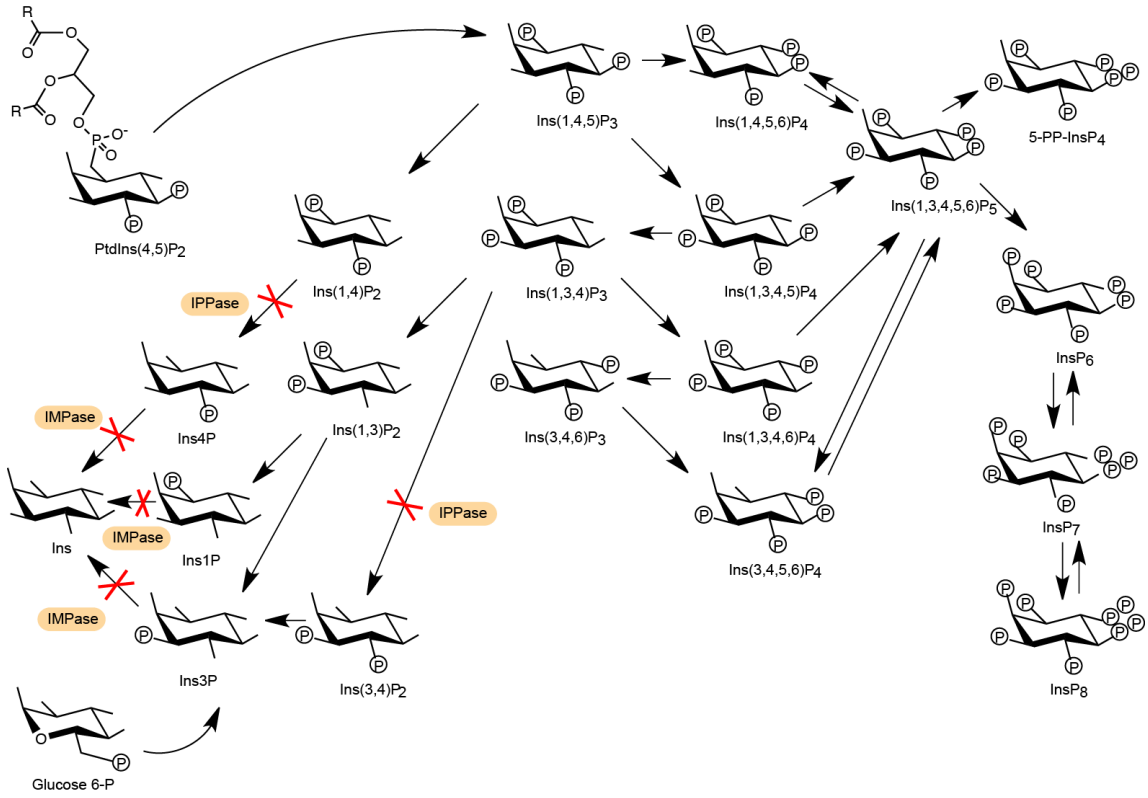


Figure 4.1.1. Inositol phosphate metabolism. The figure shows pathways of metabolism of different inositol phosphates, as identified in animals. Phosphotidylinsoitol (4,5)-bisphosphate [PtdIns $(4,5)P_2$] is converted to Inositol $(1,4,5)P_3$ which can then be metabolised in a number of different ways as shown in the figure. The enzymes that lithium is known to inhibit are shown in the boxes and the pathways inhibited are shown in the red arrows. The figure is adapted from (Irvine and Schell, 2001).

4.1.2 Aims

The aim of the investigations described in this chapter was to determine if ebselen had an effect on inositol phospholipid metabolism consistent with lithium, as well as to determine the effectiveness of ebselen in intact cells. This was achieved using the following experiments.

1. IP_1 levels in CHO-M1 cells pre-treated with ebselen were measured using an IP_1 ELISA.
2. Ebselen's effects on calcium release in response to IP_3 receptor stimulation were studied using fluorescence measurements.

3. The inositol phosphate profile in HeLa cells on ebselen and lithium pre-treatment was determined using anion exchange chromatography.
4. Mouse brain homogenate was used to determine whether ebselen crosses the blood–brain barrier, and the time-course of ebselen *ex vivo* IMPase inhibition.

4.2 Materials and Methods

4.2.1 Materials

CHO-M1 cells were obtained from Prof. John Chaliss, University of Leicester, and the HeLa cells were from Dr. Katja Rietdorf, University of Oxford. SH-SY_5Y cells were obtained from GlaxoSmithKline, UK with the permission of Dr. Martin Elliot. All media and media additives were bought from Lonza, UK. All the chemicals were purchased from Sigma–Aldrich, (Gillingham, UK) unless otherwise specified. Ebselen was purchased from Fisher Scientific, UK. L-690330 and L-690488 were purchased from Tocris, Bristol, UK. These are summarised in table 4.2.1.

The IP_1 ELISA assay kit (Cisbio Bioassays, Bagnols, France) was used to measure IIP_1 levels. [^{3}H]-inositol was bought from American Radiolabeled Chemicals (St Louis, MO, USA; # ART0261A).

Table 4.2.1. Cell lines, media, targets and agonists in the calcium release experiments

Cell lines	CHO-M_1	HeLa	SH-SY_5Y 5-HT_{2A} and 5-HT_{2C}
Medium	Alpha MEM (without nucleases) 2 mM l-glutamine 1% penicillin-streptomycin 5% Foetal calf serum 5% Newborn calf serum	DMEM 2 mM l-glutamine 1% penicillin-streptomycin 10% Foetal calf serum	DMEM 2 mM l-glutamine 10% Foetal calf serum 480 μg/ml G418
Receptor targeted	Muscarinic M_1	Purinergic P_{2Y}	Serotonergic 5-HT_{2A} and 5-HT_{2C}
Agonist	10 μM Carbachol	10 μM ATP	10 μM 5-HT

4.2.2 IP_1 ELISA

The IP-One (IP_1) ELISA assay kit (Cisbio Bioassays, Bagnols, France) was used for the determination of IP_1 levels in intact cells. The protocol was adapted from a previously published protocol (Trinquet *et al.*, 2006). The assay is based on the principle that IP_1 levels increase when IMPase is inhibited by lithium (Figure 4.2.1). Other compounds that inhibit IMPase, should replicate this effect of lithium.

Solutions used:

Stimulation buffer[5]**:** 10 mM HEPES, 1 mM $CaCl_2$, 0.5 mM $MgCl_2$, 4.2 mM KCl, 146 mM NaCl, 5.5 mM Glucose, pH 7.4.

Wash solution: 0.05% *v/v* Tween 20

Standard solution: IP1 solution (17–5000 nM).

Stop solution: (0.5 N H_2SO_4)

Additional kit contents:

A plate coated with anti-mouse IgG (ELISA plate), lysis reagent, anti-IP_1 monoclonal antibody (mAb), IP_1 –horseradish peroxidase (HRP) conjugate, 3,3',5,5'-tetramethylbenzidine (TMB) and a diluent were all provided in the kit and prepared according to the supplied instructions.

[5] The supplied stimulation buffer includes 50 mM LiCl. In order to test whether ebselen caused accumulation of IP_1 similarly to LiCl, stimulation buffer was prepared without LiCl.

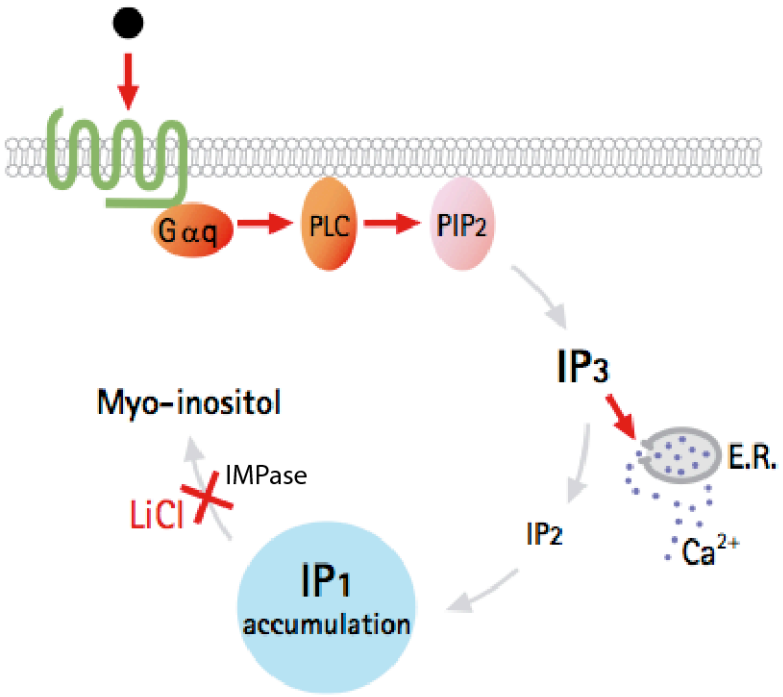


Figure 4.2.1. Pathway assayed by IP_1 ELISA. Stimulation of the $G_{\alpha q}$-coupled receptor causes the hydrolysis of PIP_2 by PLC leading to the production of IP_3. IP_3 is then recycled to myo-inositol via a succession of steps, the final of which is conversion of IP_1 to inositol. In the presence of lithium, IMPase is inhibited, which causes accumulation of IP_1 (Cisbio, 2009).

CHO-M_1 cells were grown until confluent before being plated into a 96-well plate at a density of 80000 / well (200 µL) and allowed to grow further for two days.

On the day of the experiment, the supernatant was removed from the wells. 15 µL of drug/vehicle was prepared in stimulation buffer, added to the wells and left on a rotator at R.T. for 10 min. Then, 5 µL of the agonist prepared in stimulation buffer was added to the wells, and the plate kept at 37^0C in a humidified incubator containing 5% CO_2 for 1 h. 30 µL of 1% *v/v* lysis buffer was then added, and the plate was placed back in the incubator. After 30 min, 50 µL of the well contents were transferred to the ELISA coated plate, Ins1P -HRP conjugate and the anti- IP_1 mAb were added in the order instructed, and the plate was covered and incubated on a shaker (R.T., 3 h). The wells were then washed six times with 250 µL of wash

solution, and TMB was added. The plate was incubated in the dark (R.T., 20–30 min), after which 100 μL of stop solution was added. The plate was then read at 450 nm with a correction at 595 nm.

IP-$_1$ ELISA is a competition assay kit, based on competition between free IP_1 and IP_1 –HRP conjugate for binding sites on the anti- IP_1 monoclonal antibody. Increase in IP_1 is inversely proportional to increase in optical density at 450 nm, as shown by a typical standard curve (Figure 4.2.2).

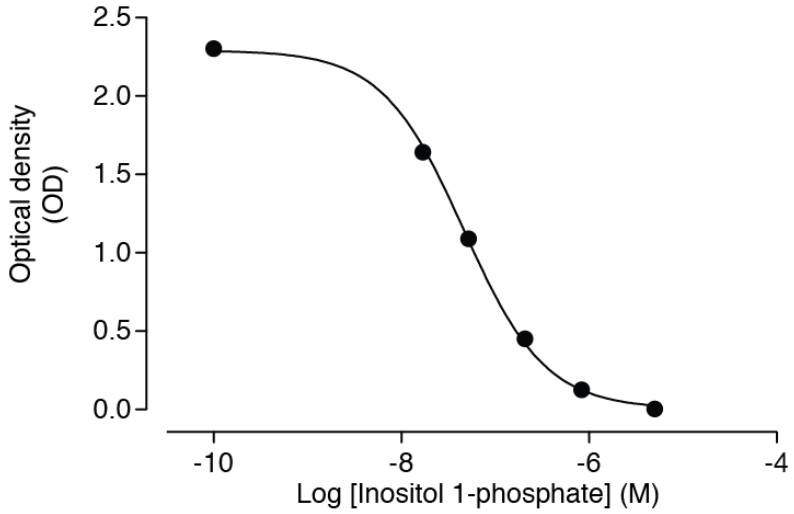


Figure 4.2.2. IP_1 ELISA standard curve. Increasing concentrations of Ins1P result in a decrease in optical density.

4.2.2.1 Test to confirm that ebselen does not interfere with the ELISA kit

Ebselen (0.1 mM or 1.0 mM) was incubated with *Hs*IMPase 1 (10 ng/well) in Tris buffer (50 mM Tris HCl, 3 mM $MgCl_2$, 150 mM KCl, 1 mM EGTA, 0.01% *v/v* Triton X) for 10 min at R.T. before the addition of varying concentrations of Ins1P (17–5000 nM) followed by incubation (37°C, 1 h). 50 μL of this solution was then transferred to an IP_1 ELISA plate coated with antibody. IP_1-HRP and anti-IP_1 mAb and the required ELISA reagents were added as above.

This experiment was also performed using the diluent provided in place of Tris buffer.

4.2.3 Michaelis–Menten kinetics with reduced ebselen

Ebselen was treated with 0.5 M dithiothreitol (DTT) in order to reduce it, and used at a final concentration of 150 μM. This reduced ebselen was incubated with *Hs*IMPase 1 for 10 minutes before the addition of Ins1P (0.1–3 mM) and further incubation (1 h, 37°C). Malachite Green (MG) reagent was added, and the absorbance measured at 595 nm. (The Malachite Green assay is described in detail in 2.2.5).

4.2.4 Calcium release assay

Calcium fluorescence studies were used to determine if ebselen inhibits the M_1, P_{2Y}, 5-HT_{2A} or 5-HT_{2C} receptors (cell/media/reagents detailed in Table 4.2.1). Stimulation of G_q-coupled receptors results in the production of IP_3, which in turn causes release of calcium from the endoplasmic reticulum (ER). The release of calcium can be observed and quantified using calcium indicator dyes such as Fura-2. (These dyes complex with free calcium and fluoresce upon excitation.) (Figure 4.2.3).

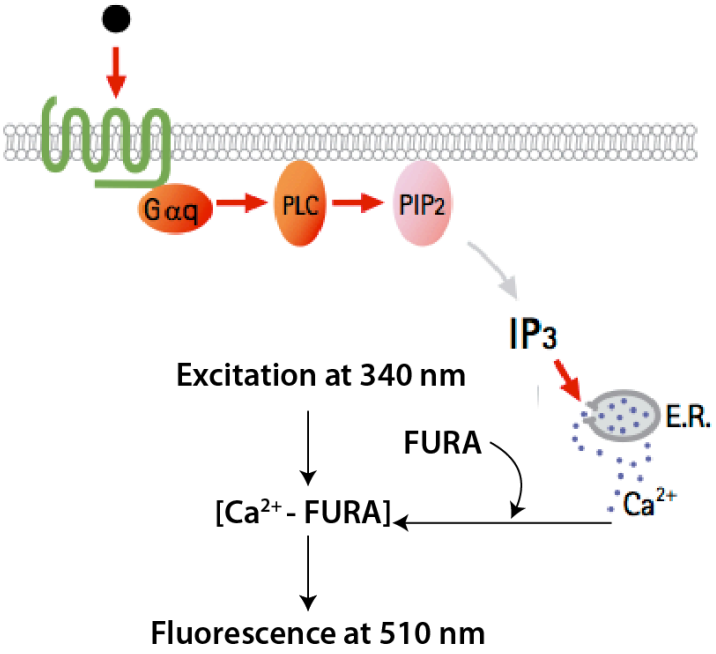


Figure 4.2.3. Calcium fluorescence. Stimulation of the $G_{\alpha q}$-coupled receptor causes the hydrolysis of PIP_2 by PLC, leading to the production of IP_3. IP_3 causes release of calcium from the ER. Calcium complexes with FURA, resulting fluorescence (510 nm, excitation at 340 nm).

The cells were plated in 96-well plates (Greiner, flat-bottomed sterile plates) and allowed to grow for two days (37°C, 5% CO_2) to 95% confluency.

On the day of the experiment, the cells were washed twice with Hank's balanced salt solution (HBSS). A 2 mM stock solution of Fura-2 AM was prepared in DMSO. This was diluted in HBSS to a final concentration of 4 μM, then 100 μL was added to each well, and the plate was left for 40 min at R.T. The cells were then washed twice with 100 μL HBSS.

The drugs were all prepared in calcium-free HBSS. Ebselen stock solution (10 mM) was made in DMSO and then diluted to the required concentration in calcium-free HBSS. All drugs were prepared at 10× concentration, and 10 μL was added to each well.

Prior to the addition of drug/vehicle, the HBSS was replaced with 90 μL calcium-free HBSS and placed in FLUOstar plate reader (BMG, Aylesbury, UK;

excitation 340 nm, emission 510 nm). Once baseline fluorescence was recorded, drug/vehicle was added and, after two minutes, the receptor agonist was added. The baseline was the average fluorescence before the addition of the agonist; the response was the fluorescence immediately after the addition of the drug. Change in fluorescence was recorded as the difference between the response and the baseline.

4.2.5 Inositol phosphate profiling and separation

The method for the inositol profiling and separation was modified from a published protocol (Azevedo and Saiardi, 2006). All the drugs were made up in HBSS. A stock solution of 5 mM ebselen in DMSO was used; this was diluted (1:100) in HBSS (final concentration 50 μM).

Buffers:

Extraction buffer: 1 M $HClO_4$, 3 mM EDTA, 0.1 mg/mL IP_6.

Neutralisation buffer: 1 M K_2CO_3, 3 mM EDTA.

Buffer A for HPLC: 1 mM EDTA

Buffer B for HPLC: 1 mM EDTA, 1.3 M $(NH_4)_2HPO_4$, pH 3.8 (with H_3PO_4).

HeLa cells were grown to 95% confluency before being plated in a 6-well plate (~50,000 cells/ well, 2 ml wells, in medium containing 20 μCi/ml [^{3}H] inositol). The plate was incubated for three days, 37^{0}C in a humidified incubator containing 5% CO_2, after which the medium was replaced with fresh medium containing 20 μCi/mL [^{3}H]inositol, and the plate was incubated for a further two days.

On the day of the experiment, the media was removed and the wells were washed twice with HBSS (2 mL/well). After washing, each well was treated with 500 μL of drug/vehicle and the plate was placed on a rotator (10 min, R.T). 5 μL of 10

mM ATP was then added to a final concentration of 100 μM, and the plate was then placed in the incubator (37°C , 1 h).

The plate was removed from the incubator and the medium was removed. 500 μL of extraction buffer was added to each well, and the plate was placed on ice and rotated for 15 min. The contents of each well were then transferred to a 2 mL screw-cap tubes, and 500 μL of neutralisation buffer was added slowly to each tube. The pH was checked to ensure that it was between pH 6 and pH 8. The tubes were loosely capped, placed on ice and rotated for 2 h. The samples were then centrifuged (9000 *g*, 10 min, 4^{o}C). Aliquots (2× 400 μL) of the supernatant were transferred into fresh tubes. The tubes were kept at −80^{o}C for future analysis. The HPLC protocol and gradient (Table 4.2.2) was modified from (Azevedo and Saiardi, 2006).

Table 4.2.2. Gradient for separation of inositol phosphates.

Time (min)	% Buffer B (start)	% Buffer B (end)
0 – 10	0	0
10 – 20	0	10
20 – 150	10	100
150 – 170	100	100
170 – 172	100	0
172 – 192	0	0

400 μL of each sample was loaded onto a Partisphere SAX column (4.6 mm × 250 mm; Whatman #4621-1505) via a perfusion pump, followed by 1 mL of ddH_2O. A flow rate of (0.5 mL/min) was applied and 1 mL fractions were collected (total, 95 fractions). A typical elution profile of inositol phosphate is shown in figure 4.2.4. [7]Scintillation vials were filled with 4 mL of scintillation fluid and 500 μL of each

[7] It was expected that inositol phosphate peaks obtained in this setup would be shifted from the representative trace shown. This is because the loading was via a perfusion pump, and although the flow-through was collected it was not recorded on the HPLC trace. Additionally, the column dimensions were different from the column used by Azevedo *et al*., 2006

fraction, and analysed using a Beckman LS6000 liquid scintillation counter. The radioactive counts (dpm) were plotted against the time of elution and compared with known values for elution of the different inositol phosphates.

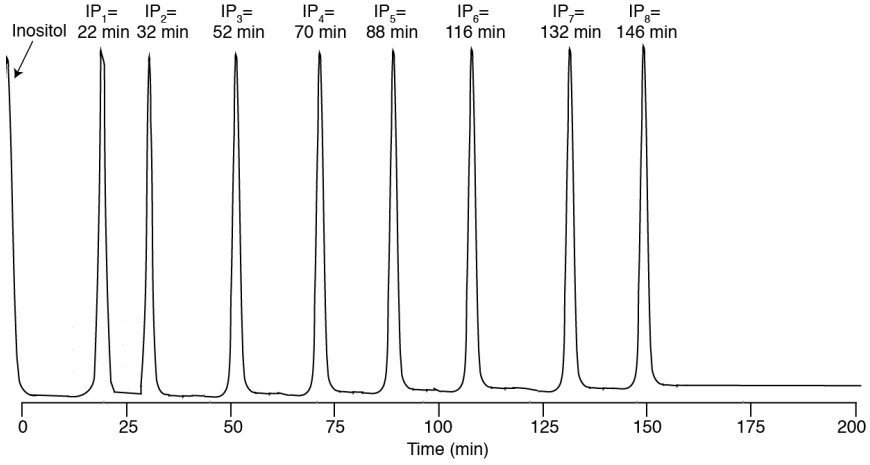


Figure 4.2.4. Typical inositol phosphate elution profile. Different inositol phosphates elute at different times. (Azevedo and Saiardi, 2006)

4.2.6 Mouse brain homogenate IMPase kinetics

Mice (C57BL/6, male, 20–25 g; Harlan, UK) administered ebselen intraperitoneally (i.p.) or vehicle (4% *w/v* β-hydroxypropyl cyclodextrin), and left for the required time. Mice were then killed by cervical dislocation, or by CO_2 followed by cervical dislocation. The brains were rapidly dissected out, divided into the separate hemispheres, and frozen by placing on dry ice immediately.

Blood was also withdrawn, using a syringe containing 0.1 mL of 10% *w/v* EDTA, and placed on ice. It was then centrifuged (9000 *g*, 10 min, 4°C) to collect the plasma fraction, which was stored at −80°C.

One half of the brain was thawed on the day of the experiment, homogenised in two volumes (for example, 250 mg in 500 μL of buffer) of Tris buffer (50 mM Tris

HCl, 3 mM $MgCl_2$, 150 mM KCl, 1 mM EGTA, 0.01% *v/v* Triton X) then diluted in Tris buffer (final concentration, 5 mg/mL). From this, 5 µL was then added to 10 µL of Ins1P (0.1–2.5 mM), the volume was made up to 50 µL in an Eppendorf tube, then vortexed and placed in a water bath (37°C, 1 h). A second Eppendorf tube was similarly prepared, but additionally with 30 mM LiCl (Lithium should eliminate IMPase activity, so any detected activity will be non-specific (Cryns *et al.*, 2008). Subtraction of non-specific activity from total activity gives total IMPase activity. A Michaelis–Menten plot was constructed (velocity of reaction against substrate concentration). The velocity was determined using the Malachite Green assay as described in a previous chapter (Section 2.2.5.1). The protein content was measured using the bicinchoninic acid method as described (Section 2.2.5.2), except that the BSA standards were prepared in Tris buffer, and the plate was left for 30 min for colour development.

4.3 Results

4.3.1 Effect of ebselen on IP_1 levels in cells

The Ins1P - ELISA assay was carried out in with CHO-M1 cells to determine the effects of ebselen on IP_1 accumulation. IP_1 levels show a negative correlation with optical density at 450 nm in the IP_1 ELISA and a thus a decrease in optical density corresponds to an increase in IP_1 levels. The optical density was measured at 450 nm and at 595 nm. The latter is a measure of baseline, and was subtracted from the former to give the final corrected optical density at 450 nm.

4.3.1.1 Lithium and L-690488 in the IP_1-ELISA assay

Both lithium and L-690488 (which is a cell permeable precursor of L-690330) have been shown to cause accumulation of IP_1 in CHO-M1 cells (Atack *et al.*, 1993a; Atack *et al.*, 1994). These were used to validate the experimental setup, as described in figure 4.3.1.

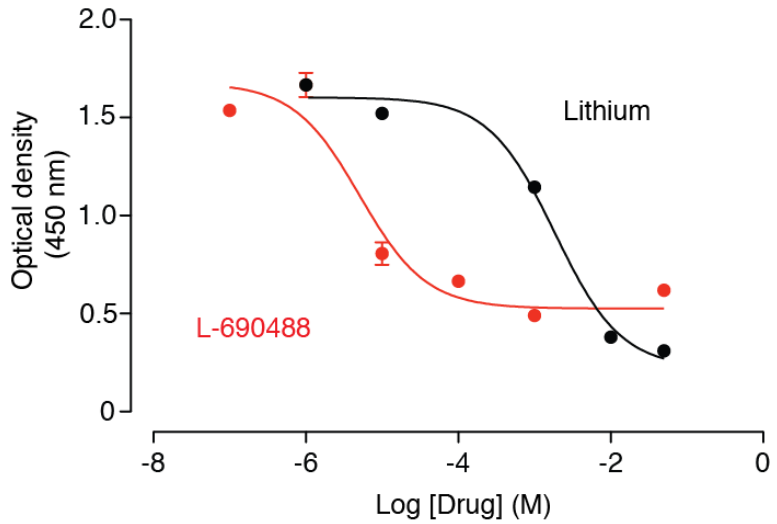


Figure 4.3.1. Concentration response curves of lithium and L-690488 in the IP_1-ELISA. Concentration-dependent IP_1 accumulation occurs in CHO-M1 cells treated with lithium or L-690488. The IC_{50} values were determined as 1.8 mM (n = 4) and 5.1 μM (n = 2), respectively.

CHO-M1 cells treated with lithium showed IP_1 accumulation (IC_{50} = 1.8 mM), as did cells treated with L-690488 (IC_{50} = 5.1 μM), as shown in figure 4.3.1. The latter is a precursor of L-690330 (competitive IMPase inhibitor) but is cell-permeable and is hydrolysed inside the cells to yield L-690330 (Atack *et al.*, 1994).

Some studies have suggested that *uncompetitive* inhibition of IMPase is necessary to cause IP_1 accumulation (Faraci *et al.*, 1993). However, other studies have shown that *competitive* inhibition also results in accumulation of the substrate (Atack *et al.*, 1993a; Atack *et al.*, 1994). The accumulation of IP_1 seen using the ELISA here confirms that it is not dependent on the mode of inhibition — both competitive and uncompetitive modes of IMPase inhibition increased IP_1 accumulation. Of course, cell permeability is essential.

4.3.1.2 Ebselen in the IP_1 ELISA

Once the assay had been validated by the positive controls, ebselen was tested in CHO-M1 cells for IP_1 accumulation.

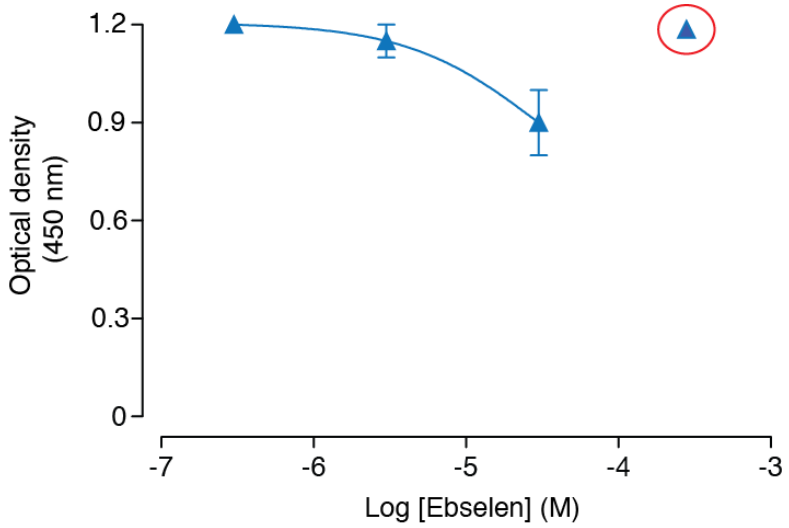


Figure 4.3.2. Effect of Ebselen in the Ins1P **-ELISA.** Ebselen caused a small increase in Ins1P accumulation at around 30 μM. This was not concentration-dependent: at 300 μM (circled in red) there was no elevated Ins1P accumulation compared to control (n=3). Only the first three data points were fitted in the curve to show the trend.

Although there did seem to be a small increase in IP_1 concentration (~25% decrease in OD at 30 μM; Figure 4.3.2), ebselen did not accumulate IP_1 to the extent that both lithium and L-690488 had.

This experiment was repeated using SH-SY_5Y cells over-expressing the 5-HT_{2C} receptor and, again, no significant IP_1 accumulation was observed.

4.3.1.3 Possible ebselen interference with the IP-One ELISA

Since ebselen did not show a significant IP_1 accumulation in the IP_1-ELISA, it was postulated that ebselen might be interfering with the reagents in the ELISA kit. Ebselen was used *in vitro* to inhibit IMPase, and the increase in Ins1P was measured using the ELISA kit. If ebselen does not interfere with the kit reagents, and there should be a decrease in optical density. In the case of the vehicle (control), *Hs*IMPase 1 will not be inhibited and there should be no accumulation of Ins1P. This reaction was carried out using Tris buffer, then repeated using the diluent provided in the kit (Figure 4.3.3).

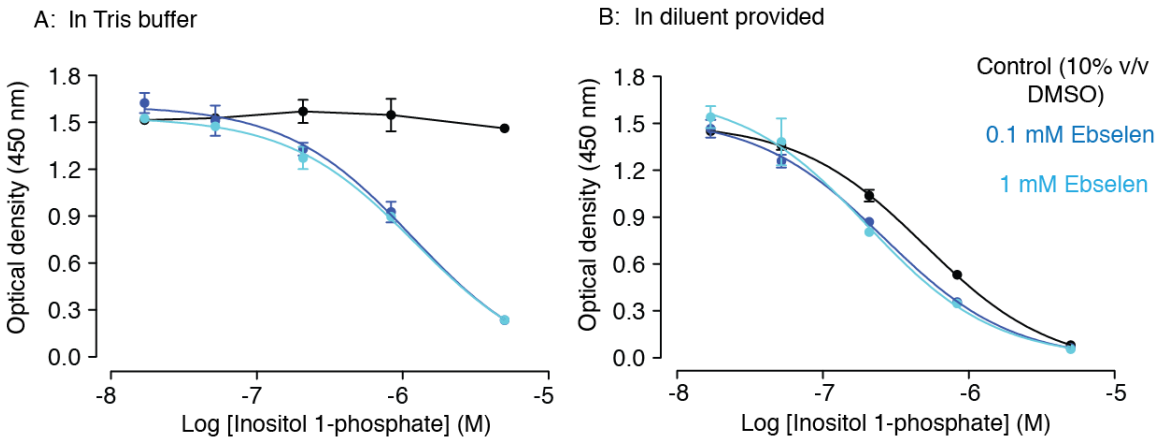


Figure 4.3.3. Effect of ebselen *in vitro* on the IP_1 ELISA assay. The effect of ebselen added *in vitro* on the Ins1P ELISA to check if ebselen, at high concentrations may be interfering with the kit reagents. A) *In vitro* effects of ebselen in Tris buffer, and B) effects when made up in the diluent provided. (n = 3).

At both concentrations, ebselen caused an increase in Ins1P, as shown by the reduction in optical density (Figure 4.3.3), while vehicle (10% *v/v* DMSO) did not increase Ins1P. However, when the experiment was repeated using the diluent provided in the kit, even the vehicle seemed to cause an increase in Ins1P (Figure 4.3.3B). It seems that the vehicle control when prepared with diluent has the same effect on Ins1P accumulation. Additionally, when Malachite green was added to IP_1 standards (17–5000 nM) in diluent there was a gradient from yellow to green, whereas the standards in Tris buffer remained yellow.

Nonetheless, figure 4.3.3 does show that the presence of high concentrations of ebselen does not interfere with the ELISA reagents.

4.3.2 Effects of reduced ebselen on IMPase activity

Another postulation was that ebselen might exist in equilibrium with its reduced form in cells due to reaction with glutathione (GSH), which is present

endogenously in cells. There is the possibility that this reduced form of ebselen does not have the ability to inhibit IMPase, and hence the concentration of active ebselen may be lower than that required to cause IP_1 accumulation. Therefore, ebselen was reduced and then tested *in vitro* for IMPase inhibitory activity.

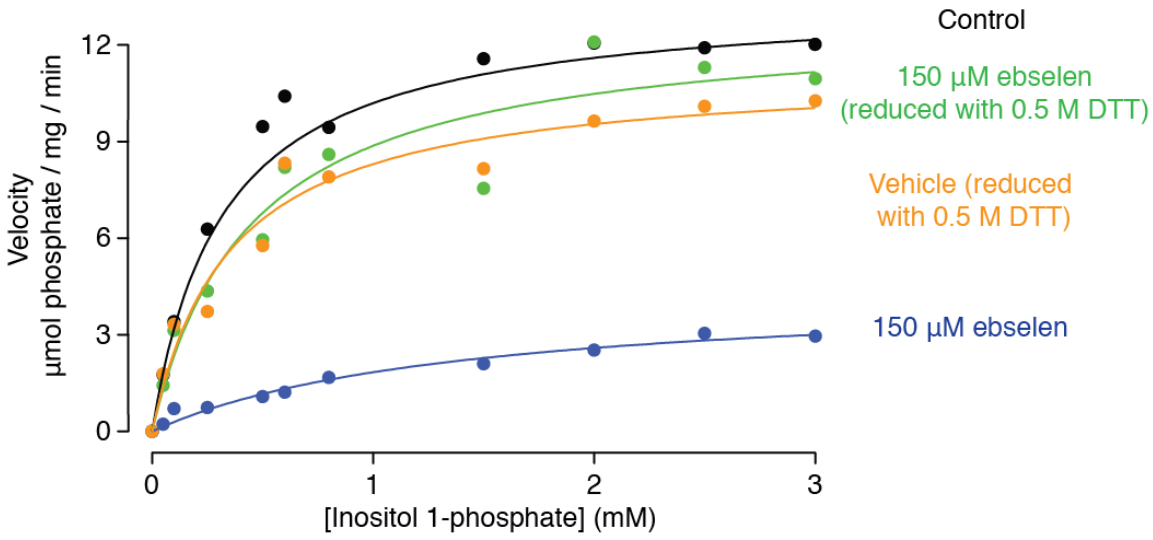


Figure 4.3.4. Effects of reduced ebselen on IMPase activity. *Hs*IMPase was treated with reduced and non-reduced ebselen at 150 µM. The latter inhibited IMPase activity whereas reduced ebselen did not. A control with and without DTT (a reducing agent) was also carried out, and no significant difference was observed between these.

The data were plotted to obtain Michaelis–Menten kinetic curves for reduced and non-reduced ebselen (Figure 4.3.4). It was concluded that the reduced form of ebselen does not inhibit IMPase activity at 150 µM.

4.3.3 Calcium release experiments

It is possible that ebselen causes inhibition of the M_1 receptor. To test this, calcium release experiments were conducted.

Fura-2 complexes with intracellular calcium and fluoresces at 510 nm. If calcium release on receptor stimulation were inhibited, there would be attenuation of fluorescence compared to the vehicle.

Ebselen was tested in CHO-M1, HeLa and SH-SY-$_5$Y cells to check for the inhibition of the muscarinic-M_1, P_{2Y}, and 5-HT_{2A}/5-HT-$_{2C}$ receptors, respectively.

4.3.3.1 Muscarinic receptors (M1)

The effect of 1, 10 and 100 μM ebselen on calcium release in CHO-M1 cells was studied by addition to the cells, before stimulation of the muscarinic receptors using 10 μM carbachol. A decrease in fluorescence units indicates that calcium release is antagonised whereas no change in fluorescence units suggests that the muscarinic receptor is not inhibited by ebselen. The trace of calcium release in the presence and absence of 10 μM ebselen is shown in Figure 4.3.5.

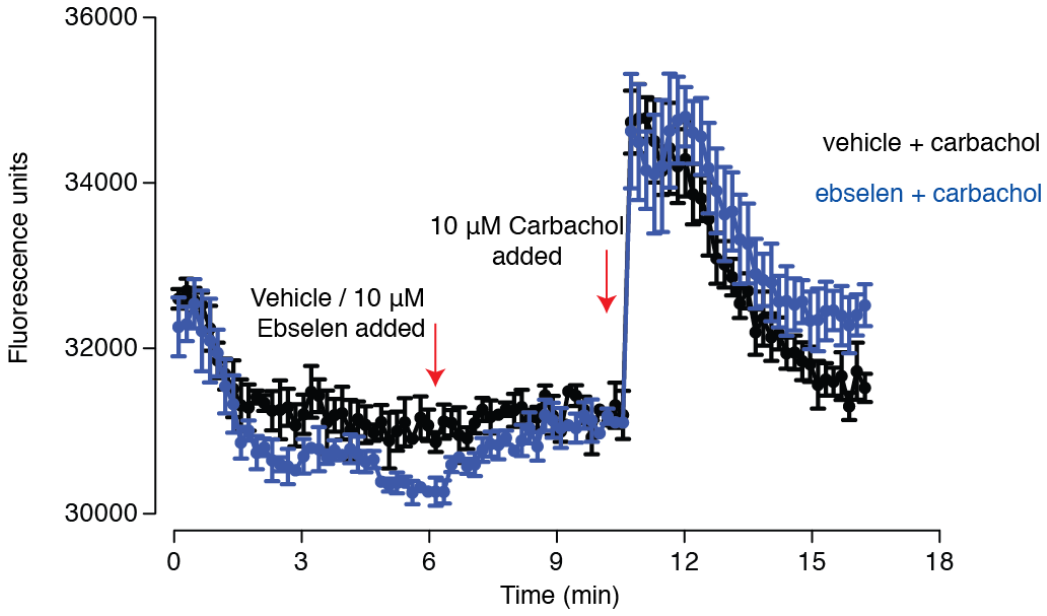


Figure 4.3.5. Effect of ebselen on calcium release following muscarinic receptor stimulation. Compared to vehicle, 10 μM ebselen did not significantly affect calcium release in CHO-M1 cells in the presence of 10 μM carbachol. Red arrows indicate the points at which ebselen/vehicle and carbachol additions were made.

There is a drop in cytosolic calcium at the start of experiments as cells are placed in calcium-free buffer. The addition of ebselen did not in itself affect cytosolic calcium, however, the addition of carbachol caused a sharp transient increase, which gradually came back to baseline.

The results for all three ebselen concentrations were analysed by using an unpaired t-test (Figure 4.3.6).

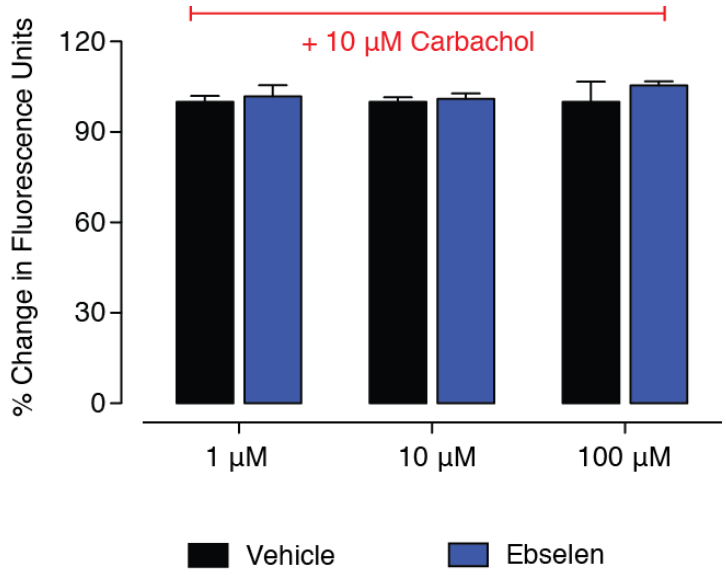


Figure 4.3.6. Effect of concentration on calcium release by muscarinic receptor stimulation. Ebselen (1, 10 and 100 µM) was tested in CHO-M1 cells for its effect on calcium release when stimulated by 10 µM carbachol. Ebselen did not inhibit calcium release on stimulation of the muscarinic receptor. None of the treatments were found to be significantly different from their vehicle controls using the unpaired t-test.

Ebselen did not antagonise the muscarinic receptor or the (release of calcium) following IP_3 receptor stimulation in this experimental setup. Higher concentrations of ebselen could not be tested because of solubility constraints. It was concluded that ebselen does not inhibit the muscarinic M_1 receptor at concentrations up to 100 µM.

4.3.3.2 Purinergic receptors (P_{2Y})

The effect of 1, 10 and 100 μM ebselen on calcium release was studied by subsequent stimulation of the purinergic receptors in HeLa cells by 10 μM ATP. The trace of calcium release in the presence and absence of 10 μM ebselen is shown in Figure 4.3.7.

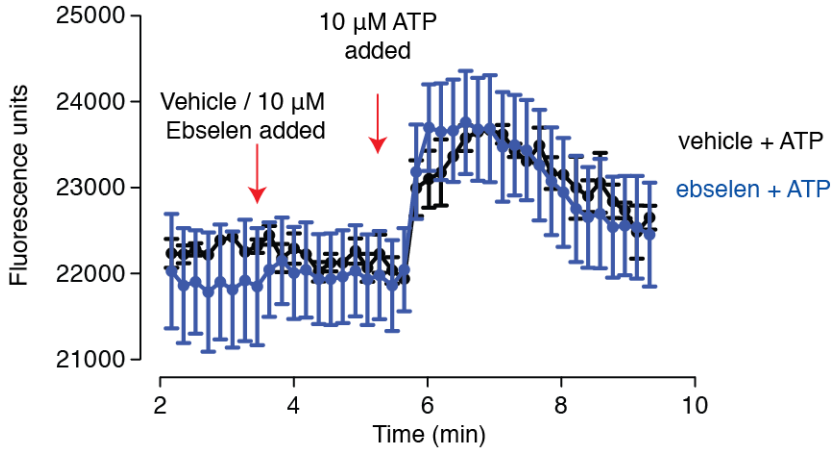


Figure 4.3.7. Effect of ebselen on calcium release following purinergic receptor stimulation. . Compared to vehicle, 10 μM ebselen did not significantly affect calcium release in HeLa cells in the presence of 10 μM ATP. Red arrows indicate the points at which ebselen/vehicle and carbachol.

The addition of ebselen did not in itself affect cytosolic calcium, however, the addition of ATP caused an increase in fluorescence intensity.

The results for all three ebselen concentrations were analysed by using an unpaired t-test (Figure 4.3.8).

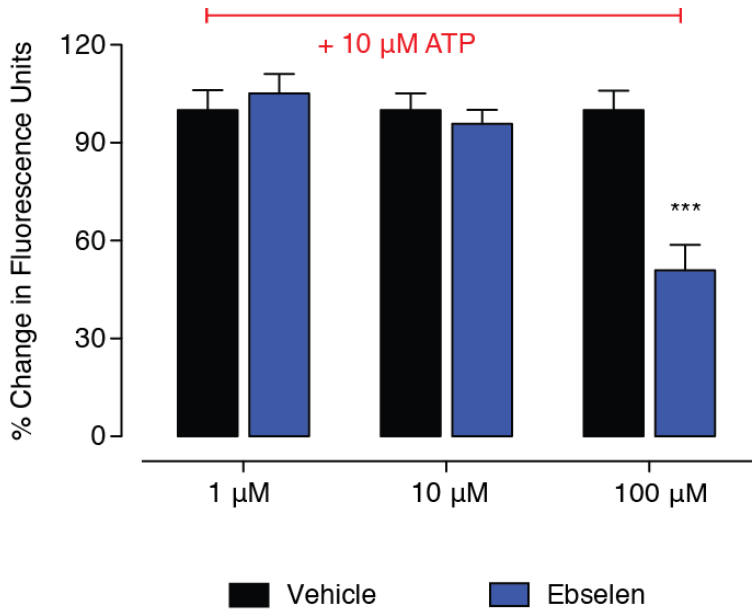


Figure 4.3.8. Effect of ebselen concentration on calcium release by P_{2Y} receptor stimulation. Ebselen (1, 10 and 100 µM) was tested in HeLa cells for its effect on calcium release when stimulated by 10 µM ATP. At 1 and 10 µM Ebselen did not inhibit calcium release upon stimulation of the purinergic receptor. However, at 100 µM there was a 50% drop in calcium fluorescence (compared to its vehicle). Statistical significance was calculated using the unpaired t-test. ***, p <0.001.

At 1 and 10 µM, Ebselen ebselen did not antagonise the P_{2Y} receptor or the (release of calcium from the IP_3 receptor-linked calcium store, in this experimental setup at 1 and 10 µM, although 100 µM ebselen did cause a 50% decrease in calcium release as shown (Figure 4.3.8).

This inhibitory effect of 100 µM ebselen might be an artefact, as there was, unusually, also a significant change in baseline (i.e. prior to ATP stimulation) for 100 µM ebselen-treated cells compared to vehicle (Figure 4.3.9). A larger baseline decrease relative to vehicle was observed compared to that with 10 µM ebselen. This might account for the reduction in fluorescence units (FU) for 100 µM ebselen cells upon stimulation with 10 µM ATP.

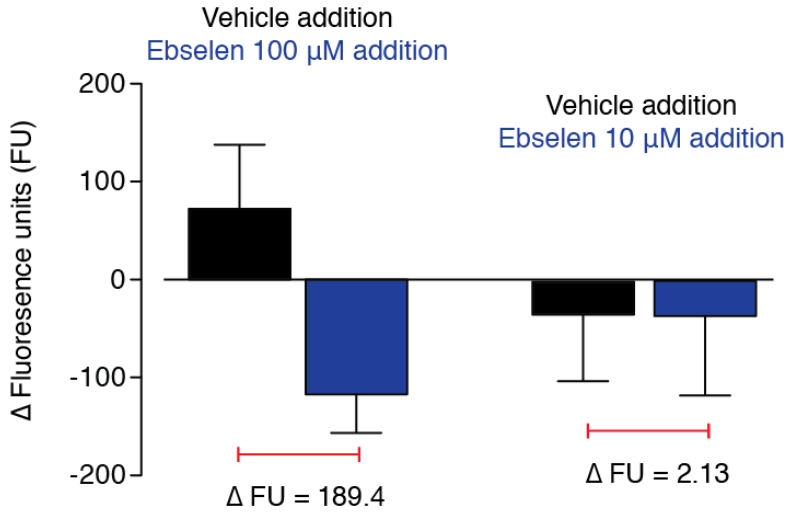


Figure 4.3.9. Baseline differences in 10 and 100 µM ebselen treated cells. Cells treated with 100 µM ebselen (blue) showed reduced fluorescence (~190 FU) than those treated with vehicle (black). This was not evident with 10 µM ebselen. This lower response might explain the differences seen in the calcium release when 100 µM ebselen was added.

However, it is yet to be established whether this baseline change is due to the presence of 100 µM ebselen or a variable response of the set of cells used for this experiment. No baseline change was seen in CHO-M1 cells using 100 µM ebselen.

4.3.3.4 Serotonergic receptors (5-HT_{2A} and 5-HT_{2C})

SH-SY_5Y 5-HT_{2C} is a human neuroblastoma-derived cell line overexpressing the 5-HT_{2C} serotonin receptor. The effects of 1, 10 and 100 µM ebselen on calcium release in SH-SY_5Y 5-HT_{2C} cells were studied, by subsequent stimulation of the serotonergic receptors with 10 µM 5-HT (5-hydroxytryptophan or serotonin). Additionally, the effect of 10 µM ebselen on 10 µM 5-HT-induced calcium release in SH-SY_5Y 5-HT_{2A} cells (5-HT_{2A} receptor) was also studied. (Two separate sets of cell lines were used; one overexpressing the 5-HT_{2C} receptor and the other overexpressing the 5-HT_{2A} receptor).

The bar graph in figure 4.3.10 show the effect of 1, 10, 100 μM ebselen and 10 μM clozapine (a known 5-HT_{2C} antagonist) on subsequent calcium release in SH-SY_5Y-5HT_{2C} cells by 10 μM 5-HT.

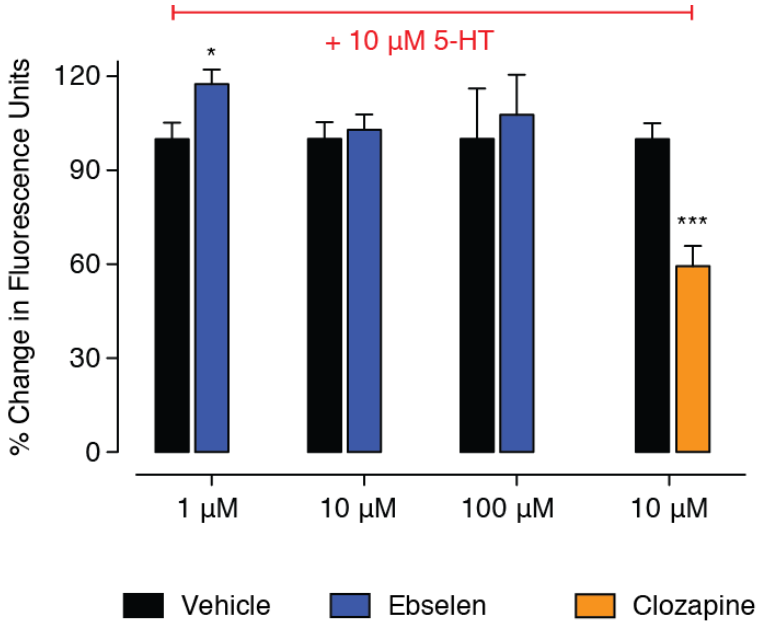


Figure 4.3.10. Effect of ebselen on calcium release following 5-HT_{2C} receptor stimulation. Ebselen (1, 10 or 100 μM), was tested in SH-SY5Y cells overexpressing the 5-HT_{2C} receptor for their effects on calcium release following stimulation by 10 μM 5-HT. Clozapine, a known antagonist at this receptor, was also used as a positive control at 10 μM. Statistical significance was calculated using the unpaired t-test. * p <0.05; *** p< 0.001.

Ebselen at 1, 10 and 100 μM did not antagonise the 5-HT_{2C} receptor (calcium release following 5-HT_{2C} stimulation). 10 μM clozapine decreased calcium release by 40% compared to its vehicle. Although 1 μM ebselen caused a ~15% increase in calcium release compared to its vehicle. However, as neither 10 nor 100 μM ebselen had a statistically significant effect, this is likely to be an experimental artefact.

The experiment was repeated with SH-SY_5Y 5HT_{2A} cells (10 μM ebselen and 10 μM clozapine, Figure 4.3.11). Ebselen at 10 μM did not antagonise calcium release on 5-HT_{2A} receptor stimulation, but 10 μM clozapine decreased calcium release by 60% compared to its vehicle.

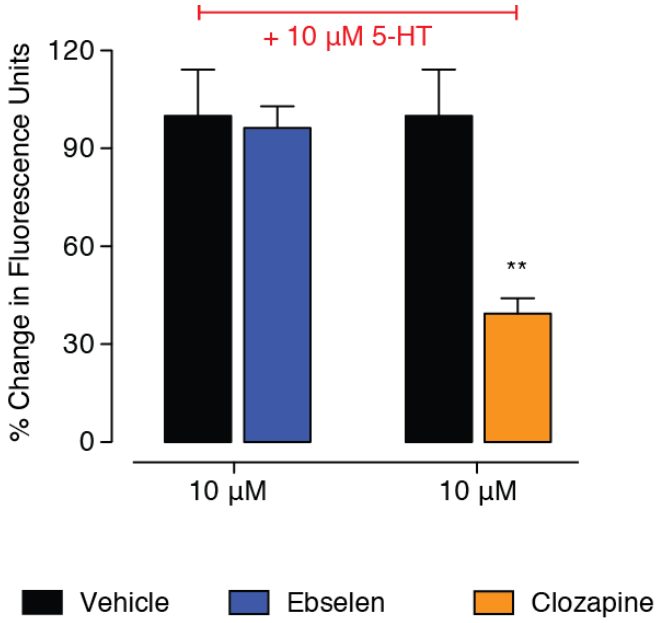


Figure 4.3.11. Effect of ebselen on calcium releasefollowing 5-HT$_{2A}$ receptor stimulation. 10 µM ebselen was tested in SH-SY$_5$Y cells overexpressing the 5-HT$_{2A}$ receptor, for its effects on calcium release when stimulated by 10 µM 5-HT. Clozapine, a known antagonist at this receptor, was used as a positive control at 10 µM. Statistical significance was calculated using the unpaired t-test. ** p <0.01.

4.3.4 Inositol phosphate profile

The recycling of IP_3 back to free inositol in cells requires a series of steps, the last of which is conversion of IP_1 into inositol. It is possible that ebselen inhibits an enzyme other than one in the G_q-coupled pathway and thus causes an increase in inositol phosphate(s) other than IP_1. In order to investigate this, the profiles of the different inositol phosphates produced upon ATP-induced stimulation in the presence of ebselen or lithium was studied.

The [^{3}H]inositol phosphate fractions obtained were analysed by plotting radioactive counts (dpm) against time (min). The inositol phosphate peaks obtained (Figure 4.3.12) were compared between the different treatments.

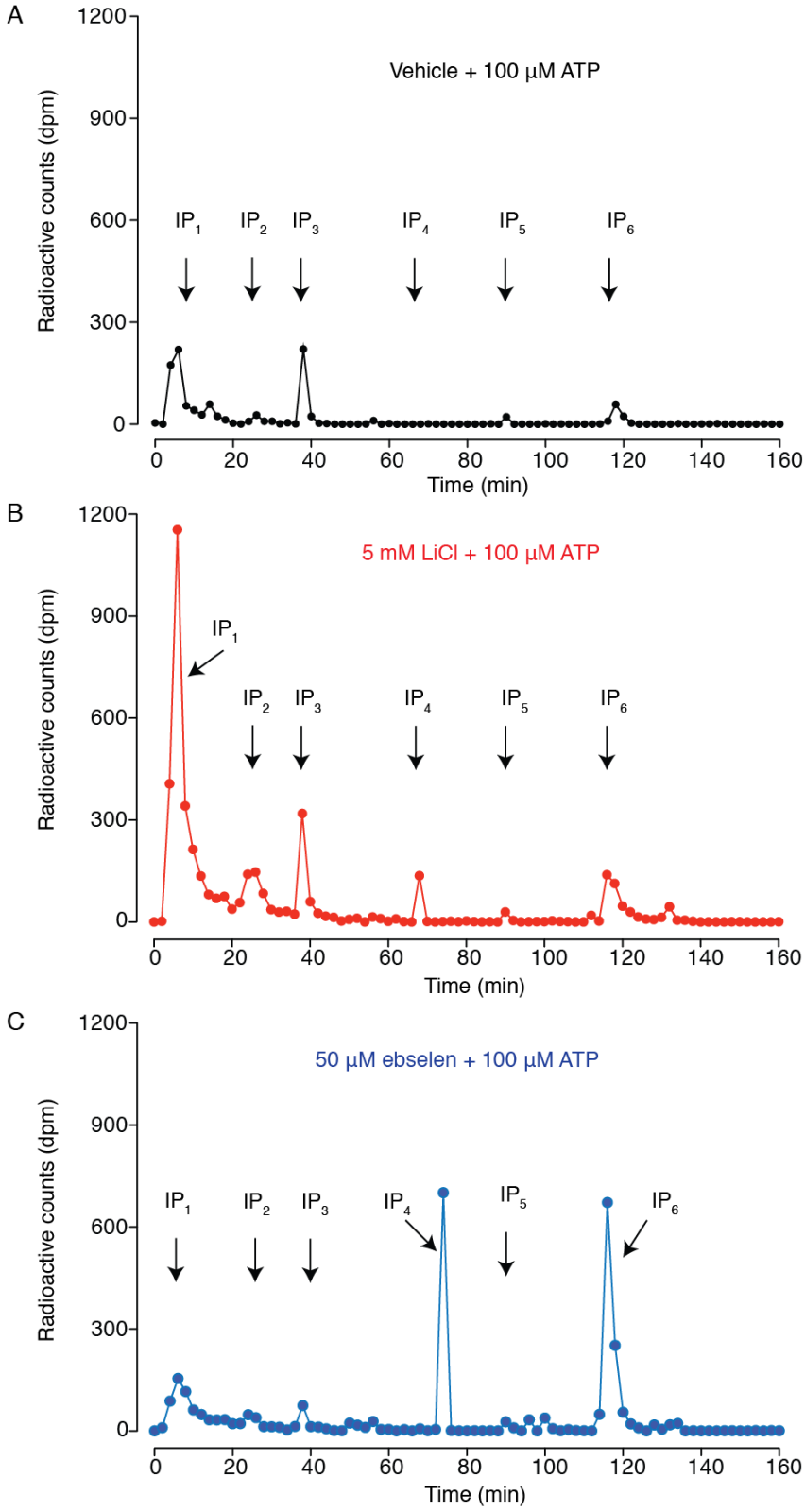


Figure 4.3.12. The inositol phosphate profile obtained with A) vehicle, B) lithium and C) ebselen. HeLa cells were treated with either vehicle, 5 mM LiCl or 50 µM ebselen, then stimulated with 100 µM ATP. The cytosolic fraction was passed though an anion exchange column and the inositol phosphates separated based on their charge and analysed by their time of elution.

In the vehicle treated stimulated cells, only IP_1 and IP_3 could be clearly seen in the HPLC trace. In comparison, lithium-treated cells showed a large increase in the IP_1 peak (Figure 4.3.12B); this was 4-fold higher than the IP_1 peak seen with vehicle treatment. There was no discernable change in IP_1 in ebselen treatment compared to the vehicle–treated cells. In contrast, ebselen treatment (4.3.12C) showed an accumulation of IP_4 and IP_6, which were not observed on vehicle treatment.

In the next experiment, a combination of 5 mM lithium and 50 μM ebselen was used to pre-treat the cells before the addition of 100 μM ATP.

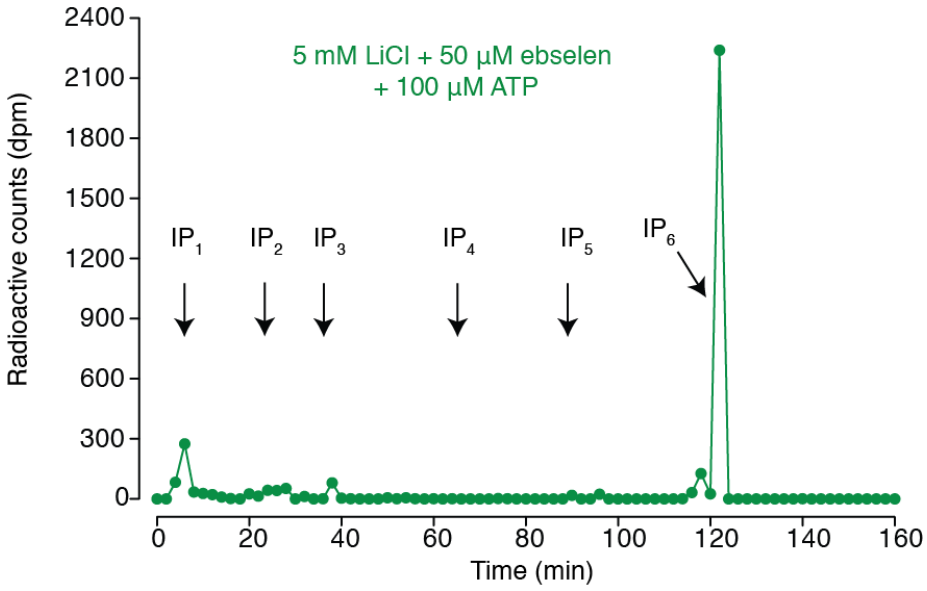


Figure 4.3.13. The inositol phosphate profile with lithium and ebselen combined. Cells were treated with 5 mM LiCl and 50 μM ebselen then stimulated with 100 μM ATP. The cytosolic fraction was passed though an anion exchange column and the inositol phosphates separated based on their charge and analysed by their time of elution.

In this case, there was a substantial increase in the IP_6 peak, which was almost 4-fold higher than the peak observed with ebselen pre-treatment alone (Figure 4.3.13. Interestingly, the large increase in IP_1 accumulation that was found in presence of

lithium alone was no longer present. The IP_1 peak was at the same level as that for vehicle-treated cells (Figure 4.3.12A).

This suggests that ebselen is likely to be inhibiting a step in the IP_3 signalling cascade prior to IP_1 and thus causing accumulation of IP_6 but not IP_1. Also, ebselen seems to abolish lithium's effect on IP_1 accumulation, and diverts it towards accumulating IP_6 instead.

4.3.5 *Ex vivo* IMPase inhibition

In order to establish if ebselen could pass the blood-brain barrier, brain homogenate from mice injected with ebselen was tested for IMPase activity, using the Malachite Green assay. Compared to the vehicle-treated mice, the ebselen-treated ones should have lower IMPase activity if ebselen is present in brain tissue.

4.3.5.1 Optimisation

The brains were dissected and homogenised from drug-naïve mice, and different dilutions of homogenate were made and tested for IMPase activity using different IP_1 concentrations. The optimal homogenate protein concentration for this assay, based of the limits of detection, was found to be 0.5 mg/mL. The IMPase activity of the mouse brain homogenate is shown in figure 4.3.14 as a Michaelis-Menten plot.

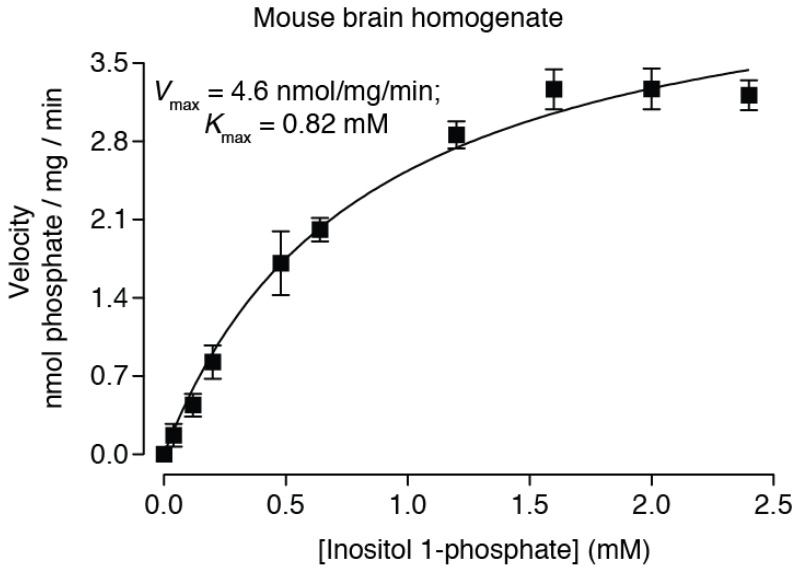


Figure 4.3.14. Michaelis–Menten plot of mouse brain homogenate phosphatase activity using Ins1P as substrate. The mouse brain homogenate was tested at different concentrations for IMPase activity. The data are corrected to eliminate background phosphates (see text).

The graph (Figure 4.3.14) shows the Michaelis–Menten kinetics plot of the velocity of phosphate released against varying substrate concentrations, using 0.5 mg/mL mouse brain homogenate. The baseline had been subtracted to eliminate background phosphate activity. The V_{max} and K_m values of the reaction were found to be 4.6 nmol phosphate/mg protein/min and 0.82 mM, respectively. Although baseline adjustment corrects for background phosphate, it does not eliminate activity from phosphatases other than IMPase.

Hence, instead of baseline correction, the activity of 30 mM lithium was used as a correction (Cryns *et al.*, 2008). At this concentration, lithium should almost completely inhibit IMPase, so any remaining phosphate activity detected would be due to other phosphatase enzymes and background phosphate present. Subtracting the activity seen in presence of 30 mM lithium, from the total activity, is the 'corrected IMPase activity' (Figure 4.3.15).

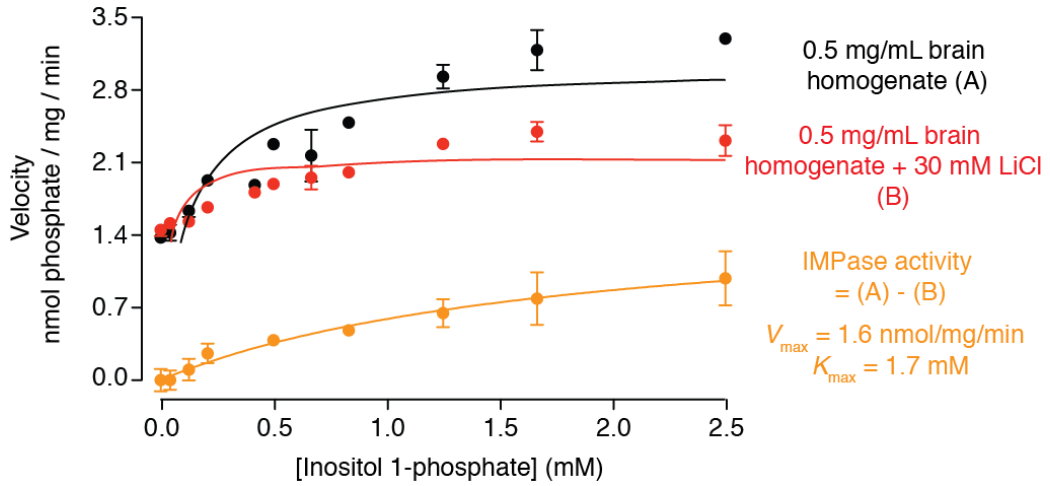


Figure 4.3.15. IMPase activity in mouse brain homogenate. The graph shows the total activity labelled as (A), the activity in the presence of 30 mM lithium (B) and the difference between the two, which is the specific IMPase activity of the mouse brain homogenate.

In all further homogenate experiments, the IMPase activity was calculated by correcting for background as shown in Figure 4.3.15.

4.3.5.2 Concentration–response of IMPase inhibitors in mouse brain homogenate

The mouse brain homogenate was spiked with varying concentrations of drug to check that inhibition of IMPase activity could be quantified using this setup. The IC_{50} values obtained were then compared to IC_{50} values previously obtained *in vitro*.

0.5 mg/mL mouse brain homogenate was spiked with increasing concentrations of lithium, L-690330 and ebselen. After the subtraction of activity in presence of 30 mM lithium from the total activity (as previously discussed), the IMPase activity was plotted (Figure 4.3.16). All three inhibited IMPase in a concentration-dependent manner, with IC_{50} values of 0.43 mM, 5.5 μM and 7.4 μM for lithium, L-690330 and ebselen, respectively.

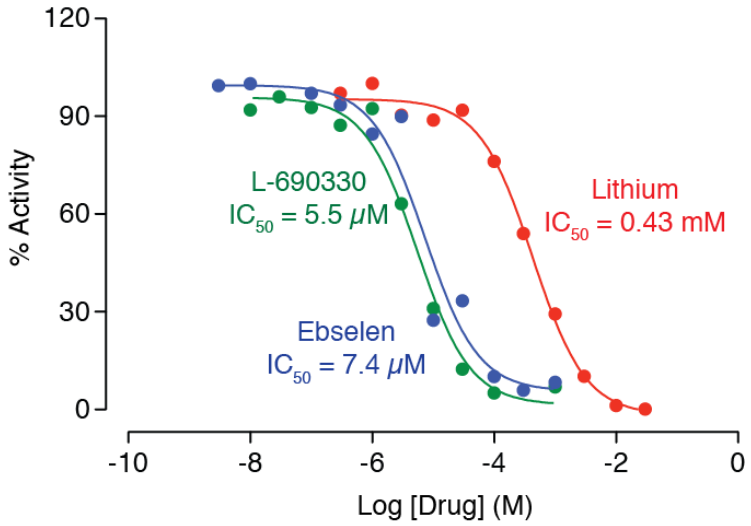


Figure 4.3.16. Concentration–response curves of IMPase inhibitors using mouse brain homogenate. Concentration–response inhibition of IMPase activity in mouse brain homogenate using lithium, L-690330 and ebselen was carried out by spiking the drugs into the mouse brain homogenate. All three showed concentration-dependent inhibition of IMPase activity (n=2).

4.3.5.3 Time-course of ebselen IMPase inhibition

The brain homogenate from mice treated with ebselen for varying lengths of time were used for this study. All the mice were treated with either vehicle or 10 mg/kg ebselen (n = 6), and after the required time point they were killed and their brains dissected out and frozen immediately. On the day of the experiment, the homogenate was prepared and incubated with varying substrate concentrations to determine IMPase activity. If ebselen has the ability to cross the blood brain barrier, the vehicle-treated mouse brain homogenate should show higher IMPase activity than brain homogenate from ebselen-treated mice.

The time points were 10 min, 1 h, 2.5 h, 5 h, 9 h and 25 h, and the velocity of IMPase activity was calculated as nmol phosphate/mg/min. The Michaelis–Menten kinetics curves for each of these time points was plotted (figure 4.3.17).

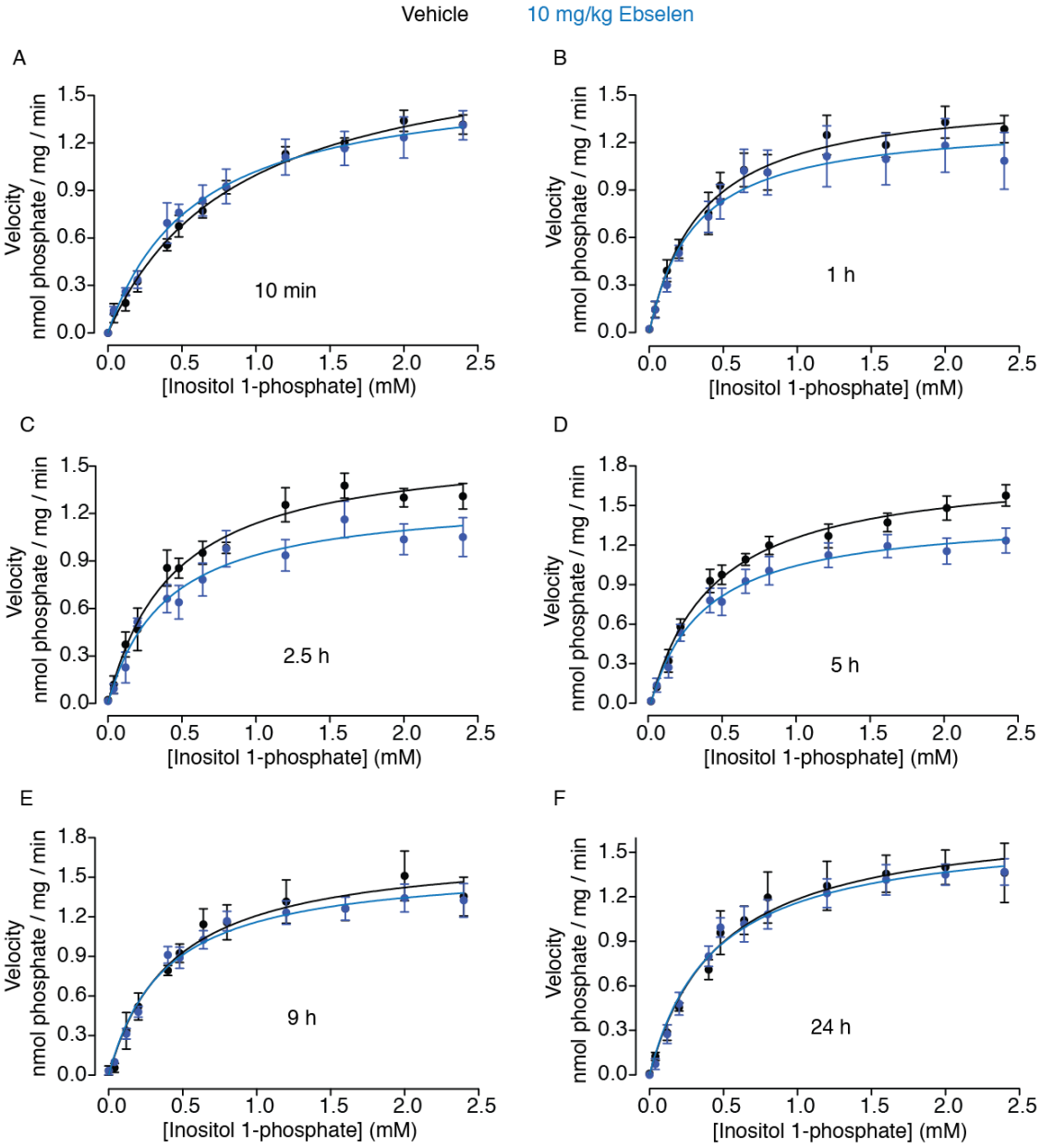


Figure 4.3.17. Time-course of ebselen IMPase inhibition using mouse brain homogenate. The graphs shows the Michaelis–Menten plots of the brain homogenates of mice treated with either vehicle (4% *w/v* cyclodextrin) (black) or 10 mg/kg ebselen (blue) at A) 10 min, B) 1 h, C) 2.5 h, D) 5 h, E) 9 h and F) 24 h post ebselen injection (n = 5–6/group). The error bars indicate SEM.

Figure 4.3.17 shows that there is a trend of reducing IMPase activity in ebselen treated mice from 1 h to 5 h post-injection; By 9 h, activity starts to increase and by 24 h post-injection, there is no appreciable difference in activity. The strongest inhibitory effect seems to be about 5 h post ebselen treatment. The V_{max} values

obtained at these different time-points were further analysed for statistical significance (Figure 4.3.18). The paired t-test with global fitting was used.

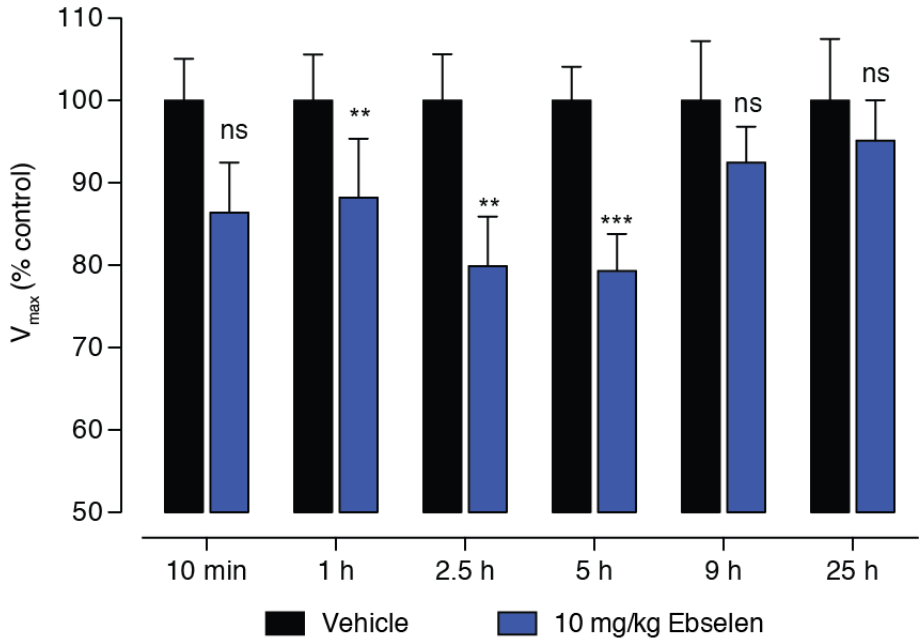


Figure 4.3.18. Effect of 10 mg/kg ebselen expressed as % V_{max} at different time-points. The bar chart compares V_{max} values obtained using brain homogenate from 10 mg/kg ebselen-treated mice to those for vehicle-treated mice at different time points. The difference is statistically significant at 1 h to 5 h, after which this trend starts to reverse. The maximum inhibition was 21% of the vehicle activity (2.5 h and 5 h after administration). The statistical significance was calculated using the paired t-test for the kinetic curve. ** p <0.01; *** p <0.001; ns, not significant.

The statistical analysis of V_{max} values confirmed that the strongest and most consistent inhibitory effect was seen 5 h post ebselen administration. The inhibitory effect was also observed at 1 h and 2.5 h but not after 9 h. This is consistent with the behavioural results (see Chapter 5). The K_m and V_{max} values over the time course is shown in Table 4.3.1.

Table 4.3.1. V_{max} and K_m values for vehicle and ebselen (10 mg/kg) treated mouse brain homogenate.

Time	Measure	Vehicle	Ebselen 10 mg/kg
10 min	K_m (mM)	0.88	0.57
	V_{max} (nmol/mg/min)	1.88	1.68
1 h	K_m (mM)	0.35	0.30
	V_{max} (nmol/mg/min)	1.52	1.34
2.5 h	K_m (mM)	0.44	0.40
	V_{max} (nmol/mg/min)	1.64	1.31
5 h	K_m (mM)	0.43	0.36
	V_{max} (nmol/mg/min)	1.80	1.43
9 h	K_m (mM)	0.43	0.38
	V_{max} (nmol/mg/min)	1.73	1.60
24 h	K_m (mM)	0.47	0.43
	V_{max} (nmol/mg/min)	1.74	1.70

This study confirms that ebselen has the ability to cross the blood–brain barrier, that its IMPase inhibitory activity is detectable within 1 h of injection and up to 5 h, and that inhibition is reversed by 25 h.

4.4 Discussion

4.4.1 Effect of ebselen on PI-linked signalling pathway in cells

Ebselen did not inhibit the muscarinic M_1 receptors in CHO-M1 cells or the serotonergic 5-HT_{2A} and 5-HT_{2C} receptors in SH-SY_5Y cells at concentrations up to 100 μM and the P_{2Y} purinergic receptors at concentrations up to 10 μM. This was important, since a lot of the behavioural tests, dealt with in the next chapter, can be modulated using receptor agonists and/or antagonists. Lithium produces effects in the behavioural tests, not by acting at the receptor level, but downstream of it. Hence, in order for ebselen to mimic lithium's effects in rodents, it was useful to know that ebselen did not inhibit the receptor itself, and any effect observed would be downstream of receptor inhibition. Additionally, ebselen's lack of IP_1 accumulation in the CHO cells cannot be attributed to inhibition of the muscarinic M1 receptor.

Unlike lithium and L-690330, ebselen did not cause accumulation of IP_1 in the ELISA assay (Figure 4.3.1). At low micromolar concentrations (1–30 μM) ebselen did cause up to a 25% increase in IP_1 levels in CHO-M1 cells, and because of solubility constraints, it was not possible to increase the concentration further (ebselen is soluble up to ~100 μM in ddH_2O). The reason a greater accumulation of IP_1 is not seen, may also be due to the reaction of ebselen with endogenous cellular GSH, Ebselen may exist in equilibrium with its reduced form. As shown in Figure 4.3.4, reduced ebselen does not inhibit IMPase. In the experiment, however, very strong reducing conditions were used, and it is improbable that cells would have such a strong reducing environment. Hence, although reduced ebselen did not inhibit IMPase, it is likely that within cells not all of it will be reduced. The extent and rate of

reduction of ebselen *in vivo*, however, has not been measured. However, it is interesting to note that despite being the most potent inhibitor of IMPase, beryllium does not show IP_1 accumulation either (Faraci *et al.*, 1993).

In HeLa cells stimulated with ATP, the inositol phosphate profile showed that ebselen caused an increase in IP_4 and IP_6. Also, when combined with lithium, it completely eliminated the Ins1P accumulation effect of lithium. This suggests that ebselen possibly inhibits another enzyme in the IP_3 recycling pathway. For example, ebselen might be inhibiting inositol polyphosphate 5-phosphatase (IP-5Pase), the enzyme that converts IP_3 to IP_2. Usually, IP_3 is converted into IP_2 and IP_4 (which is then converted into a different isomer of IP_3 before being converted into IP_2). IP_2 is then converted into IP_1 and finally into inositol (Figure 4.4.1).

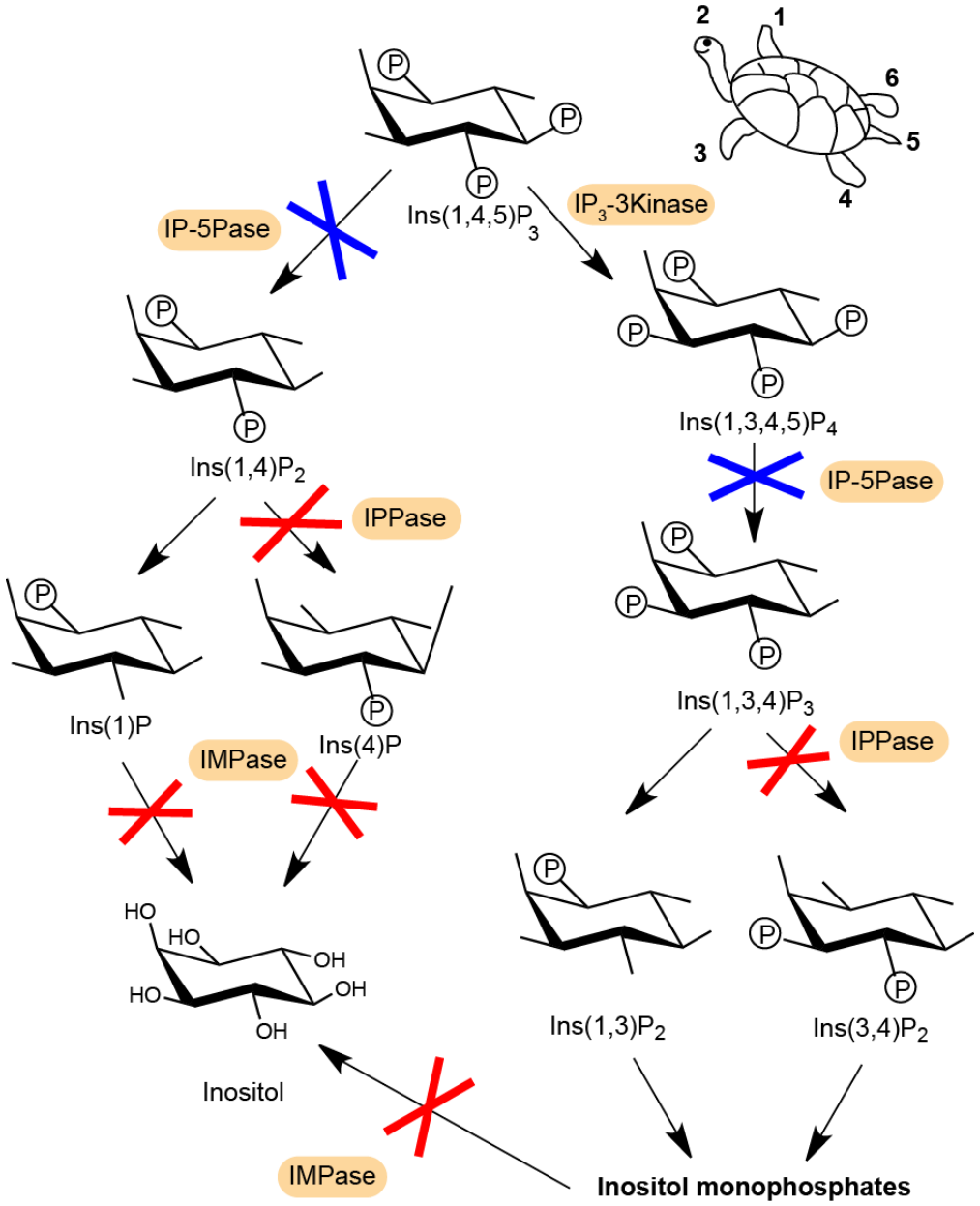


Figure 4.4.1. Stages in the recycling of IP_3 to inositol. In the conversion of IP_3 into inositol via a succession of steps, Ins(1,4,5)P_3 is recycled back to myo-inositol via a series of dephosphorylation steps or via the phosphorylation to inositol 1,3,4,5-tetrakisphosphate [Ins(1,3,4,5)P_4] which is then converted to myo-inositol via a series of dephosphorylation steps. This leads to formation of inositol bisphosphates followed by the formation of inositol monophosphates (IP_1) and finally to myo-inositol. The enzymes inositol polyphosphate 5-phosphatase (IP-5Pase), inositol polyphosphate 1-phosphatase (IPPase), inositol (1,4,5)-trisphosphate-3kinase (IP_3-3kinase) and inositol monophosphatase (IMPase) are shown in orange boxes. The red crosses show the pathways inhibited by lithium. The blue crosses show the pathways that ebselen might be inhibiting. Ebselen might inhibit IP-5Pase to cause the accumulation of higher inositol phosphates.

However, other pathways exist, including the conversion of IP_3 into higher phosphates like IP_5 and IP_6. For example, inositol (1, 4, 5)-trisphosphate can either be

hydrolysed by inositol polyphosphate 5-phosphatase (IP-5Pase) to form inositol (1, 4)-bisphosphate or, alternatively, phosphorylated by inositol (1, 4, 5) 3-kinase (IP_3-3kinase) to form inositol (1, 3, 4, 5)-tetrakisphosphate (Figure 4.4.1), which is then further phosphorylated into IP_5 and IP_6 (Irvine and Schell, 2001; Majerus, 1992). The three enzymes compete for the same substrate, inositol (1, 4, 5)-trisphosphate and therefore, if one pathway is inhibited, this will lead to a substantial increase in the activity of the other. For example, if ebselen inhibits IP-5Pase, it does not allow the conversion of inositol (1, 4, 5)-trisphosphate to inositol (1, 4)-bisphosphate or the conversion of inositol (1, 3, 4, 5)-tetrakisphosphate to inositol (1, 3, 4)-trispohsphate.

This causes accumulation of inositol (1, 3, 4, 5)-tetrakisphosphate and of inositol (1, 4, 5, 6)-tetrakisphosphate. These are further phosphorylated to form the higher inositol phosphates, IP_5 and IP_6. (Figure 4.4.2).

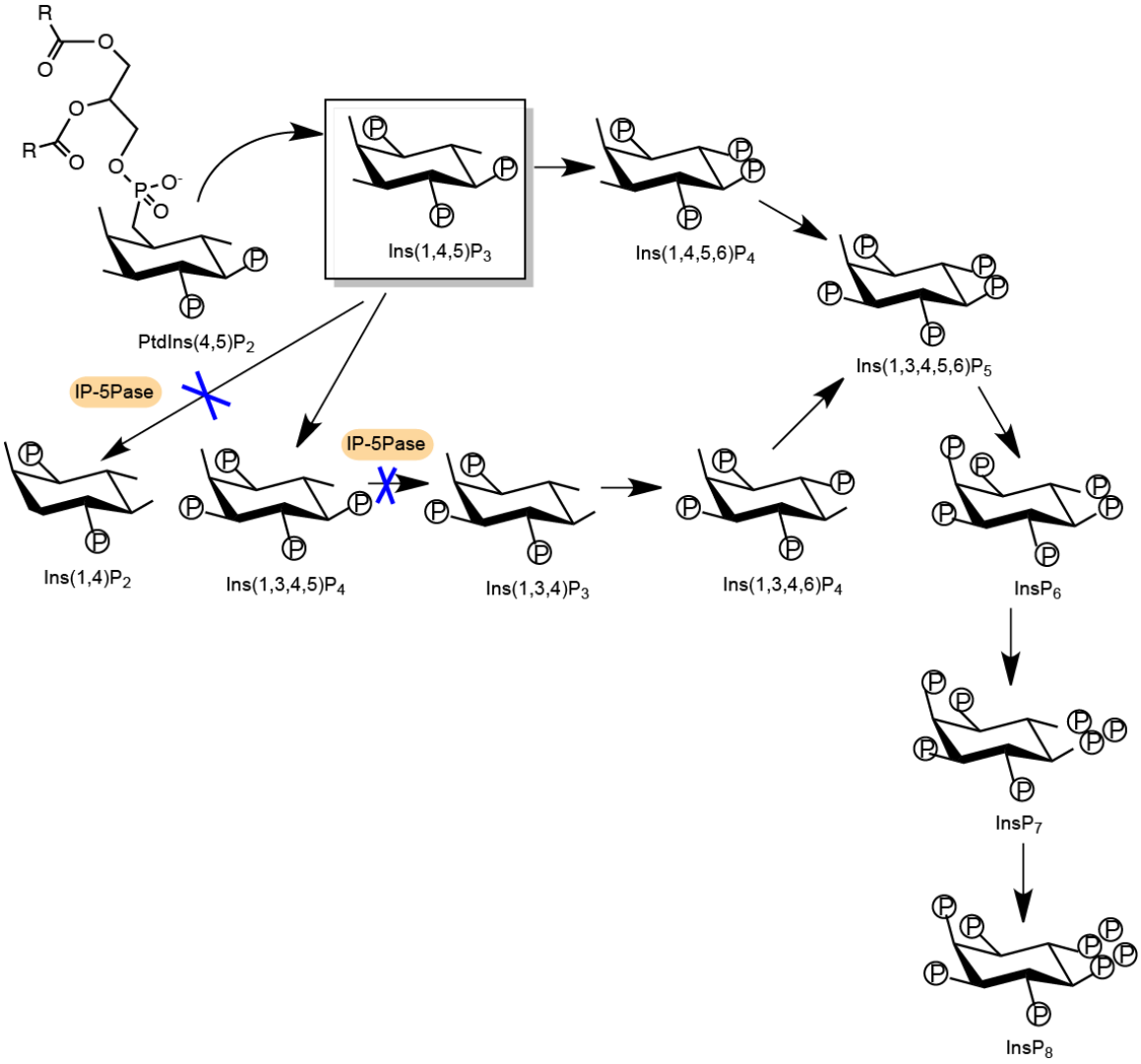


Figure 4.4.2. Metabolism of IP_3 to higher inositol phosphates. Phosphatidylinositol 4,5-bisphosphate (PIP_2) is hydrolysed to inositol 1,4,5-trisphosphate [$Ins(1,4,5)P_3$] which can be converted to either inositol 1,4,5,6-tetrakisphosphate [$Ins(1,4,5,6)P_4$] or inositol 1,3,4,5-tetrakisphsophate [$Ins(1,3,4,5)P_4$]. $Ins(1,4,5,6)P_4$ is then converted via $Ins(1,3,4,5,6)P_5$ to inositol hexakisphosphate (IP_6), which is then further phosphorylated to inositol pentakisphosphate-pyrophosphate ($InsP_7$) and finally to inositol tetrakisphosphate-bispyrophosphate ($InsP_8$). $Ins(1,3,4,5)P_4$ is initially dephosphorylated to inositol 1,3,4-trisphosphate [$Ins(1,3,4)P_3$] after which it is phosphorylated to inositol 1,3,4,6-tetrakisphosphate [$Ins(1,3,4,6)P_4$]. The latter is then phosphorylated to form $Ins(1,3,4,5,6)P_5$ and so on. Adapted from (Irvine and Schell, 2001).

There is some indirect evidence of ebselen's inhibition of IP-5Pase. Ebselen besides inhibiting IMPase, also inhibits PKC (Cotgreave *et al.*, 1989). PKC has been shown to activate IP-5Pase in platelets (Connolly *et al.*, 1986), and hence inhibition of the former may indirectly result in the inhibition of IP-5Pase by ebselen.

In the inositol profile obtained with ebselen there was an increase in IP_4 and IP_6, which is consistent with the hypothesis that ebselen inhibits IP-5Pase resulting the conversion of IP_3 to higher phosphates instead of metabolism into inositol. A peak in IP_5 however, was not observed, and this might be due to differential kinetics properties of the enzymes in this pathway. In the presence of lithium (which blocks IPPase and IMPase) and ebselen, only a large increase in IP_6 was seen. No IP_1 accumulation (seen with lithium alone) was observed, nor was a peak in the IP_4 region (seen with ebselen alone). This may be a consequence of increased inhibitory action on the conversion of IP_3 into lower inositol phosphates in presence of ebselen. Since IP_2 and IP_1 are not formed, no accumulation of the latter will be seen. Increased inhibitory effects of lithium and ebselen may cause a further enhancement of the shift in the inositol cycle towards the production of higher inositol phosphates. For example, the IP_6 peak was twice the size of the IP_1 peak seen with lithium alone and about four times the size of the IP_6 peak with ebselen alone.

This is a complex network of pathways involving many different isomers of inositol phosphates, and hence further validation and confirmation of the different inositol phosphates would be required. Additionally, a time-course is being conducted to measure the inositol phosphate profile at various different time points instead of just the 1 h time point. This might shed light on the rate of formation and conversion of the higher inositol phosphates.

This might be why IP_1 accumulation is not detected in the presence of ebselen in the IP_1 ELISA assay; it would be instructive to test the combination of lithium and ebselen in this assay to see if the IP_1 accumulation produced by lithium can be removed by the addition of ebselen.

It is interesting to note that ebselen may have a whole host of other actions in cellular physiology, since IP_6 is an active inositol phosphate, unlike IP_1. A time-couse study (measuring IP_1 at different time-points) with the addition of ebselen might prove useful to determine if there is an initial increase in IP_1 that ceases if conversion of ebselen into an inactive form occurs. It has already been demonstrated that this is not due to its competitive mode of inhibition, since L-690330 (a competitive inhibitor) does show IP_1 accumulation in two different experimental setups. So the reason beryllium and ebselen do not show IP_1 accumulation may not be related to IMPase, but to some other mechanism. Some studies have suggested that elevation in IP_1 levels are not necessarily attributable to IMPase inhibition, but may be due to direct hydrolysis of PI and PIP to IP_1 (Batty and Nahorski, 1985; Gee *et al.*, 1988).

In conclusion, despite the fact that lithium causes accumulation of IP_1, this is not therapeutically relevant, but is a marker for lithium inhibition of IMPase. IP_1 is an inactive metabolite. However, if ebselen does cause IP_6 accumulation, this may have physiological consequences, since IP_6 plays a role in the cell's energy metabolism and trafficking (Irvine and Schell, 2001; Saiardi *et al.*, 2002). IP_6 is believed to have antioxidant properties, to inhibit synaptogamins and to serve as a co-factor with some enzymes (Irvine and Schell, 2001). Additionally, the overall effect of the conversion into higher phosphates is the depletion of cellular inositol and lower inositol phosphates. Therefore, overall, the effects of ebselen and lithium are the same: a decrease in inositol.

4.4.2 Effect of ebselen on PI-linked signalling pathway in cells

In this chapter, the ability of ebselen to cross the blood–brain barrier has also been demonstrated. Since ebselen is relatively hydrophobic, the fact that it has the

ability to cross the blood brain barrier is not surprising. Comparison of the IC_{50} values for IMPase inhibition obtained revealed that the lithium and the ebselen values are not significantly different from those previously obtained *in vitro*, although the L-690330 IC_{50} value was higher than previously seen. This suggests that ebselen and L-690330 probably inhibit IMPase by targeting different amino acid residues, since the latter inhibits one isoform more potently than the other.

The study of activity in homogenate at different time points has shown that ebselen effects are likely to be prominent within the first hour post injection, and up to about five hours post injection. This information is particularly pertinent to the behavioural experiments (Chapter 5). It is also interesting to note that the inhibitory effect of ebselen had subsided nine hours after administration (dose, 10 mg/kg).

The ideal test of ebselen's effect in the context of the inositol depletion hypothesis would be to establish whether ebselen has the ability to deplete inositol *in vivo*, since it is possible that this, rather than accumulation of IP_1 accounts for lithium's therapeutic actions. On-going experiments are being conducted to test whether or not ebselen has the ability to decrease inositol levels in mouse brain using magnetic resonance spectroscopic techniques.

CHAPTER 5

EBSELEN AND BEHAVIOUR

5 Ebselen and Behaviour

5.1 Introduction

Animal models are usually evaluated based on three criteria (Kato *et al.*, 2007). The first is 'face validity', which is the association between human symptoms of disease and features of the model; the second is 'construct validity', the association between mechanism of the model and the disease pathology; and the final is 'predictive validity', which is based on the efficacy of drugs used therapeutically in the model.

In this chapter, I report ebselen's effects using phenotypic mice models in which lithium has been known to have a distinct and reproducible effect. Some of these models have been selected to mimic certain facets of the disease; for example, the open-field test (Hall, 1936) examines exploratory activity in a novel environment that is indicative of sensation-seeking (Zuckerman, 1984); amphetamine-induced hyperactivity test (Moore, 1978) represents the manic phase; and the forced-swim test (Porsolt *et al.*, 1978) represents the depressive phase. It is important to note that though all of these models mimic symptoms of bipolar disorder, they may or may not be related to the disease at all; i.e., they have good face validity and some predictive validity, but no established construct validity.

5.1.1 Exploratory activity using the open-field test

These tests generally measure activity in a novel environment. Rodents are, by nature, inquisitive animals and will explore a new environment. Zuckerman has linked this ambulatory activity in a novel open field to sensation seeking (Zuckerman,

1984; Zuckerman and Neeb, 1979). Impulsivity and sensation seeking are characteristic traits for bipolar patients in the manic phase of the illness. This behaviour has been correlated with the serotonergic and the noradrenergic systems. Increased levels of 3-Methoxy-4-hydroxyphenylglycol (MHPG; a metabolite of noradrenaline degradation) were seen in sensation-seeking humans (Roy *et al.*, 1989).

The OFT involves placing the animals in the centre of an open arena and measuring the activity of the animal. Different parameters can be measured, such as movement in the horizontal plane, rearing (movement in the vertical plane), defecation, thigmotaxis (time spent close to the walls of the cage) or time spent in the centre of the field, depending on requirement. The field may also be adjusted to be less stressful or highly stressful. The latter is usually achieved by strong lighting in the centre of the field.

Lithium decreases ambulatory behaviour, both horizontal and vertical (rearing) , when mice are in a novel environment, although the effects are stronger on rearing than on ambulation (Johnson, 1972; Johnson and Wormington, 1972; Smith and Smith, 1973). Strain-dependent behavioural differences exist, however, and C57BL/6 mice are usually considered to be the most appropriate for the OFT.

Since lithium's effect on rodent exploratory activity seems to be consistent (predictive validity), and since this test may correlate with sensation-seeking behaviour in bipolar patients (face validity), I decided to test ebselen's effects on exploration in a novel environment in the OFT.

5.1.2 Amphetamine-induced hyperactivity test

This experiments is used to model the manic phase of bipolar disorder. It involves administering rodents with a stimulant that causes hypermobility, which can

be used as a model of the hyperactivity seen in bipolar mania. The most common stimulant used is d-amphetamine, although combinations of d-amphetamine and chlordiazepoxide, apomorphine or phencyclidine have also been used (O'Donnell and Gould, 2007). This test involves the dopaminergic system (amphetamine increases dopamine levels in the synapses). In some patients, treatment with dopaminergic agonists, such as bromocriptine and piribedil can precipitate mania in bipolar patients (Gerner *et al.*, 1976; Silverstone, 1984). Additionally, in patients with bipolar depression, but not unipolar depression, amphetamine itself was seen to precipitate mania (Van Kammen and Murphy, 1975). Hence, this model also has a degree of face validity.

In the AIH model, rodents are administered with stimulant and their movement or activity is measured and compared with control animals. The aim in this test is to assess reduced hyperactivity by drugs that have (or may have) anti-manic properties. The drugs may be administered prior to or with the stimulant, and the behaviour is compared with that of naive animals administered the stimulant. A decrease in hyperactivity (produced by the stimulant) in presence of the drug indicates an anti-manic effect of the drug.

Lithium consistently attenuates AIH in rodents, although different strains have differential responses to d-amphetamine and lithium (Gould *et al.*, 2007b). However, it does not completely abolish the hyperactivity. Other drugs used in the treatment of bipolar disorder, such as anti-psychotics, also reduce psychostimulant-induced hyperactivity (Arnt, 1995), as expected, and are used for the treatment of manic episodes.

Since the amphetamine-induced hyperactivity model has good predictive validity for lithium, I decided to test ebselen in this model.

5.1.3 Behavioural despair test (forced swim test, FST)

The behavioural despair test, also known as FST, is frequently used for screening antidepressants (Cryan *et al.*, 2002; Porsolt *et al.*, 1978). The test involves measuring the time spent immobile by a rodent when placed in a cylinder of water, without being able to touch the base. Rodents placed under acute stress will respond by trying to escape the environment that is causing them this stress. Therefore, immobility is the equivalent of 'giving up' and correlates with a state of depression.

Antidepressants have a robust effect reducing immobility time. This test is highly sensitive to the strain of animal and experimental setup and lacks face validity (Petit-Demouliere *et al.*, 2005). However, it has strong predictive validity for antidepressants acting through the serotonergic and noradrenergic pathways. This test has a strong monoaminergic component, and drugs that increase levels of catecholamines (and, to a lesser, extent serotonin), have a strong positive correlation with decreased immobility time in the FST (Porsolt *et al.*, 1979). As many as 83% of the different classes of drugs decrease immobility time in the FST (Borsini and Meli, 1988). Acute and chronic lithium also decrease immobility time, although not as much as some antidepressants do (Gould *et al.*, 2007a).

The FST though has good predictive validity for antidepressants and, to a lesser extent, for lithium. However, it was considered a useful test to ascertain if ebselen had any antidepressant-like activity.

5.1.4 Pilocarpine seizure test

All of the three behavioural tests mentioned previously, i.e., the OFT, AIH and the FST, are all associated to the monoamine neurotransmitter systems. The pilocarpine seizure model shows lithium's effects on the cholinergic system in rodents

(Honchar *et al.*, 1983). Pilocarpine is a muscarinic agonist, and when administered at high doses to rodents has the ability to cause seizures. 'Sub-convulsive' doses of pilocarpine do not have this effect.

Lithium, when administered in rodents prior to a sub-convulsive dose of pilocarpine, can to produce tonic-clonic seizures, which follow a defined pattern (Jope *et al.*, 1986). Lithium on its own does not have this effect, and seems to sensitise the rodents to pilocarpine-induced seizures. These seizures can be reversed by inositol and were also seen in *impa*1 knockout mice (Agam *et al.*, 2009), and hence are significant in light of the inositol depletion hypothesis (Kofman and Belmaker, 1990; Kofman *et al.*, 1991).

However, this potentiation of seizures is not seen in primates or in any other species except, rat, mouse and goldfish (Belmaker and Bersudsky, 2007; Dixon *et al.*, 1992). This effect is extremely robust and unique to lithium, as none of the other drugs that are used in bipolar disorder produce seizures when combined with pilocarpine. This test also lacks any face or construct validity.

Ebselen was tested in this model only because of this model's strong correlation with the inositol depletion hypothesis. When administered alone, pilocarpine at sub-convulsive doses produces tremors in rodents. It also increases the expression of immediate early genes (IEGs), for example c-Fos, which are markers of neuronal activation (Barone *et al.*, 1993). Ebselen's effect on pilocarpine-induced tremor and pilocarpine-induced c-Fos expression was also measured, in order to determine what effect, if any, it had on these.

5.1.5 Aims

The aims of the research described in this chapter were primarily to test the effects of ebselen in four different behavioural tests that have shown consistent effects with lithium and/or simulate certain symptoms of bipolar disorder. The tests were OFT, AIH, FST and the pilocarpine seizure model described previously. The results obtained with ebselen were compared to those obtained with lithium, either using lithium in my own experiments, or wherever possible, published data on lithium effects.

5.2 Materials and Methods

5.2.1 Legal compliance

All experimental procedures in this thesis were carried out in accordance with the UK Home Office Animals (Scientific Procedures) Act (1986) and associated code of practice guidelines under the following licences. Some experiments, as mentioned, were carried out at Ben-Gurion University under Prof. Belmaker's license.

Project licence: Licence holder- Dr. Trevor Sharp; PPL 80/2445

Personal Licence: Licence holder: Nisha Singh; PIL 80/8054

All experiments were carried out between 1st October 2008 and 31st December 2011 at the Biomedical Sciences Building, University of Oxford. The exceptions were the pilocarpine seizure experiments that were carried out in Ben-Gurion University, Israel.

5.2.2 Experimental animals

Except where otherwise specified, all studies used male C57BL/6 mice from Harlan Olac, UK. All mice were between 20–25 g and 10–12 weeks old at the time of the experiments. The mice were housed in the Biomedical Sciences Building, University of Oxford, and were allowed to acclimatize for one week before the start of experimentation. They were housed in groups of four, kept on a 12 h light/12 h dark cycle (lights off 20:00–8:00) at 21 ± 1°C, with free access to food (standard lab chow), water and environmental enrichment. All the mice were weighed before the start of the experiment.

The cages were always cleaned with soap and water and dried between the each experimental run.

5.2.3 Drugs

Unless otherwise specified, all drugs were obtained from Sigma–Aldrich, Gillingham, UK. Ebselen was obtained from Fisher Scientific (UK). All animals were dosed intra-peritoneally (i.p.) at 0.01 mL/g weight of mouse, unless otherwise specified. Lithium was dosed at 0.067 mL/g weight of mouse. The details of all the drugs used, the doses and the vehicles are given in Table 5.2.1.

Table 5.2.1. Drugs and doses.

Drug	Dose used	Vehicle
Ebselen[1]	1 - 10 mg/kg	4% *w/v* (2-hydroxy propyl)-β-cyclodextrin
D-amphetamine	1 - 4 mg/kg	Saline
Lithium chloride	10 - 20 mmol/kg	ddH_2O
Pilocarpine hydrochloride	100 – 300 mg/kg	Saline
Imipramine hydrochloride	16 mg/kg	Saline

[1] A 0.5 M (137.1 mg/mL) stock of solution of ebselen was prepared in DMSO. This was diluted in 4% cyclodextrin gradually with vortexing, to the required concentration

5.2.4 Activity monitor setup

For the open field and the amphetamine-induced hyperactivity tests, the Linton AM1053 X, Y, Z IR Activity Monitor (San Diego Instruments) with dual grid was used (Figure 5.2.1). Each activity monitor has 48 infrared beams, 24 on each level arranged in an 8×16, 1” (25.4 mm) grid. The lower grid measures normal X, Y

movement, whilst the upper grid measures rearing. The grid height was adjusted to 70 mm. The activity monitors are connected to a computer running AMLOGGER (Linton) software. AMLOGGER software discriminates between different types and speeds of movement, and records the data according to the various categories of activity. The types of movements that can be measured are described in Table 5.2.2.

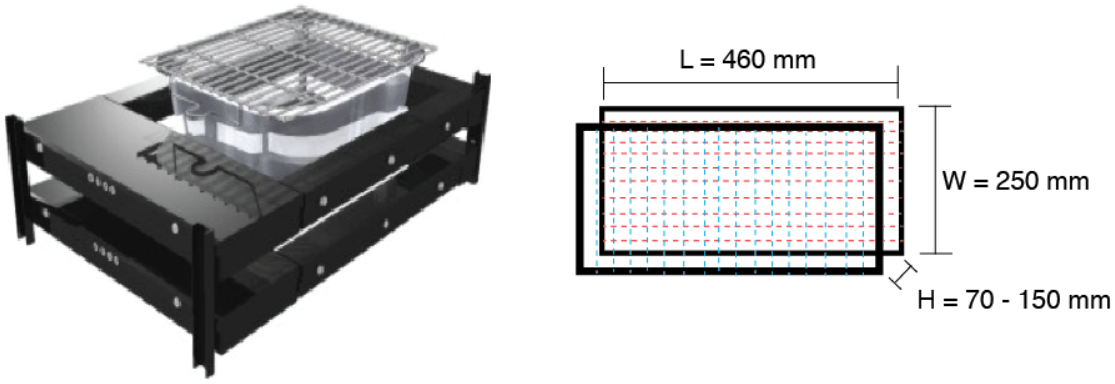


Figure 5.2.1. Linton AM1053 activity monitor. Linton activity monitor (left) and a schematic representation of the two grids (right). Each grid consists of 24 infrared emitters/detectors (8×16) . The infrared beams on the bottom grid (red) detect movement in the lower plane. The upper beams (blue) measure movement in the upper plane. The separation (H) of the grids is adjustable (70–150 mm).

Table 5.2.2. Description of movements that can be measured using the activity monitor.

Activity	Number of valid beam breaks
Rearing	Number of rearing beam breaks
Centre rear	Number or rearing beam breaks which occurred away from the cage walls.
FR-Count	Front to Rear Movement counts.
Activity (S)	Time Spent Active (Seconds). Beams broken.
Mobility (S)	Time Spent Mobile (Seconds) More than one beam broken in x or y axis.
Rearing (S)	Time Spent Rearing (Seconds)

Four monitors were used simultaneously in all experiments, with one mouse in each. All treatments were rotated between the four different monitors to eliminate monitor-specific effects.

Activity was detected as a single-beam break in the horizontal plane (x/y-axes). Rearing (single-beam breaks in the top grid) was movement in the z-axis. The measure of mobility takes into account the time spent moving in either the x/y axes or the z-axis, but requires more than one beam to be broken.

5.2.5 Open field test

The mice were injected with drug/vehicle and placed in the activity monitor cages (novel environment) for 1 h. The activity was measured throughout that time.

5.2.5.1 Time course of ebselen effect

Mice were injected with drug/vehicle and then placed into the activity monitor for 1 h after different time periods post-injection (Figure 5.2.2).

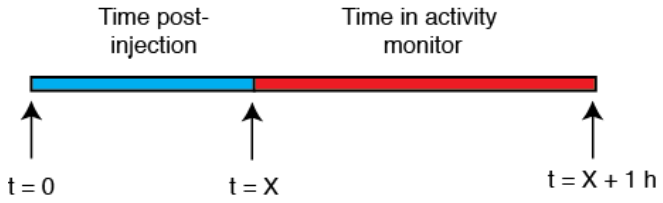


Figure 5.2.2. Time course method. Mice were injected at t = 0 with drug/vehicle. They were placed into the activity monitor at t = X (the chosen time point), and the activity was monitored for 1 h.

The animals were killed using CO_2, and the brains were excised and frozen on dry ice rapidly. Blood (800 μL) was taken from the heart in a syringe containing 100 μL of 10% EDTA, mixed, and placed on ice immediately. The blood was spun at 10,000 *g* for 10 min at 4°C and the plasma was collected and stored at -80°C for analysis of ebselen levels at a latter date.

5.2.6 Amphetamine-induced hyperactivity

5.2.6.1 Amphetamine dose response

Mice were habituated to the room and the activity monitor cage for 30 min before being injected with d-amphetamine/saline and placed in the activity monitor cage for 1 h for monitoring.

5.2.6.2 Effect of ebselen on amphetamine-induced hyperactivity

Mice were brought into the injection room 10 min before the start of the experiment. They were treated with drug/vehicle and immediately placed, individually, in the activity monitor cages for 1 h to habituate. The mice were then injected with d-amphetamine/saline, and then placed back into the same cage in the activity monitor. The amphetamine injections were always made on the side of the midline alternate to the drug/vehicle injection. The mice were monitored for an additional 1 h (Figure 5.2.3).

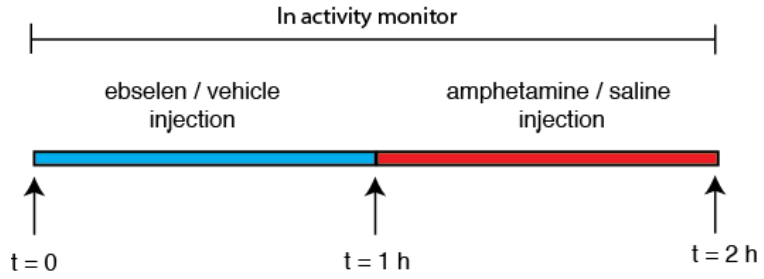


Figure 5.2.3. Amphetamine-induced hyperactivity method. Ebselen/vehicle) was injected at t = 0 and 1 h post-injection, amphetamine was administered. The mice were monitored for the whole 2 h period.

5.2.7 Forced swim test (FST)

The FST was performed in a Plexiglas cylinder (height 25 cm, diameter 20 cm). It was filled with water (23 ± 1°C) to 15 cm so that the mouse could not touch the bottom with its tail. Mice were treated with drug and relevant vehicles at various times before monitoring activity. Each mouse was kept in the water-filled cylinder for 6 min, of which only the last 4 min were used for analysis. The experiment was video recorded and analysed for immobility at a later time by an observer who was blind to the dosing. Immobility was defined as the period of time during which the mouse did not make movements beyond those required to keep its head above the water.

5.2.8 Pilocarpine seizures

CD-1 male mice (12 weeks old, 25–30 g) were obtained from Harlan, Israel. Mice were placed singly in cages in the experimentation room overnight. LiCl (10 mmol/kg) was injected 18–20 h before pilocarpine HCl. The mice were observed and rated every 10 min according to the Patel scale (Patel *et al.*, 1988); as shown in Table 5.2.3. Stages 1–3 were categorised as non-seizure states and stages 4–5 as seizure states.

The mice were killed by CO_2 as soon as the test was complete or the humane end-point was reached, whichever was earlier.

CD-1 mice were used in this case since they respond better in this test, and all previous studies have employed CD-1 strain rather than C57Bl/6.

Table 5.2.3. Patel scoring.

Observation	Score
No change	0
Gnawing, chewing, gustatory movements, tears	1
Shivering	2
Head-bobbing	3
Rearing, limb clonus	4
Rearing, falling, seizures	5

5.2.8.1 Effect of ebselen on pilocarpine-induced seizures

A preliminary experiment was performed using ebselen (10 mg/kg)/vehicle, injected 1 h before an injection of pilocarpine (300 mg/kg) to confirm that ebselen does not inhibit seizures induced by pilocarpine.

5.2.8.2 Effect of Ebselen on Pilocarpine seizures

Mice were divided into groups; each group received drug/vehicle at a different time point prior to the pilocarpine injection (100 mg/kg). Mice were observed individually and scored every 10 min.

5.2.8.3 Sensitization experiment

LiCl (1 mmol/kg) was injected 18 h prior to drug/vehicle injection. pilocarpine (100 mg/kg) was injected 1 h post injection, and the mice were observed individually and scored every 10 min.

5.2.8.4 Tremor monitoring

Mice (CD-1, male, 25 g; Harlan, UK) were injected with drug/vehicle, and 1 h later with 200 mg/kg pilocarpine/saline. After 25 minutes, they were placed in the tremor monitor (SDI, San Diego, USA) individually for 1 min. The tremor monitor measures and records continuous movement up to 128 Hz; it can distinguish this from ambulatory and stereotypical movements. After recording for 1 min in the tremor

monitor, the mice were killed by cervical dislocation, the brains were rapidly excised and frozen by placing in dry ice.

We used tremor as the end point, since our license in Oxford, did not allow us to measure pilocarpine-induced seizures. Hence, we used tremor as measure of pilocarpine induced activity as our end point. Additionally, since the seizures rating was a subjective test, it was decided to use the tremor monitor to provide a more objective measure that maybe sensitive to slight variations that would be missed by the seizure ratings.

5.2.9 *In situ* hybridisation

Mouse brains from the tremor analysis (5.2.8) were used for *in situ* hybridisation (ISH). Fos expression was measured in brain slices in the frontal cortex, striatum and hippocampus regions.

5.2.9.1 Sectioning

Slides were prepared by dipping twice in warm subbing solution (2.5 g/L gelatin, 0.25 g/L chrome alum) and oven-dried before use. The cerebellum was removed from brains and discarded. Brains were halved with a surgical blade. The right half was mounted in Cryo-M-Bed embedding medium, frozen and clamped in a Bright 5030 cryostat (−20°C). Sections (12 μm) were collected at levels of Bregma 2.22 mm (Frontal Cortex), Bregma 1.10 (Striatum) and Bregma −1.70 (hippocampus) (Franklin and Paxinos, 2008). The left half of the brain was left frozen, in case we needed it for further analysis at a later date.

5.2.9.2 Slide Pre-treatment

Diethylpyrocarbonate (DEPC) water was prepared (0.1% *v/v* in deionised water). Phosphate buffered saline (PBS, 0.2M) and triethanolamine (TEA) buffer (19.5 g/L TEA, 9 g/L NaCl, pH 8) was made up in DEPC water and autoclaved (121°C, 15 psi, 15 min). A 4% Paraformaldehyde (PFA) buffer (4% in 0.1M in PBS) was prepared by heating to 60°C, and the pH was adjusted to 7.5.

Slides were taken and allowed to warm to room temperature. They were sequentially fixed with PFA for 5 minutes, rinsed twice in PBS, and then treated in TEA buffer with acetic anhydride (final concentration 0.25%) for 10 minutes. They were then dehydrated in 70% ethanol (1 min), 80% ethanol (1 min), 95% ethanol (2 min) and 100% ethanol (1 min). Finally, they were delipidated in chloroform (10 min), 100% ethanol (1 min) and 95% ethanol (1 min). The slides were air dried and replaced in boxes for storage at −20°C.

5.2.9.3 Hybridisation

A solution of 20× saline sodium citrate (SSC) was prepared (3 M NaCl and 300 mM trisodium citrate pH 7) in DEPC water. This was left overnight and autoclaved the following day. The oligonucleotide mixture was prepared by adding 17 µL of DEPC water to 6 µL of ^{35}S-dATP (37 MBq; 10 mCi/mmol; Hartmann Analytics, Germany), with 7µL of terminal deoxynucleotidyl transferase (TdT) forward buffer and 3µL of oligonucleotide probe. The probe (CTTCA GGGTA GGTGA AGACA AAGGA AGACG TGTAA GTAGT GCAGC) was designed to target the murine *Fos* gene. Samples were centrifuged (15 s) before the addition of 2 µL TdT enzyme, followed by another brief spin. The mixture was incubated (30 min, 37°C) in a water bath and then placed on ice for about 30 min.

A Sephadex™ column was prepared by tipping off the storage solution, washing gently with TE buffer (10 mM Tris, 1mM EDTA). Labelled oligonucleotide probe was added to each section (10^6 cpm/slide) in hybridisation buffer (50% *v/v* formamide, 4× SSC, 5× Denhardt's solution, 0.4 mg/mL herring sperm DNA, 0.1 mg/mL polyA tail, 0.12 mg/mL heparin, 10% *w/v* dextran sulphate and 20 mM DTT).

Rinsed plastic incubation trays were inlaid with 4 sheets of filter paper moistened in 50 ml formamide buffer (10 mL 20× SSC, 25 mL formamide, 15 mL DEPC water) to keep the chambers humid during hybridisation. Slides were arranged in the trays, and left for 30 minutes to thaw. Oligonucleotide mixture (200 μL) was added to each slide, cover slips were placed on top and the trays were covered and incubated (34°C, 18 h).

The coverslips were removed by washing in 1× SSC, and the slides were placed in 1× SSC at R.T. They were washed once with 1× SSC and then with 1× SSC at 55°C and placed in a water bath (55°C, 20 min); the 55°C wash procedure was repeated three times. The slides were then left in 1× SSC at R.T. for 1 h, rinsed in deionised water, and left to dry overnight.

5.2.9.4 Film Autoradiography

The dried slides were arranged into photographic cassettes with ^{14}C standard microscale (Amersham Life Sciences, UK) and Biomax film (Sigma–Aldrich) for 8 days for autoradiographic development.

5.2.9.5 Computerised Analysis of Autoradiographs

The relative abundance of *fos* mRNA in selected areas was determined using Core™ software (MCID, St Catherines, Ontario, Canada). Optical Density values were calibrated to ^{35}S tissue equivalents using the ^{14}C microscale. Areas of interest

were according to figures 12, 22 and 45 of the Franklin & Paxinos Mouse Brain Atlas (Franklin and Paxinos, 2008). Regions analysed were: frontal cortex (prelimbic, orbital, motor cortex), striatum (caudate putamen, inner and outer parietal, piriform) and the hippocampus (inner and outer parietal, CA1, CA3). Densitometric values were measured for three sections from each animal, averaged and calculated as nCi/g tissue. Data in the figures are presented as mean +/- SEM and expressed as percentage of controls. A one-way analysis of variance ANOVA with Dunnett's post-test was used to calculate significance.

5.3 Results

5.3.1 Open field test

The mice were assessed for the effect of 10 mg/kg ebselen using an OFT. Four mice were monitored at a time (2 vehicle-treated and 2 ebselen-treated mice). The paired t-test was used to analyse the results (comparing ebselen- and vehicle-treated groups).

5.3.1.1 Effect of ebselen on activity

Figure 5.3.1 shows the effect of 10 mg/kg ebselen on ambulatory activity in the horizontal plane. The activity (total number of beams broken in the whole period of testing) and the 'Front to rear' (FR) counts (total beams broken when a complete run from one end of the cage to the other takes place) were used as measure of activity. The FR count is a measure of the number of times the mouse moves from one end to the other in one complete linear motion. The infrared beams from the lower grid alone measure these movements.

Mice treated with ebselen (10 mg/kg) showed a significant decrease in overall activity immediatly after, 1.5 and 4 h post administration compared to the vehicle-treated mice (Figure 5.3.1A). The decrease was ~50% up to 2.5 h after treatment and, no significant difference was seen by 24 h

Treatment with ebselen at 10 mg/kg caused a maximal decrease in activity and FR movement of 51%.

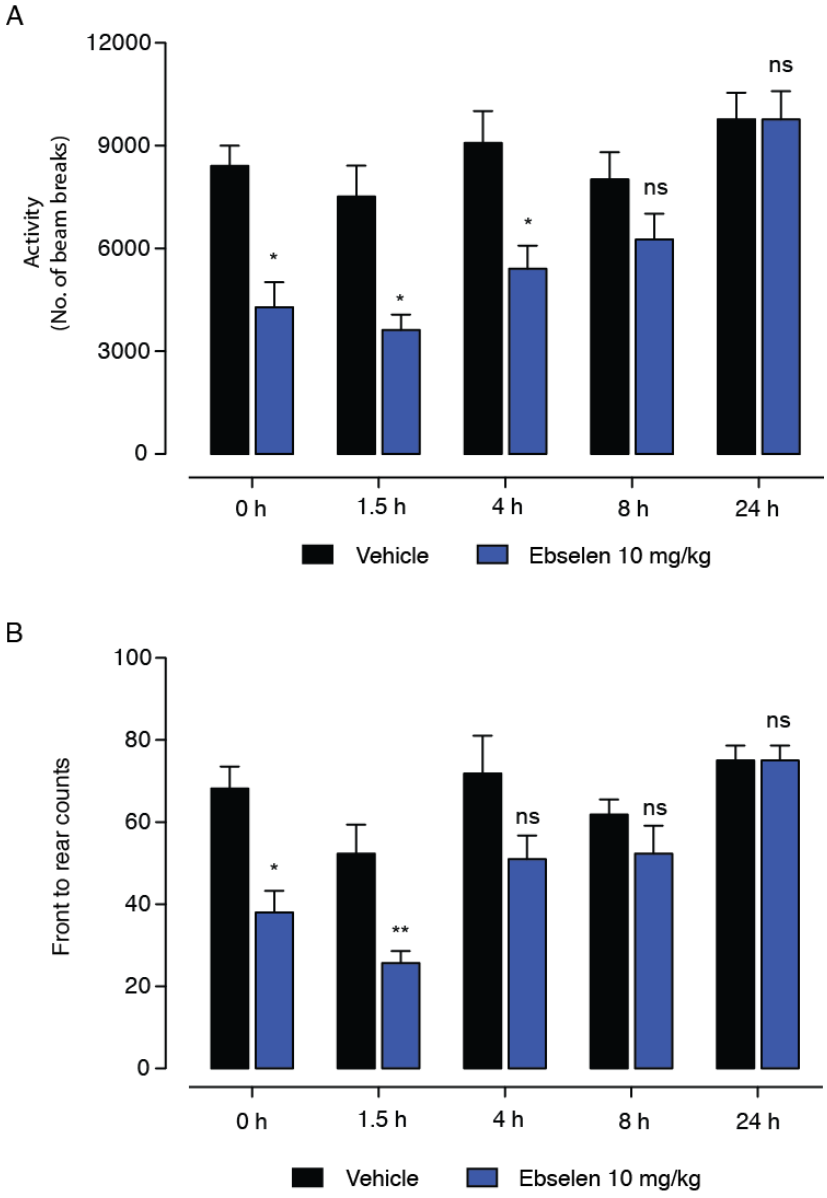


Figure 5.3.1. Effect of ebselen on horizontal ambulatory movement (OFT). Activity was measured for an hour from the indicated times post-injection. **A)** Activity measured as the total number of beam breaks, and **B)** counts of FR movement. This movement is in the horizontal plane and is measured by beam breaks in the lower grid of the activity monitor (n = 6.).Paired t-test was used. * p <0.05;** p <0.01; ns, not significant.

5.3.1.2 Effect of ebselen on rearing

The effect of ebselen on rearing (vertical movement) was assessed by a similar test but including the upper grid of sensors. Centre-rearing behaviour is a measure of

the rearing activity away from the sides of the cage (thigmotaxis). This is when the mouse stands on its hind paws without the need for support from the cage walls.

Total rearing (Figure 5.3.2A) in ebselen-treated mice dropped to ~10% relative to vehicle-treated mice within an hour of treatment and remains at this level to about 2.5 h. By 5 h post-injection the total rearing increased, but still at ~30% of control. At 8 h, the rearing was ~50%, and by 24 h no differences in rearing was detected.

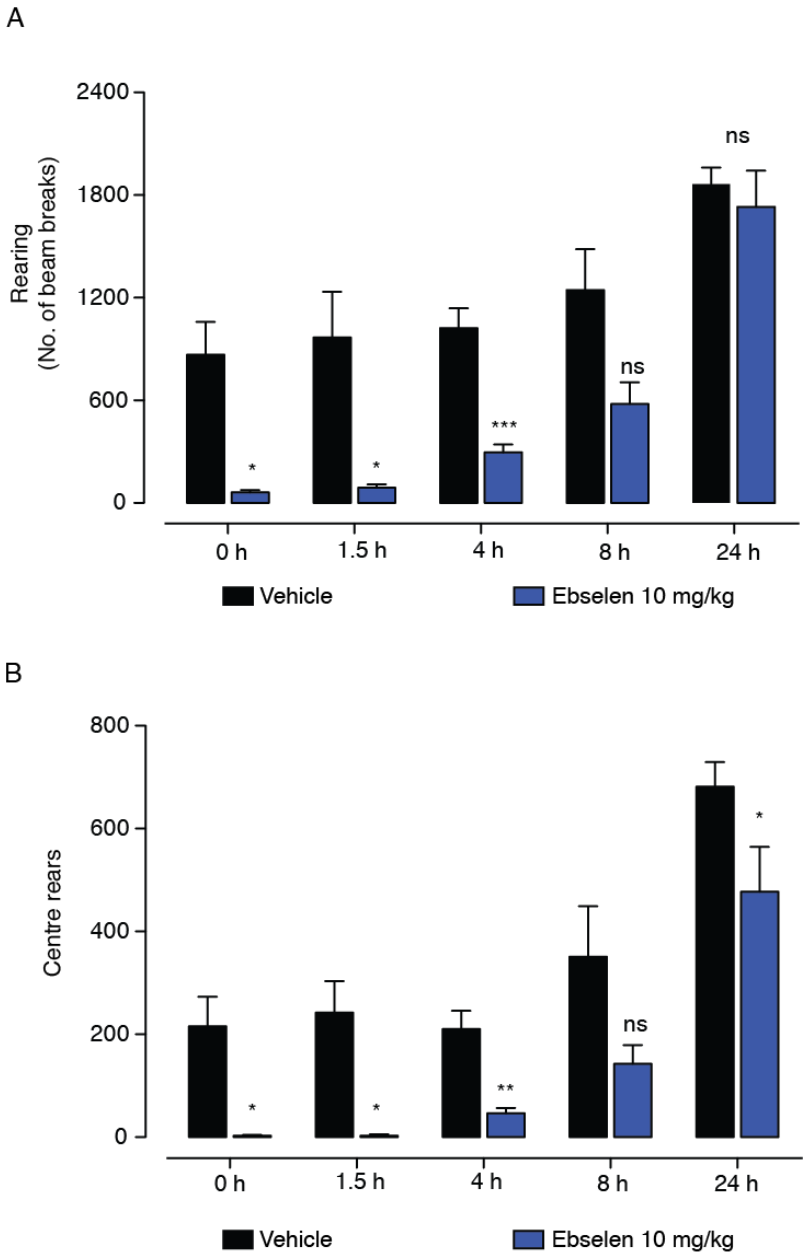


Figure 5.3.2. Effect of ebselen on rearing behaviour (OFT). Rearing was measured for an hour from indicated times post injection. A) Total rearing (number of beam breaks in the top grid of the activity monitor) and B) rears in the centre of the cage area. n = 6 Paired t-test was used.. * p <0.05;** p <0.01; ns, not significant.

Centre rearing behaviour (Figure 5.3.2B) was even more profoundly influenced by ebselen. This was reduced by ~99% during the initial 2.5 h. Between 4–5 hours it increases by about 20% and by 9 hours it reached 50%. Even after 24 h the centre rearing behaviour showed a decrease of 25% in the ebselen treated mice.

5.3.1.3 Effect of ebselen on mobility

Mobility is a combined measure of movement in horizontal. This event is recorded only when there is more than a single beam break. Hence, it is a more accurate ambulatory measure.

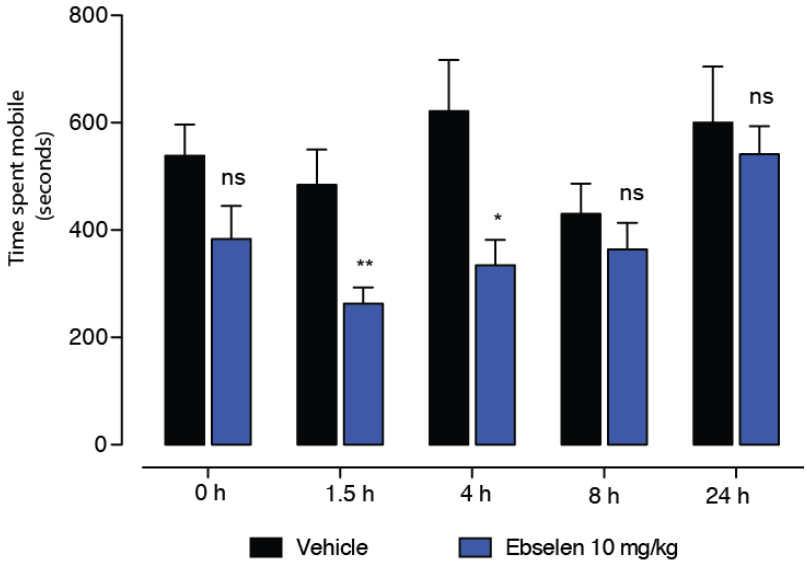


Figure 5.3.3. Ebselen's effect on mobility in the OFT. The figure shows the time spent mobile by ebselen treated animals (blue) compared to vehicle treated animals (black). This includes both, horizontal and vertical movement, and is measured by more than one beam break in either of the two grids. The unpaired t-test was used as a measure of significance (n = 6). Paired t-test was used. * p <0.05;** p <0.01; ns, not significant.

Ebselen, as expected, decreases the time spent mobile (Figure 5.3.3). There was a 30% reduction within the first hour, and this increased to ~50% by 2.5 h and stayed at this level till about 5 h post-injection. By 9 h the decrease was just ~15% , and no difference in mobility was detected 24 h post injection.

5.3.2 Amphetamine-induced hyperactivity

The effect of ebselen treatment on amphetamine-induced hyperactivity was investigated. The activity was analysed for significance using the paired t-test between the vehicle+saline group and the ebselen+saline group; and between the

vehicle+amphetamine group and the ebselen+amphetamine group (unless otherwise specified).

5.3.2.1 Amphetamine dose response

An initial experiment to ascertain dose-related effects of amphetamine on activity were conducted. Studies suggest that at high doses of amphetamine the animals do not show hyperactivity, but instead show stereotypic behaviour. Hence, doses above 4 mg/kg were not investigated.

The dose–response relationship of amphetamine on activity (Figure 5.3.4) shows that 4 mg/kg amphetamine was the most effective at producing hyperactivity. At 1 and 2 mg/kg amphetamine, the increase in activity was not so significant. Hence, for the following experiment, it was decided that 4 mg/kg of amphetamine would be used. It was also observed that 30 min was too short a habitation period, (mice were still actively exploring at the end of the 30 min habituation period) so it was decided that for the ebselen experiments, the habituation time would be increased to 1 h. Although the mice were monitored for the whole 1 h time period post-amphetamine, only the most active phase (15 to 45 min post amphetamine injection) was used in the subsequent tests. It was decided that ebselen's effect on hyperactivity would be analysed during this 30 min period.

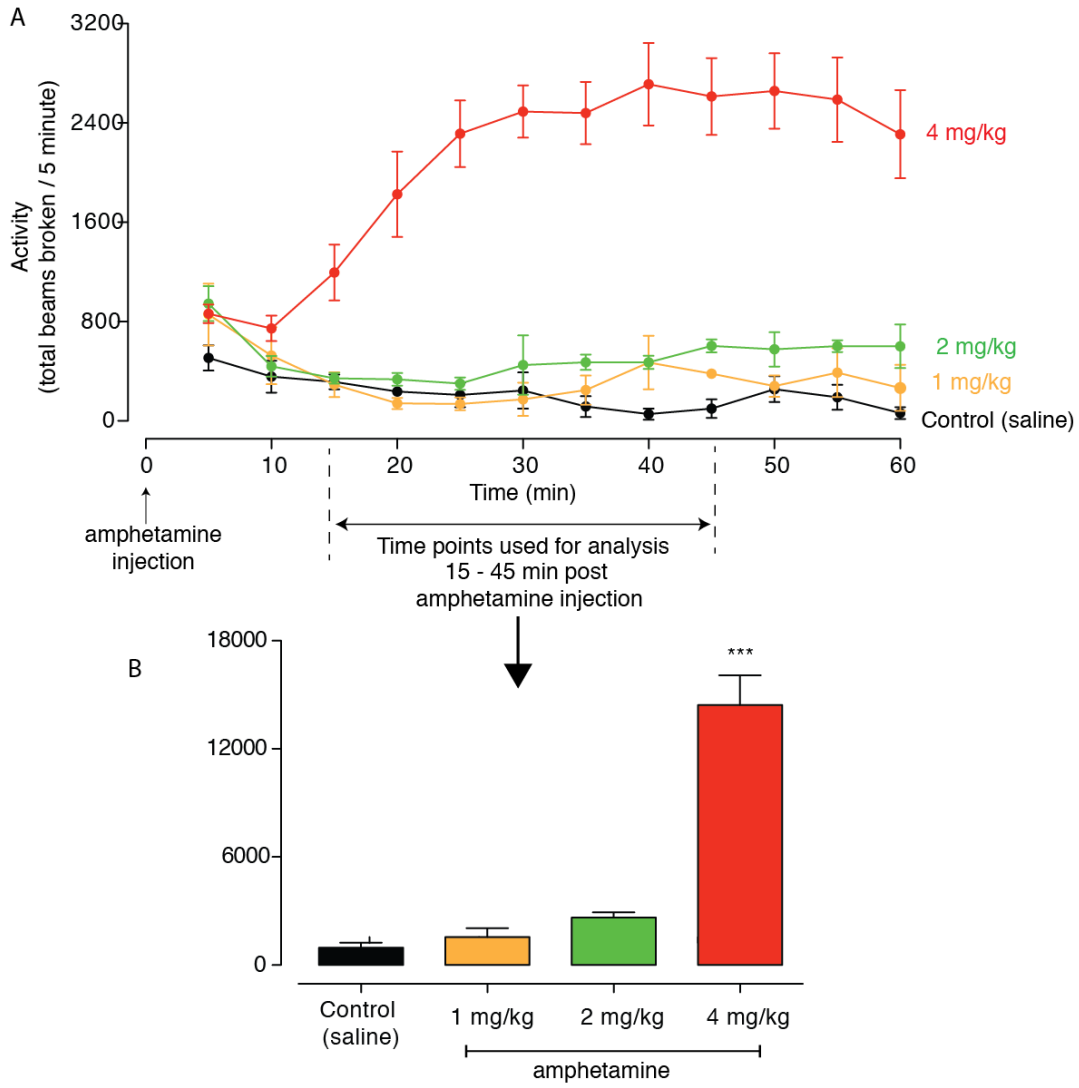


Figure 5.3.4. Amphetamine dose–response. A) Effect of three different doses of d-amphetamine, 1, 2 and 4 mg/kg, on activity was measured over 60 min (total number of beam breaks in a 5 min interval). **B)** The most active period (15 to 45 min post-amphetamine injection) was analysed by one-way ANOVA with a Dunnett's post-test for the three doses and the control.

5.3.2.2 Ebselen's effect on 4 mg/k amphetamine-induced hyperactivity

Initially, 4 mg/kg d-amphetamine was used. The unpaired t-test was used to analyse the results by comparing the ebselen (or vehicle) and amphetamine (or saline) treated groups.

Mice were divided into four groups (n = 8), and each group was injected with one of the following combinations of drugs: vehicle+saline, ebselen+saline,

vehicle+amphetamine and ebselen+amphetamine. Each group was rotated between the activity monitor cages to negate any cage-specific effects. Mice were first injected with vehicle/ebselen and placed in the activity monitor cages for habituation for 1 h, then administered amphetamine/saline and monitored for a further 1 h. The activity was determined as the total beam breaks per 5 min and plotted against time (min) as shown in figure 5.3.5.

Amphetamine treatment caused an increase in activity compared to saline (Figure 5.3.5B–D); the increase was reduced by prior administration of ebselen at 5mg/kg (Figure 5.3.5C) and 10mg/kg (Figure 5.3.5D).

In order to compare the trends, bar graphs were plotted (Figure 5.3.6). The activity, measured as the total number of beams broken over the 75-105 min post-ebselen/vehicle administration period show that 1 mg/kg ebselen did not affect hyperactivity, whereas 5 and 10 mg/kg reduced it but only the latter was found to be significant using the paired t-test.

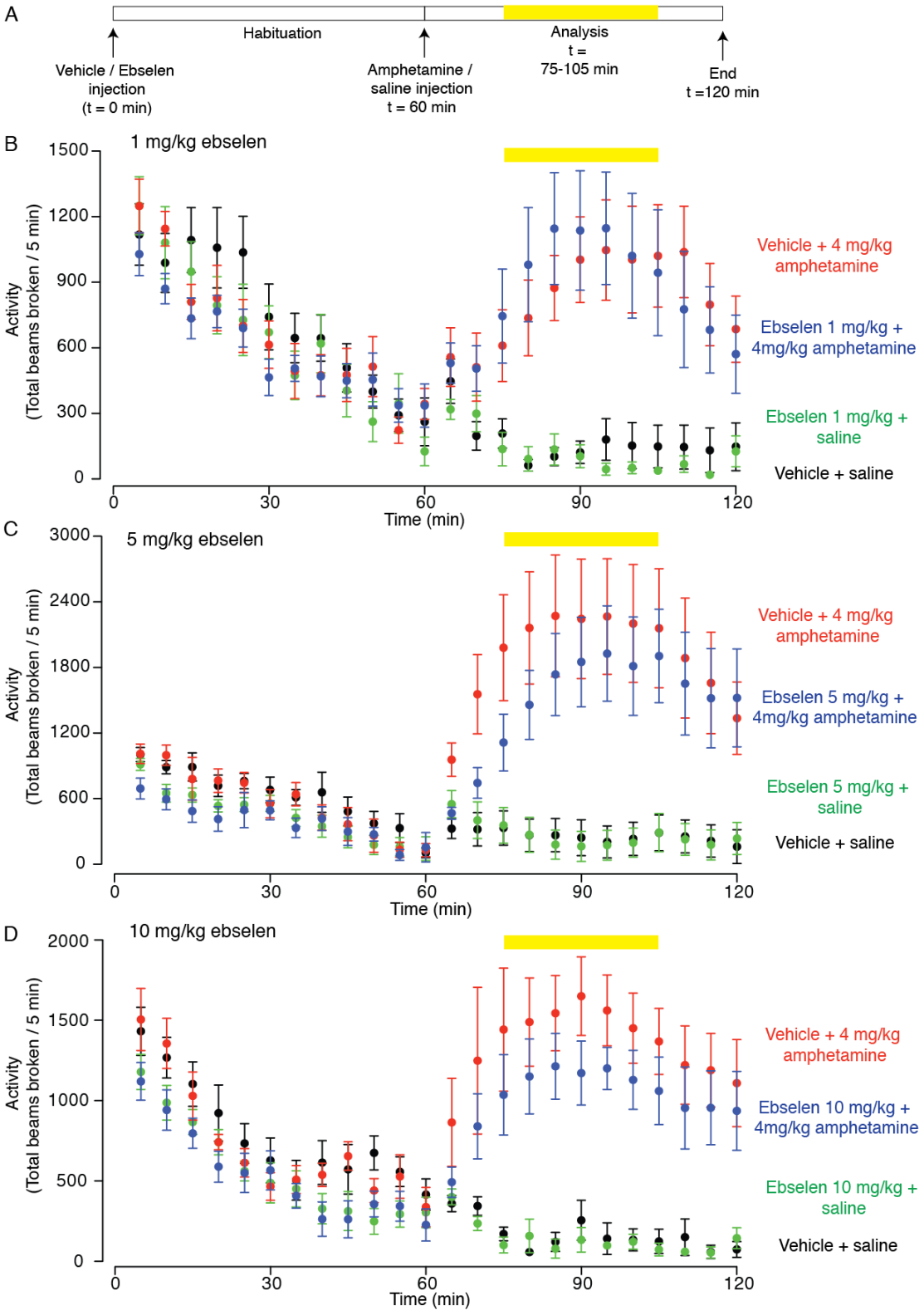


Figure 5.3.5. Effect of ebselen on amphetamine-induced hyperactivity. A) Amphetamine (4 mg/kg) (or saline) was injected 60 min post injection of ebselen (or vehicle). The yellow bar shows the period (75–105 min) that was used for analysis. Ebselen was tested at **B)** 1, **C)** 5 and D) 10 mg/kg. The graphs show the activity (total beam breaks in a 5 min interval) against time for four groups with the indicated administration of drugs. n = 6-8.

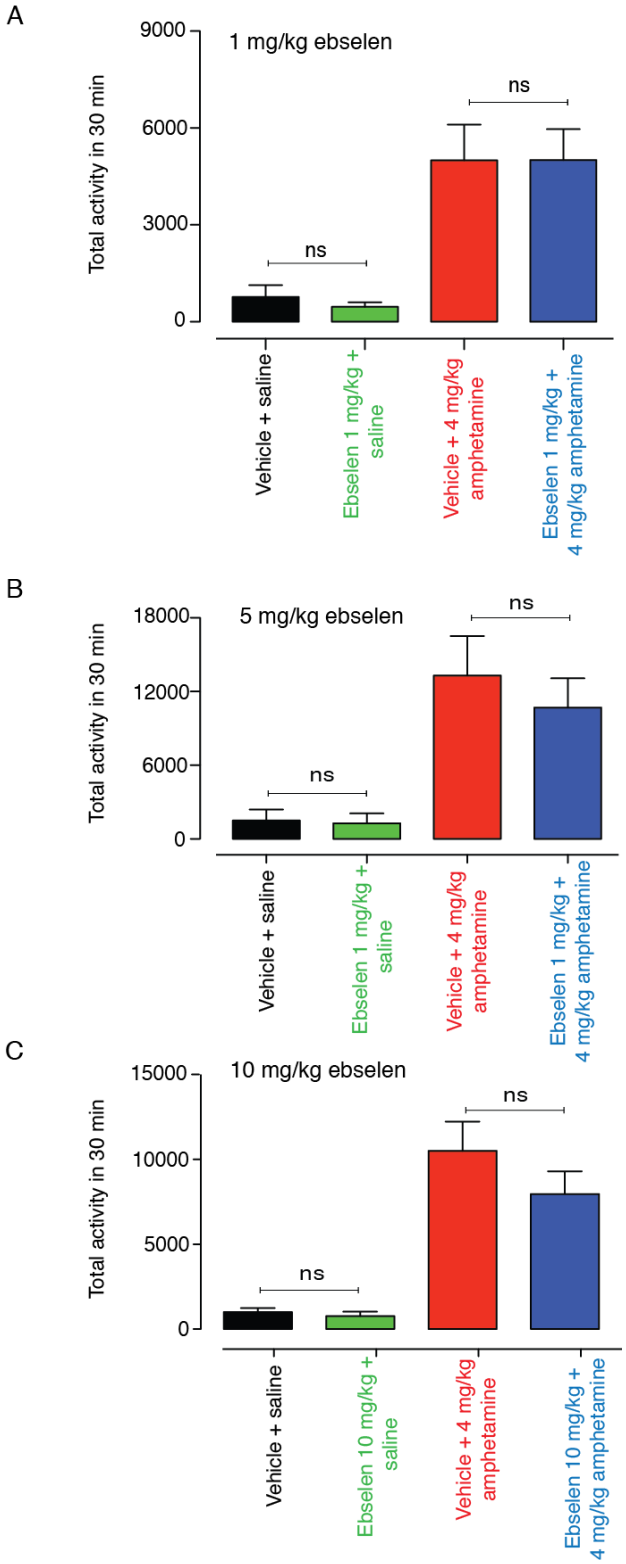


Figure 5.3.6. Effect of ebselen on amphetamine-induced hyperactivity. Bar graphs show the effect of ebselen at **A)** 1**, B)** 5, and **C)** 10 mg/kg during the period t = 75–105 min (see Figure 5.3.5). The y-axis shows the total activity in the 30 min period for the 4 different treatment groups. n = 6-8. The paired t-test was used to determine significance between the groups indicated by the line. * p <0.05; ns, not significant.

A dose of 1 mg/kg ebselen had no effect on amphetamine hyperactivity, while 5 mg/kg caused a decrease in activity. Using mean values, the difference between the vehicle and ebselen is a reduction of 20% in ebselen-treated mice. However, this was not seen to be significant. With 10 mg/kg ebselen there was a 25% decrease in the ebselen treated mice compared to the vehicle treated mice administered amphetamine. This decrease was found to be significant ($p=0.0308$) using the paired t-test. No significant difference was seen between the vehicle and the ebselen treated groups administered saline, instead of amphetamine.

5.3.2.3 Effect of ebselen on 2 mg/kg amphetamine-induced hyperactivity

In another experiment, the effect of ebselen on the hyperactivity elicited by 2 mg/kg d-amphetamine was investigated. For this, mice were divided into two groups ($n = 8$) and two combinations of drugs were used: vehicle + amphetamine and ebselen + amphetamine.

Amphetamine-induced increase in activity was reduced by prior administration of ebselen at 2 mg/kg (Figure 5.3.7C) and 5 mg/kg (Figure 5.3.7D). Additionally, with the 1 mg/kg ebselen-treated group there was a decrease in activity, but only after $t = 100$ min (Figure 5.3.7B).

In order to compare the data directly, bar graphs were plotted (Figure 5.3.8).

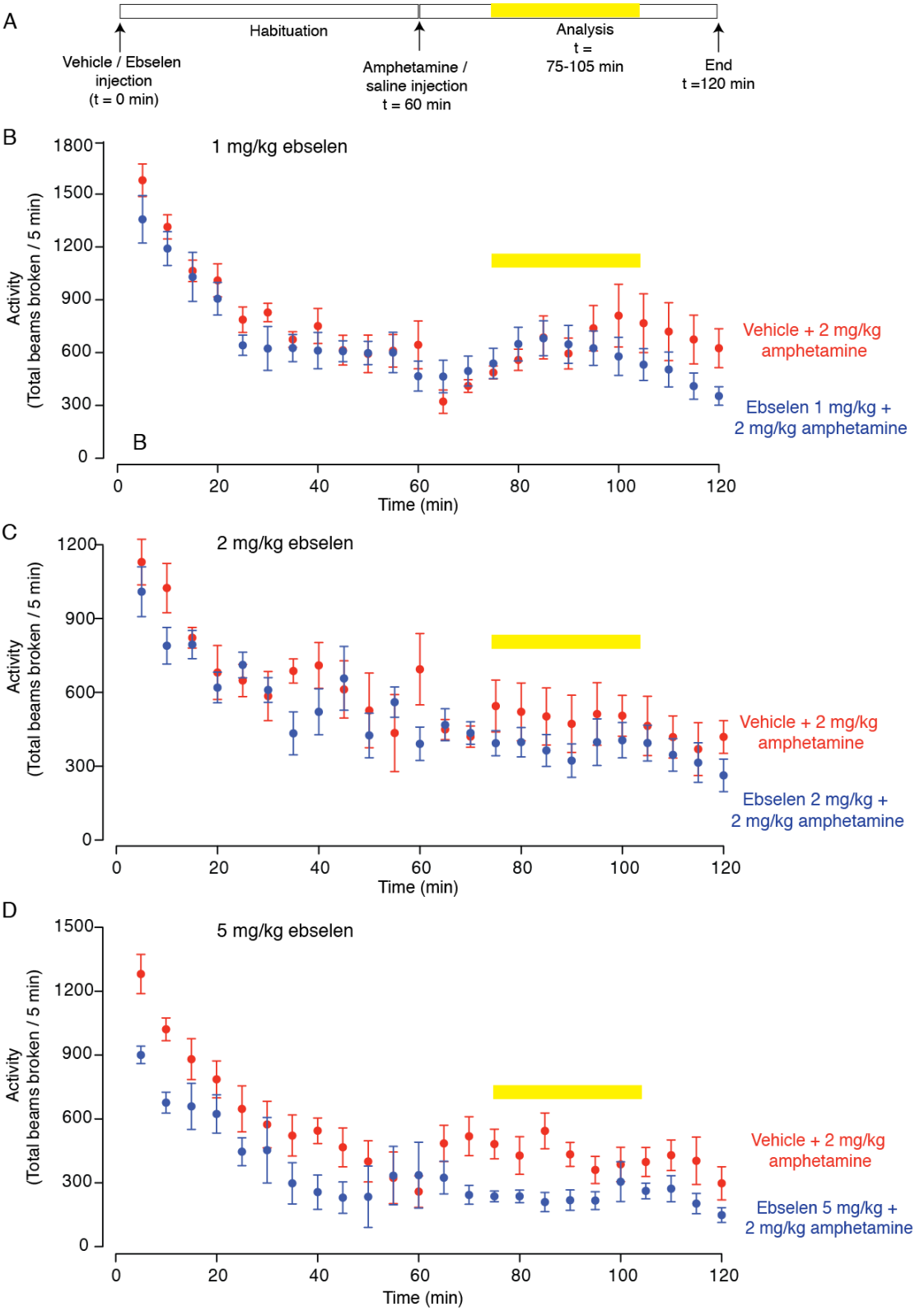


Figure 5.3.7. Effect of ebselen on amphetamine-induced hyperactivity. A) Amphetamine (2 mg/kg) (or saline) was injected 60 min post injection of ebselen (or vehicle). The yellow bar shows the period (75–105 min) that was used for analysis. Ebselen was tested at **B)** 1, **C)** 2 and **D)** 5 mg/kg. The graphs show the activity (total beam breaks in a 5 min interval) against time for two groups with the indicated administration of drugs. n = 6-8

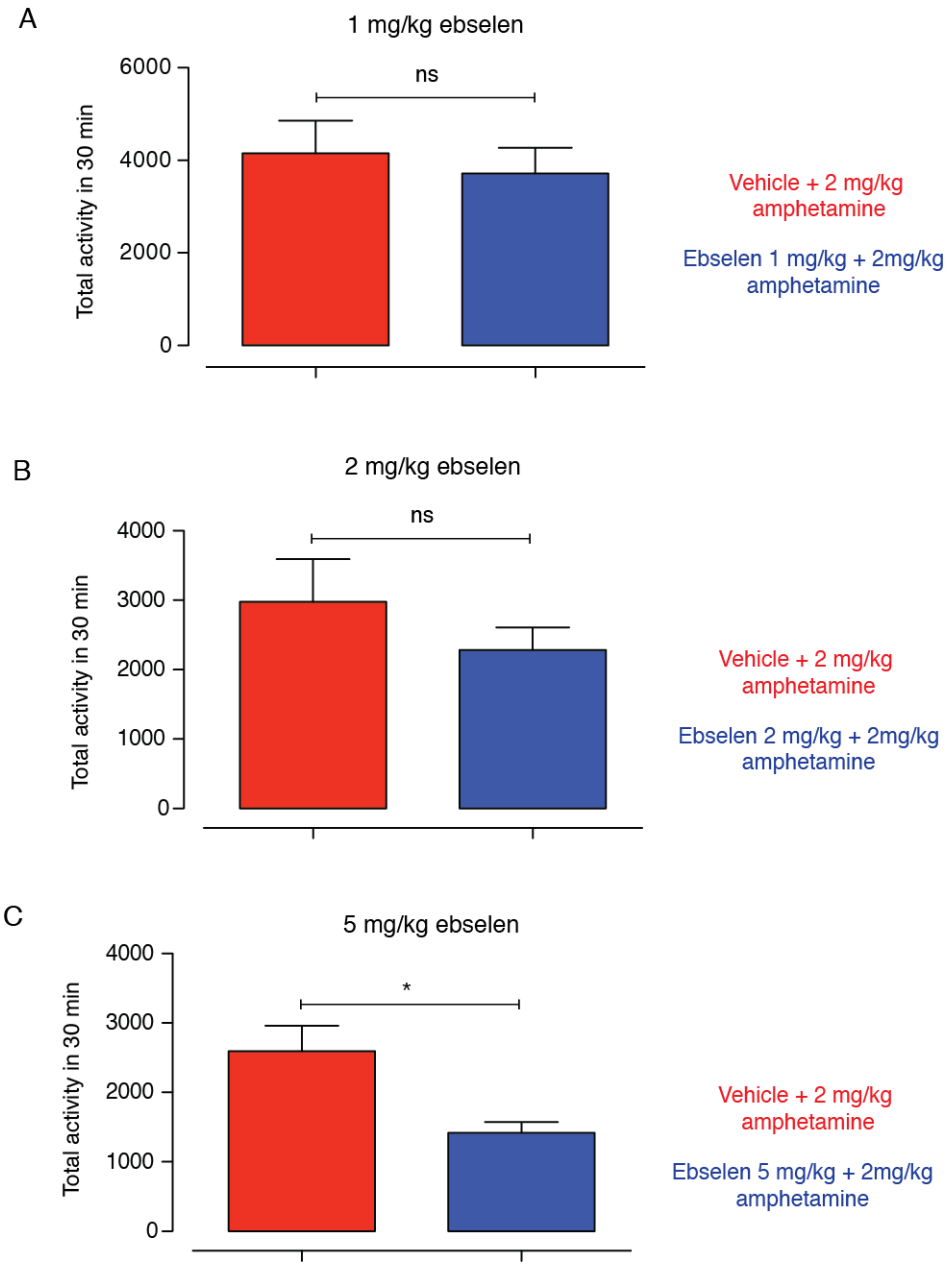


Figure 5.3.8. Effect of ebselen on amphetamine-induced hyperactivity. Bar graphs show the effect of ebselen at **A)** 1, **B)** 2, and **C)** 5 mg/kg during the period t = 75–105 min (see Figure 5.3.5). The y-axis shows the total activity in the 30 min period for the 2 different treatment groups. n = 6-8.. The paired t-test was used to determine significance between the groups indicated by the line. * p <0.05; ns, not significant).

Ebselen at 1 mg/kg and 2 mg/kg did not have a significant effect on 2 mg/kg amphetamine-induced activity (Figure 5.3.8A and B). However, 5 mg/kg ebselen did cause a significant decrease in activity (Figure 5.3.8C).

At 5 mg/kg ebselen, 2mg/kg amphetamine-induced hyperactivity dropped by 45% compared to the vehicle-treated group, which was greater than in the case of 4 mg/kg amphetamine and was found to be significant using the paired t-test ($p = 0.0195$). At this dose (5 mg/kg ebselen) no significant difference in baseline (time in activity monitor before the administration of amphetamine) was observed.

5.3.3 Forced swim test

Ebselen at the three doses was administered in the FST. Imipramine, a tricyclic antidepressant, was used as a positive control (16 mg/kg, administered 30 min before the start of the testing). LiCl (10 mmol/kg) and NaCl administered 18 h before the FST were also tested. The one-way ANOVA with a Dunnett's post-test was used to analyse the results obtained by comparing the ebselen- and lithium-treated groups against the vehicle-treated groups. Immobility was recorded as the time in which the mouse made no movement other then necessary to keep it's head above water (Porsolt *et al.*, 1977).

CD-1 mice were used, since these mice are considered to be superior to the C57Bl/6 in the FST (David *et al.*, 2003).

5.3.3.1 Ebselen in CD-1 mice

Administration of ebselen 1 h prior to testing

The effect of 5 and 10 mg/kg ebselen (n = 6 /group), administered 1 h prior to the test, in CD-1 mice is shown in Figure 5.3.9.

Imipramine showed a significant decrease in immobility compared to vehicle treated mice (Figure 5.3.9). No significant differences were seen with 5 and 10 mg/kg ebselen.

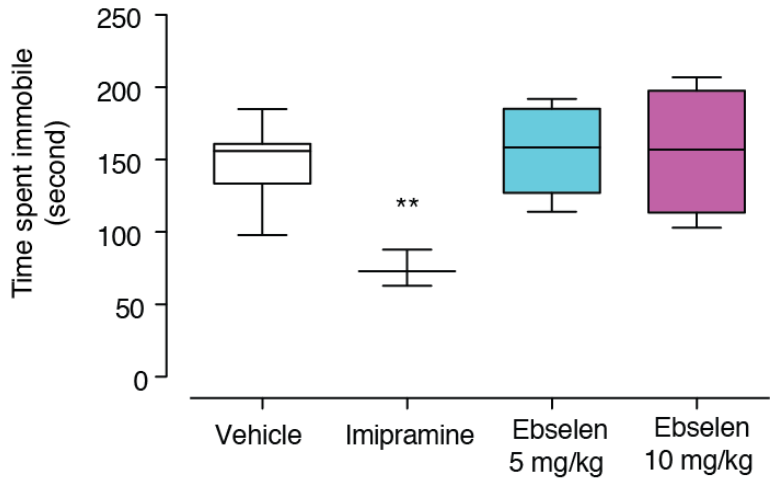


Figure 5.3.9. Ebselen, administered acutely, in an FST using CD-1 mice. The box plot shows the effects of ebselen (5 and 10 mg/kg) vehicle and Imipramine (16 mg/kg, positive control). Drugs were injected 1 h prior to the test. A one-way ANOVA with a Dunnett's post-test was used for statistical analysis (n = 6 / group). Only the imipramine group was significantly different from the vehicle treated mice. ** p <0.01.

Sub-acute and chronic administration of ebselen prior to testing

Since the mice treated with the acute doses of ebselen did not show any significant difference compared to the vehicle-treated mice, sub-acute and a chronic administration of ebselen (5 mg/kg) were tested in CD-1 mice. This was injected twice daily for two days for the sub-acute group and twice daily for a week for the chronic group. The mice were then tested in the FST. Neither the sub-acute nor the chronic ebselen treatment showed any significant change in immobility time compared to the vehicle-treated mice (Figure 5.3.10).

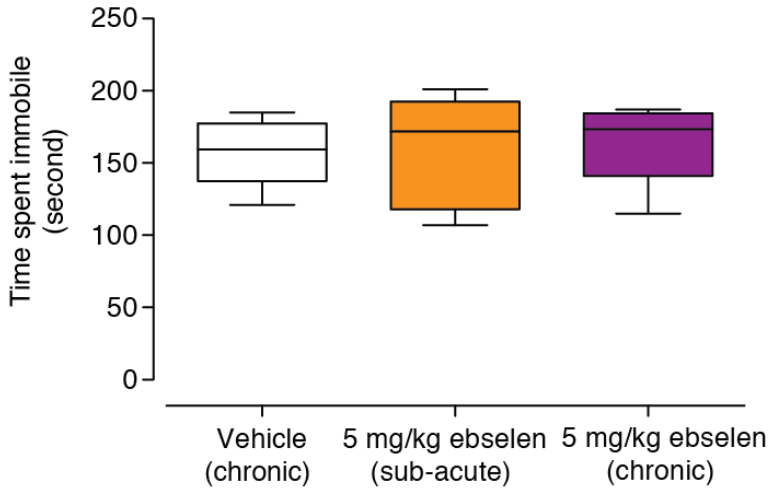


Figure 5.3.10. Ebselen, administered sub-acutely and chronically, in an FST using CD-1 mice. The sub-acute treatment involved twice daily dosing for 2 days. The chronic treatment involved twice daily injections for one week. A one-way ANOVA with a Dunnett's post-test was used for statistical analysis (n = 6 / group) and neither group was significantly different from the vehicle treated group.

5.3.3.2 Ebselen in C57BL/6 mice

The FST was then carried out using C57BL/6 mice, to investigate strain-specific differences; the FST is sensitive to strain differences (David *et al.*, 2003). Ebselen (5 or 10 mg/kg) was administered 1 h prior to testing; however, no significant difference was observed in the immobility time compared to the vehicle treated mice. This was repeated using a 30 min post-injection period before the FST.

Acute administration of ebselen 30 min prior to FST

The FST was repeated using the same doses (5 and 10 mg/kg), but administered 30 min prior to testing. The mice were then tested as before (Figure 5.3.11A).

Ebselen produced a dose-dependent increase in immobility time in the FST. Lithium, when administered chronically, reduces the immobility time and shows antidepressant effects (Can *et al.*, 2011; O'Donnell and Gould, 2007). This is in contrast to a study which showed that ebselen decreased immobility time in NIH-Swiss mice (Posser *et al.*, 2009). The experiment was repeated with NIH-Swiss mice

(Figure 5.3.11B), and the dose-dependent increase in immobility time was again observed.

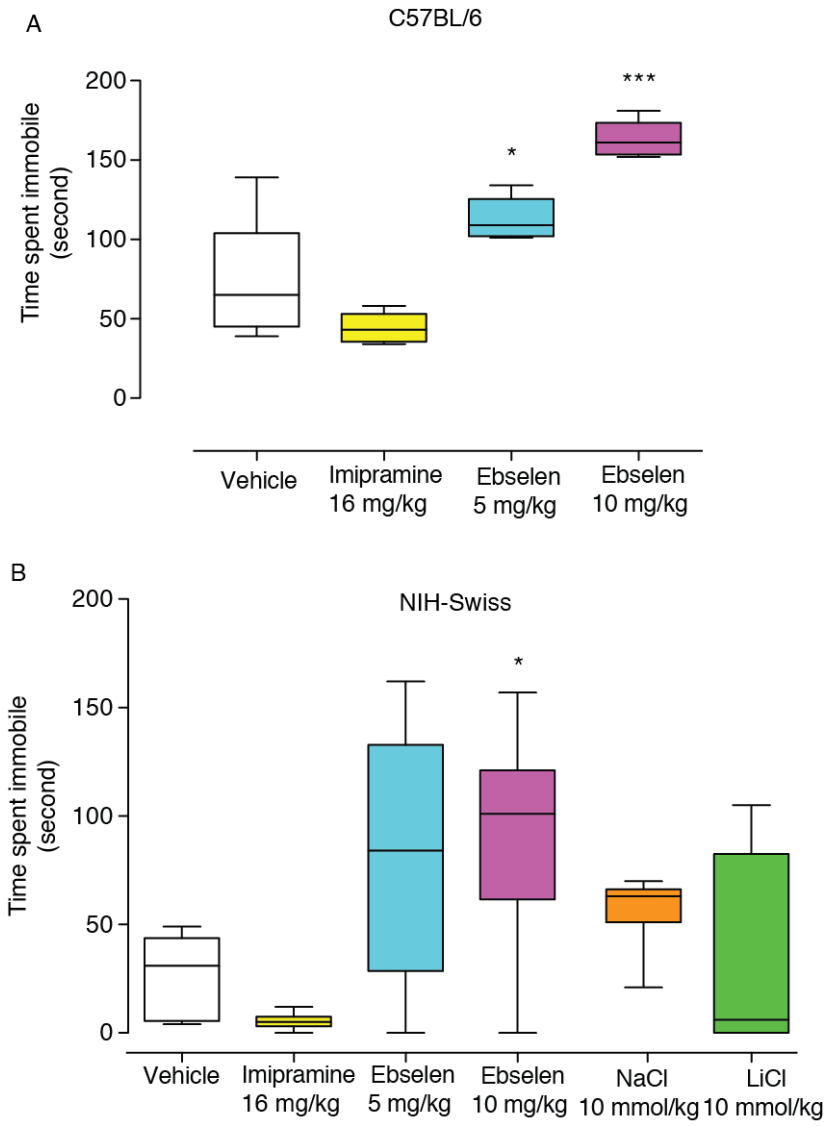


Figure 5.3.11. Ebselen administered 30 min prior to FST using A) C57BL/6 mice and B) NIH Swiss mice. Ebselen (5 or 10 mg/kg) vehicle or Imipramine (control) was injected 30 min prior to the test. A one-way ANOVA with a Dunnett's post-test was used for statistical analysis (n = 8 / group). The ebselen treated mice showed a significant dose-dependent increase in immobility time, although imipramine was not significantly different from the vehicle treated mice. * p <0.05; *** p <0.001.

Effect of 1 mg/kg ebselen and lithium in the FST

Next, a lower ebselen dose (1 mg/kg) was used, administered 30 min prior to testing, along with lithium (10 mmol/kg, administered 18 h prior to the FST). C57BL/6 mice (n = 6/group) were treated, the immobility times are presented in Figure 5.3.12.

At 1 mg/kg, ebselen did not produce any change in immobility time compared to the vehicle. Lithium showed a decrease in immobility time compared to its vehicle (NaCl), although this was not statistically significant. Imipramine (not shown) was significantly different from the vehicle in this experiment.

Lithium (20 mmol/kg), was also tested 1 h prior to the FST, but no difference was detected from the control. Hence, in this experimental setup, lithium showed a decrease in immobility time only when administered 18 h prior to the FST.

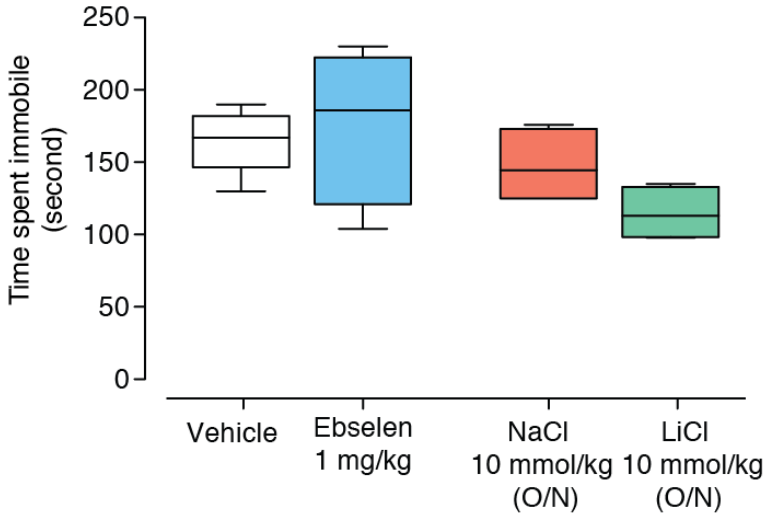


Figure 5.3.12. Effect of acute treatment of ebselen (1 mg/kg) in the FST. C57BL/6 mice were tested with ebselen/vehicle injected 30 min prior to the test, or with lithium/NaCl (10 mmol/kg) overnight (O/N). One-way ANOVA with a Dunnett's post-test was used for statistical analysis (n = 6 / group). Neither ebselen nor lithium were found to be significantly different from their vehicles although lithium did show decrease in immobility time.

5.3.4 Pilocarpine seizure test

Lithium, when given in conjunction with a sub-convulsive dose of pilocarpine causes seizure. This effect is reversed by myo-inositol treatment and hence the seizures are attributed to a depletion of inositol; this provides evidence for the hypothesis that lithium causes inositol depletion (Belmaker and Bersudsky, 2007; Kofman and Belmaker, 1990).

The experiment was repeated using ebselen, to investigate what effect this has on sub-convulsive doses of pilocarpine. Mice were injected with ebselen/vehicle followed by pilocarpine after a pre-determined time. They were then observed and assigned a score every 10 min according to the Patel scale (Patel *et al.*, 1988) shown in Table 5.2.3. Observer scores were plotted against time post-pilocarpine injection

5.3.4.1 Ebselen's effect on a convulsive dose of pilocarpine

The initial experiment was carried out with 300 mg/kg pilocarpine (a convulsive dose), in conjunction with 10 mg/kg ebselen. This was to ascertain whether ebselen blocks pilocarpine-induced convulsions at an acute dose (1 h prior to testing) of 10 mg/kg.

The mice were injected with ebselen or vehicle 1 h prior to the administration of pilocarpine (300 mg/kg) and the animals were scored every 10 min until the humane end-point was reached (Figure 5.3.13).

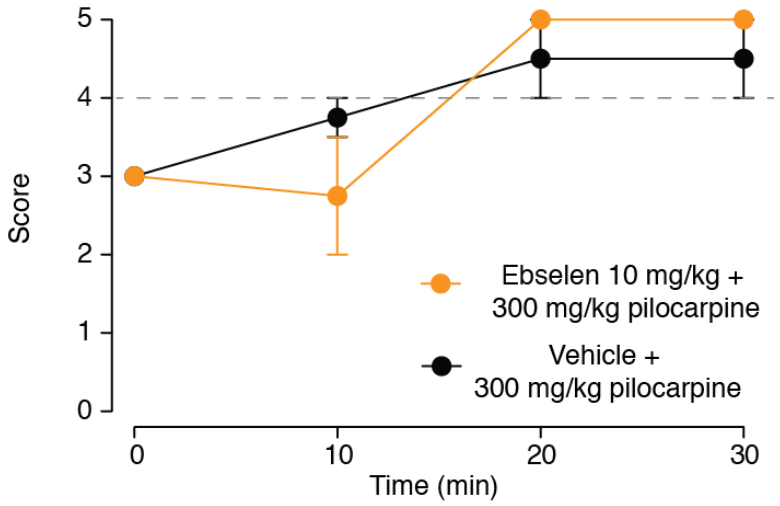


Figure 5.3.13. Effect of ebselen on a convulsive dose of pilocarpine. Ebdelen (10 mg/kg) was administered 1 h prior to pilocarpine (300 mg/kg) (n = 4). Patel scale scores assessed at 10 min intervals are plotted against time post pilocarpine injection. The dashed line indicates the seizure states (score ≥ 4).

All mice developed seizures, and that there was no observable difference between the ebselen- and vehicle-treated mice.

5.3.4.2 Effect of Lithium on sub-convulsive doses of pilocarpine

Next, lithium was assessed in the pilocarpine seizure test. Lithium would serve as a positive control in this paradigm and if seizures were seen in mice treated with lithium + pilocarpine at a sub-convulsive dose (100 mg/kg). Lithium was administered 18 h prior to the pilocarpine injection, and the mice (n = 6/group) were scored (Figure 5.3.14).

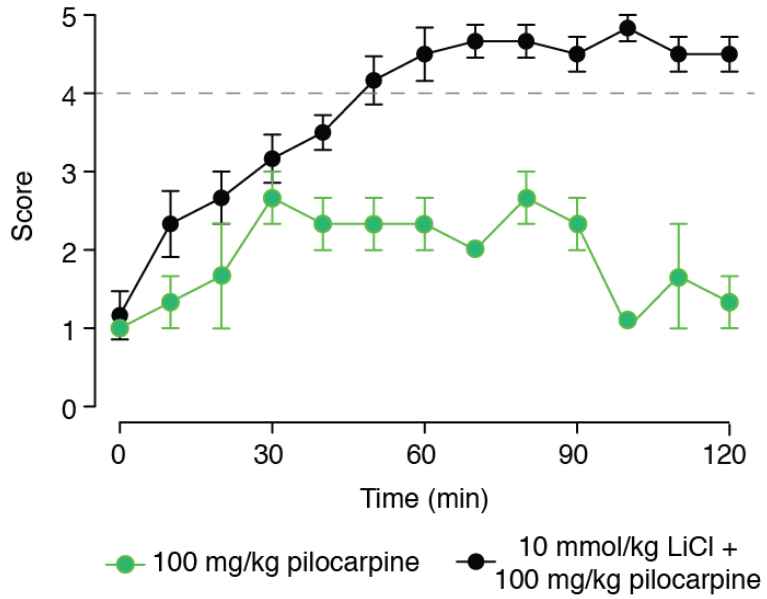


Figure 5.3.14. Effect of Lithium on 100 mg/kg pilocarpine. Mice administered pilocarpine with or without prior (18 h) treatment with lithium (10 mmol/kg) . Scores, according to the Patel scale, are plotted against time post pilocarpine injection. All mice subjected to both drugs experienced seizure. Dashed line indicates seizure states (score ≥ 4). n = 6/group.

Pilocarpine at 100 mg/kg alone did not cause seizures, but 10 mmol/kg lithium when injected prior to pilocarpine caused seizures. 100% of the mice in the latter group developed generalised seizures and none of the mice in the former group developed seizures. Hence, it was concluded that the assay setup was functionally valid.

5.3.4.3 Effect of 5 mg/kg ebselen on pilocarpine seizures

Once the effect of lithium, the positive control, was established in the assay, ebselen (5 mg/kg) was tested in combination with 100 mg/kg pilocarpine. Ebselen was administered at different times prior to pilocarpine: overnight for 16 h (O/N), 1 h, 3.5 h, and chronically (2 weeks, twice a day). The scoring was as above.

None of the mice developed seizures with the different treatments (Figure 5.3.15). One mouse in the overnight group convulsed, but since this was not reproducible, it was considered to be an artefact.

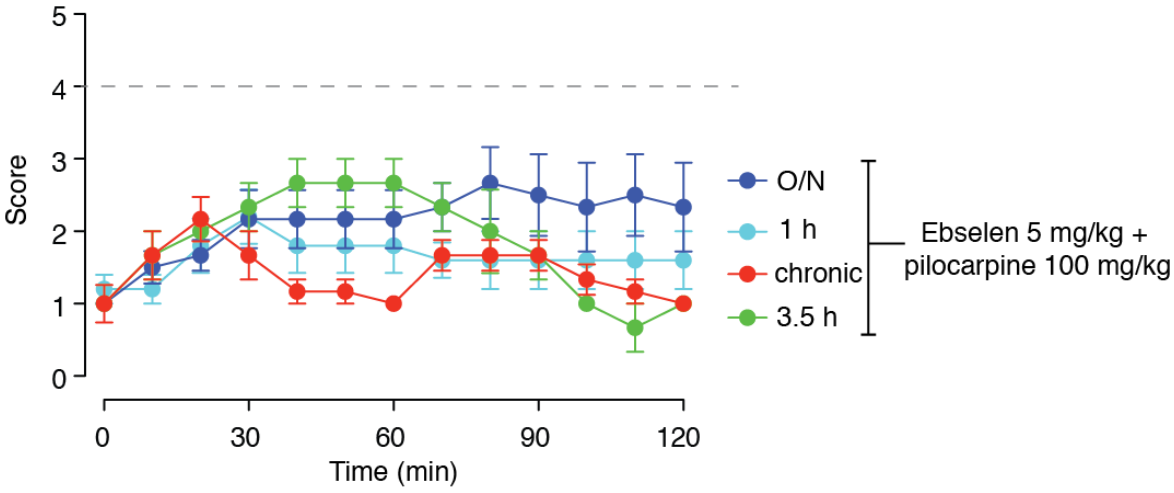


Figure 5.3.15. Effect of 5 mg/kg ebselen with 100 mg/kg pilocarpine. Ebselen was injected at different times prior to pilocarpine: 1 h, 3.5 h, O/N and chronic. Scores, according to the Patel scale, are plotted against time post pilocarpine injection. The dashed line indicates the seizure states (score ≥ 4). n= 6/group.

5.3.4.4 Effect of 10 mg/kg ebselen on pilocarpine seizures

Since 5 mg/kg ebselen did not have an effect with 100 mg/kg pilocarpine, a higher dose of ebselen (10 mg/kg) was tested. Ebselen was injected 1 h, 3.5 h, and 16 h (O/N) before pilocarpine.

None of the mice developed seizures (Figure 5.3.16). It was concluded that neither 5 nor 10 mg/kg of ebselen in combination with 100 mg/kg pilocarpine had the ability to produce seizures, unlike 10 mmol/kg lithium.

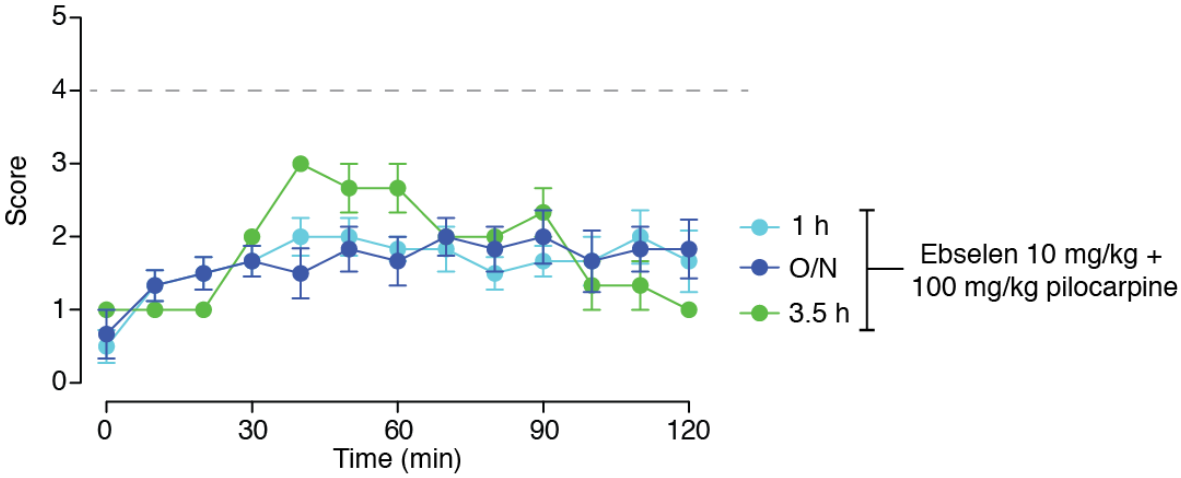


Figure 5.3.16. Effect of 10 mg/kg ebselen with 100 mg/kg pilocarpine. Ebselen was injected either 1 h, 3.5 h or 16 h prior to pilocarpine. Scores, according to the Patel scale, are plotted against time post-pilocarpine injection. None of the mice convulsed. The dashed line indicates the seizure states (score ≥4). n = 6/group.

5.3.4.5 Ebselen sensitisation of lithium-pilocarpine seizures

It had been shown that the combination of ebselen and pilocarpine did not cause seizure. It was conjectured that ebselen with pilocarpine might cause seizure in mice that had previously been given a small dose of lithium. As lithium (1 mmol/kg) administered 18 h prior to pilocarpine (100 mg/kg) did not cause seizure, this combination was tested again, but supplemented with ebselen (10 mg/kg) 1 h prior to the pilocarpine injection.

No seizures were observed in either the ebselen or the vehicle group (Figure 5.3.17). It was concluded that ebselen (10 mg/kg) given 1 h prior to pilocarpine, did not sensitise the mice.

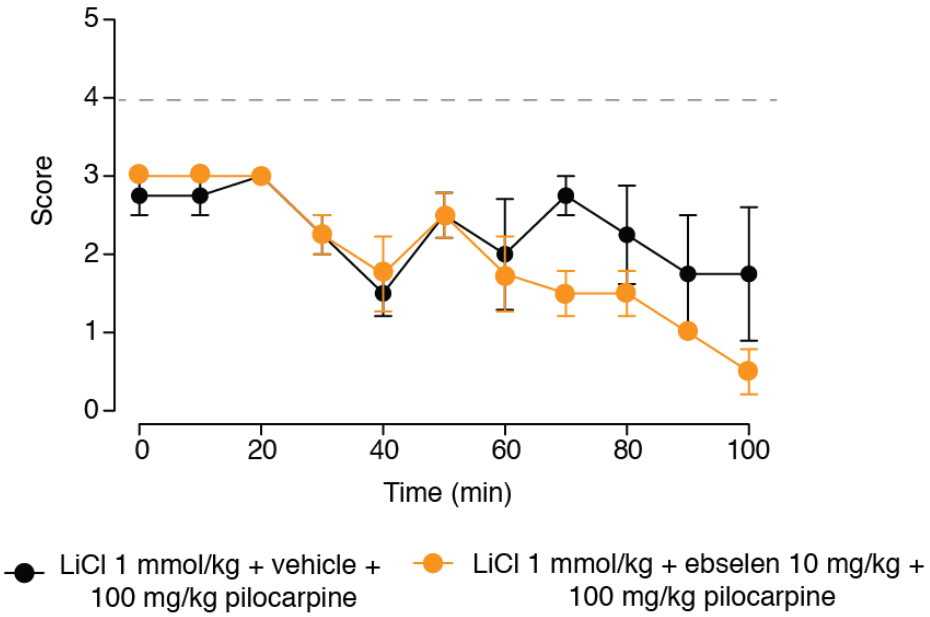


Figure 5.3.17. Effect of 10 mg/kg ebselen with 1 mmol lithium and 100 mg/kg pilocarpine. Lithium was administered 18 h prior to ebselen/vehicle, then pilocarpine 1 h later. Scores, according to the Patel scale, are plotted against time post-pilocarpine injection. The dashed line indicates the seizure states, (score ≥4).

Neither 5 nor 10 mg/kg ebselen with 100 mg/kg pilocarpine had the ability to produce seizures (unlike 10 mmol/kg lithium), nor did this sensitise to seizure by mmol/kg lithium with 100 mg/kg pilocarpine to seizures.

5.3.5 Tremor analysis

It had been established that ebselen did not potentiate pilocarpine seizure. However, it might be that this combination of drugs might have some other detectable effects. Two avenues of investigation were followed: behaviour change and gene expression.

The tremor monitor method offers a quantitative analysis of effects that ebselen might have. This is preferable to the subjective (observational) assessment of the Patel scale scoring used in the seizure experiments.

Mice were treated with either vehicle + saline, 1 mg/kg ebselen + saline, vehicle + 200 mg/kg pilocarpine or 1mg/kg ebselen + 200 mg/kg pilocarpine. Vehicle/drug was administered 1 h prior to pilocarpine. Then, 25 min later the mice were placed in the tremor monitor and observed for 1 min. The tremor monitor measures the amplitude and frequency of tremors.

Ebselen (1 mg/kg) reduced the amplitude of tremors produced by 200 mg/kg pilocarpine (Figure 5.3.18C and D).

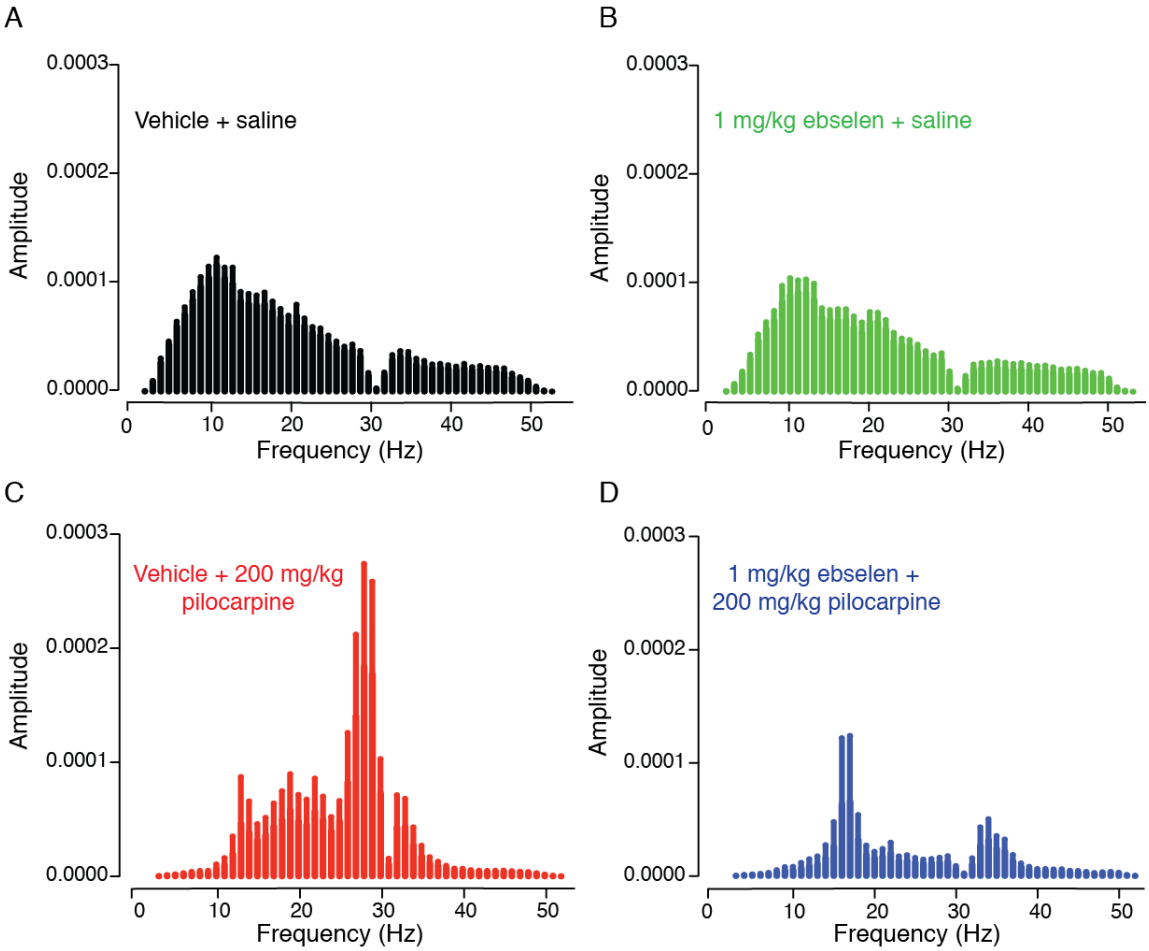


Figure 5.3.18. Effect on 1 mg/kg ebselen on tremors induced by 200 mg/kg pilocarpine. The amplitude and the frequency of tremor are plotted for the four combinations of drugs/controls (n = 4/group).

5.3.6 *In situ* hybridisation

The mice were removed after 1 min in the tremor monitor and immediately killed and their brains removed. As inhibition of pilocarpine tremors by ebselen had been shown, the brains from those mice were used to analyse *c-Fos* mRNA expression by in situ hybridisation.

c-Fos is a proto-oncogene belonging to the family of immediate early genes (IEG) transcription factors. It is a marker for neuronal activation and is activated by a number of neurotransmitters, hormones and growth factors.

The mouse brain regions examined were frontal cortex (cingulate, orbital, and secondary motor cortex; Figure 5.3.19A) striatum (caudate putamen, inner and outer parietal cortex, piriform cortex; Figure 5.3.20A) and the hippocampus (inner and outer parietal cortex, CA1 and CA3; Figure 5.3.21A). Graphs were drawn from normalised data of regions across all treatment groups with respect to the control (vehicle + saline) group, whose average value in any given region was defined as 100%. A one-way ANOVA with a Dunnett's post-test was used to determine statistical significance (n = 4 / group). All groups were compared to the control group.

5.3.6.1 *c-Fos* expression in the frontal cortex

The cingulate cortex, the orbital cortex and the secondary motor cortex (M2) regions were analysed for any changes in *c-Fos* mRNA expression following administration of 200 mg/kg pilocarpine and/or 1 mg/kg ebselen.

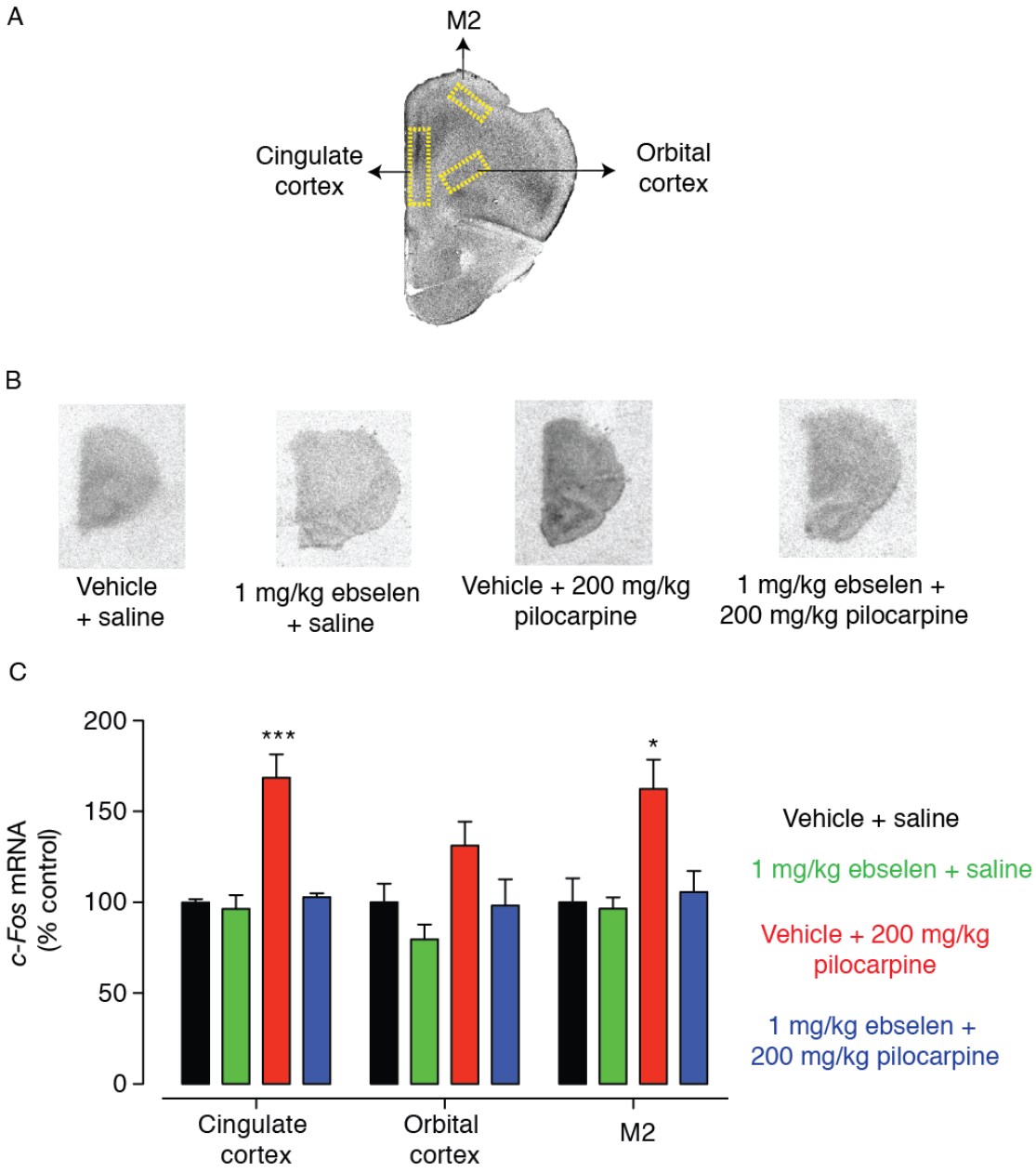


Figure 5.3.19. *c-Fos* mRNA expression in the frontal cortex. The effects of 1 mg/kg ebselen and/or 200 mg/kg pilocarpine on *c-Fos* expression were investigated in the frontal cortex. **A)** Shows the schematic representation of the different regions of the frontal cortex that were used for analysis; the cingulate cortex, orbital cortex and secondary motor cortex (M2). **B)** Shows the sample images of the sections observed for each of the 4 treatment groups. **C)** Shows the bar graph with of the data relative to control (100%). Analysis of statistical significance was done using a one-way ANOVA was used with a Dunnet's post-test. * p <0.05; *** p <0.001.

Pilocarpine caused an increase in the expression of *c-Fos* in the cingulate cortex and the secondary motor cortex (M2) regions of the frontal cortex (Figure

5.3.19 B and C). Interestingly, ebselen at 1 mg/kg almost completely ablated pilocarpine-induced *c-Fos* expression in all three regions of the frontal cortex.

5.3.6.2 c-Fos expression in striatum

Next *c-Fos* expression in four regions at the level of the striatum was examined. In the striatum, although there was an increase in expression in the pilocarpine-treated group, this was not as prominent as in case of the frontal cortex regions, and was not considered significant. However, in the caudate putamen and the outer parietal cortex there is a clear reduction of *c-Fos* mRNA in the ebselen + pilocarpine group compared to the vehicle + pilocarpine group. In the striatum, it appears that ebselen alone decreases *c-Fos* mRNA compared to the control (Figure 5.3.20B and C). This was, however, insignificant.

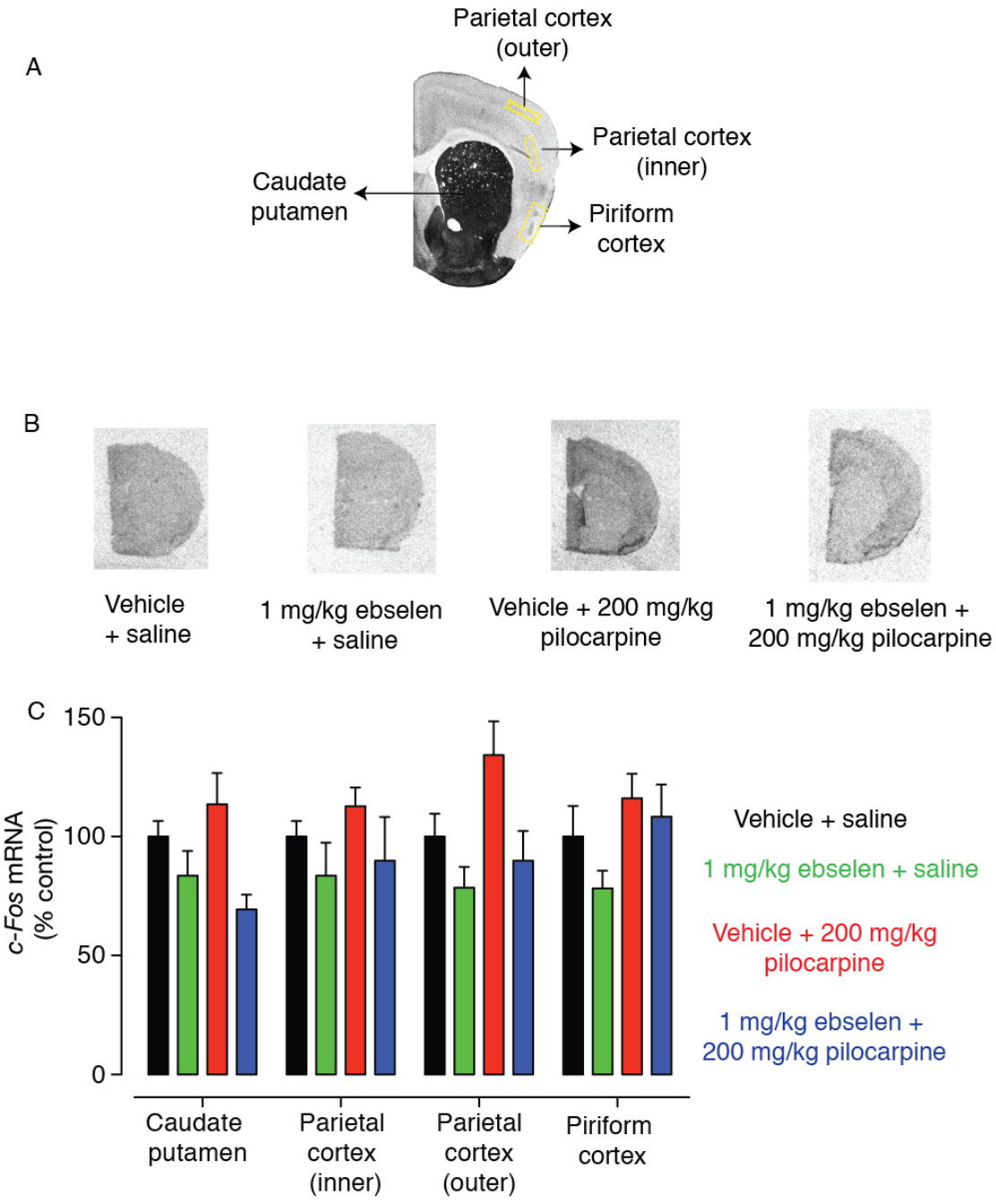


Figure 5.3.20. *c-Fos* mRNA expression in the striatum. The effects of 1 mg/kg ebselen and/or 200 mg/kg pilocarpine on *c-Fos* expression were investigated in the striatum. **A)** Shows the schematic representation of the different regions of the striatum that were used for analysis; the caudate putamen, the inner and outer parietal cortex and the piriform cortex. **B)** Shows the sample images of the sections observed for each of the 4 treatment groups. **C)** Shows the bar graph with of the data relative to control (100%). Analysis of statistical significance was done using a one-way ANOVA was used with a Dunnet's post-test.

5.3.6.3 c-Fos expression in the hippocampus

In the hippocampus, pilocarpine significantly increased *c-Fos* expression in the CA1, inner and out parietal cortex regions of the hippocampus (Figure 5.3.21B and C). The increase was not so pronounced in the CA3 region. Ebselen reduces the expression in all the four regions, however, not to the extent observed in the frontal cortex.

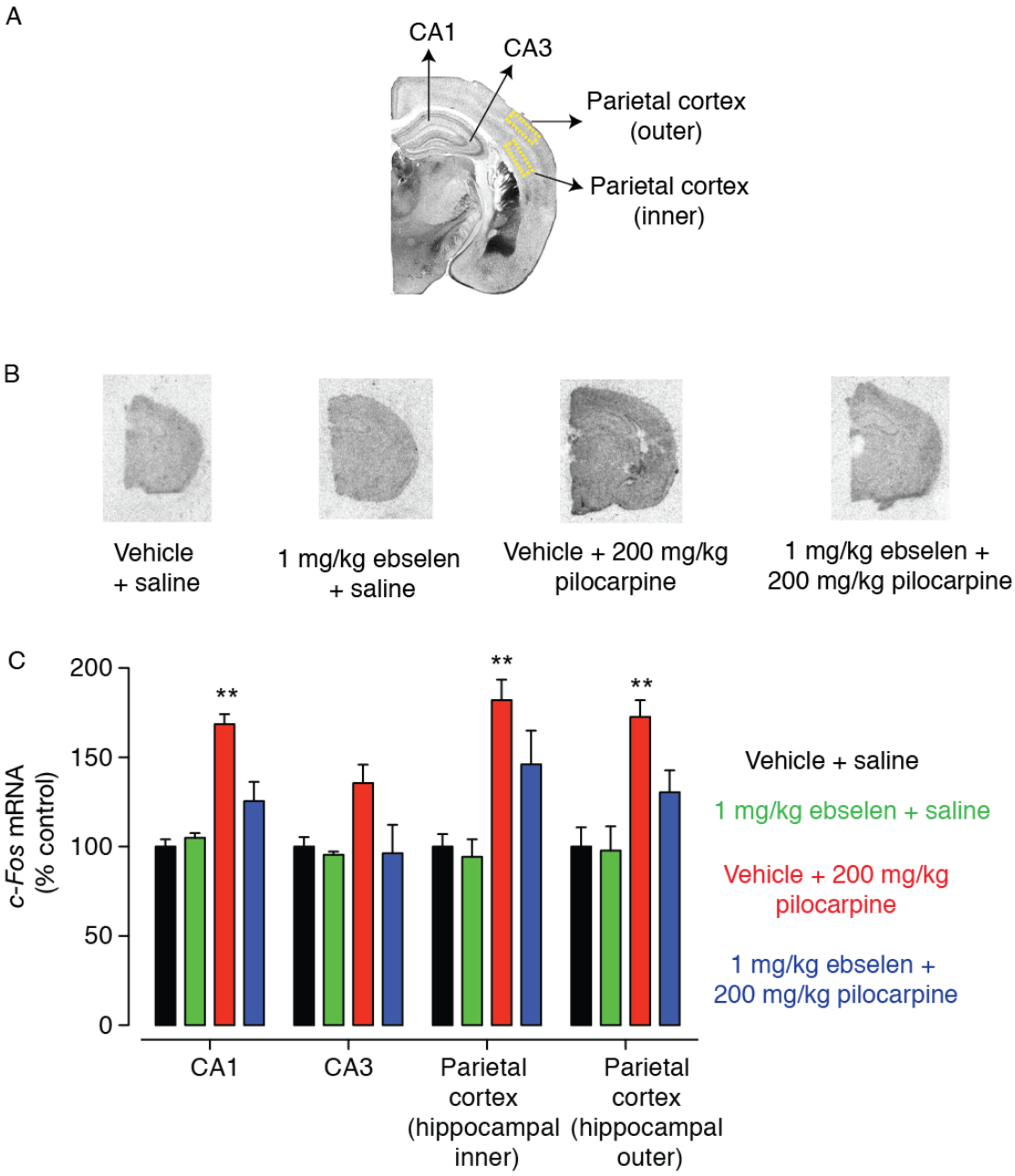


Figure 5.3.21. *c-Fos* mRNA expression in the hippocampus. The effects of 1 mg/kg ebselen and/or 200 mg/kg pilocarpine on *c-Fos* expression in the hippocampus. **A)** Shows the schematic representation of the different regions of the hippocampus that were used for analysis; the CA1, CA2 and the inner and outer parietal cortex. **B)** Shows the images of the sections that were observed for each of the 4 treatment groups. **C)** Shows the bar graph of the data relative to control (100%). Analysis of statistical significance was done using a one-way ANOVA with a Dunnet's post-test. ** p <0.01.

The expression levels of *c-Fos* mRNA in all the tested regions and treatment groups is given in table 5.3.1.

Table 5.3.1. *c-Fos* mRNA expression with and without treatment in the different brain regions.

Region	Basal expression (optical density units)	Ebselen induced expression (optical density units)	Pilocarpine induced expression (optical density units)	Pilocarpine + ebselen induced expression (optical density units)
Frontal Cortex				
Cingulate cortex	315.61	304.28	532.23	324.54
Orbital cortex	347.73	456.26	276.78	341.58
M2	243.40	395.49	234.93	257.32
Striatum				
Caudate putamen	274.04	228.87	311.08	190.08
Parietal cortex inner (Ptxi)	288.56	241.16	325.29	259.10
Parietal cortex outer (Ptxo)	309.3	242.78	415.21	277.76
Piriform cortex	514.97	402.48	767.40	557.78
Hippocampus				
CA 1	283.64	478.37	297.76	356.01
CA 3	357.95	485.38	341.66	344.81
Hippocampal parietal cortex inner (hip Ptxi)	307.38	559.31	289.87	449.14
Hippocampal parietal cortex outer (hip Ptxo)	308.47	532.45	301.62	402.34

5.4 Discussion

In this chapter it has been shown that ebselen exhibits some, but not all, of the behavioural effects of lithium in established rodent models of mania and depression. However, unlike lithium's dual-role therapeutic effects, antimanic and antidepressant, ebselen seems to have just antimanic activity. Nevertheless, this is the first study that shows that an *in vitro* inositol monophosphatase inhibitor shares some of the behavioural effects of lithium.

5.4.1 Ebselen's effect on exploratory activity

Ebselen had a definite reduction in exploratory activity and if we assume that the correlation between time spent active by mice in a novel open field and sensation-seeking behaviour in man are true then by extrapolation (Zuckerman, 1984; Zuckerman and Neeb, 1979), lithium reduces sensation seeking in man. Ebselen, by virtue of its lithium like effects in this test, should also reduce this behaviour in man. This is interesting because the manic phase in bipolar patients is characterised by sensation and novelty seeking, for example, gambling and substance abuse is commonly seen in bipolar manic patients. Lithium reduces exploratory behaviour in the OFT and its effect is more significant on rearing than on activity (Johnson, 1972). Ebselen similarly decreased ambulatory activity and rearing behaviour in the OFT and like lithium, ebselen's effect in decreasing rearing behaviour is more significant and robust than that in the horizontal plane, compared to vehicle treatment. Whether or not this effect is related to IMPase can be tested by inositol reversibility of this behaviour. However, these effects were paralleled by the inhibition of IMPase seen *ex vivo* in the previous chapter (Figure 4.3.18). Lithium was not tested in this

experimental setup; however, this test was chosen because of lithium's effects in it are well recognised. It would be useful to further characterise ebselen's effect under different treatment regimes, and directly compare it to lithium's effects in the OFT. Despite this, ebselen caused a distinct reduction in exploratory behaviour in a novel environment, however whether this effect is related to IMPase inhibition is unknown. Although the mice under the testing conditions, were awake and active it cannot be ruled out that ebselen might be having a sedative-like effect. However, lithium itself was discovered for its effect of reducing activity in guinea pigs (Cade, 1949).

5.4.2 Ebselen's effect in amphetamine-induced hyperactivity

The amphetamine hyperactivity test is a rodent test that is said to mimic the manic state in bipolar patients. In the amphetamine-induced hyperactivity test, lithium decreases the hyperactivity produced by 2 mg/kg amphetamine (Gould *et al.*, 2007b; Gould *et al.*, 2005). Two different doses of amphetamine were tried : 2 and 4 mg/kg. Initially 4 mg/kg amphetamine was administered, since this produced a distinct increase in activity. Ebselen at 10 mg/kg did effect a significant reduction in hyperactivity induced by 4 mg/kg amphetamine, although this was seen to be a small effect (about 25%). It was concluded that 4 mg/kg might have been too high a dose to show a reduction in hyperactivity. At this dose, saturation might have been reached so small differences in activity might be undetectable. Other groups have almost consistently used 2 mg/kg amphetamine in this test and therefore, 2 mg/kg amphetamine was used in subsequent experiments.

Ebselen at 5 mg/kg did produce a significant decrease in activity with 2 mg/kg amphetamine-induced hyperactivity (about 45%). This experiment was repeated in another setup, the Ethovision setup in Dr. Belmaker's laboratory, Ben Gurion

University. This decrease in amphetamine-induced hyperactivity in mice treated with 5 mg/kg ebselen was reproducible in the other setup. This is useful, since sometimes varying conditions can have varying effects on behavioural tests. Hence, it is possible to conclude that ebselen, like lithium, causes a reduction in amphetamine-induced hyperactivity hence it might be that ebselen had the ability to reduce manic symptoms in bipolar patients. Interestingly, tamoxifen, a protein kinase C inhibitor also has the ability to reduce AIH in rodents, and so does a GSK-3 inhibitor (Einat *et al.*, 2007; Gould *et al.*, 2004a) so it is not possible to relate this effect to IMPase inhibition since ebselen inhibits all three enzymes. Tamoxifen was successful in clinical trials for bipolar mania, hence this test has seen clinical validation as well (Bebchuk *et al.*, 2000).

5.4.3 Ebselen's effect in the forced swim test

The preceding experiments demonstrated that ebselen mimics the anti-manic aspects of lithium in rodent models of mania. However, ebselen did not mimic lithium antidepressant effects in the FST.

Antidepressants decrease immobility time in the FST, as does lithium. . Ebselen was tested at different time points, with different doses and in different mice strains. CD-1 mice are commonly used in the FST for antidepressant screening. In CD-1 mice, no significant effect was observed with ebselen, while imipramine showed a significant decrease in immobility time. However, in C57BL/6 and NIH-Swiss mice, ebselen increased immobility time significantly, and in a dose-dependent manner, when injected 30 min before testing.

These latter findings were contrary to the ones showing that ebselen reduced immobility time (Posser *et al.*, 2009) in NIH-Swiss mice when dosed at 10–30 mg/kg,

subcutaneously. Their experimental setup was slightly different (cylinder dimensions). Additionally, a drug injected subcutaneously is absorbed more slowly than a drug injected intra-peritoneally. It is possible that ebselen absorption (at the same dose) was slower in the case of Posser *et al.*. It has been shown that the FST is sensitive to both cylinder dimension and route of injection. Hence, it is possible, that these differences underlie the conflicting results.

A lower dose of ebselen, 1 mg/kg, was also tried, since it might have been possible that ebselen was having a depressant effect only at higher doses, but this still resulted in an immobility time similar to vehicle, although with a large variation (Figure 5.3.12). Additionally, mice were only habituated to the environment for 30 min before the start of the test; it is possible that this is not sufficient for ebselen testing. This might have been a novel environment, and it has already been established that ebselen decreases activity in a novel environment. This is why there might have been an increase in immobility time, instead of a decrease. Another consideration is the possibility that lithium's antidepressant effects are not affected through IMPase, but by some other mechanism.

Some studies have shown that sub-active doses of lithium, when given in conjunction with sub-active doses of some antidepressants, like fluoxetine and moclobemide, a decrease in immobility time is observed (Nixon *et al.*, 1994). Hence, it may be useful test ebselen's effect in conjunction with sub-active doses of antidepressants in order to test if it has any additive effects.

It is seen that drugs that inhibit NA action and dopaminergic activity, show an increase in immobility time (Cryan *et al.*, 2002; Cryan *et al.*, 2005; O'Leary *et al.*, 2007). Chronically dosed SSRIs also show an increase in immobility time (Hansen *et al.*, 1997).

5.4.4 Ebselen's effect in the pilocarpine seizure test

In the pilocarpine seizure test, ebselen did not mimic lithium. Lithium in conjunction with a sub-convulsive dose of pilocarpine causes seizures, while ebselen, at various doses and time points did not produce any seizures. However, this seizure test is observational, and thus subjective. In order to ascertain the effect of lithium on pilocarpine-induced changes more objectively, the tremor monitor was used. After injection with pilocarpine, even at sub-convulsive doses, the mice show tremors. This offered a more sensitive and accurate measure of ebselen's effect on pilocarpine-induced tremors.

Vehicle-treated animals administered pilocarpine showed increased tremor behaviour (Figure 5.3.18); this was not observed in ebselen-treated animals administered pilocarpine. Ebselen at 10 mg/kg did not block the seizures produced by pilocarpine (Figure 5.3.13); however, even at 1 mg/kg, ebselen eliminated the tremor elicited by 200 mg/kg of pilocarpine. This suggests that ebselen might be eliciting this effect through another pathway. Alternatively, lithium itself might be eliciting this effect through another target, but possibly one related to inositol, since the addition of inositol caused the ablation of seizures. For example, since lithium-sensitized pilocarpine-induced seizures can be reversed by inositol, it is believed that lithium promotes these seizures through the inhibition of IMPase. Additionally, *impa*1 knockout mice, when administered 100 mg/kg pilocarpine, also developed seizures which could be reversed by inositol (Kofman *et al.*, 1991). However, when the IMPase-specific inhibitor L-690330 was injected subcutaneously, there were no seizures reported in presence of 100 mg/kg (Atack *et al.*, 1993b). Also, L-690330, when injected intra-cerebroventicularly, inhibited seizures with pilocarpine (Belmaker

lab, unpublished data). This suggests that some other mechanism of lithium is involved in seizure potentiation.

This may be through the other arm of the PI signalling cascade. Lithium by inhibiting IMPase may lead to decreasing inositol levels in the membrane. This causes temporary increase in DAG in the membrane, which then leads to PKC activation. This results in seizures. This hypothesis is further strengthened by the fact that phorbol esters, which are activators of PKC, have the ability to cause seizures in mice at picomolar concentrations (Smith and Meldrum, 1992). The pattern of onset of seizures is also very similar to that seen in the pilocarpine seizure model. This hypothesis could be tested by pretreating mice with staurosporine, a PKC antagonist, before injecting lithium and pilocarpine. This mechanism is especially interesting, because there is a study that suggests that ebselen also has the ability to inhibit PKC (Cotgreave *et al.*, 1989).

If PKC activation is responsible for seizure production in the pilocarpine-seizure model, ebselen, by virtue of its ability to inhibit PKC, would inhibit these seizures.

Pilocarpine also caused increase of *c-Fos* expression in certain areas of the brain; this was much attenuated in the presence of ebselen. Since it was shown that ebselen does not inhibit the muscarinic receptor directly (see previous chapter), it is possible that inhibition of *c-Fos* expression occurs downstream of receptor activation. Ebselen also reduced the expression of *c-Fos* elicited by 2,5-dimethoxy-4-iodoamphetamine (DOI), which is a 5-HT_2 agonist (experiments done by Verity Blackburn). Since both pilocarpine and DOI act through G_q-coupled pathways, it is possible that ebselen is inhibiting a second messenger; IMPase and/or PKC will also cause a decrease in *c-Fos* expression. This study on *c-Fos* expression, confirms that

ebselen crosses the blood–brain barrier and has the ability to influence brain signalling, i.e. not acting solely at the periphery. It also demonstrates that ebselen, like lithium, has the ability to modulate activity downstream of the receptor.

In conclusion, ebselen seems to have an overall effect of attenuating hyperactivity, rather than mimicking the bi-variant effects of lithium. However, like lithium, ebselen is also acting downstream of the receptor and seems to have actions on multiple components of the cell signalling cascade.

To determine conclusively that ebselen elicits some of these effects through IMPase inhibition, inositol reversibility must be demonstrated in ebselen-elicited behaviour. This is currently the subject of on-going investigation in this lab.

CHAPTER 6

FINAL DISCUSSION

6 Final Discussion

In this investigation, the primary aim was to find a lithium-mimetic drug by screening for IMPase inhibitory activity. Two approaches were employed: virtual screening using Ins1P as the model ligand, and repositioning of an orphan drug.

Repositioning has proved highly effective for developing and studying new effects of existing drugs (Cavalla, 2009). But it has not enjoyed such success in delivering new drugs to the market. This is due to licensing obstacles. For example, if a company repositions an existing antihistamine as a novel antidepressant, it does not require a license or a prescription, particularly if it can be bought over the counter. Thus there is no incentive for a company to invest in the necessary additional research if this is not going to translate into additional profit. However, in the case of ebselen and similar drugs this is not a key issue. These drugs are not yet in the market, so there is the potential for them to generate profit. Rather, the problem in this case lies in ownership and the willingness of the parent company to share data with the company wishing to reposition the drug.

Ebselen was identified as an IMPase inhibitor by the repositioning approach, and was considered suitable to be further evaluation in cellular and behavioural tests. In cells, ebselen exhibited overall inositol depletion, and this was judged to be likely by inhibition of IMPase and IP-5Pase, as seen by the elevation of IP_4 and IP_6. In contrast, lithium is believed to inhibit IMPase directly, thereby resulting in an elevation of $Ins1P_{lter}$ levels. In *ex vivo* experiments, ebselen showed a time-dependent IMPase inhibition profile, with maximum inhibitory activity between 2.5 and 5 hours post-administration and reversal of inhibition by 24 hours. Ebselen evoked lithium-like properties in behavioural tests for mania; however, it showed depressant-like activity in the forced swim test. Additionally, ebselen did not precipitate seizures in

the pilocarpine seizure test, unlike lithium. Based on this evidence, therefore, ebselen may well have potential therapeutic application for bipolar mania, though not necessarily for bipolar depression. However, ebselen may still prove to be clinically useful in the treatment of bipolar disorder by virtue of its ability to inhibit a number of targets that have been strongly linked with bipolar disorder.

Ebselen has been shown to inhibit PKC (Cotgreave *et al.*, 1989). Relatedly, tamoxifen, a PKC inhibitor, has also been shown to be clinically useful in the treatment of bipolar mania (Bebchuk *et al.*, 2000). Ebselen's effects in the behavioural tests show pharmacological isomorphism with tamoxifen. Ebselsen also inhibits GSK-3, a target that has been validated in a number of mouse models of mania and depression (Gould *et al.*, 2004a; Gould *et al.*, 2004b). Additionally, ebselen is a known antioxidant (Narayanaswami and Sies, 1990; Parnham and Kindt, 1984), and bipolar disorder has a strong oxidative stress component (Buttner *et al.*, 2007; Frey *et al.*, 2007; Steckert *et al.*, 2010). Clinical trials with *N*-acetylcysteine showed that it was useful as adjunct therapy for bipolar depression (Berk *et al.*, 2008).

By virtue of ebselen's ability to inhibit multiple sites, all of which are targeted directly or indirectly by lithium; and additionally because of its antioxidant capabilities, ebselen seems to be an excellent candidate drug for the treatment of bipolar disorder.

Psychiatric illness represents 37% of the total population disease burden (Hughes, 2009; Lopez, 2006), yet there is a paucity of drugs treating psychiatric illnesses, with novel mechanisms of action in the market at present (Hughes, 2009). All the drugs used in the treatment of schizophrenia or depression (or even anticonvulsants) are modifications of parent molecules that were discovered, mostly serendipitously, around the 1970s (Tohen, 2008). Target-based discovery is still a

relatively new concept in drug discovery since most drugs were discovered without any prior information of their targets, including lithium (Ayd, 1991). The focus of drug discovery in the last three decades has shifted to the development of specific and selective inhibitors of a known target (Swinney and Anthony, 2011). Additionally, a new focus of biological research has been genetics: creating knock-out and knock-in mice to unravel the mechanisms of disease pathology and to prove the importance of a selected target. This has not proven to be fruitful, since in a number of cases, the target of the therapeutic agent, may be completely unrelated to the disease itself. Even in diseases where the pathological target has been established unequivocally, such as for cystic fibrosis, no drugs are yet available to treat the disease.

What we have now is a huge chasm because we know that most drugs don't act selectively, and that knocking out a single gene in a mouse, will hardly ever produce a disease state. Additionally, with regards to a CNS disorder establishing the disease state in mice is incredibly difficult, since the animals do not have the ability to convey to us that they are depressed, or that they are feeling manic.

Rodent models of psychiatric disorders are as challenging as they were a few decades ago. We are also greatly constrained by our limited understanding of the neurobiology of most psychiatric disorders. Genetic technology has provided a wide selection of mutant mice strains, but their phenotyping and relation to disease pathology leaves much to be desired (Wotjak, 2004).

Eglumegad, a metabotropic glutamate receptor agonist developed by Eli Lilly, the recently proposed new anti-psychotic with a novel mechanism of action. Eglumegad had shown all the appropriate results in the standard animal models of psychosis and anxiety. Clinical trials, however, showed that eglumegad was no better than placebo (Patil *et al.*, 2007). But can the converse also be true? Drugs that

disappoint in animal models might have efficacy in humans. And, if the effects of lithium were discovered today, instead of six decades ago by John Cade, would it be approved by the regulatory authorities?

Animal models can be useful for some disease conditions. They may also be useful for predicting toxicity. But in case of psychiatric disorders, they are not reliable indicators of efficacy. Conn and Roth conducted a study of about 500 compounds, classified as antidepressant, antipsychotic or anxiolytic, in 2008 (Conn and Roth, 2008). In this, they reviewed whether the preclinical models were efficient in predicting the clinical outcomes. Essentially, they found that preclinical models were good at predicting some adverse effects, such as extrapyramidal symptoms, and were therefore useful in differentiating between typical and atypical antipsychotics. However, for predicting overall efficacy, or efficacy compared to the conventional treatment, preclinical models were of limited use.

More often than not, clinical trials initially reveal a drug-related effect, and this is subsequently investigated in animal models to elucidate the underlying cause of that effect. For example, ketamine has recently been shown to have antidepressant properties (Berman *et al.*, 2000); however, this was initially observed in the clinic setting, and subsequently found to be valid in preclinical antidepressant tests. Clozapine, an atypical antipsychotic, did not show extrapyramidal symptoms in preclinical models, so was initially rejected as an anti-psychotic. In a later reinvestigation, it was found to be clinically useful in the treatment of psychotic symptoms of schizophrenia — without producing the adverse effects associated with typical antipsychotics such as haloperidol. Two novel antidepressants, agomelatine and mifepristone, do not show antidepressant activity in the various standard behavioural tests for antidepressants (Conn and Roth, 2008). However, these have

shown clinical efficacy in the treatment of depression; aglomelatine was especially useful in the treatment of severe depression (San and Arranz, 2008). Lithium is better known for its ability to treat mania than depression, but it has been found to be beneficial in the treatment of resistant depression that is not responsive to traditional antidepressants (Bauer and Dopfmer, 1999). It is probable that all these drugs have mechanism of actions in the treatment of depression that are different to those of traditional antidepressants. Hence, testing these in traditional models may not always lead to positive phenotypic effects. By the same analysis, should ebselen be excluded from clinically testing as a novel mood stabiliser because it did not exhibit all the effects of lithium in preclinical models?

It is possible, based on the results presented here, that ebselen might prove effective in the treatment of mania or even as a novel anti-psychotic. Additionally, although we know that lithium inhibits IMPase and a number of other targets *in vitro,* there is insufficient information to establish the mechanisms by which it produces its effects *in vivo*. However, is it possible to conclude, based on all that has been demonstrated, that ebselen will (or will not) be better than lithium clinically? This can only be answered by clinical testing.

Progressing ebselen into clinical trials for bipolar disorder is a formidable challenge. The most important attribute of ebselen is that it has already been used in clinical trials, and has been found to be safe under the conditions tested. Additionally, ebselen is cell-permeable and has the ability to cross the blood–brain barrier — a major impediment in CNS drug discovery (Pardridge, 2005). Finally, ebselen targets multiple systems that are known to play roles in bipolar disorder.

Only once ebselen is tested in clinical trials in bipolar patients will its true therapeutic impact be known. Ebselen hits many targets and this is a problem for it as

a small molecule tool, but not as a drug. In their study, Conn and Roth found that drugs that hit multiple receptors were more effective in treating schizophrenia and related disorders compared to drugs that were selective (single targets) (Conn and Roth, 2008).

So all along, maybe condemning lithium as a 'bad drug' because of its polypharmacology is the wrong way of looking at it. Perhaps lithium is the 'perfect drug'—, for precisely the same reasons.

Bibliography

Agam, G., Bersudsky, Y., Berry, G.T., Moechars, D., Lavi-Avnon, Y., and Belmaker, R.H. (2009). Knockout mice in understanding the mechanism of action of lithium. Biochem Soc Trans *37*, 1121-1125.

Ahluwalia, P., and Singhal, R.L. (1980). Effect of low-dose lithium administration and subsequent withdrawal on biogenic amines in rat brain. Br J Pharmacol *71*, 601-607.

Allison, J.H., Blisner, M.E., Holland, W.H., Hipps, P.P., and Sherman, W.R. (1976). Increased brain myo-inositol 1-phosphate in lithium-treated rats. Biochem Biophys Res Commun *71*, 664-670.

Allison, J.H., and Stewart, M.A. (1971). Reduced brain inositol in lithium-treated rats. Nat New Biol *233*, 267-268.

American Psychiatric Association (2000). Diagnostic and statistical manual of mental health disorders, Fourth Edition, Text Revision (Washington DC).

Apparsundaram, S., Schroeter, S., Giovanetti, E., and Blakely, R.D. (1998). Acute regulation of norepinephrine transport: II. PKC-modulated surface expression of human norepinephrine transporter proteins. J Pharmacol Exp Ther *287*, 744-751.

Arai, R., Ito, K., Ohnishi, T., Ohba, H., Akasaka, R., Bessho, Y., Hanawa-Suetsugu, K., Yoshikawa, T., Shirouzu, M., and Yokoyama, S. (2007). Crystal structure of human myo-inositol monophosphatase 2, the product of the putative susceptibility gene for bipolar disorder, schizophrenia, and febrile seizures. Proteins *67*, 732-742.

Ashburn, T.T., and Thor, K.B. (2004). Drug repositioning: identifying and developing new uses for existing drugs. Nat Rev Drug Discov *3*, 673-683.

Atack, J.R. (1996). Inositol monophosphatase, the putative therapeutic target for lithium. Brain Res Brain Res Rev *22*, 183-190.

Atack, J.R. (1997). Inositol monophosphatase inhibitors--lithium mimetics? Med Res Rev *17*, 215-224.

Atack, J.R., Cook, S.M., Watt, A.P., Fletcher, S.R., and Ragan, C.I. (1993a). In vitro and in vivo inhibition of inositol monophosphatase by the bisphosphonate L-690,330. J Neurochem *60*, 652-658.

Atack, J.R., Cook, S.M., Watt, A.P., and Ragan, C.I. (1992). Measurement of lithium-induced changes in mouse inositol(1)phosphate levels in vivo. J Neurochem *59*, 1946-1954.

Atack, J.R., Prior, A.M., Fletcher, S.R., Quirk, K., McKernan, R., and Ragan, C.I. (1994). Effects of L-690,488, a prodrug of the bisphosphonate inositol

monophosphatase inhibitor L-690,330, on phosphatidylinositol cycle markers. J Pharmacol Exp Ther *270*, 70-76.

Atack, J.R., Prior, A.M., Griffith, D., and Ragan, C.I. (1993b). Characterization of the Effects of Lithium on Phosphatidylinositol (Pi) Cycle Activity in Human Muscarinic M1 Receptor-Transfected Cho Cells. Br J Pharmacol *110*, 809-815.

Ayd, F.J., Jr. (1991). Invited ACNP Lecture. The early history of modern psychopharmacology. Neuropsychopharmacology *5*, 71-84.

Azevedo, C., and Saiardi, A. (2006). Extraction and analysis of soluble inositol polyphosphates from yeast. Nat Protoc *1*, 2416-2422.

Babic, T. (1999). The cholinergic hypothesis of Alzheimer's disease: a review of progress. J Neurol Neurosurg Psychiatry *67*, 558.

Bakchine, S., Lacomblez, L., Benoit, N., Parisot, D., Chain, F., and Lhermitte, F. (1989). Manic-like state after bilateral orbitofrontal and right temporoparietal injury: efficacy of clonidine. Neurology *39*, 777-781.

Ballenger, J.C., and Post, R.M. (1984). Neurobiology of mood disorders (Baltimore, Williams & Wilkins).

Barkai, A.I. (1981). Myo-inositol turnover in the intact rat brain: increased production after d-amphetamine. J Neurochem *36*, 1485-1491.

Barone, P., Morelli, M., Cicarelli, G., Cozzolino, A., DeJoanna, G., Campanella, G., and DiChiara, G. (1993). Expression of c-fos protein in the experimental epilepsy induced by pilocarpine. Synapse *14*, 1-9.

Barrett, T.B., Hauger, R.L., Kennedy, J.L., Sadovnick, A.D., Remick, R.A., Keck, P.E., McElroy, S.L., Alexander, M., Shaw, S.H., and Kelsoe, J.R. (2003). Evidence that a single nucleotide polymorphism in the promoter of the G protein receptor kinase 3 gene is associated with bipolar disorder. Mol Psychiatry *8*, 546-557.

Batty, I., and Nahorski, S.R. (1985). Differential effects of lithium on muscarinic receptor stimulation of inositol phosphates in rat cerebral cortex slices. J Neurochem *45*, 1514-1521.

Battye, T.G., Kontogiannis, L., Johnson, O., Powell, H.R., and Leslie, A.G. (2011). iMOSFLM: a new graphical interface for diffraction-image processing with MOSFLM. Acta Crystallogr D Biol Crystallogr *67*, 271-281.

Bauer, M., and Dopfmer, S. (1999). Lithium augmentation in treatment-resistant depression: meta-analysis of placebo-controlled studies. J Clin Psychopharmacol *19*, 427-434.

Baum, A.E., Akula, N., Cabanero, M., Cardona, I., Corona, W., Klemens, B., Schulze, T.G., Cichon, S., Rietschel, M., Nothen, M.M.*, et al.* (2008). A genome-

wide association study implicates diacylglycerol kinase eta (DGKH) and several other genes in the etiology of bipolar disorder. Mol Psychiatry *13*, 197-207.

Bebchuk, J.M., Arfken, C.L., Dolan-Manji, S., Murphy, J., Hasanat, K., and Manji, H.K. (2000). A preliminary investigation of a protein kinase C inhibitor in the treatment of acute mania. Arch Gen Psychiatry *57*, 95-97.

Bellivier, F., Leboyer, M., Courtet, P., Buresi, C., Beaufils, B., Samolyk, D., Allilaire, J.F., Feingold, J., Mallet, J., and Malafosse, A. (1998). Association between the tryptophan hydroxylase gene and manic-depressive illness. Arch Gen Psychiatry *55*, 33-37.

Belmaker, R.H., and Bersudsky, Y. (2007). Lithium-pilocarpine seizures as a model for lithium action in mania. Neurosci Biobehav Rev *31*, 843-849.

Benes, F.M., Matzilevich, D., Burke, R.E., and Walsh, J. (2006). The expression of proapoptosis genes is increased in bipolar disorder, but not in schizophrenia. Mol Psychiatry *11*, 241-251.

Benes, F.M., Walsh, J., Bhattacharyya, S., Sheth, A., and Berretta, S. (2003). DNA fragmentation decreased in schizophrenia but not bipolar disorder. Arch Gen Psychiatry *60*, 359-364.

Berk, M., Copolov, D.L., Dean, O., Lu, K., Jeavons, S., Schapkaitz, I., Anderson-Hunt, M., and Bush, A.I. (2008). N-acetyl cysteine for depressive symptoms in bipolar disorder--a double-blind randomized placebo-controlled trial. Biol Psychiatry *64*, 468-475.

Berman, R.M., Cappiello, A., Anand, A., Oren, D.A., Heninger, G.R., Charney, D.S., and Krystal, J.H. (2000). Antidepressant effects of ketamine in depressed patients. Biol Psychiatry *47*, 351-354.

Berridge, M.J., Downes, C.P., and Hanley, M.R. (1982). Lithium amplifies agonist-dependent phosphatidylinositol responses in brain and salivary glands. Biochem J *206*, 587-595.

Berridge, M.J., Downes, C.P., and Hanley, M.R. (1989). Neural and developmental actions of lithium: a unifying hypothesis. Cell *59*, 411-419.

Bertelsen, A., Harvald, B., and Hauge, M. (1977). A Danish twin study of manic-depressive disorders. Br J Psychiatry *130*, 330-351.

Bitran, J.A., Manji, H.K., Potter, W.Z., and Gusovsky, F. (1995). Down-regulation of PKC alpha by lithium in vitro. Psychopharmacol Bull *31*, 449-452.

Blackwell, J.R., and Horgan, R. (1991). A novel strategy for production of a highly expressed recombinant protein in an active form. FEBS Lett *295*, 10-12.

Blakely, R.D., Ramamoorthy, S., Schroeter, S., Qian, Y., Apparsundaram, S., Galli, A., and DeFelice, L.J. (1998). Regulated phosphorylation and trafficking of antidepressant-sensitive serotonin transporter proteins. Biol Psychiatry *44*, 169-178.

Blanchet, P.J., Fang, J., Gillespie, M., Sabounjian, L., Locke, K.W., Gammans, R., Mouradian, M.M., and Chase, T.N. (1998). Effects of the full dopamine D1 receptor agonist dihydrexidine in Parkinson's disease. Clin Neuropharmacol *21*, 339-343.

Bodick, N.C., Offen, W.W., Levey, A.I., Cutler, N.R., Gauthier, S.G., Satlin, A., Shannon, H.E., Tollefson, G.D., Rasmussen, K., Bymaster, F.P.*, et al.* (1997). Effects of xanomeline, a selective muscarinic receptor agonist, on cognitive function and behavioral symptoms in Alzheimer disease. Arch Neurol *54*, 465-473.

Bond, P.A. (1972). The determination of 4-hydroxy-3-methoxyphenylethylene glycol in urine and CSF using gas chromatography. Biochem Med *6*, 36-45.

Bone, R., Frank, L., Springer, J.P., Pollack, S.J., Osborne, S.A., Atack, J.R., Knowles, M.R., McAllister, G., Ragan, C.I., Broughton, H.B.*, et al.* (1994). Structural analysis of inositol monophosphatase complexes with substrates. Biochemistry *33*, 9460-9467.

Bone, R., Springer, J.P., and Atack, J.R. (1992). Structure of inositol monophosphatase, the putative target of lithium therapy. Proc Natl Acad Sci U S A *89*, 10031-10035.

Borsini, F., and Meli, A. (1988). Is the forced swimming test a suitable model for revealing antidepressant activity? Psychopharmacology (Berl) *94*, 147-160.

Brown, E., Kendall, D.A., and Nahorski, S.R. (1984). Inositol phospholipid hydrolysis in rat cerebral cortical slices: I. Receptor characterisation. J Neurochem *42*, 1379-1387.

Bunney, W.E. (1978). Psychopharmacology of the switch process in affective illness (New York, Raven Press.).

Bunney, W.E., and Garland-Bunney, B.L. (1987). Mechanisms of action of lithium in affective illness: Basic and clinical implications. In Psychopharmacology: The Third Generation of Progress, H.Y. Meltzer, ed. (New York, Raven Press.), pp. 553-565.

Bunney, W.E., Jr., and Davis, J.M. (1965). Norepinephrine in depressive reactions. A review. Arch Gen Psychiatry *13*, 483-494.

Buttner, N., Bhattacharyya, S., Walsh, J., and Benes, F.M. (2007). DNA fragmentation is increased in non-GABAergic neurons in bipolar disorder but not in schizophrenia. Schizophr Res *93*, 33-41.

Cade, J.F. (1949). Lithium salts in the treatment of psychotic excitement. Med J Aust *2*, 349-352.

Calabrese, J.R., Bowden, C.L., Sachs, G., Yatham, L.N., Behnke, K., Mehtonen, O.P., Montgomery, P., Ascher, J., Paska, W., Earl, N.*, et al.* (2003). A placebo-controlled

18-month trial of lamotrigine and lithium maintenance treatment in recently depressed patients with bipolar I disorder. J Clin Psychiatry *64*, 1013-1024.

Can, A., Blackwell, R.A., Piantadosi, S.C., Dao, D.T., O'Donnell, K.C., and Gould, T.D. (2011). Antidepressant-like responses to lithium in genetically diverse mouse strains. Genes Brain Behav *10*, 434-443.

Cavalla, D. (2009). APT drug R&D: the right active ingredient in the right presentation for the right therapeutic use. Nat Rev Drug Discov *8*, 849-853.

Chen, G., Masana, M.I., and Manji, H.K. (2000). Lithium regulates PKC-mediated intracellular cross-talk and gene expression in the CNS in vivo. Bipolar Disord *2*, 217-236.

Chen, G., Yuan, P.X., Jiang, Y.M., Huang, L.D., and Manji, H.K. (1998). Lithium increases tyrosine hydroxylase levels both in vivo and in vitro. J Neurochem *70*, 1768-1771.

Chen, L., and Roberts, M.F. (1998). Cloning and expression of the inositol monophosphatase gene from Methanococcus jannaschii and characterization of the enzyme. Appl Environ Microbiol *64*, 2609-2615.

Cipriani, A., Pretty, H., Hawton, K., and Geddes, J.R. (2005). Lithium in the prevention of suicidal behavior and all-cause mortality in patients with mood disorders: a systematic review of randomized trials. Am J Psychiatry *162*, 1805-1819.

Cisbio (2009). IP-One ELISA.

Conn, P.J., and Roth, B.L. (2008). Opportunities and challenges of psychiatric drug discovery: roles for scientists in academic, industry, and government settings. Neuropsychopharmacology *33*, 2048-2060.

Connolly, T.M., Lawing, W.J., Jr., and Majerus, P.W. (1986). Protein kinase C phosphorylates human platelet inositol trisphosphate 5'-phosphomonoesterase, increasing the phosphatase activity. Cell *46*, 951-958.

Copeland, R.A. (2005). Evaluation of Enzyme Inhibitors in Drug Discovery (John Wiley and Sons).

Coppen, A., Standish-Barry, H., Bailey, J., Houston, G., Silcocks, P., and Hermon, C. (1991). Does lithium reduce the mortality of recurrent mood disorders? J Affect Disord *23*, 1-7.

Cotgreave, I.A., Duddy, S.K., Kass, G.E., Thompson, D., and Moldeus, P. (1989). Studies on the anti-inflammatory activity of ebselen. Ebselen interferes with granulocyte oxidative burst by dual inhibition of NADPH oxidase and protein kinase C? Biochem Pharmacol *38*, 649-656.

Coxhead, N., Silverstone, T., and Cookson, J. (1992). Carbamazepine versus lithium in the prophylaxis of bipolar affective disorder. Acta Psychiatr Scand *85*, 114-118.

Cryan, J.F., Markou, A., and Lucki, I. (2002). Assessing antidepressant activity in rodents: recent developments and future needs. Trends Pharmacol Sci *23*, 238-245.

Cryan, J.F., Page, M.E., and Lucki, I. (2005). Differential behavioral effects of the antidepressants reboxetine, fluoxetine, and moclobemide in a modified forced swim test following chronic treatment. Psychopharmacology (Berl) *182*, 335-344.

Cryan, J.F., and Slattery, D.A. (2007). Animal models of mood disorders: Recent developments. Curr Opin Psychiatry *20*, 1-7.

Cryns, K., Shamir, A., Shapiro, J., Daneels, G., Goris, I., Van Craenendonck, H., Straetemans, R., Belmaker, R.H., Agam, G., Moechars, D.*, et al.* (2007). Lack of lithium-like behavioral and molecular effects in IMPA2 knockout mice. Neuropsychopharmacology *32*, 881-891.

Cryns, K., Shamir, A., Van Acker, N., Levi, I., Daneels, G., Goris, I., Bouwknecht, J.A., Andries, L., Kass, S., Agam, G.*, et al.* (2008). IMPA1 is essential for embryonic development and lithium-like pilocarpine sensitivity. Neuropsychopharmacology *33*, 674-684.

David, D.J., Renard, C.E., Jolliet, P., Hascoet, M., and Bourin, M. (2003). Antidepressant-like effects in various mice strains in the forced swimming test. Psychopharmacology (Berl) *166*, 373-382.

Diacicov, S., and Tudorache, B. (1990). [Clonidine treatment in manic episodes]. Rev Med Interna Neurol Psihiatr Neurochir Dermatovenerol Neurol Psihiatr Neurochir *35*, 29-32.

Diehl, R.E., Whiting, P., Potter, J., Gee, N., Ragan, C.I., Linemeyer, D., Schoepfer, R., Bennett, C., and Dixon, R.A. (1990). Cloning and expression of bovine brain inositol monophosphatase. J Biol Chem *265*, 5946-5949.

Dixon, J.F., Lee, C.H., Los, G.V., and Hokin, L.E. (1992). Lithium enhances accumulation of [3H]inositol radioactivity and mass of second messenger inositol 1,4,5-trisphosphate in monkey cerebral cortex slices. J Neurochem *59*, 2332-2335.

Drummond, A.H., Joels, L.A., and Hughes, P.J. (1987). The interaction of lithium ions with inositol lipid signalling systems. Biochem Soc Trans *15*, 32-35.

Einat, H., Yuan, P., Szabo, S.T., Dogra, S., and Manji, H.K. (2007). Protein kinase C inhibition by tamoxifen antagonizes manic-like behavior in rats: implications for the development of novel therapeutics for bipolar disorder. Neuropsychobiology *55*, 123-131.

Ellis, J., and Lenox, R.H. (1990). Chronic lithium treatment prevents atropine-induced supersensitivity of the muscarinic phosphoinositide response in rat hippocampus. Biol Psychiatry *28*, 609-619.

Emsley, P., Lohkamp, B., Scott, W.G., and Cowtan, K. (2010). Features and development of Coot. Acta Crystallogr D Biol Crystallogr *66*, 486-501.

Esterling, L.E., Cox Matise, T., Sanders, A.R., Yoshikawa, T., Overhauser, J., Gershon, E.S., Moskowitz, M.T., and Detera-Wadleigh, S.D. (1997). An integrated physical map of 18p11.2: a susceptibility region for bipolar disorder. Mol Psychiatry *2*, 501-504.

Evans, P. (2006). Scaling and assessment of data quality. Acta Crystallogr D Biol Crystallogr *62*, 72-82.

Fain, J.N., and Berridge, M.J. (1979). Relationship between phosphatidylinositol synthesis and recovery of 5-hydroxytryptamine-responsive Ca2+ flux in blowfly salivary glands. Biochem J *180*, 655-661.

Faraci, W.S., Zorn, S.H., Bakker, A.V., Jackson, E., and Pratt, K. (1993). Beryllium competitively inhibits brain myo-inositol monophosphatase, but unlike lithium does not enhance agonist-induced inositol phosphate accumulation. Biochem J *291 (Pt 2)*, 369-374.

Franklin, K.B.J., and Paxinos, G. (2008). The mouse brain in stereotaxic coordinates, 3rd compact edn (New York, N.Y., London : Elsevier/Academic Press).

Frey, B.N., Andreazza, A.C., Kunz, M., Gomes, F.A., Quevedo, J., Salvador, M., Goncalves, C.A., and Kapczinski, F. (2007). Increased oxidative stress and DNA damage in bipolar disorder: a twin-case report. Prog Neuropsychopharmacol Biol Psychiatry *31*, 283-285.

Gee, N.S., Ragan, C.I., Watling, K.J., Aspley, S., Jackson, R.G., Reid, G.G., Gani, D., and Shute, J.K. (1988). The purification and properties of myo-inositol monophosphatase from bovine brain. Biochem J *249*, 883-889.

George, M.S., Molnar, C.E., Grenesko, E.L., Anderson, B., Mu, Q., Johnson, K., Nahas, Z., Knable, M., Fernandes, P., Juncos, J.*, et al.* (2007). A single 20 mg dose of dihydrexidine (DAR-0100), a full dopamine D1 agonist, is safe and tolerated in patients with schizophrenia. Schizophr Res *93*, 42-50.

Gerner, R.H., Post, R.M., and Bunney, W.E., Jr. (1976). A dopaminergic mechanism in mania. Am J Psychiatry *133*, 1177-1180.

Gershon, E.S. (1982). Genetic studies of affective disorders and schizophrenia. Prog Clin Biol Res *103 Pt A*, 417-432.

Gershon, E.S., Goldin, L.R., Guroff, J.J., and Hamovit, J.R. (1989). Description of the National Institute of Mental Health family study of affective disorders. Genet Epidemiol *6*, 183-185.

Gilbert, J., Henske, P., and Singh, A. (2003). Rebuilding Big Pharma's Business Model. In In Vivo The Business and Medicine Report (Windhoven Information Inc.).

Gill, R., Mohammed, F., Badyal, R., Coates, L., Erskine, P., Thompson, D., Cooper, J., Gore, M., and Wood, S. (2005). High-resolution structure of myo-inositol

monophosphatase, the putative target of lithium therapy. Acta Crystallogr D Biol Crystallogr *61*, 545-555.

Gillaspy, G.E., Keddie, J.S., Oda, K., and Gruissem, W. (1995). Plant inositol monophosphatase is a lithium-sensitive enzyme encoded by a multigene family. Plant Cell *7*, 2175-2185.

Gleick, J. (1988). Chaos : making a new science (London, Heinemann).
Goodwin, F.K., Fireman, B., Simon, G.E., Hunkeler, E.M., Lee, J., and Revicki, D. (2003). Suicide risk in bipolar disorder during treatment with lithium and divalproex. Jama *290*, 1467-1473.

Goodwin, F.K., Jamison, K.R., and Ghaemi, S.N. (2007). Manic-depressive illness : bipolar disorders and recurrent depression, 2nd edn (New York ; Oxford, Oxford University Press).

Goodwin, F.K., Murphy, D.L., Brodie, H.K., and Bunney, W.E., Jr. (1970). L-DOPA, catecholamines, and behavior: a clinical and biochemical study in depressed patients. Biol Psychiatry *2*, 341-366.

Goodwin, G.M., DeSouza, R.J., Wood, A.J., and Green, A.R. (1986). Lithium decreases 5-HT1A and 5-HT2 receptor and alpha 2-adrenoceptor mediated function in mice. Psychopharmacology (Berl) *90*, 482-487.

Goodwin, G.M., and Geddes, J.R. (2003). Latest maintenance data on lithium in bipolar disorder. Eur Neuropsychopharmacol *13 Suppl 2*, S51-55.

Gottesman, II, and Gould, T.D. (2003). The endophenotype concept in psychiatry: etymology and strategic intentions. Am J Psychiatry *160*, 636-645.

Gottesman, II, and Shields, J. (1973). Genetic theorizing and schizophrenia. Br J Psychiatry *122*, 15-30.

Gould, T.D., Einat, H., Bhat, R., and Manji, H.K. (2004a). AR-A014418, a selective GSK-3 inhibitor, produces antidepressant-like effects in the forced swim test. Int J Neuropsychopharmacol *7*, 387-390.

Gould, T.D., Einat, H., O'Donnell, K.C., Picchini, A.M., Schloesser, R.J., and Manji, H.K. (2007a). Beta-catenin overexpression in the mouse brain phenocopies lithium-sensitive behaviors. Neuropsychopharmacology *32*, 2173-2183.

Gould, T.D., and Manji, H.K. (2002). The Wnt signaling pathway in bipolar disorder. Neuroscientist *8*, 497-511.

Gould, T.D., and Manji, H.K. (2005). Glycogen synthase kinase-3: a putative molecular target for lithium mimetic drugs. Neuropsychopharmacology *30*, 1223-1237.

Gould, T.D., O'Donnell, K.C., Picchini, A.M., and Manji, H.K. (2007b). Strain differences in lithium attenuation of d-amphetamine-induced hyperlocomotion: a

mouse model for the genetics of clinical response to lithium. Neuropsychopharmacology *32*, 1321-1333.

Gould, T.D., Picchini, A.M., O'Donnell, K.C., Schloesser, R.J., and Manji, H.K. (2005). Mouse strain differences in single dose lithium attenuation of amphetamine hyperactivity. Neuropsychopharmacology *30*, S172-S172.

Gould, T.D., Zarate, C.A., and Manji, H.K. (2004b). Glycogen synthase kinase-3: a target for novel bipolar disorder treatments. J Clin Psychiatry *65*, 10-21.

Greasley, P.J., Gore, M.G., Ragan, C.I., Knowles, M.R., Gee, N.S., and McAllister, G. (1992). Bovine inositol monophosphatase; observation of the modification of a cysteine residue using protein fluorescence. Biochem Soc Trans *20*, 290S.

Greenspan, K., Schildkraut, J.J., Gordon, E.K., Baer, L., Aronoff, M.S., and Durell, J. (1970). Catecholamine metabolism in affective disorders. 3. MHPG and other catecholamine metabolites in patients treated with lithium carbonate. J Psychiatr Res *7*, 171-183.

Grossman, F., and Potter, W.Z. (1999). Catecholamines in depression: a cumulative study of urinary norepinephrine and its major metabolites in unipolar and bipolar depressed patients versus healthy volunteers at the NIMH. Psychiatry Res *87*, 21-27.

Grossman, F., Potter, W.Z., Brown, E.A., and Maislin, G. (1999). A double-blind study comparing idazoxan and bupropion in bipolar depressed patients. J Affect Disord *56*, 237-243.

Hall, C.S. (1936). Emotional behavior in the rat. III. The relationship between emotionality and ambulatory activity. Journal of Comparative Psychology *22*, 345-352.

Hallcher, L.M., and Sherman, W.R. (1980). The effects of lithium ion and other agents on the activity of myo-inositol-1-phosphatase from bovine brain. J Biol Chem *255*, 10896-10901.

Hansen, H.H., Sanchez, C., and Meier, E. (1997). Neonatal administration of the selective serotonin reuptake inhibitor Lu 10-134-C increases forced swimming-induced immobility in adult rats: A putative animal model of depression? Journal of Pharmacology and Experimental Therapeutics *283*, 1333-1341.

Harwood, A.J. (2005). Lithium and bipolar mood disorder: the inositol-depletion hypothesis revisited. Mol Psychiatry *10*, 117-126.

Hasler, G., Drevets, W.C., Gould, T.D., Gottesman, II, and Manji, H.K. (2006). Toward constructing an endophenotype strategy for bipolar disorders. Biol Psychiatry *60*, 93-105.

Hauser, G. (1969). Myo-inositol transport in slices of rat kidney cortex. I. Effect of incubation conditions and inhibitors. Biochim Biophys Acta *173*, 257-266.

Hayes, J., Prah, P., Nazareth, I., King, M., Walters, K., Petersen, I., and Osborn, D. (2011). Prescribing trends in bipolar disorder: cohort study in the United Kingdom THIN primary care database 1995-2009. PLoS One *6*, e28725.

Hayes, P.E., and Schulz, S.C. (1987). Beta-blockers in anxiety disorders. J Affect Disord *13*, 119-130.

Hesketh, J.E., Glen, A.I., and Reading, H.W. (1977). Membrane ATPase activities in depressive illness. J Neurochem *28*, 1401-1402.

Ho, A.K., Loh, H.H., Craves, F., Hitzemann, R.J., and Gershon, S. (1970). The effect of prolonged lithium treatment on the synthesis rate and turnover of monoamines in brain regions of rats. Eur J Pharmacol *10*, 72-78.

Honchar, M.P., Olney, J.W., and Sherman, W.R. (1983). Systemic cholinergic agents induce seizures and brain damage in lithium-treated rats. Science *220*, 323-325.

Hopkins, A.L., and Groom, C.R. (2002). The druggable genome. Nat Rev Drug Discov *1*, 727-730.

Hughes, B. (2009). Novel consortium to address shortfall in innovative medicines for psychiatric disorders. Nat Rev Drug Discov *8*, 523-524.

Hughes, J.H., Dunne, F., and Young, A.H. (2000). Effects of acute tryptophan depletion on mood and suicidal ideation in bipolar patients symptomatically stable on lithium. Br J Psychiatry *177*, 447-451.

Inhorn, R.C., and Majerus, P.W. (1987). Inositol polyphosphate 1-phosphatase from calf brain. Purification and inhibition by Li+, Ca2+, and Mn2+. J Biol Chem *262*, 15946-15952.

Irvine, R.F., and Schell, M.J. (2001). Back in the water: the return of the inositol phosphates. Nat Rev Mol Cell Biol *2*, 327-338.

Irwin, J., and Shoichet, B. (2005). ZINC - A free database of commercially available compounds for virtual screening. J Chem Inf Model *45*, 177-182.

Itaya, K., and Ui, M. (1966). A new micromethod for the colorimetric determination of inorganic phosphate. Clin Chim Acta *14*, 361-366.

Jackson, S.W. (1986). Melancholia and depression : from Hippocratic times to modern times (New Haven ; London, Yale University Press).

Janowsky, D.S., el-Yousef, M.K., Davis, J.M., and Sekerke, H.J. (1972). A cholinergic-adrenergic hypothesis of mania and depression. Lancet *2*, 632-635.

Janowsky, D.S., and Risch, S.C. (1984). Cholinomimetic and Anticholinergic Drugs Used To Investigate an Acetylcholine Hypothesis of Affective Disorders and Stress. Drug Development Research *4*, 125-142.

Jenkinson, S., Nahorski, S.R., and Challiss, R.A. (1994). Disruption by lithium of phosphatidylinositol-4,5-bisphosphate supply and inositol-1,4,5-trisphosphate generation in Chinese hamster ovary cells expressing human recombinant m1 muscarinic receptors. Mol Pharmacol *46*, 1138-1148.

Johnson, F.N. (1972). Dissociation of vertical and horizontal components of activity in rats treated with lithium chloride. Experientia *28*, 533-535.

Johnson, F.N., and Wormington, S. (1972). Effect of lithium on rearing activity in rats. Nat New Biol *235*, 159-160.

Jope, R. (1979). Effects of lithium treatment in vitro and in vivo on acetylcholine metabolism in rat brain. J Neurochem *33*, 487-495.

Jope, R.S., Morrisett, R.A., and Snead, O.C. (1986). Characterization of lithium potentiation of pilocarpine-induced status epilepticus in rats. Exp Neurol *91*, 471-480.

Joyce, P.R., Fergusson, D.M., Woollard, G., Abbott, R.M., Horwood, L.J., and Upton, J. (1995). Urinary Catecholamines and Plasma Hormones Predict Mood State in Rapid-Cycling Bipolar Affective-Disorder. J Affect Disord *33*, 233-243.

Kato, T., Kubota, M., and Kasahara, T. (2007). Animal models of bipolar disorder. Neurosci Biobehav Rev *31*, 832-842.

Kato, T., Takahashi, S., and Inubushi, T. (1992). Brain lithium concentration by 7Li- and 1H-magnetic resonance spectroscopy in bipolar disorder. Psychiatry Res *45*, 53-63.

Kessler, R.C., Berglund, P., Demler, O., Jin, R., Merikangas, K.R., and Walters, E.E. (2005). Lifetime prevalence and age-of-onset distributions of DSM-IV disorders in the National Comorbidity Survey Replication. Arch Gen Psychiatry *62*, 593-602.

Kil, J., Pierce, C., Tran, H., Gu, R., and Lynch, E.D. (2007). Ebselen treatment reduces noise induced hearing loss via the mimicry and induction of glutathione peroxidase. Hear Res *226*, 44-51.

Kirshenbaum, G.S., Clapcote, S.J., Duffy, S., Burgess, C.R., Petersen, J., Jarowek, K.J., Yucel, Y.H., Cortez, M.A., Snead, O.C., 3rd, Vilsen, B.*, et al.* (2011). Mania-like behavior induced by genetic dysfunction of the neuron-specific Na+,K+-ATPase alpha3 sodium pump. Proc Natl Acad Sci U S A *108*, 18144-18149.

Klein, P.S., and Melton, D.A. (1996). A molecular mechanism for the effect of lithium on development. Proc Natl Acad Sci U S A *93*, 8455-8459.

Knapp, S., and Mandell, A.J. (1973). Short- and long-term lithium administration: effects on the brain's serotonergic biosynthetic systems. Science *180*, 645-647.

Knowles, M.R., Gee, N., McAllister, G., Ragan, C.I., Greasley, P.J., and Gore, M.G. (1992). Bovine inositol monophosphatase. Modification, identification and mutagenesis of reactive cysteine residues. Biochem J *285 (Pt 2)*, 461-468.

Kofman, O., and Belmaker, R.H. (1990). Intracerebroventricular myo-inositol antagonizes lithium-induced suppression of rearing behaviour in rats. Brain Res *534*, 345-347.

Kofman, O., Belmaker, R.H., Grisaru, N., Alpert, C., Fuchs, I., Katz, V., and Rigler, O. (1991). Myo-inositol attenuates two specific behavioral effects of acute lithium in rats. Psychopharmacol Bull *27*, 185-190.

Kraepelin, E., and Robertson, G.M. (1921). Manic-depressive insanity and paranoia (Edinburgh, E. & S. Livingstone).

Kusumakar, V., and Yatham, L.N. (1997). Lamotrigine treatment of rapid cycling bipolar disorder. Am J Psychiatry *154*, 1171-1172.

Leech, A.P., Baker, G.R., Shute, J.K., Cohen, M.A., and Gani, D. (1993). Chemical and kinetic mechanism of the inositol monophosphatase reaction and its inhibition by Li+. Eur J Biochem *212*, 693-704.

Lenox, R.H., Gould, T.D., and Manji, H.K. (2002). Endophenotypes in bipolar disorder. Am J Med Genet *114*, 391-406.

Linnoila, M., Karoum, F., and Potter, W.Z. (1983). Effects of antidepressant treatments on dopamine turnover in depressed patients. Arch Gen Psychiatry *40*, 1015-1017.

Linnoila, M., Miller, T.L., Bartko, J., and Potter, W.Z. (1984). Five antidepressant treatments in depressed patients. Effects on urinary serotonin and 5-hydroxyindoleacetic acid output. Arch Gen Psychiatry *41*, 688-692.

Livingstone, C., and Rampes, H. (2006). Lithium: a review of its metabolic adverse effects. J Psychopharmacol *20*, 347-355.

Lopez, A.D. (2006). Global burden of disease and risk factors (New York, NY Washington, DC, Oxford University Press ;
World Bank).

Lovell, S.C., Davis, I.W., Arendall, W.B., 3rd, de Bakker, P.I., Word, J.M., Prisant, M.G., Richardson, J.S., and Richardson, D.C. (2003). Structure validation by Calpha geometry: phi,psi and Cbeta deviation. Proteins *50*, 437-450.

Lovenberg, T.W., Brewster, W.K., Mottola, D.M., Lee, R.C., Riggs, R.M., Nichols, D.E., Lewis, M.H., and Mailman, R.B. (1989). Dihydrexidine, a novel selective high potency full dopamine D-1 receptor agonist. Eur J Pharmacol *166*, 111-113.

Lynch, E.D., and Kil, J. (2009). Development of Ebselen, a Glutathione Peroxidase Mimic, for the Prevention and Treatment of Noise-Induced Hearing Loss. Seminars in hearing/volume *30*, 47-55.

Maas, J.W., Fawcett, J., and Dekirmenjian, H. (1968). 3-Methoxy-4-hydroxy phenylglycol (MHPG) excretion in depressive states. A pilot study. Arch Gen Psychiatry *19*, 129-134.

Mackinnon, D.F., and Pies, R. (2006). Affective instability as rapid cycling: theoretical and clinical implications for borderline personality and bipolar spectrum disorders. Bipolar Disord *8*, 1-14.

Majerus, P.W. (1992). Inositol phosphate biochemistry. Annu Rev Biochem *61*, 225-250.

Majumder, A.L., Johnson, M.D., and Henry, S.A. (1997). 1L-myo-inositol-1-phosphate synthase. Biochim Biophys Acta *1348*, 245-256.

McAllister, G., Whiting, P., Hammond, E.A., Knowles, M.R., Atack, J.R., Bailey, F.J., Maigetter, R., and Ragan, C.I. (1992). cDNA cloning of human and rat brain myo-inositol monophosphatase. Expression and characterization of the human recombinant enzyme. Biochem J *284 (Pt 3)*, 749-754.

McCoy, A.J., Grosse-Kunstleve, R.W., Adams, P.D., Winn, M.D., Storoni, L.C., and Read, R.J. (2007). Phaser crystallographic software. J Appl Crystallogr *40*, 658-674.
Mishory, A., Yaroslavsky, Y., Bersudsky, Y., and Belmaker, R.H. (2000). Phenytoin as an antimanic anticonvulsant: a controlled study. Am J Psychiatry *157*, 463-465.

Mizuno, K., Yamamoto, S., and Lands, W.E. (1982). Effects of non-steroidal anti-inflammatory drugs on fatty acid cyclooxygenase and prostaglandin hydroperoxidase activities. Prostaglandins *23*, 743-757.

Monaco, M.E., and Woods, D. (1983). Characterization of the hormone-sensitive phosphatidylinositol pool in WRK-1 cells. J Biol Chem *258*, 15125-15129.

Moore, G.J., Bebchuk, J.M., Parrish, J.K., Faulk, M.W., Arfken, C.L., Strahl-Bevacqua, J., and Manji, H.K. (1999). Temporal dissociation between lithium-induced changes in frontal lobe myo-inositol and clinical response in manic-depressive illness. Am J Psychiatry *156*, 1902-1908.

Moore, K. (1978). Amphetamines: Biochemical and behavioural actions in animals. In Handbook of Psychopharmacology, I. L.L., I. S.D., and S. S.A., eds. (New York, Plenum Press), pp. 41-98.

Mork, A., Geisler, A., and Hollund, P. (1992). Effects of lithium on second messenger systems in the brain. Pharmacol Toxicol *71 Suppl 1*, 4-17.

Mu, Q., Johnson, K., Morgan, P.S., Grenesko, E.L., Molnar, C.E., Anderson, B., Nahas, Z., Kozel, F.A., Kose, S., Knable, M.*, et al.* (2007). A single 20 mg dose of the full D1 dopamine agonist dihydrexidine (DAR-0100) increases prefrontal perfusion in schizophrenia. Schizophr Res *94*, 332-341.

Murphy, D.L., Brodie, H.K., Goodwin, F.K., and Bunney, W.E., Jr. (1971). Regular induction of hypomania by L-dopa in "bipolar" manic-depressive patients. Nature *229*, 135-136.

Murshudov, G.N., Skubak, P., Lebedev, A.A., Pannu, N.S., Steiner, R.A., Nicholls, R.A., Winn, M.D., Long, F., and Vagin, A.A. (2011). REFMAC5 for the refinement of macromolecular crystal structures. Acta Crystallogr D Biol Crystallogr *67*, 355-367.

Nahorski, S.R., Ragan, C.I., and Challiss, R.A. (1991). Lithium and the phosphoinositide cycle: an example of uncompetitive inhibition and its pharmacological consequences. Trends Pharmacol Sci *12*, 297-303.

Narayanaswami, V., and Sies, H. (1990). Antioxidant activity of ebselen and related selenoorganic compounds in microsomal lipid peroxidation. Free Radic Res Commun *10*, 237-244.

Naylor, E., Arredouani, A., Vasudevan, S.R., Lewis, A.M., Parkesh, R., Mizote, A., Rosen, D., Thomas, J.M., Izumi, M., Ganesan, A*., et al.* (2009). Identification of a chemical probe for NAADP by virtual screening. Nat Chem Biol *5*, 220-226.

Naylor, G.J., Dick, D.A., Dick, E.G., Le Poidevin, D., and Whyte, S.F. (1973). Erythrocyte membrane cation carrier in depressive illness. Psychol Med *3*, 502-508.

Naylor, G.J., Dick, D.A., Dick, E.G., and Moody, J.P. (1974). Lithium therapy and erythrocyte membrane cation carrier. Psychopharmacologia *37*, 81-86.

Nixon, M.K., Hascoet, M., Bourin, M., and Colombel, M.C. (1994). Additive effects of lithium and antidepressants in the forced swimming test: further evidence for involvement of the serotoninergic system. Psychopharmacology (Berl) *115*, 59-64.

Noack, C.H., and Trautner, E.M. (1951). The lithium treatment of maniacal psychosis. Med J Aust *2*, 219-222.

Nonaka, S., Hough, C.J., and Chuang, D.M. (1998). Chronic lithium treatment robustly protects neurons in the central nervous system against excitotoxicity by inhibiting N-methyl-D-aspartate receptor-mediated calcium influx. Proc Natl Acad Sci U S A *95*, 2642-2647.

O'Brien, W.T., Harper, A.D., Jove, F., Woodgett, J.R., Maretto, S., Piccolo, S., and Klein, P.S. (2004). Glycogen synthase kinase-3beta haploinsufficiency mimics the behavioral and molecular effects of lithium. J Neurosci *24*, 6791-6798.

O'Donnell, K.C., and Gould, T.D. (2007). The behavioral actions of lithium in rodent models: leads to develop novel therapeutics. Neurosci Biobehav Rev *31*, 932-962.

O'Leary, O.F., Bechtholt, A.J., Crowley, J.J., Hill, T.E., Page, M.E., and Lucki, I. (2007). Depletion of serotonin and catecholamines block the acute behavioral response to different classes of antidepressant drugs in the mouse tail suspension test. Psychopharmacology (Berl) *192*, 357-371.

Ohnishi, T., Ohba, H., Seo, K.C., Im, J., Sato, Y., Iwayama, Y., Furuichi, T., Chung, S.K., and Yoshikawa, T. (2007a). Spatial expression patterns and biochemical properties distinguish a second myo-inositol monophosphatase IMPA2 from IMPA1. J Biol Chem *282*, 637-646.

Ohnishi, T., Watanabe, A., Ohba, H., Iwayama, Y., Maekawa, M., and Yoshikawa, T. (2010). Behavioral analyses of transgenic mice harboring bipolar disorder candidate genes, IMPA1 and IMPA2. Neurosci Res *67*, 86-94.

Ohnishi, T., Yamada, K., Ohba, H., Iwayama, Y., Toyota, T., Hattori, E., Inada, T., Kunugi, H., Tatsumi, M., Ozaki, N.*, et al.* (2007b). A promoter haplotype of the inositol monophosphatase 2 gene (IMPA2) at 18p11.2 confers a possible risk for bipolar disorder by enhancing transcription. Neuropsychopharmacology *32*, 1727-1737.

Oppenheim, G., Ebstein, R.P., and Belmaker, R.H. (1979). Effect of lithium on the physostigmine-induced behavioral syndrome and plasma cyclic GMP. J Psychiatr Res *15*, 133-138.

Pardridge, W.M. (2005). The blood-brain barrier: bottleneck in brain drug development. NeuroRx *2*, 3-14.

Parnham, M., and Sies, H. (2000). Ebselen: prospective therapy for cerebral ischaemia. Expert Opin Investig Drugs *9*, 607-619.

Parnham, M.J., and Kindt, S. (1984). A novel biologically active seleno-organic compound--III. Effects of PZ 51 (Ebselen) on glutathione peroxidase and secretory activities of mouse macrophages. Biochem Pharmacol *33*, 3247-3250.

Patel, S., Meldrum, B.S., and Fine, A. (1988). Susceptibility to pilocarpine-induced seizures in rats increases with age. Behav Brain Res *31*, 165-167.

Patil, S.T., Zhang, L., Martenyi, F., Lowe, S.L., Jackson, K.A., Andreev, B.V., Avedisova, A.S., Bardenstein, L.M., Gurovich, I.Y., Morozova, M.A.*, et al.* (2007). Activation of mGlu2/3 receptors as a new approach to treat schizophrenia: a randomized Phase 2 clinical trial. Nat Med *13*, 1102-1107.

Peet, M. (1994). Induction of mania with selective serotonin re-uptake inhibitors and tricyclic antidepressants. Br J Psychiatry *164*, 549-550.

Perry, W., Minassian, A., Paulus, M.P., Young, J.W., Kincaid, M.J., Ferguson, E.J., Henry, B.L., Zhuang, X., Masten, V.L., Sharp, R.F.*, et al.* (2009). A reverse-translational study of dysfunctional exploration in psychiatric disorders: from mice to men. Arch Gen Psychiatry *66*, 1072-1080.

Petit-Demouliere, B., Chenu, F., and Bourin, M. (2005). Forced swimming test in mice: a review of antidepressant activity. Psychopharmacology (Berl) *177*, 245-255.
Pichot, P. (2004). [Circular insanity, 150 years on]. Bull Acad Natl Med *188*, 275-284.

Plenge, P., and Mellerup, E.T. (1982). 3H-Imipramine high-affinity binding sites in rat brain. Effects of imipramine and lithium. Psychopharmacology (Berl) *77*, 94-97.

Poitou, P., and Bohuon, C. (1975). Catecholamine metabolism in the rat brain after short and long term lithium administration. J Neurochem *25*, 535-537.

Pollack, S.J., Atack, J.R., Knowles, M.R., McAllister, G., Ragan, C.I., Baker, R., Fletcher, S.R., Iversen, L.L., and Broughton, H.B. (1994). Mechanism of inositol monophosphatase, the putative target of lithium therapy. Proc Natl Acad Sci U S A *91*, 5766-5770.

Pollack, S.J., Knowles, M.R., Atack, J.R., Broughton, H.B., Ragan, C.I., Osborne, S., and McAllister, G. (1993). Probing the role of metal ions in the mechanism of inositol monophosphatase by site-directed mutagenesis. Eur J Biochem *217*, 281-287.

Porcelli, S., Savoia, E.M., Bonafede, R., Moretti, F., Carchia, G., Belvedere, M., De Ronchi, D., and Serretti, A. (2011). Bipolar depression: quetiapine extended release effectiveness. Eur Neuropsychopharm *21*, S432-S432.

Porsolt, R.D., Anton, G., Blavet, N., and Jalfre, M. (1978). Behavioural despair in rats: a new model sensitive to antidepressant treatments. Eur J Pharmacol *47*, 379-391.

Porsolt, R.D., Bertin, A., Blavet, N., Deniel, M., and Jalfre, M. (1979). Immobility induced by forced swimming in rats: effects of agents which modify central catecholamine and serotonin activity. Eur J Pharmacol *57*, 201-210.

Porsolt, R.D., Le Pichon, M., and Jalfre, M. (1977). Depression: a new animal model sensitive to antidepressant treatments. Nature *266*, 730-732.

Posser, T., Kaster, M.P., Barauna, S.C., Rocha, J.B., Rodrigues, A.L., and Leal, R.B. (2009). Antidepressant-like effect of the organoselenium compound ebselen in mice: evidence for the involvement of the monoaminergic system. Eur J Pharmacol *602*, 85-91.

Potter, W.Z., and Linnoila, M. (1989). Biochemical classifications of diagnostic subgroups and D-type scores. Arch Gen Psychiatry *46*, 269-271.

Potter, W.Z., and Manji, H.K. (1994). Catecholamines in depression: an update. Clin Chem *40*, 279-287.

Price, L.H., Charney, D.S., Delgado, P.L., and Heninger, G.R. (1990). Lithium and serotonin function: implications for the serotonin hypothesis of depression. Psychopharmacology (Berl) *100*, 3-12.

Reisberg, B., Doody, R., Stoffler, A., Schmitt, F., Ferris, S., and Mobius, H.J. (2003). Memantine in moderate-to-severe Alzheimer's disease. N Engl J Med *348*, 1333-1341.

Rice, P.L., I. and Bleasby,A. (2000). EMBOSS: The European Molecular Biology Open Software Suite. Trends in Genetics *16*, 276-277.

Riemann, D., Hohagen, F., Bahro, M., and Berger, M. (1994). Sleep in depression: the influence of age, gender and diagnostic subtype on baseline sleep and the cholinergic REM induction test with RS 86. Eur Arch Psychiatry Clin Neurosci *243*, 279-290.

Risch, S.C., Cohen, R.M., Janowsky, D.S., Kalin, N.H., Sitaram, N., Gillin, J.C., and Murphy, D.L. (1981). Physostigmine induction of depressive symptomatology in normal human subjects. Psychiatry Res *4*, 89-94.

Roccatagliata, G. (1986). A history of ancient psychiatry (New York, Greenwood Press).

Roy, A., De Jong, J., and Linnoila, M. (1989). Extraversion in pathological gamblers. Correlates with indexes of noradrenergic function. Arch Gen Psychiatry *46*, 679-681.
Roy, A., Pickar, D., Linnoila, M., and Potter, W.Z. (1985). Plasma norepinephrine level in affective disorders. Relationship to melancholia. Arch Gen Psychiatry *42*, 1181-1185.

Rubin, A.L., Price, L.H., Charney, D.S., and Heninger, G.R. (1985). Noradrenergic function and the cortisol response to dexamethasone in depression. Psychiatry Res *15*, 5-15.

Rudorfer, M.V., Ross, R.J., Linnoila, M., Sherer, M.A., and Potter, W.Z. (1985). Exaggerated orthostatic responsivity of plasma norepinephrine in depression. Arch Gen Psychiatry *42*, 1186-1192.

Sachs, G.S., Printz, D.J., Kahn, D.A., Carpenter, D., and Docherty, J.P. (2000). The Expert Consensus Guideline Series: Medication Treatment of Bipolar Disorder 2000. Postgrad Med *Spec No*, 1-104.

Saiardi, A., Sciambi, C., McCaffery, J.M., Wendland, B., and Snyder, S.H. (2002). Inositol pyrophosphates regulate endocytic trafficking. Proc Natl Acad Sci U S A *99*, 14206-14211.

Saito, I., Asano, T., Sano, K., Takakura, K., Abe, H., Yoshimoto, T., Kikuchi, H., Ohta, T., and Ishibashi, S. (1998). Neuroprotective effect of an antioxidant, ebselen, in patients with delayed neurological deficits after aneurysmal subarachnoid hemorrhage. Neurosurgery *42*, 269-277; discussion 277-268.

Sambrook, J., Fritsch, E.F., and Maniatis, T. (1989). Molecular cloning : a laboratory manual, 2nd edn (Cold Spring Harbor, Cold Spring Harbor Laboratory Press).

San, L., and Arranz, B. (2008). Agomelatine: a novel mechanism of antidepressant action involving the melatonergic and the serotonergic system. Eur Psychiatry *23*, 396-402.

Saudek, V., Vincendon, P., Do, Q.T., Atkinson, R.A., Sklenar, V., Pelton, P.D., Piriou, F., and Ganzhorn, A.J. (1996). 7Li nuclear-magnetic-resonance study of lithium binding to myo-inositolmonophosphatase. Eur J Biochem *240*, 288-291.

Schanberg, S.M., Breese, G.R., Schildkraut, K.K., Gordon, E.K., and Kopin, I.J. (1968a). 3-methoxy-4-hydroxyphenylglycol sulfate in brain and cerebrospinal fluid. Biochem Pharmacol *17*, 2006-2008.

Schanberg, S.M., Schildkraut, J.J., Breese, G.R., and Kopin, I.J. (1968b). Metabolism of normetanephrine-H3 in rat brain--identification of conjugated 3-methoxy-4-hydrophenylglycol as the major metabolite. Biochem Pharmacol *17*, 247-254.

Schewe, T. (1995). Molecular actions of ebselen--an antiinflammatory antioxidant. Gen Pharmacol *26*, 1153-1169.

Schildkraut, J.J. (1965). The catecholamine hypothesis of affective disorders: a review of supporting evidence. Am J Psychiatry *122*, 509-522.

Schildkraut, J.J., Gordon, E.K., and Durell, J. (1965). Catecholamine metabolism in affective disorders. I. Normetanephrine and VMA excretion in depressed patients treated with imipramine. J Psychiatr Res *3*, 213-228.

Schildkraut, J.J., Logue, M.A., and Dodge, G.A. (1969). The effects of lthium salts on the turnover and metabolism of norepinephrine in rat brain. Psychopharmacologia *14*, 135-141.

Schildkraut, J.J., Schanberg, S.M., and Kopin, I.J. (1966). The effects of lithium ion on H3-norepinephrine metabolism in brain. Life Sci *5*, 1479-1483.

Schoepfer, R. (1993). The pRSET family of T7 promoter expression vectors for Escherichia coli. Gene *124*, 83-85.

Schou, M., Juel-Nielsen, N., Stromgren, E., and Voldby, H. (1954). The treatment of manic psychoses by the administration of lithium salts. J Neurol Neurosurg Psychiatry *17*, 250-260.

Schultz, J.E., Siggins, G.R., Schocker, F.W., Turck, M., and Bloom, F.E. (1981). Effects of prolonged treatment with lithium and tricyclic antidepressants on discharge frequency, norepinephrine responses and beta receptor binding in rat cerebellum: electrophysiological and biochemical comparison. J Pharmacol Exp Ther *216*, 28-38.

Seeman, P., and Van Tol, H.H. (1994). Dopamine receptor pharmacology. Trends Pharmacol Sci *15*, 264-270.

Segal, D.S., Callaghan, M., and Mandell, A.J. (1975). Alterations in behaviour and catecholamine biosynthesis induced by lithium. Nature *254*, 58-59.

Sengupta, N., Datta, S.C., Sengupta, D., and Bal, S. (1980). Platelet and erythrocyte-membrane adenosine triphosphatase activity in depressive and manic-depressive illness. Psychiatry Res *3*, 337-344.

Shamir, A., Sjoholt, G., Ebstein, R.P., Agam, G., and Steen, V.M. (2001). Characterization of two genes, Impa1 and Impa2 encoding mouse myo-inositol monophosphatases. Gene *271*, 285-291.

Shimon, H., Agam, G., Belmaker, R.H., Hyde, T.M., and Kleinman, J.E. (1997). Reduced frontal cortex inositol levels in postmortem brain of suicide victims and patients with bipolar disorder. Am J Psychiatry *154*, 1148-1150.

Shin, J.M., Cho, Y.M., and Sachs, G. (2004). Chemistry of covalent inhibition of the gastric (H+, K+)-ATPase by proton pump inhibitors. J Am Chem Soc *126*, 7800-7811.

Shorter, E. (2009). The history of lithium therapy. Bipolar Disord *11 Suppl 2*, 4-9.

Siever, L.J. (1987). Role of noradrenergic mechanisms in the etiology of the affective disorders. In Psychopharmacology: The Third Generation of Progress, H.Y. Meltzer, ed. (New York, Raven Press.), pp. 493-504.

Silverstone, P.H., McGrath, B.M., and Kim, H. (2005). Bipolar disorder and myo-inositol: a review of the magnetic resonance spectroscopy findings. Bipolar Disord *7*, 1-10.

Silverstone, T. (1984). Response to bromocriptine distinguishes bipolar from unipolar depression. Lancet *1*, 903-904.

Simon, J.R., and Kuhar, M.J. (1976). High affinity choline uptake: ionic and energy requirements. J Neurochem *27*, 93-99.

Singh, J., Petter, R.C., Baillie, T.A., and Whitty, A. (2011). The resurgence of covalent drugs. Nat Rev Drug Discov *10*, 307-317.

Sjoholt, G., Ebstein, R.P., Lie, R.T., Berle, J.O., Mallet, J., Deleuze, J.F., Levinson, D.F., Laurent, C., Mujahed, M., Bannoura, I.*, et al.* (2004). Examination of IMPA1 and IMPA2 genes in manic-depressive patients: association between IMPA2 promoter polymorphisms and bipolar disorder. Mol Psychiatry *9*, 621-629.

Sjoholt, G., Molven, A., Lovlie, R., Wilcox, A., Sikela, J.M., and Steen, V.M. (1997). Genomic structure and chromosomal localization of a human myo-inositol monophosphatase gene (IMPA). Genomics *45*, 113-122.

Smith, D.F. (1988). Lithium attenuates clonidine-induced hypoactivity: further studies in inbred mouse strains. Psychopharmacology (Berl) *94*, 428-430.

Smith, D.F., and Smith, H.B. (1973). The effect of prolonged lithium administration on activity, reactivity, and endurance in the rat. Psychopharmacologia *30*, 83-88.

Smith, P.K., Krohn, R.I., Hermanson, G.T., Mallia, A.K., Gartner, F.H., Provenzano, M.D., Fujimoto, E.K., Goeke, N.M., Olson, B.J., and Klenk, D.C. (1985). Measurement of protein using bicinchoninic acid. Anal Biochem *150*, 76-85.

Smith, S.E., and Meldrum, B.S. (1992). The protein kinase C activators, phorbol 12-myristate,13-acetate and phorbol 12,13-dibutyrate, are convulsant in the pico-nanomolar range in mice. Eur J Pharmacol *213*, 133-135.

Soares, J.C., Chen, G., Dippold, C.S., Wells, K.F., Frank, E., Kupfer, D.J., Manji, H.K., and Mallinger, A.G. (2000a). Concurrent measures of protein kinase C and phosphoinositides in lithium-treated bipolar patients and healthy individuals: a preliminary study. Psychiatry Res *95*, 109-118.

Soares, J.C., Mallinger, A.G., Dippold, C.S., Forster Wells, K., Frank, E., and Kupfer, D.J. (2000b). Effects of lithium on platelet membrane phosphoinositides in bipolar disorder patients: a pilot study. Psychopharmacology (Berl) *149*, 12-16.

Sobczak, S., Riedel, W.J., Booij, I., Aan Het Rot, M., Deutz, N.E., and Honig, A. (2002). Cognition following acute tryptophan depletion: difference between first-degree relatives of bipolar disorder patients and matched healthy control volunteers. Psychol Med *32*, 503-515.

Steckert, A.V., Valvassori, S.S., Moretti, M., Dal-Pizzol, F., and Quevedo, J. (2010). Role of oxidative stress in the pathophysiology of bipolar disorder. Neurochem Res *35*, 1295-1301.

Stieglitz, K.A., Johnson, K.A., Yang, H., Roberts, M.F., Seaton, B.A., Head, J.F., and Stec, B. (2002). Crystal structure of a dual activity IMPase/FBPase (AF2372) from Archaeoglobus fulgidus. The story of a mobile loop. J Biol Chem *277*, 22863-22874.

Strasser, F., Pelton, P.D., and Ganzhorn, A.J. (1995). Kinetic characterization of enzyme forms involved in metal ion activation and inhibition of myo-inositol monophosphatase. Biochem J *307 (Pt 2)*, 585-593.

Swinney, D.C., and Anthony, J. (2011). How were new medicines discovered? Nat Rev Drug Discov *10*, 507-519.

Takimoto, K., Okada, M., Matsuda, Y., and Nakagawa, H. (1985). Purification and properties of myo-inositol-1-phosphatase from rat brain. J Biochem *98*, 363-370.

Teague, S.J., Davis, A.M., Leeson, P.D., and Oprea, T. (1999). The Design of Leadlike Combinatorial Libraries. Angew Chem Int Ed Engl *38*, 3743-3748.

Tietze, F. (1969). Enzymic method for quantitative determination of nanogram amounts of total and oxidized glutathione: applications to mammalian blood and other tissues. Anal Biochem *27*, 502-522.

Tohen, M. (2008). Clinical trials in bipolar mania: implications in study design and drug development. Arch Gen Psychiatry *65*, 252-253.

Treiser, S.L., Cascio, C.S., O'Donohue, T.L., Thoa, N.B., Jacobowitz, D.M., and Kellar, K.J. (1981). Lithium increases serotonin release and decreases serotonin receptors in the hippocampus. Science *213*, 1529-1531.

Trinquet, E., Fink, M., Bazin, H., Grillet, F., Maurin, F., Bourrier, E., Ansanay, H., Leroy, C., Michaud, A., Durroux, T.*, et al.* (2006). D-myo-inositol 1-phosphate as a surrogate of D-myo-inositol 1,4,5-tris phosphate to monitor G protein-coupled receptor activation. Anal Biochem *358*, 126-135.

Tudorache, B., and Diacicov, S. (1991). The effect of clonidine in the treatment of acute mania. Rom J Neurol Psychiatry *29*, 209-213.

Vadnal, R.E., Parthasarathy, R., Parthasarathy, L., Ramesh, T.G., and Shyamaladevi, C.S. (1992). The identification of a membrane-bound myo-inositol 1-phosphatase in rat brain, liver, and testes. Biochem Int *26*, 935-941.

Van Kammen, D.P., and Murphy, D.L. (1975). Attenuation of the euphoriant and activating effects of d- and l-amphetamine by lithium carbonate treatment. Psychopharmacologia *44*, 215-224.

van Praag, H.M., and Korf, J. (1975). Central monoamine deficiency in depressions: causative of secondary phenomenon? Pharmakopsychiatr Neuropsychopharmakol *8*, 322-326.

Varma, S.D., Chakrapani, B., and Reddy, V.N. (1970). Intraocular transport of myoinositol. II. Accumulation in the rabbit lens in vitro. Invest Ophthalmol *9*, 794-800.

Verdonk, M.L., Cole, J.C., Hartshorn, M.J., Murray, C.W., and Taylor, R.D. (2003). Improved protein-ligand docking using GOLD. Proteins *52*, 609-623.

Walters, W.P., Stahl, M.T., and Murcko, M.A. (1998). Virtual screening - an overview. Drug Discov Today *3*, 160-178.

Williams, R.S., Cheng, L., Mudge, A.W., and Harwood, A.J. (2002). A common mechanism of action for three mood-stabilizing drugs. Nature *417*, 292-295.

Willner, P. (1985). Antidepressants and serotonergic neurotransmission: an integrative review. Psychopharmacology (Berl) *85*, 387-404.

Wilson, C.O., Gisvold, O., Block, J.H., and Beale, J.M. (2004). Wilson and Gisvold's textbook of organic medicinal and pharmaceutical chemistry / edited by John H. Block, John M. Beale Jr, 11th edn (Philadelphia, Lippincott Williams & Wilkins).

Wotjak, C.T. (2004). Of mice and men: Potentials and caveats of behavioural experiments with mice. BIF Futura *19*, 158-168.

Yamaguchi, T., Sano, K., Takakura, K., Saito, I., Shinohara, Y., Asano, T., and Yasuhara, H. (1998). Ebselen in acute ischemic stroke: a placebo-controlled, double-blind clinical trial. Ebselen Study Group. Stroke *29*, 12-17.

Yoshikawa, T., Turner, G., Esterling, L.E., Sanders, A.R., and Detera-Wadleigh, S.D. (1997). A novel human myo-inositol monophosphatase gene, IMP.18p, maps to a susceptibility region for bipolar disorder. Mol Psychiatry *2*, 393-397.

Young, A.H., Calabrese, J.R., Gustafsson, U., Paulsson, B., Malhi, G.S., Bond, D.J., and Ferrier, N. (2010a). The efficacy of quetiapine monotherapy in bipolar II depression: combined data from the BOLDER and EMBOLDEN studies. Bipolar Disord *12*, 58-59.

Young, A.H., McElroy, S.L., Bauer, M., Philips, N., Chang, W., Olausson, B., Paulsson, B., Brecher, M., and Investigators, E.I.T. (2010b). A Double-Blind, Placebo-Controlled Study of Quetiapine and Lithium Monotherapy in Adults in the Acute Phase of Bipolar Depression (EMBOLDEN I). J Clin Psychiat *71*, 150-162.

Young, L.T., Warsh, J.J., Kish, S.J., Shannak, K., and Hornykeiwicz, O. (1994). Reduced brain 5-HT and elevated NE turnover and metabolites in bipolar affective disorder. Biol Psychiatry *35*, 121-127.

Yuan, P.X., Chen, G., Huang, L.D., and Manji, H.K. (1998). Lithium stimulates gene expression through the AP-1 transcription factor pathway. Brain Res Mol Brain Res *58*, 225-230.

Zerahn, K. (1955). Studies on the active transport of lithium in the isolated frog skin. Acta Physiol Scand *33*, 347-358.

Zhang, F., Phiel, C.J., Spece, L., Gurvich, N., and Klein, P.S. (2003). Inhibitory phosphorylation of glycogen synthase kinase-3 (GSK-3) in response to lithium - Evidence for autoregulation of GSK-3. Journal of Biological Chemistry *278*, 33067-33077.

Zhang, L., Elmer, L.W., and Little, K.Y. (1998). Expression and regulation of the human dopamine transporter in a neuronal cell line. Brain Res Mol Brain Res *59*, 66-73.

Zhou, R., Gray, N.A., Yuan, P., Li, X., Chen, J., Chen, G., Damschroder-Williams, P., Du, J., Zhang, L., and Manji, H.K. (2005). The anti-apoptotic, glucocorticoid receptor cochaperone protein BAG-1 is a long-term target for the actions of mood stabilizers. J Neurosci *25*, 4493-4502.

Zuckerman, M. (1984). Sensation Seeking - a Comparative Approach to a Human Trait. Behav Brain Sci *7*, 413-434.

Zuckerman, M., and Neeb, M. (1979). Sensation seeking and psychopathology. Psychiatry Res *1*, 255-264.